CLIMATE VARIABILITY: CHANGING WEATHER PATTERNS OVER NEW ZEALAND

A thesis submitted in partial fulfilment of the requirements for the
Degree of Doctor of Philosophy in Physics
at the University of Canterbury

by

SIMON PARSONS

Department of Physics and Astronomy
College of Science
University of Canterbury

– February 2015 –

Big whirls have little whirls that feed on their velocity,
and little whirls have lesser whirls and so on to viscosity.

— Lewis Fry Richardson

The reasonable man adapts himself to the world; the unreasonable one persists in trying to adapt the world to himself. Therefore, all progress depends on the unreasonable man.

— George Bernard Shaw

ABSTRACT

The original intention of this thesis was to investigate Climate Change (CC), in particular the meteorological impacts of CC on New Zealand (NZ). Succinctly, "to understand what NZ's future weather may entail". However, as the research progressed it has led to the larger circulation and has highlighted the teleconnections that are present and the importance of the wider circulation and to NZ. It is apparent that the larger scale circulation needs to be considered in conjunction with, if not before, the synoptic scale. Thus, in order to understand NZ's future weather first we must understand the Southern Hemisphere and the circulation within it.

CC is often described in a broad global scale and it is difficult to translate and relate these mechanisms into day to day weather terms, which have the advantage of being commonly understood. Synoptic Climatology (SC) can bridge this gap by simplifying the wide variety of weather into a small grouping of types, and thus can provide an understandable alternative.

To undertake this research an existing SC scheme known as the Kidson Types (KTs) was extended with the use of General Circulation Model (GCM) output. The KTs have been widely used in NZ, thus work detailing their future would be advantageous. The GCMs were able to reproduce the observed frequencies of occurrence of the KTs during the late 20th century. Future projections for the late 21st century surprisingly showed little change in annual type frequencies. To investigate this further a sensitivity study was undertaken, which revealed that the methodology was insensitive to annual type frequency change. The range of response from the GCM projections also inhibited determining significant changes in KT frequencies. Additionally, trend analysis using four realisations from one GCM noted both positive and negative trends in some of the types. This also

highlights the difficulty in using GCM output, as a larger ensemble can diffuse results and in a small ensemble individual GCMs can unduly bias the results.

Further scrutiny of the KT was then undertaken. An investigation of the KTs to ascertain their influence in the wider circulation using the ERA Interim (ERA-I) reanalysis and trends within the KT using a long term reanalysis data set, the Twentieth Century Reanalysis (20CR). Due to the high year to year variability in the KTs, significant trends were only determined in the 20CR with a reduction in the Zonal Regime representing the occurrence of strong westerly flows over NZ. A composite analysis was also undertaken to evaluate the KTs within the Southern Hemisphere (SH). A positive pressure anomaly was detected far from the Kidson domain, which is defined over NZ, during the SW type. This motivated another study on SH Blocking.

Blocking is a large scale phenomena that can influence the paths of synoptic systems and thus potentially cause or exacerbate adverse weather events. Blocking is an area of climate research that requires further work, as there is a deficit of GCM studies in the SH. This study utilised a Persistent Positive Anomaly (PPA) methodology which is advantageous as the spatial pattern, latitude and longitude, of the Blocking Events (BEs) is determined. To our knowledge, this is the first study to use GCM output using the PPA methodology in the SH and this is also the first blocking study using Coupled Model Inter-comparison Project (CMIP)5 GCM output in the SH. A reduction of BEs was observed over the South Pacific Ocean (SPO) region during summer and spring, in the GCM projections between 2041-2070 and 2071-2100. The Southern Annular Mode (SAM) has been suggested as an influence on blocking frequency in previous work and this relationship was studied. A high negative correlation between SAM+ and BEs was observed in summer with the reanalysis and GCM historical output. This correlation was reduced in 21st century. However, further work is needed in this study in order to gain an understanding of the mechanisms and linkages between SAM and the BEs.

Deputy Vice-Chancellor's Office
Postgraduate Office

UNIVERSITY OF CANTERBURY
Te Whare Wānanga o Waitaha
CHRISTCHURCH NEW ZEALAND

Co-authorship Form

This form is to accompany the submission of any thesis that contains research reported in co-authored work that has been published, accepted for publication, or submitted for publication. A copy of this form should be included for each co-authored work that is included in the thesis. Completed forms should be included at the front (after the thesis abstract) of each copy of the thesis submitted for examination and library deposit.

Please indicate the chapter/section/pages of this thesis that are extracted from co-authored work and provide details of the publication or submission from which the extract comes:

Chapter 4, SYNOPTIC CLIMATOLOGY WITH GCM OUTPUT OVER NEW ZEALAND, *published in the International Journal of Climatology, 2014 (Parsons et al., 2014).*

Please detail the nature and extent (%) of contribution by the candidate:

Simon Parsons was the lead author of this article; contribution 70%.

Certification by co-authors:

If there is more than one co-author then a single co-author can sign on behalf of all.

The undersigned certifies that:

- the above statement correctly reflects the nature and extent of the PhD candidate's contribution to this co-authored work;
- in cases where the candidate was the lead author of the co-authored work he or she wrote the text.

Name: Signature: Date:

ACKNOWLEDGMENTS

Firstly, I would like to acknowledge and thank Jeanelle for her continued support and encouragement throughout this thesis. Without her this thesis would not have happened. Thanks my darling wife.

My primary supervisor Dr Adrian McDonald for his constant support and understanding despite the many suspensions and delays of this thesis. My secondary supervisor Dr James Renwick for his continued support and interest in my work, despite Skypes concerted efforts to thwart communication. Thank you both, especially for laughing at my attempts at humour.

The Atmospheric Physics group at the University of Canterbury, past and present, Nikolai Kuetzmann, Jack Coggins, Ben Jolly, Simon Fullick, Robert Ward, Madeline Smith, Fraser Dennison and Graeme Plank. Department of Physics and Astronomy for the P.hD. scholarship.

This project has been based on data that many groups and organizations have supplied. Thank you to the many modeling groups that enabled this work to occur.

CONTENTS

LIST OF FIGURES

LIST OF TABLES

ACRONYMS

20CR Twentieth Century Reanalysis

3D-VAR Three Dimensional Variational Assimilation

4D-VAR Four Dimensional Variational Assimilation

AC Anticyclone

ACC Antarctic Circumpolar Current

AOH Antarctic Ozone Hole

AR4 IPCC Fourth Assessment Report

AR5 IPCC Fifth Assessment Report

BE Blocking Event

CC Climate Change

CMIP Coupled Model Inter-comparison Project

CMIP3 Coupled Model Inter-comparison Project 3

CMIP5 Coupled Model Inter-comparison Project 5

ECMWF European Centre for Medium-Range Weather Forecasts

ENI East North Island

ENSO El Niño - Southern Oscillation

EOF Empirical Orthogonal Function

ERA40 European Reanalysis 40

ERA-I ERA Interim

ESI East South Island

GCM General Circulation Model

GHG Green House Gas

HSE High South East

IO Indian Ocean

IPCC Intergovernmental Panel on Climate Change

KT Kidson Type

LMC Lund Map Classification

MSLP Mean Sea Level Pressure

NCEP1 NCEP/NCAR1

NCEP2 NCEP/NCAR2

NH Northern Hemisphere

NI North Island

NWP Numerical Weather Prediction

NZ New Zealand

PC Principal Component

PCA Principal Component Analysis

PPA Persistent Positive Anomaly

PSL Pressure at Sea Level

RCM Regional Climate Model

RCP Representative Concentration Pathway

SAM Southern Annular Mode

SAM- Southern Annular Mode Negative Phase

SAM+ Southern Annular Mode Positive Phase

SC Synoptic Climatology

SH Southern Hemisphere

SI South Island

SO Southern Ocean

SOI Southern Oscillation Index

SOI- Southern Oscillation Index Negative Phase

SOI+ Southern Oscillation Index Positive Phase

SOM Self Organised Map

SP South Pacific

SPO South Pacific Ocean

SRES Special Report on Emissions Scenarios

SST Sea Surface Temperature

SW South Westerly

WGCM Working Group on Coupled Modelling

WRCP World Climate Research Project

WSI West South Island

ZW3 Zonal Wave 3

1

INTRODUCTION

1.1 MOTIVATION

The goal of this thesis is to further the understanding of Climate Change (CC) on the Southern Hemisphere (SH) and ascertain it's meteorological impacts on New Zealand (NZ). Succinctly, "to understand what NZ's future weather may entail". Whilst the intention of this thesis is simple to paraphrase, the process has been more complicated.

CC is often described in a broad global scale and it is difficult to translate and relate these mechanisms into day to day weather terms, which have the advantage of being commonly understood. The intention of this thesis is to be able to describe projected CC in terms of general weather patterns. The weather, which is tangible to everyone, and how the impacts of how CC will perturb weather patterns. Thus, assist in demystifying CC so its impacts can be widely understood.

Synoptic Climatology (SC) relates meteorological patterns to the local environment (Yarnal, 1993). The intention of this work is to build on previous SC research done in NZ, rather than establish a new system. Kidson (2000) devised twelve synoptic pattens for NZ, these are now known as the Kidson Types (KTs). The KTs have been widely used in NZ and the investigation of KTs under climate change projections is one of the intentions of this thesis.

While this thesis is broad in focus, it does follow a logical progression which has been an enlightening journey. As each chapter segues into another it became apparent that in order to understand the smaller scale regional variations a comprehensive understanding of the larger scale hemispheric variations is also required.

1.2 THESIS OUTLINE

Several paths of investigation were conducted in this thesis. The original concept was to use the SC method of Kidson (2000), known as the KTs, and then extend this research with the use of General Circulation Models (GCMs). Once an understanding of the likelihood of the future weather patterns was determined these results would then be used in downscaling back to the local level within NZ. However, due to the findings of this research, presented in Chapter 4, principally a lack of sensitivity to change in the KT methodology the downscaling was not undertaken.

Chapter 2 provides a summary of the current literature, environs and relevant physical processes to this thesis. All of the data used in this thesis is derived from model output, either reanalysis or General Circulation Model (GCM). Due to the importance of the model output Chapter 3 is devoted to this topic.

The research presented in this thesis starts in Chapter 4, with the SC method of Kidson (2000). This work has been peer reviewed and published as Parsons et al. (2014).

The outcome from Chapter 4 led to an investigation of the KTs situated within the larger hemispheric scale using composite analysis, Chapter 5. Whilst this thesis is interested in future weather patterns the Kidson analysis was also extended back to 1871, using the Twentieth Century Reanalysis (20CR) data which became available during this project. This chapter also investigates trends and inter-annual variability of the KTs. This work is also in preparation for publication and it is to be submitted to the New Zealand journal Weather and Climate.

It is apparent from Chapter 5 that the weather in the mid latitudes, affecting NZ, can be considered as anomalies superimposed on the mean background state. Simply New Zealand's weather is the passage of high (anticyclone) and low (cylone) pressure systems. A positive pressure anomaly was detected far from the Kidson domain, which is defined over NZ, during the composite analysis. This motivated another study on SH Blocking, Chapter 6.

Blocking is a large scale phenomena that can persist and interfere with the passage of transient cyclonic systems. A detailed survey of blocking in the SH was undertaken using reanalysis data and GCM projections, Chapter 6. Finally, Chapter 7 provides a thesis summary and details some potential future work.

Chapter 4 has been published in the International Journal of Climatology Parsons et al. (2014). Chapter 5 is in preparation for submission in the NZ journal Weather and Climate. Chapter 6 is in preparation for submission in the Monthly Weather Review. Thus, the style and content of Chapters 4, 5 and 6 reflect this and their introduction sections may overlap with material that is presented in Chapter 2.

This thesis is somewhat broad and the final outcome involves larger scales and not the downscaling to NZ as originally envisioned. It does follow a logical path which highlights the importance of understanding the larger scale climatology before attempting to understand regional climates.

2

BACKGROUND

This chapter introduces and discusses the environs, background and processes detailed in this thesis. It is organised in the following manner.

1. Introduction and climate change is briefly discussed.
2. An overview of Synoptic Climatology (SC) and methodologies.
3. The Southern Hemisphere (SH) and New Zealand.

The lack of observational data and quality of the reanalysis data, prior to the satellite era, has inhibited studies in the SH when compared to the Northern Hemisphere (NH) (Simmonds et al., 2003; Hoskins and Hodges, 2005; Renwick, 2005). Additionally, General Circulation Models (GCMs) require quality observational data for validation. This is a common theme amongst studies that utilise model output in the SH. Chapter 3 discusses this issue and the reanalysis and GCM output in further detail.

2.1 INTRODUCTION AND CLIMATE CHANGE

It is virtually certain (99-100%) that anthropogenic influences have warmed the global climate, (Bindoff et al., 2013 and references within). However, interpreting climate change at the regional level is as an area of research that requires more investigation (Solomon et al., 2007). This has been further refined in the IPCC Fifth Assessment Report (AR5) with new research

initiatives quantifying the near term and regional ramifications of climate change (Meehl et al., 2009; Moss et al., 2010; Bindoff et al., 2013). To these ends climate change research is shifting towards examination of regional variation and assessing anomalous or extreme climate and weather events at a regional scale. An increased understanding of the regional impacts of climate change is of importance for policy makers to assist in appropriate planning decisions (Doherty et al., 2009).

The spatial and temporal scale of meteorological events are linked. Small spatial weather events occur on small time scales and larger events exist on larger time scales (Oke, 1987; Sturman and Tapper, 2006). This thesis is primarily interested in the synoptic scale. The synoptic scale includes weather systems such as cyclones and anticyclones and blocking highs, which are approximately 500-2000 km in size and last 3-10 days. However, these synoptic systems cannot be analysed in isolation, the larger circulation also needs consideration as the smaller scale synoptic features are influenced and reside within it.

The intention of this work is to provide further understanding of future weather patterns affecting New Zealand (NZ). GCM projections from the Coupled Model Inter-comparison Project (CMIP) 3 and 5 archives provide the data for this study (Meehl et al., 2000, 2007; Taylor et al., 2012). However, the coarse resolution of GCM data can make them unsuitable for investigations of regional and local climates, particularly concerning interactions with orography (Kidson and Thompson, 1998; Ackerley et al., 2012; Lee and Sheridan, 2012). In order to remedy this downscaling can be undertaken, this can be either dynamical or statistical.

Dynamical downscaling requires another model to be nested within the GCM. The GCM provides the boundary conditions, or the forcing, for the Regional Climate Model (RCM). The RCM operates at a higher spatial resolution which can more accurately portray the interaction with the orography. However, dynamical downscaling is still computationally demanding (Drost et al., 2007; Renwick et al., 2009; Ackerley et al., 2012). This

approach is also commonly employed in Numerical Weather Prediction (NWP) for short term weather forecasting.

Statistical downscaling determines relationships between the larger meteorological fields and local observed variables, extrapolation based on these relationships can then be undertaken. It has the advantage of being computationally less demanding than dynamical downscaling (Kidson and Thompson, 1998).

One of the statistical methods used is SC. SC techniques are often employed to reduce the complexity of weather data in order to simplify the extrapolation procedure (Huth et al., 2008). SC is used in this thesis to relate the GCM future projections to local weather patterns over NZ and examine the potential for change.

2.2 SYNOPTIC CLIMATOLOGY

Synoptic Climatology (SC) attempts to group similar weather patterns together to enable linking between atmospheric circulation and environmental variables (Yarnal, 1993). This can reduce the complexity of the daily weather into a smaller grouping of weather types. The weather types can then provide a proxy for a correlation between weather events and other variables such as precipitation, heat indices and flooding, (Griffiths, 2011; McKerchar et al., 2010). The terms maps, nodes, centroids, types, clusters or centres are often used in SC studies and describe the same element.

Climate regimes or classifications originated from meteorologists initially looking for improved weather forecasting techniques. Many different methods have been used and explored, however they all attempt to achieve the same purpose. To group similar synoptic situations in an effort to help interpret climatic variability (Huth et al., 2008). Advances in computational power combined with an increase in data availability, both reanalysis and GCMs, have lead to a resurgence of interest in syn-

optic climatology and climate classifications (Sheridan and Lee, 2010).

These classifications have been undertaken independently in different regions, hence there is a lack of standardised methodologies. For example the Hess-Brezowsky classification was developed for Germany and the Lamb catalogue for the British Isles (Huth et al., 2008). The diversity of methodologies and domains has also limited comparison of these classification systems (Huth et al., 2008). This is especially true for climate studies, which require a long time series in order to capture the longer modes of variability. Huth et al. (2008) provides a review of current synoptic classifications, however this is from a very Eurocentric point of view and concludes that a new European system is needed due to the diverse nature and the many different classifications systems.

Classification systems can be broadly grouped into three categories; subjective, mixed and objective.

SUBJECTIVE Requires expert knowledge, time intensive, hard to be consistent and reproduce results.

MIXED / HYBRID Expert knowledge combined with physical parameters.

OBJECTIVE Based on physical parameters. Can be automated and should be reproducible.

Subjective methods have been replaced by objective methods due to the labour intensive requirement, subjectivity of the operator and availability of large data sets such as reanalysis and the ability for these to be automated. However, all of these methods still retain a subjective component and these decisions on methodology will affect the outcomes. Subjective terms such as the number of classes/clusters and thresholds used in the methodology can strongly affect the results. Once these subjective terms or thresholds are determined the data can then be processed objectively. Despite these methods being considered objective, since they can be automated, they still retain a subjective component, namely the thresholds and number of

classes. These subjective decisions applied in the methodology can strongly influence the outcome and the detail and rationale behind the subjective decisions taken when determining the clusters are not always fully explained in the literature (Huth et al., 2008; Sheridan and Lee, 2011). The remainder of this section is focused on objective methodologies.

A conceptually simple SC method is that of map correlations, determining similarity between maps and grouping like maps together. Lund (1963) describes an early implementation of this method, whereby each map (n) is correlated against every other map, forming a n x n matrix. The maps with the highest number of correlated maps, above a subjective threshold, become the groups. The mean of these groups becomes the centres and the correlation process is repeated with the new centres. This approach is used in Chapter 4.

2.2.1 *PCA & Clustering*

Clustering schemes are frequently used in SC. An Empirical Orthogonal Function (EOF) analysis followed by a clustering on the resultant Principal Components (PCs) is used in many schemes (Christensen and Bryson, 1966; Barry and Perry, 1973; Bjornsson, 1997). The majority of the variation within the data can be explained by the first several PCs and provide an acceptable method of data reduction (Cuell and Bonsal, 2009). In NZ, this approach has been used for the Kidson Types (KTs), which is discussed in Section 2.2.3.

As with centres and clusters in SC, the terminology involved in Principal Component Analysis (PCA) and EOF can differ depending on the source, often these terms are used interchangeably. We define the EOF as the spatial pattern and the PC as the time component loadings.

The following description is based on Wilks (2011) and Bjornsson (1997) who provides a simplified manual for PCA.

Firstly, the time series mean of the data is removed. The data is then reformatted so each row, $x_{11,12,\cdots,1p}$, represents a single observation map and each column, $x_{11,21,\cdots,n1}$, is the time series for a particular grid point within the map. The data formed in this manner is known as S mode. If the matrix is rotated, so the columns are grid points and rows the time series, it is known as T mode.

$$F = \begin{bmatrix} x_{11} & x_{12} & \cdots & x_{1p} \\ x_{21} & x_{22} & \cdots & x_{2p} \\ \vdots & \vdots & \ddots & \\ x_{n1} & x_{n2} & \cdots & x_{np} \end{bmatrix}$$

The covariance matrix, R is then formed.

$$R = \frac{1}{n-1} F^t F$$

Eigenvalue and eigenvectors are then determined.

$$R = C \Lambda C^t$$

$$RC = C\Lambda$$

Λ contains the eigenvalues (λ_i) of R and C contains the corresponding eigenvectors (c_i). The EOFs are the eigenvectors and represent the spatial pattern of variations. The λ_i represent the amount of variance for each EOF. The first EOF has the largest eigenvalues, thus it explains the highest amount of the variability in F.

The time series for the EOF is known as the PC, $\overrightarrow{a_1}$.

$$\overrightarrow{a_1} = F\overrightarrow{c_1}$$

The original data, F, can be reconstructed as the sum of the EOFs and PCs.

$$F = \sum_{j=1}^{p} \overrightarrow{a_j}(EOF_j)$$

However, as this procedure is often undertaken for data reduction only a few of EOFs are retained and the majority of the data variability can be explained by these. Clustering is often undertaken on the retained PCs from the EOF analysis. The clustering methods seek to minimise the intra-type differences while maximizing the inter-type differences (Mahlstein and Knutti, 2010). One such method is k-means clustering (MacQueen, 1967).

In k-means clustering data points are randomly selected from the data, this is known as "seeding". The distance between the seeds and remaining data is then determined. Euclidean distance was used in Kidson (2000), however different metrics and weighting schemes could also be applied. The closest data point and seed are merged to form a new cluster and the process repeats. This process can be iterative, which will eventually result in all of the data being assigned to a single centre. Often the clustering process follows a Monte Carlo method, in which the clustering procedure is repeated multiple times and a dominant set of repeatable clusters emerges.

The steps of k-means clustering are as follows: A prior amount of clusters k

1. k data points are randomly selected, seeded, within the data.
2. The data is assigned to the "closest" k point to form a cluster. This is often done with Euclidean distance, or a weighted metric.
3. The mean of the clusters is determined and this is the new position for k.
4. Steps 2-3 are repeated, until the system is stable or a minimising condition is met.

Variations of this scheme also exist. In Kidson (2000) an iterative or agglomerative k-means was used. Whereby the closest

clusters are merged together and the process is repeated with $k-1$ clusters. Eventually this method will converge at 1 cluster.

2.2.2 *Self Organised Maps*

The use of Self Organised Maps (SOMs) is a relatively new occurrence for SC (Sheridan and Lee, 2011) and is similar to cluster analysis (Hewitson and Crane, 2002). SOMs attempt to locate nodes that are representative of the range of data, then distribute the nodes across the range. This generates a continuum of patterns which encompass the data series, with more maps or nodes being allocated to denser data regions and the corners of the SOM grid represent the furthest removed or extreme of the data (Hewitson and Crane, 2002; Sheridan and Lee, 2011). They are considered to be able to display the transitions between nodes better than other commonly used methods, such as PCA followed by a k-means clustering Sheridan and Lee (2011).

In the SH, Hope et al. (2006) studied Australian rainfall patterns in relation to changes in the circulation and a SOM approach was employed in this study. This work was further extended with the use of GCM output in Hope (2006). Jiang et al. (2013a) investigated air quality in Auckland with 25 maps devised using a SOM. The 25 maps were similar to previous work, such as (Kidson, 2000; Jiang, 2010), and were also useful in visualizing the westerly progression of the synoptic types. Jiang et al. (2013a) is the first synoptic climate SOM work for NZ, however further SOM schemes for NZ and the SH are currently being developed (pers.comm McDonald., 2014).

2.2.3 *Kidson Types*

In NZ, the work of John Kidson's KTs forms the de facto standard for synoptic classification work. Other SC schemes for NZ do exist, Jiang (2010) used NCEP/NCAR1 (NCEP1) output to de-

vise 12 synoptic types for NZ, using rotated PCA and k-means clustering, and these types were then used in a later study investigating inter-annual variability (Jiang et al., 2013b). The 12 types determined by Jiang (2010) are similar to the types previously determined by Kidson (2000).

The KTs are a widely used synoptic classification scheme for NZ comprising of twelve weather patterns which can also be grouped into three regimes. The KTs are the result of a series of work (Kidson, 1994a,b, 1997, 2000). The KTs have been used extensively in NZ and over a wide variety of research areas, ranging from riverflows, palaeoclimate, extreme weather and future weather (McKerchar et al., 2010; Ackerley et al., 2011; Griffiths, 2011; Parsons et al., 2014). Due to the continued use of the KTs the original results of Kidson (2000) were updated by Renwick (2011), thereby extending the KTs to mid 2010. The KTs as determined in Kidson (2000) are displayed Figure 2.1.

Due to the widespread use of the KTs they provide an ideal candidate for research into future weather patterns and climate variability for NZ, hence they are of great interest to this thesis and are used in Chapters 4 and 5.

The KTs have been connected to modes of inter annual variability, temperature and precipitation. Griffiths (2011) investigated extreme participation in NZ using the KTs. The TSW, TNW, and NE types were associated with increased precipitation events, however there are regional differences which are consistent with the effects of orography on circulation. The orographic result on precipitation is observed during the Zonal regime when there is a reduction in precipitation across NZ, apart from the west coast and the south of the south Island.

Renwick (2011) presented the following results using the Kidson Regimes in conjunction with daily observations from the virtual climate station network (VCSN) (Tait et al., 2006). During the Trough regime there is an increase in rainfall over the NZ, between 50-100% while the east coast of the North Island (NI) receives a slight increase in precipitation. A reduction in the max daily temperature is also observed in the West South

Island (WSI) region. The Zonal regime brings an increase in temperature in particularly East of the Southern Alpine range of 1-1.5°C, due to foehn. During Blocking Regimes there is an increase in mean temperature observed across NZ, apart from the eastern regions, East South Island (ESI) and East North Island (ENI), where it is reduced by -0.5°C and -0.5°C. Precipitation is also reduced during the Blocking regime in NZ, apart from ENI and the top of the NI. The observed regime affects on temperature and precipitation make "meteorological sense" when considering the circulation patterns and topography.

The KTs are formed by Principal Component Analysis (PCA) on 1000 hPa geopotential height field from NCEP1 reanalysis output between 1958-1997. An iterative k-means clustering scheme is then applied to the five leading principal components. The clustering process was initialised with 100 randomly seeded centres. Over multiple runs it converged to a common set of twelve clusters. These clusters are then used for the assigning process, which is based on minimum Euclidean distance to the clusters (Kidson, 2000).

The KTs domain is bounded by a latitude 25°S-55°S and longitude 160°E-175°W as seen in Figure 2.2 and encompasses NZ. The size of the domain was chosen to restrict the number of synoptic scale events, as opposed to a larger domain which could contain combinations of weather systems that would require a greater number of classes (Kidson, 2000). While the KT domain is defined and thereby constrained over NZ, the larger circulation is still important. This is evident in Chapter 5, Figure 5.4, where anomalies are apparent and interact well outside of the Kidson domain.

An outcome from chapter 4 highlighted a lack of sensitivity with the KTs. Additionally in Chapter 5 trends using the latest reanalysis data show that previous work may have overstated trends in KTs. This is due to the original methodology using NCEP1 reanalysis data, see section 3.1, as the earlier NCEP1 reanalysis has been proven to contain some spurious data in the SH and is influenced by suboptimal data coverage in the pre satellite era (Kanamitsu et al., 2002; Marshall, 2003). How-

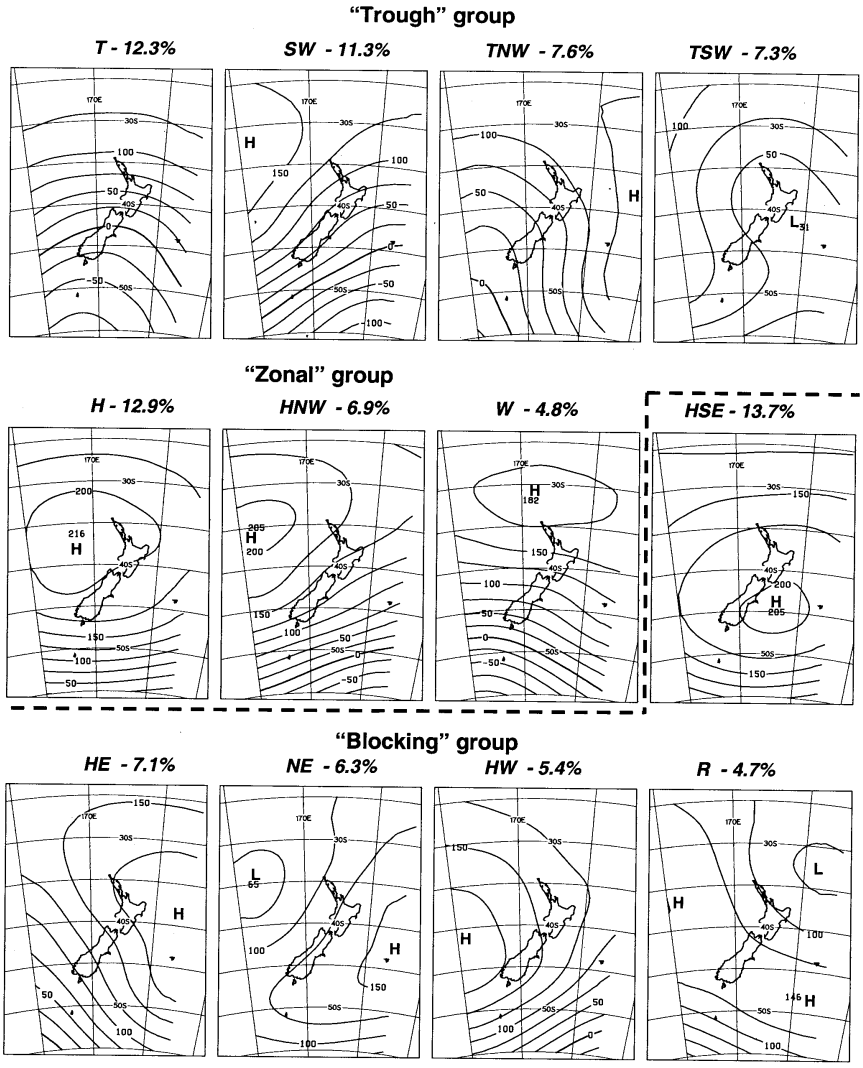

Figure 2.1: The Kidson Types. Each type is given a descriptive name, Trough (T), South Westerly (SW), Trough North West (TNW), Trough South West (TSW), High (H), High North West (HNW), Westerly (W), High South East (HSE), High East (HE), North Easterly (NE), High West (HW) and Ridge (R). The occurrence frequency (%). Reproduced from Kidson (2000)

ever, the KTs still provide utility in understanding and linking weather patterns to other phenomena (Renwick, 2011).

2.2.4 *Synoptic Climatology using GCM projections*

Synoptic climatology has experienced a resurgence with the increased availability of reanalysis data. This has continued as the availability and veracity of GCM output has improved. Since SC can provide a computationally inexpensive method to downscale GCM output (Sheridan and Lee, 2010). SC techniques have been applied to GCM output in a wide variety of locations in an effort to better understand the projected circulation changes under climate change and the local regional responses to these changes.

Schuenemann and Cassano (2009) and Schuenemann and Cassano (2010) investigated future Arctic synoptic circulation using SOMs and CMIP3 output. In the formation of the SOM centres the entire data set, reanalysis and model output, was used. This approach allows for the clustering to span the entire data range. Thus when comparing historical and future cluster frequencies, the bias from initial cluster formation is reduced.

Hope (2006), expanding on previous work detailed in Hope et al. (2006), used SOMs and CMIP3 GCMs output to investigate future precipitation patterns in Australia. Mahlstein and Knutti (2010) used a clustering scheme to determine distinct climate regions, as opposed to traditional national borders. Based on temperature and precipitation from an ensemble of 23 CMIP3 GCMs. Lee and Sheridan (2012) present a six step procedure, clustering and PCA, to assist in standardising the fragmented methodologies in use in synoptic climatology. Sheridan and Lee (2010) reviews the use of GCM output and SC and notes that often the rationale for GCM selection is often not stated or validated. See Section 3.2.1 for further discussion on GCM validation.

Chapter 4 investigates the KTs applied to CMIP3 output in detail.

2.3 SOUTHERN HEMISPHERE AND NEW ZEALAND

This section introduces modes of inter-annual variability, large scale features and other modes of climate variability relevant to the SH, the midlatitudes and NZ.

Figure 2.2 displays the annual average Mean Sea Level Pressure (MSLP) from the ERA Interim (ERA-I) reanalysis data set between 1979-2008. The geostrophic approximation indicates that the wind flows parallel to the isobars, thus the strong zonal flow of the westerlies is apparent with the lack of a significant land mass in the SH to act as a barrier (Mayewski et al., 2009). NZ is positioned between a belt of high pressure to the north and zonal flow to the south.

In order to understand weather patterns for NZ it is also necessary to consider the modes of inter-annual variability and how these modes are affected by climate change. Of particular interest to this research is the Southern Annular Mode (SAM) and El Niño - Southern Oscillation (ENSO), as these two modes can strongly influence NZ's weather and climate (Kidson and Renwick, 2002a; Sturman and Tapper, 2006; Kidston et al., 2009).

2.3.1 *New Zealand*

New Zealand (NZ) is situated in the midlatitudes between 35°-48°South, with two major land masses the NI and South Island (SI). The circumpolar westerly flow is the dominant meteorological feature of the SH and thus it significantly impacts NZ (Sturman and Tapper, 2006), as seen in Figure 2.2. This zonal circulation has a strong control on temperature of NZ, as it meanders in a more southerly or northerly direction (Trenberth, 1976; Dean and Stott, 2009). Inter-annual variability is also important to NZ. The NI is linked more to the tropical pacific and ENSO, while the SI to the midlatitudes and circumpolar circulation and SAM (Ummenhofer and England, 2007).

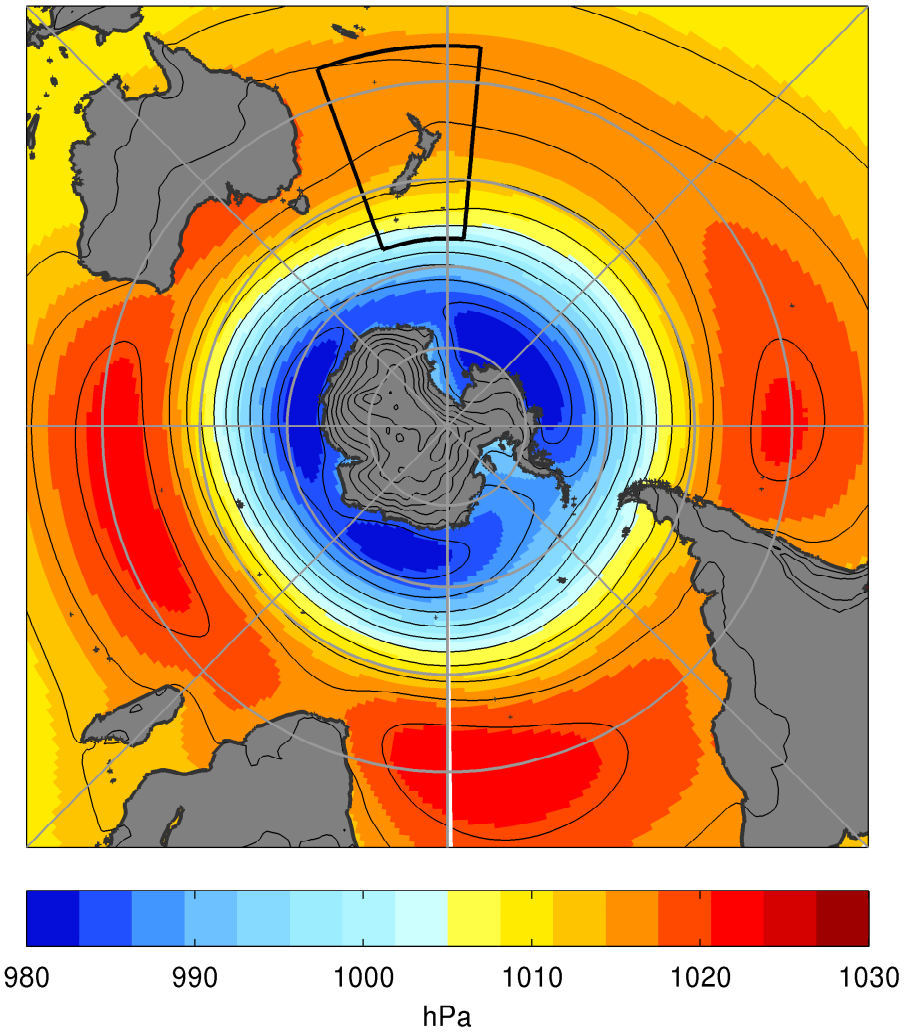

Figure 2.2: Southern Hemisphere mean MSLP. ERA-I 1979-2008. Contours are at 4 hPa. The Kidson domain is displayed over New Zealand.

In the midlatitudes weather is modulated by the passage of synoptic scale features, anticyclones and cyclones, imposed on the mean flow. Extra-tropical cyclones from the North and Tasman sea can impact the NI. However, there is still some influence of polar flows in the SI and tropical flows in the NI (Ackerley et al., 2012).

Regional differences in NZ's climate can be largely related to differences in topography. The Southern Alpine range runs the length of the SI, forming the only mountainous barrier at that latitude. Strong orographic precipitation is present on the West coast due to the predominant direction of flow and with less precipitation on the East coast. Elegantly summarised by Drost et al. (2007); "In a nut shell, New Zealand's climate is dominated by the ocean and the main regional differences are induced by the topography".

This is evident through the work of Mullan (1998) who determined six climate regions in NZ by subjectively categorising precipitation data using EOF analysis. Figure 2.3 displays the six regions and the rainfall station locations used in the analysis. The boundaries of the six climate regions reflect the main topographic features of the NI and SI. They are simply named in relation to the location of the region on the island, such as ENI. These regions have been utilised in other studies (Kidson, 2000; Kidson and Renwick, 2002a; Lorrey et al., 2007).

Due to the strong influence of topography on the climate in NZ, statistical downscaling of GCM output is an alternative to dynamical downscaling (Kidson and Thompson, 1998; Renwick et al., 2009).

Trenberth (1976) determined a series of indices based on pressure differences between stations to describe the meridional and zonal flows in the NZ and Australian region. The pressure difference between Hobart and the Chatham Islands is known as the M1 meridional index. The M1 is well correlated with NZ temperature trends (Salinger and Mullan, 1999). As previously mentioned the topography plays a very important part in the

local climate, in particular the orographic precipitation on the west coast of the SI, or the WSI district.

A detection and attribution study of the NZ temperature trend was conducted by Dean and Stott (2009), using GCM output with the intention of separating the trends into the natural and anthropogenic components. However, the GCM representation of the circulation was questionable.

Kidson and Thompson (1998) investigated the benefits of statistical and dynamical downscaling for NZ. The European Reanalysis 40 (ERA40) reanalysis provided the boundary conditions from 1980-1994. Statistical downscaling was undertaken using EOF and a regression analysis and dynamical downscaling conducted using the mesoscale model RAMS and compared to local station data. Statistical downscaling was more suited to continuous fields such as temperature than non continuous fields like precipitation (Kidson and Thompson, 1998). Similar results were obtained from both methods. However, the dynamical downscaling required a higher investment in computational resources than the statistical methodology, this was also noted in Renwick et al. (1998).

Dynamical downscaling of GCMs for NZ has also been undertaken. Renwick et al. (1998) noted an improvement in the skill of a higher resolution RCM (50km) nested within a GCM (125km). This was also noted in Drost et al. (2007), where a nested RCM was also used. The RCM used in Drost et al. (2007) had a 40km spatial resolution, this higher resolution assisted in accurately portraying the topography that heavily influences the observed climate in NZ.

2.3.2 *El Niño - Southern Oscillation*

The El Niño - Southern Oscillation (ENSO) is used to describe a coupled mode of variability, a Sea Surface Temperature (SST) anomaly and an atmospheric pressure oscillation. El Niño / La Niña is the phenomena associated with the SST component. El Niño is Spanish for the "little boy" and La Niña for "little girl".

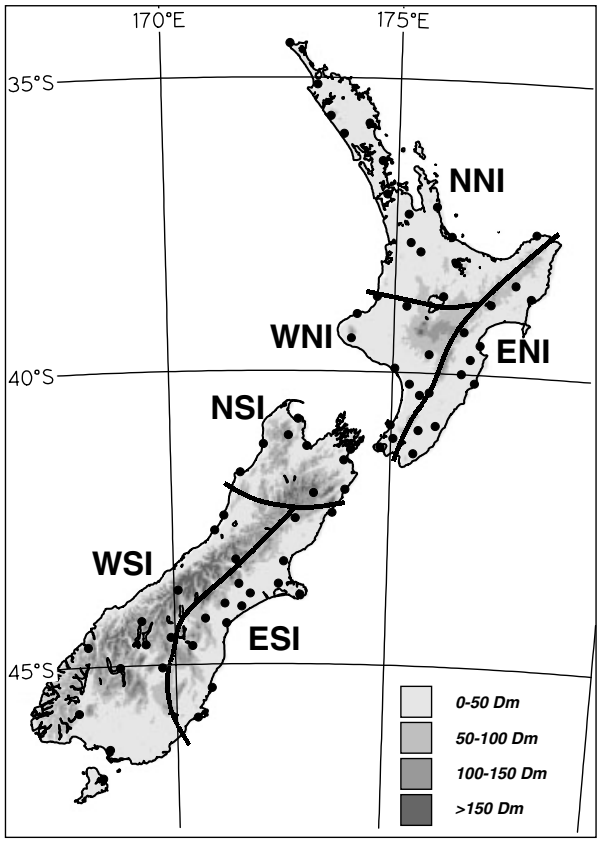

Figure 2.3: New Zealand Climate Regions. Each region is named after its location and Island, thus East South Island (ESI). The black dots represent the location of 78 climate stations from which the regions were formed. The shading represents the relief. Reproduced from Kidson and Renwick (2002a)

El Niño known as a 'warm event', with increased SST in the tropical eastern Pacific ocean. The atmospheric component is known as the Southern Oscillation. The pressure oscillation was first noted by Sir Gilbert Walker, in a series of work in the 1920s (Troup, 1965). The coupling of the SST and Southern Oscillation Index (SOI) was first linked together in the work of Bjerknes (1966).

The physical process of ENSO is as follows. The easterly tradewinds push the warm surface water to the west pacific, resulting in cold water upwelling in the east. This temperature gradient induces a pressure gradient that drives the trade winds is reinforced by the temperature gradient. However, during El Niño the trade winds are reduced as pressure rises in the west and the warm SST extends across the equatorial Pacific Ocean from the South American coast (McPhaden et al., 2006). The SOI describes a oscillating pressure between the Indian and Pacific Oceans it is based on observations of pressure data from stations at Darwin and Tahiti and correlates with the strength of the trade winds (McPhaden et al., 2006).

These coupled modes, El Niño and Southern Oscillation are highly negatively correlated with each other and generally occur on a 2 to 7 year time scale (McPhaden et al., 2006). A particularly strong El Niño event occurred in 1997-1998, this further encouraged interest in this mode of variability as the teleconnections from this event were observed across the globe (McPhaden et al., 2006). Statistically significant teleconnections have been determined between the SOI and the high latitudes of the SH (Turner, 2004).

There are several variations of the SOI, however they all prescribe the same phenomena. The Troup method, from Troup (1965), is used by the Australian Bureau of Meteorology and also in Chapter 5. The SOI is a normalised monthly pressure difference between Darwin and Tahiti, see equation 2.1. The factor of 10 is a standard convention. Figure 2.4 displays the SOI as calculated with the Troup method using ERA-I data for a period between 1979-2008.

$$\text{SOI} = 10\,\frac{\Delta_{TD} - \Delta_{TDavg}}{\sigma_{TDavg}} \tag{2.1}$$

where Δ_{TD} = monthly mean pressure difference between Tahit and Darwin
Δ_{TDavg} = climatological monthly mean of Δ_{TD} for that month
σ_{TDavg} = climatological standard deviation of Δ_{TD} for that month

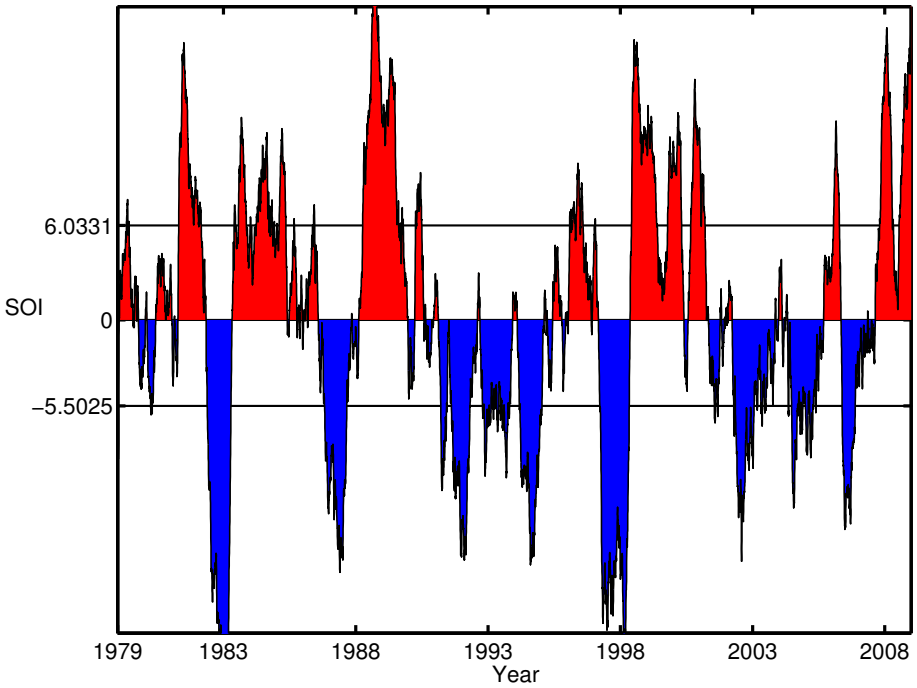

Figure 2.4: Southern Oscillation Index, generated using ERA-Interim 1979-2008. The SOI is unit-less index and the y axis values indicate the location of the upper and lower quartiles. The SOI+ La Niña (red) and SOI- El Niño (blue)

2.3.3 *Southern Annular Mode*

The Southern Annular Mode (SAM) is an annular structure and is the dominant mode of variability in the mid to high latitudes of the SH, with the austral summer showing the SAM strongest signals (Mayewski et al., 2009; Kidston et al., 2009; Fogt et al., 2012).

SAM has been trending to its positive phase, SAM+, and this has been linked to the Antarctic Ozone Hole (AOH) (Arblaster and Meehl, 2006; Thompson et al., 2011). A reduction of stratospheric ozone in the austral autumn and winter reduces the stratospheric temperature. This temperature reduction then causes a change in the geopotential height, which in turn causes a strengthening of the circumpolar flow (Thompson et al., 2011).

A variety of SAM indices exist, each derived using a different methodology. These different methods capture the same broad features of SAM and can be grouped into two approaches, PCA and pressure differences. Data is either sourced from observation stations or gridded model output. The advantage of the station data is the length of the climate record, as there are known "issues" with reanalysis products in the SH prior to the inclusion of satellite data in 1979 (Marshall, 2003; Ho et al., 2012), see Section 3.1.

Gong and Wang (1999) uses a normalised monthly zonal mean MSLP difference between latitude 40 & 65; Marshall (2003) uses the MSLP pressure differences from island stations situated close to the 45th & 65th parallels and the first PC of the 500 hPa geopotential data South of 20°from reanalyses is also used (Thompson and Wallace, 2000). An advantage of Marshall (2003) methodology is that it has a longer series of data that is based on surface station observations. However, as we are interested in future climate projections this study uses the method of Gong and Wang (1999), as this method utilises gridded surface data and thus is well suited to GCM output.

However, there are competing forcings, ozone and Green House Gases (GHGs). As the ozone depletion recovers GHGs are expected to continue to rise. Ozone is more important in the 20th century and GHGs will be more important than ozone by the middle of the 21st century, depending on future emissions (Son et al., 2010; Arblaster et al., 2011).

In the SH midlatitudes a positive phase of SAM+ is related to an increase in surface pressure in the region eastward of NZ

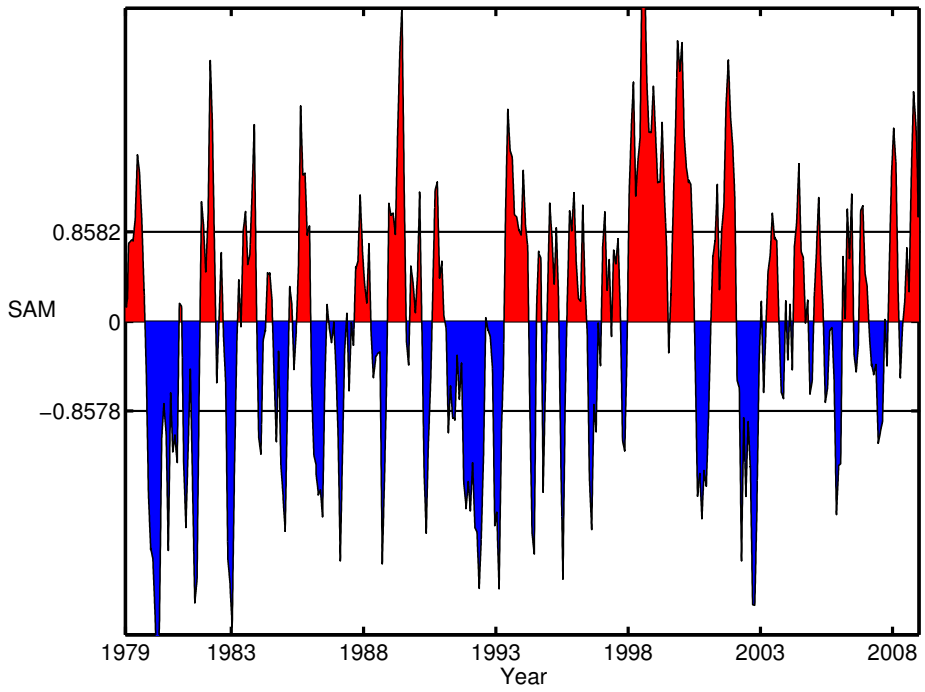

Figure 2.5: Southern Annular Mode, generated using ERA-Interim 1979-2008. The SAM is unit-less and the y axis values indicate the location of the upper and lower quartiles.

and a reduction in pressure over Antarctica (Gillett et al., 2006; Mayewski et al., 2009; Thompson et al., 2011).

2.3.4 *Influence of ENSO and SAM on New Zealand*

ENSO

NZ is almost equidistant from the Southern Oscillation centres of action at Darwin and Tahiti, thus the SOI is uncorrelated with the MSLP in NZ as the pressure fluctuates either side of NZ. However, there is enough of a pressure gradient to cause an anomalous flow in the region (Gordon, 1986). Thus, during Southern Oscillation Index Negative Phase (SOI-) there is an anomalous south westerly flow over NZ and an anomalous north easterly flow during Southern Oscillation Index Positive Phase (SOI+).

Kidson and Renwick (2002a) investigated ENSO in relation to NZ's weather. El Niño and La Niña periods were determined from a cluster analysis on satellite data of outgoing long wave radiation, centred in the tropics, based on previous work in (Kidson and Renwick, 2002b). Three clusters representing a strong El Niño , moderate El Niño and La Niña were investigated in conjunction with the NCEP1 reanalysis and NZ climate station data. During a strong El Niño an increase in westerlies is observed, which also corresponds to a increase in the KT Zonal regime and a reduction in the KT Blocking regime (Kidson and Renwick, 2002a). Using composite analysis the strong El Niño was associated with above normal temperatures and wetter conditions in the southwest and drier in the east. However, this was a short record and contained only two strong El Niño periods, 1982-83 and 1997-98.

Ummenhofer and England (2007) investigated precipitation in NZ with respect to inter-annual variability. Observational and model output was utilised, however due to GCM resolution NZ was partitioned into the NI and SI regions. The results were also tested using ERA40 and found to be consistent. The NI is influenced more by ENSO and the SI by SAM. During La Niña

the WSI experiences increased precipitation. Drier conditions occur in the NI and the top of the SI during El Niño , while increased precipitation occurs on the south western edge of the SI (Ummenhofer and England, 2007).

SAM

During SAM+ the increase in mid latitude surface pressure equates to a reduction in the intensity of the dominant westerly flow over NZ, which can be observed as easterly wind anomalies (Renwick and Thompson, 2006; Kidston et al., 2009). This change in the dominant wind circulation affects the amount of orographic precipitation generated, resulting in a reduction of precipitation on the West Coast of the SI and increased daily maximum temperature of up to 1.4°C in the WSI and west of the NI (Renwick and Thompson, 2006).

2.3.5 *Cyclones and Anticyclones*

Cyclones and anticyclones strongly influence weather in NZ and the midlatitudes (Trenberth and Mo, 1985; Sinclair, 1996). The first study of these migratory systems in the SH was by Taljaard (1967) using data gathered during the International Geophysical year of 1957-1958. Previous to this period, studies were limited in their spatial domain and more regional in nature (Jones and Simmonds, 1994).

There are two common methodologies that are applied to this problem, an Eulerian and Lagrangian approach. The Eulerian method applies a statistical analysis of baroclinic instability and is undertaken in an fixed region. This process follows the work of Blackmon (1976) and Wallace et al. (1988) and is commonly referred to as "storm track" analysis. The Lagrangian method determines and tracks individual cyclones or anticyclones, in the SH the work of (Murray and Simmonds, 1991; Sinclair, 1994; Hoskins and Hodges, 2005) is generally followed.

Substantial SH cyclone tracking research has also focused on cyclones and extra-tropical cyclones. Anticyclones (ACs) may be considered slow moving benign features when compared to cyclones they remain an important synoptic feature. ACs can be stable and long lived synoptic weather systems that can disrupt and block the passage of cyclonic systems (Sinclair, 1996). These long lived features and their extended persistence can exacerbate weather conditions, such as droughts and heatwaves (Barnes et al., 2012). However, studies of ACs utilising GCM projections in the SH are rare. For this reason and because of the importance of these features in the midlatitudes this topic is seen as a possible avenue for future work, see Section 7.1.2.

Tracking systems are well established as an objective tool and have replaced earlier subjective processing that involved labour intensive manual examination (Sinclair, 1996). Often the same core tracking methodology can be applied to cyclones and anticyclones, with changes in the subjective thresholds and parameters (Murray and Simmonds, 1991; Sinclair, 1994). These methodologies have been continually refined over time and subsequent publications (Murray and Simmonds, 1991; Sinclair, 1997).

In the SH cyclone tracking studies have been undertaken and climatologies established by Trenberth and Mo (1985); Murray and Simmonds (1991); Jones and Simmonds (1994); Sinclair (1994); Hoskins and Hodges (2005). However, some studies utilised earlier reanalysis data sets that have since been found to contain erroneous data, see section 3.1. Anticyclone climatologies in the SH have been determined by Jones and Simmonds (1994); Sinclair (1996); Pezza et al. (2007).

A poleward shift in cyclone activity was determined by Yin (2005), using a storm track approach using eddy kinetic energy from fifteen GCMs. Reduction in cyclone frequency but increase in intensity were identified.

Ulbrich et al. (2009) provides a comprehensive review on the cyclone tracking methods and their use with reanalysis and GCM output for the SH and NH. For the SH, a projected poleward shift

of storm tracks, resulting in less cyclonic activity at 50°S and increased at 60°S is indicated, this shift has also been the focus of other studies (Yin, 2005; Harvey et al., 2012). Another important finding from this review is that the diversity of methodologies employed in cyclone research has inhibited intercomparisons of these studies, thus the lack of intercomparative studies has impeded wider understanding of this important phenomena (Ulbrich et al., 2009).

Neu et al. (2012) compared 15 cyclone tracking schemes as part of the Inter comparison of Mid Latitude Storm Diagnostics (IMILAST) project. The schemes displayed similar performance when tracking well defined features. However, the subjective definitions and thresholds for events can lead to varied results. For example, the threshold for the start and end of a cyclone, genesis and lysis, which could lead to greater disparity between studies when determining the duration of events. Therefore care needs to be taken when comparing statistics between methodologies, especially genesis, lysis and density. While the migratory nature of synoptic activity affects local weather, the cyclonic systems are in turn affected by larger climatic modes of variability (Pezza et al., 2007).

A cyclone tracking scheme was developed during this thesis. Influenced by the work of Sinclair (1994, 1995, 1997) with the intention on expanding this work using GCM projections. However, it became apparent that the algorithm would be too slow for processing the quantity of GCM output required. This is seen as a possible avenue for further research, as mentioned in Section 7.1.2. Thus, an alternative Eulerian approach was used to investigate blocking.

2.3.6 *Blocking*

Blocking is a large scale phenomenon that can perturb the position of mean flow, storm tracks, cyclones and anticyclones in the midlatitudes (Trenberth and Mo, 1985; Kidson and Sinclair, 1995; Renwick, 2005). Blocking Events (BEs) are long lived sta-

tionary ACs. Various definitions and methodologies of determining blocking exist. This has sometimes impeded comparison between studies (Barriopedro et al., 2010b; Barnes et al., 2012). Early work by Rex (1950a,b) in the NH defined a BE when the mean flow was split by the BE, this has become known as the classic definition.

Blocking has been linked to extreme weather (Barnes et al., 2012; Dunn-Sigouin and Son, 2013). As BE are stable and long-lived and by their definition they can impede other synoptic systems. Fronts can be slowed, or stalled, thus increasing precipitation events or droughts can be exacerbated (Barnes et al., 2012). The location of BEs is also important, as the mean flow can be diverted and this can also modify precipitation patterns (Cowan et al., 2013).

Three common methodologies are used in blocking studies, these are indices, tracking and Persistent Positive Anomalies (PPAs). Indices determine events where the gradient or meridional flow in a fixed region becomes greater than a certain threshold (Tibaldi and Molteni, 1990). Tracking is a Lagrangian approach in which individual events are identifying and tracked (Sinclair, 1996). PPA which locates fixed anomalies above and longer than subjective thresholds (Renwick, 2005), this methodology is used in Chapter 6. All of these methods are objective, in that the algorithm can be automated for processing as opposed to subjective which require an operator.

Whilst blocking has been investigated, particularly in the NH, the underlying mechanisms are still not completely understood (Barnes et al., 2012; Cowan et al., 2013; Christensen et al., 2013). However, it has been suggested that BE reinforce themselves by absorbing smaller transient eddies (Yamazaki and Itoh, 2009). Additionally, GCM studies have under reported blocking (Palmer et al., 2008) which has been attributed to the coarse resolution of the GCM. Matsueda et al. (2009) investigated blocking frequency at three different GCM resolutions. The highest resolution, 20km, was best able to simulate the blocking frequencies observed in reanalysis output. It has been suggested that is due to the high resolution being able to model transient eddies that

are considered to play an important role in maintaining blocking events (Matsueda et al., 2009).

The majority of SH blocking studies have utilised reanalysis data and not GCM projections. BEs in the SH are also thought to be less persistent than the NH, due to the higher zonal wind speed (Trenberth and Mo, 1985; Kiladis and Mo, 1998). These studies have used different methodologies, thus comparison of results can be fraught with difficulty. However, there is a broad consensus in some results. For example the South Pacific Ocean (SPO), east of NZ, is a primary region of blocking activity in the SH and BEs occur mostly during winter (Trenberth and Mo, 1985; Kiladis and Mo, 1998; Sinclair, 1996; Renwick, 2005). Figure 2.6 displays the annual SH spatial patterns for the PPA, as determined by Renwick (2005), as discussed the majority of PPA are located in the SPO region.

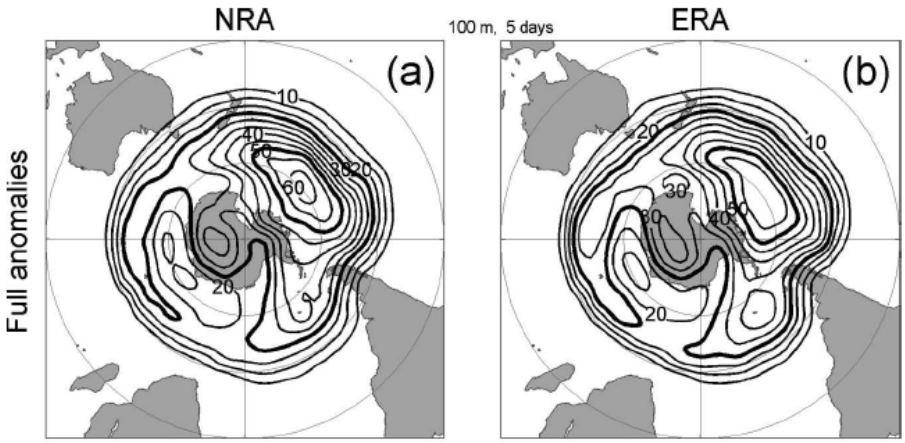

Figure 2.6: Long-term annual mean frequency (day yr) of PPA events of at least 100 m lasting at least 5 days: (a), (b) anomalies only from the seasonal cycle, and (left) Uses NRA fields (NCEP1), and (right) uses ERA. The contour interval is 5, starting at 10. The 25 and 50 contours are thickened. Figure and caption is sourced from Renwick (2005)

In the SH the Intergovernmental Panel on Climate Change (IPCC) AR5 report has stated, with medium confidence, that the SH blocking will not increase (Christensen et al., 2013). Chapter 6 expands on the work of Renwick (2005) with CMIP5 GCM out-

put, the intention of this work is to provide more confidence in the current understanding of SH blocking projections.

2.3.7 *Zonal Wave 3*

Zonal Wave 3 (ZW3) has been linked to BEs in the SH (Trenberth and Mo, 1985; Renwick, 2005; Berrisford et al., 2007). This is due to the breakdown of the zonal winds due to the ridges associated with the ZW3 pattern (Renwick and Revell, 1999). At 50°S zonal waves 1 and 3 account for 99% of the total variance in the annual mean 500 mb pattern (van Loon and Jenne, 1972). ZW3 has its maximum peak during winter (van Loon and Jenne, 1972).

Raphael (2004) determined a ZW3 index using three fixed locations, at 45-50°S and the longitudes 45-60°E, 161-171°E and 71-81°W. These areas are derived from work by van Loon and Jenne (1972) in which the ZW3 ridges were located. Raphael (2004) represented results based on the 500 gph level; however, the methodology can also be applied to MSLP level data because the surface and 500 gph level indices are well correlated ($r > 0.84$). The ZW3 index is the normalised average of the three locations, see Equation 2.2. A similar methodology to determine a ZW3 index was also used by Mo and White (1985) with three slightly different geographical locations.

$$
\begin{aligned}
I_i &= \frac{X_{mthly} - \bar{X}_{mthly}}{\sigma_{mthly}} \qquad (2.2)\\
I_{ZW3} &= \frac{I_1 + I_2 + I_3}{3}
\end{aligned}
$$

where I_{ZW3} = is the average of the three I_i values
X_{mthly} = three monthly value
$\bar{X}_{mthly}$ = climatological three monthly mean
σ_{mthly} = the standard deviation of the three monthly mean

A positive ZW3 corresponds to a strong meridional flow and the negative a stronger zonal flow. Thus BEs should be reduced during the negative phase of the ZW3 index. This methodology

is advantageous as it is a simple metric that can be easily understood and applied to data. However, due to the nature of the fixed locations this metric could be insensitive to a ZW3 phase change. Hobbs and Raphael (2010) used a Fourier transform instead of the Raphael (2004) ZW3 index, "because of its inability to separate the effects of strength and location." and the latitude band was north of the area of interest. The Fourier transform was applied along the longitudinal coordinate of the 500 hPa geopotential height for each month (Hobbs and Raphael, 2010). If further ZW3 and blocking studies are conducted the zonal wave methodology used in Hobbs and Raphael (2007) and Hobbs and Raphael (2010) would be applied.

3

DATA

The data used in the research is model output. This can be divided into two types; Reanalysis models and General Circulation Models (GCMs). During this work later generations of reanalyses and GCMs became available; with Chapter 4 using the earlier Coupled Model Inter-comparison Project (CMIP)3 GCMs and reanalysis; Chapter 5 uses both generations of reanalyses and Chapter 6 uses the later CMIP5 GCMs and the latest reanalysis. Due to the importance of these models this chapter is devoted to them.

3.1 REANALYSIS DATA

Retrospective analysis, or reanalysis, are data products based on previous observations. The reanalysis provides a baseline for climate research, they represent the previous state of the climate to the best of our knowledge and render a smoothed global gridded data set (Kalnay et al., 1996; Bromwich et al., 2007).

Numerical Weather Prediction (NWP) output, from weather forecasts, is not suitable for climate studies as the operational model undergoes regular improvements and changes to methodology, during the time span needed for climate studies (Compo et al., 2006; Bromwich et al., 2011). Reanalyses use a "frozen" system, with stable model and constant data assimilation methodology (Saha et al., 2010). However, changes to the observational net-

work during the reanalysis period can introduce bias, for example the inclusion of new satellite observations in a previous data sparse region such as the high latitudes of the Southern Hemisphere (SH) (Simmons et al., 2004; Bengtsson et al., 2004; Bromwich et al., 2011).

The reanalysis data are model output, from a model forced and constrained by assimilated observational data. The observations can be obtained from a variety of sources; satellites, radiosondes, ocean buoys and weather stations etc (Kistler et al., 2001). The observations are assimilated to provide regular nudging for the model. This assimilation is the essential difference between GCMs and reanalysis models.

Three Dimensional Variational Assimilation (3D-Var) is the process in which the data are assimilated and errors are minimised between the observations and reanalysis output. This is done in three dimensional space, hence 3D-Var. Four Dimensional Variational Assimilation (4D-Var) incorporates time as the fourth dimension (Dee et al., 2011). This allows for a forecasting diagnostic step within the model. A forecast is made and this is compared to the observations. This information is then used to nudge/constrain the previous state. However 4D-Var is computationally more expensive than 3D-Var (Uppala et al., 2005).

Since the reanalyses are based on observations the quality and quantity of observations will affect the ability of the reanalysis to reflect the current state (Kistler et al., 2001; Bengtsson et al., 2004; Simmons et al., 2004; Compo et al., 2006). The Northern Hemisphere (NH), with a higher population density and landmass has had the benefit of a denser observational network when compared to the SH. For example, the dearth of radiosonde observations in the SH is apparent in Figure 3.1, which displays the radiosonde network assimilated in 1979 for the European Reanalysis 40 (ERA40) reanalysis (Uppala et al., 2005). Figure 3.2 displays the amount of surface observations used in the Twentieth Century Reanalysis (20CR) (Compo et al., 2011). The NH has over 100 observations by 1900, however it is not until 1950 that the SH has 100 observations.

Thus prior to inclusion of satellite observations, circa 1979, the reanalysis products are considered less reliable in the SH (Renwick, 2004; Jones and Lister, 2007). Hence the later generation of reanalyses, such as NCEP/NCAR2 (NCEP2) and ERA Interim (ERA-I), both begin post satellite. The reanalyses products that are utilised in this thesis are detailed in Table 3.1.

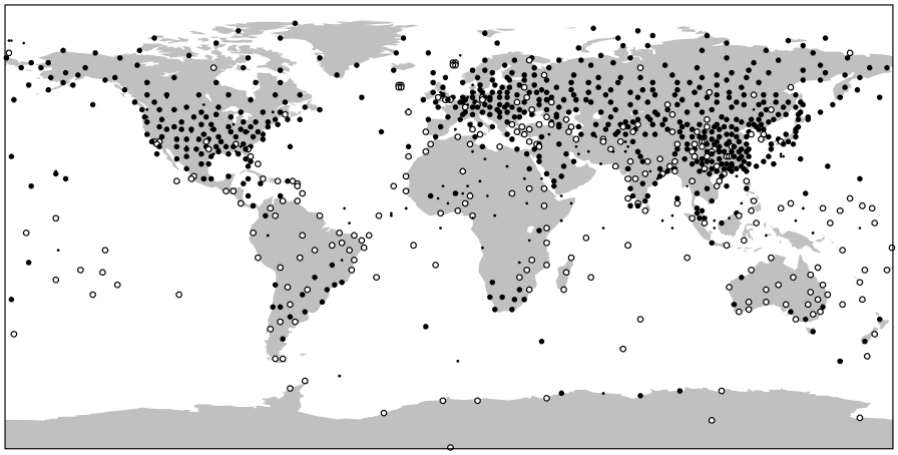

Figure 3.1: Frequency of radiosonde reports for 1979 utilised in ERA40. Solid circles denote stations from which at least three reports are available every 2 days on average, open circles denote other stations reporting at least once every 2 days, and small dots represent stations reporting at least once per week. Caption and Figure reproduced from Uppala et al. (2005)

Table 3.1: Reanalysis models used in this thesis

Name	Resolution	Period	Reference
NCEP/NCAR1	2.5°x 2.5°	1957-1996	Kalnay et al. (1996)
NCEP/NCAR2	2.5°x 2.5°	1979-present	Kanamitsu et al. (2002)
ERA40	2.5°x 2.5°	1957-2002	Uppala et al. (2005)
ERA Interim	0.5°x 0.5°	1979-present	Dee et al. (2011)
20Cth Reanalysis V2	2°x 2°	1871-2010	Compo et al. (2011)

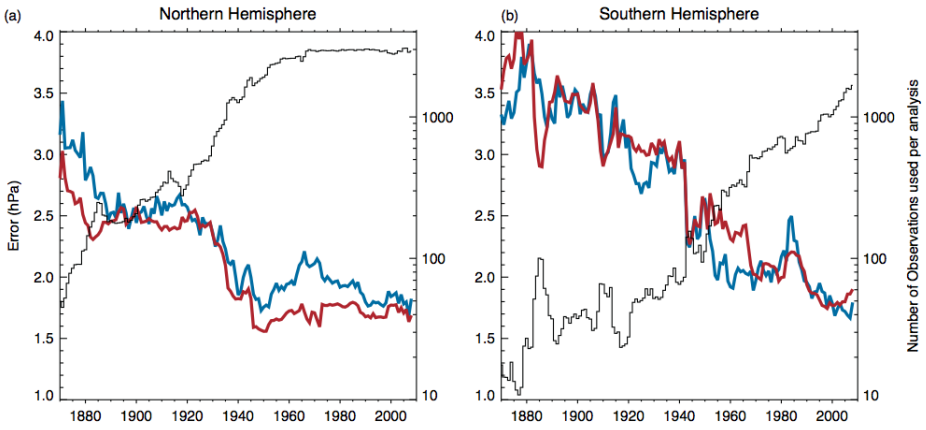

Figure 3.2: 20CR Time series of the 6 hourly first guess root mean square (r.m.s.) difference from pressure observations (blue) and expected r.m.s. difference (red) calculated over individual years from 1870 to 2008 for the extratropical (a) Northern Hemisphere (20°N 90°N) and (b) Southern Hemisphere (20°S 90°S). The square root is calculated on the annual mean square values. The thin black curve shows the average number of pressure observations for each analysis in the indicated year. Figure and caption reproduced from Compo et al. (2011)

NCEP/NCAR 1 and 2

NCEP/NCAR1 (NCEP1) has an initial 40 year period, starting in 1957, with the intention of continuing updates and extending the reanalysis back to 1948. However, between 1979-1992 some observations were incorrectly assimilated over the SH. Further analysis determined the SH mid and high latitudes were adversely affected, mostly at the surface level and during winter (Kidson, 1999). In particular, the Southern Annular Mode (SAM) is over represented in NCEP1 leading to a overly positive trend (Marshall, 2003).

NCEP/NCAR2 (NCEP2) is an incremental evolution from NCEP1. It therefore retains the same resolution and format, this is to enable easy integration and replacement of the previous NCEP1 (Kanamitsu et al., 2002). NCEP2 addresses the erroneous data assimilation that caused issues in the SH (Kistler et al., 2001). It also incorporates additional refinements in some parametrised processes, such as cloud and snow (Kanamitsu et al., 2002). NCEP2 starts from 1979, the satellite era, and continues to the present.

ERA40 and ERA-Interim

European Reanalysis 40 (ERA40) is a 45 year reanalysis data set from the European Centre for Medium-Range Weather Forecasts (ECMWF) from 1957-2002. It is a second generation reanalysis set and builds on the previous reanalysis, ERA15. 3D-Var is used instead of 4D-Var, due to the computationally expensive requirements of 4D-Var (Uppala et al., 2005).

ERA Interim (ERA-I) expands on ERA40, beginning from the post satellite era. Spatial and temporal resolution is increased to 6 hourly and 0.5°and 4D-Var is used. It is an intermediate product that address data assimilation problems that were encountered in ERA40, while also preparing for the next generation of ECMWF reanalysis (Dee et al., 2011).

Twentieth Century Reanalysis

The Twentieth Century Reanalysis (20CR) is a reanalysis data set based on surface observations only. There are no upper atmosphere measurements, such as radiosondes and satellites, assimilated into this data set and thus this avoids any discontinuity associated with the inclusion of changing observing technologies (Compo et al., 2011). The 20CR is the first reanalysis data set to extend back to 1871. The longer time series of the 20CR is also useful in the study of inter-annual variability. This data set is used extensively in Chapter 5. However, as seen in Figure 3.2, there is a lack of observations in the SH before the 1950s.

3.2 GENERAL CIRCULATION MODELS

As we are concerned with future weather patterns, an appropriate tool for this research is the use of General Circulation Models (GCMs). GCMs are in a constant state of evolution and refinement. The growth of computational power has allowed for increased resolution, spatial and temporal, and the inclusion of more complex processes that were previously empirical approximations (McGuffie and Henderson-Sellers, 2005). The GCMs are required to create multiple simulations, with and without anthropogenic forcing, pre-industrial control runs, twentieth century and future emission scenarios. A coarser spatial resolution is used due to the high computational requirements when compared to operational NWP models, due to the longer simulation time and amount of simulations. However, despite the increases in computer power, GCMs still require substantial investment in computational resources to provide capability for future modelling requirements (Shapiro et al., 2010).

To resolve smaller terrain features and local circulations that might impact regional climates a higher resolution model or statistical downscaling is necessary (Liang et al., 2008; Doherty et al., 2009; Flato et al., 2013). However, both of these methods

still require the boundary conditions to be supplied from a GCM. Thus, the ability of the GCM to accurately portray the observed climate is of critical importance (Flato et al., 2013).

The World Climate Research Project (WRCP) is an international body tasked with organising global climate research. A sub group the, Working Group on Coupled Modelling (WGCM), is responsible for the CMIP. The CMIP serves as a repository for the GCM output (Meehl et al., 2000). Two generations of model output are used in this research, CMIP3 (Meehl et al., 2007) and CMIP5 (Taylor et al., 2012). Whilst the CMIP archives provide a vast database of output, not all of the modeling groups provide a full complement of variable fields and time resolutions, this availability can also provide some limitations in GCMs selection.

The GCMs control runs are based on our understanding of the past and present climate, the scenarios and forcings that contribute to the future projections need to be based on some form of extrapolation of our current climate (Moss et al., 2010). In short what type of future will global society have? Will there be a reduction of emissions and if so how much? Shorter term, decadal (defined as 10-30 year), projections are also currently being investigated to address concerns from policy and decision makers (Doherty et al., 2009; Taylor et al., 2012). This method uses a GCM initialised from reanalysis output (Meehl et al., 2009).

The IPCC Fourth Assessment Report (AR4) adopted a qualitative description of the future with "storylines" and the IPCC Fifth Assessment Report (AR5) reverted to a physical quantity to explain possible scenarios, known as Representative Concentration Pathways (RCPs). In Chapter 4 the A1B and A2 scenarios are used and two RCPs are used in Chapter 6, RCP 8.5 and RCP 4.5. The discussion is limited to the forcing scenarios used in the research, firstly the AR4, then the AR5.

The Special Report on Emissions Scenarios (SRES) uses four "story lines" to describe the future environment in the AR4 (Nakicenovic et al., 2000). These story lines are qualitative descriptions that encompass the social, economic and political environ-

ment that contribute to the global emissions. With each story there is also a subset.

The A1 scenario describes a future world of rapid growth and global population peaking mid century then declining. There are 3 subsets within the A1 SRES which describe the energy use. The A1B is a "balanced" version of the A1 scenario, with energy supplied from fossil and non fossil sources. With the global sharing of new and efficient technology, the A1B is known as the "Star Trek Future". The A2 focusses on regional development, there is limited global sharing and take up of new technologies. This can be considered as " Business as usual" (Nakicenovic et al., 2000). In general the AR4 scenarios have been too conservative with current emissions exceeding the highest scenario, A2, and the B1 and B2 are now considered overly optimistic (Peters et al., 2013). Figure 3.3 displays the forcing of the SRES families.

The RCPs that are used in the AR5 and CMIP5 replace the SRES scenarios used in CMIP3 for two reasons.

1. The forcing scenarios need to be re-evaluated to address new concerns, changing global circumstances or questions that scientific advances have revealed (Moss et al., 2010; Peters et al., 2013), such as interest in near term or decadal studies, these also required new climate scenarios (Meehl et al., 2009).

2. By allowing climate studies to divorce themselves from the socio-economic storyline, they can concentrate on the science. "The radiative forcing trajectories are not associated with unique socio-economic or emissions scenarios, and instead can result from different combinations of economic, technological, demographic, policy and institutional futures." (Moss et al., 2010).

Figure 3.4 displays the relative forcing of the RCPs. The RCPs increase until 2050; then 2.6 deceases; 4.5 stabilizes; 6.0 and 8.5 continue to increase.

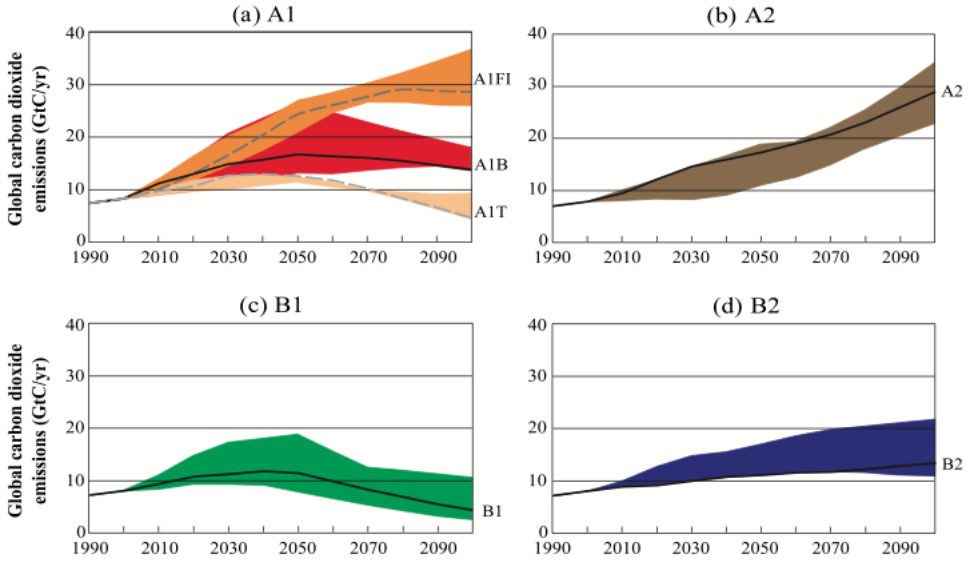

Figure 3.3: Total global annual CO_2 emissions from all sources (energy, industry, and land-use change) from 1990 to 2100 (in gigatonnes of carbon (GtC/yr)) for the four families (A1, A2, B1, and B2) and six scenario groups: the fossil-intensive A1FI (comprising the high-coal and high-oil-and-gas scenarios), the predominantly non-fossil fuel A1T, the balanced A1B in (a); A2 in (b); B1 in (c), and B2 in (d). Each coloured emission band shows the range of harmonized and non-harmonized scenarios within each group. For each of the six scenario groups an illustrative scenario is provided, including the four illustrative marker scenarios (A1, A2, B1, B2, solid lines) and two illustrative scenarios for A1FI and A1T (dashed lines). Figure and caption is reproduced from Nakicenovic et al. (2000)

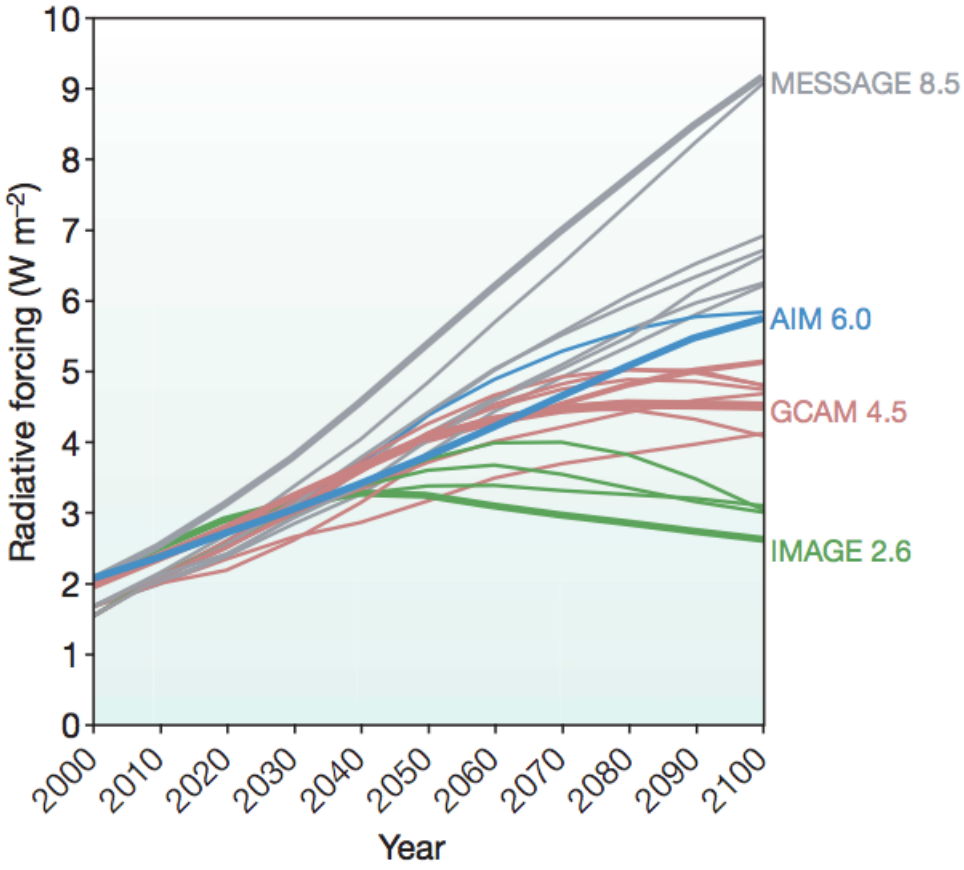

Figure 3.4: Representative concentration pathways. Changes in radiative forcing relative to pre-industrial conditions. Bold coloured lines show the four RCPs; thin lines show individual scenarios from other candidate RCP scenarios. Caption and Figure reproduced from Moss et al. (2010)

Table 3.2: Representative Concentration Pathways CMIP5, adapted from Moss et al. (2010)

	RCP 8.5	RCP 6.0	RCP 4.5	RCP 2.6
Radiative Forcing	$> 8.5 Wm^{-2}$ in 2100	$6 Wm^{-2}$ stablize 2100	$4.5 Wm^{-2}$ stablize 2100	$3 Wm^{-2}$ peak at 2100
Concentration (p.p.m)	1370 CO_2 in 2100	850 CO_2 stabilise 2100	650 CO_2 stabilise 2100	490 CO_2 peak at 2100
Pathway	Rising	stabilise at 2100	stabilise at 2100	Peak-Decline
RCP	MESSAGE 8.5	AIM 6.0	GCAM 4.5	IMAGE 2.6

3.2.1 *GCM Validation*

Rarely is a single GCM used in climate studies, instead ensembles of GCM output are used. Thus the internal variability in one GCM realization can be countered by the different GCMs members of the ensemble. The ensemble of GCMs often performing better than a single GCM, when considering multiple variables (Tebaldi and Knutti, 2007; Knutti et al., 2010).

As GCMs are diverse and developed by different modelling groups around the world. They have different parametrisations, resolutions and internal variability and therefore provide different projections from the same forcing. Whilst GCMs are improving, there are areas that require further work.

1. The westerly winds in the SH are positioned too far North (Mullan and Dean, 2009; Kidston and Gerber, 2010; Swart and Fyfe, 2012).
2. The ability of some GCMs to accurately display Antarctica sea ice is questionable (Ainley et al., 2010; Mahlstein et al., 2013; Turner et al., 2013).
3. Inter-annual variability, El Niño - Southern Oscillation (ENSO) simulation (Jin et al., 2008; Collins et al., 2010; Stevenson, 2012).

Some GCMs perform better in certain environments. Thus it can be desirable to use a smaller selection of better performing GCMs for the study in question. A multitude of parameters can be used in this selection process.

For example, Ainley et al. (2010) required a reliable Antarctic climatology, particularly variables relating to sea ice extent. They were concerned at the ability of GCMs to accurately portray the present (observational record). Therefore, they refined the model selection from the 18 available GCMs to 4. The first order of selection was a comparison between the pre-industrial westerly winds and the strength of the Antarctic Circumpolar Current (ACC). Then the location of westerly winds and sea ice extent. There was considerable variability in the models with regards to the sea ice extent, these models were then excluded. Lastly the model selection process compared the boundaries

of the ACC and annual sea ice thickness to the observational record.

An integrated metric, whereby if the model in question can achieve a realistic distribution of circulation patterns can be used as a guide in model selection. Synoptic Climatology (SC) provides one such measure and has been used in this capacity. Using Self Organised Maps (SOMs) Schuenemann and Cassano (2010) selected 3 GCMs from 17 for their investigation in projected circulation changes regarding precipitation in the Arctic region. Anagnostopoulou et al. (2009) used Principal Component Analysis (PCA) to validate a GCMs ability to recreate circulation patterns in the Mediterranean Basin. Thus, SC methods are an established methodology of GCM validation. In Chapter 4 the SC Kidson Type (KT) methodology is used to select the five highest performing GCMs from fifteen.

For New Zealand (NZ) Mullan and Dean (2009) investigated AR4 GCMs in regards to their ability to replicate the observed SH climate and other meteorological indicators that are important for NZ, such as the location of the Westerly wind. A 30 year period, 1971-2000, of monthly output from 17 GCMs using the CMIP3 20C3M control run was tested against 62 performance indicators. The highest performing was a 12 model average, followed by a 17 model average. Thus the smaller ensemble, with the worst performing members removed was ranked higher than any single model. However, there are some distinct shortcomings as none of the models accurately positioned the westerly wind maximum in the NZ region between the longitudes of 160°- 190°.

3.3 SUMMARY

The lack of observational data and some erroneous assimilation issues in the SH has impeded the quality of the earlier reanalysis data, in particular NCEP1. The inclusion of satellite data since 1979 has somewhat alleviated this concern. Thus it is advisable to avoid the earlier generation of reanalysis where possible.

GCM validation is required when engaging in climate projections. This is applicable to both statistical and dynamical downscaling. The quality of the reanalyses and the ability of GCM control runs to accurately portray the observed climate are important in order for confidence to be obtained for future climate projections. Smaller ensembles can be beneficial in downscaling by reducing the variability within the ensemble. However, it is important to establish a justifiable methodology for the selection of the GCMs employed in a reduced ensemble.

4

THE USE OF SYNOPTIC CLIMATOLOGY WITH GENERAL CIRCULATION MODEL OUTPUT OVER NEW ZEALAND

4.1 ABSTRACT

A cluster analysis-based synoptic classification scheme, known as the Kidson Types (KTs), was applied to reanalyses and CMIP3 General Circulation Model (GCM) output over New Zealand to identify the potential for future changes in regional circulation. Results indicate that a number of GCM 20th century control runs reproduce the type frequencies observed in reanalysis data. Application to future scenario runs for the periods 2046-2065 and 2081-2100 display little variation in the annual frequency of the synoptic types relative to the 20th century, especially when uncertainty associated with the model ensemble is considered. This is surprising in the context of previous work on possible future movements in jet position and subsequent impacts on weather patterns. A sensitivity analysis that mimics the movement of the jet position was performed, revealing that the annual type frequencies are relatively insensitive to change. To determine whether this is a problem with the synoptic typing scheme, a correlation-based classification technique was also used, but showed similar results. This work highlights issues with applying synoptic classification schemes to GCM output and indicates that if such schemes are to be used they should be designed and tested with this application in mind.

4.2 INTRODUCTION

Understanding climate change and variability at a regional level is a significant challenge, highlighted by the Intergovernmental Panel on Climate Change (IPCC) IPCC Fourth Assessment Report (AR4) as an area of research that urgently requires further investigation (IPCC, 2007; Doherty et al., 2009). In particular, the ramifications of regional climate change need to be better understood to inform policy decisions (Doherty et al., 2009). The large uncertainties associated with regional climate predictions also need to be reduced where possible and the local effects of climate change need to be quantified (Hawkins and Sutton, 2009). One approach to this problem is through synoptic classification.

Synoptic classification systems group similar synoptic situations together in an effort to reduce complexity, while potentially providing a useful proxy that can help to interpret climatic variability at regional scales (Yarnal, 1993). Synoptic Climatology (SC) can also provide a methodology to relate large-scale circulation to changes in the frequency of particular weather patterns. The application of synoptic classification schemes to General Circulation Model (GCM) output therefore offers a useful and intuitive way of identifying climate change variations, particularly circulation changes.

Synoptic classification methods can be divided into two main categories, subjective and objective. Subjective techniques require an"operator" to manually decide each pattern's class, while objective schemes use a set of mathematical rules and defined limits, hence can be automated. Most methodologies still retain a subjective component, such as the number of classes selected and domain size, but are identified as objective (Huth et al., 2008).

Synoptic classification evolved from early weather forecasting techniques, and was originally envisioned as a method of providing extended forecasts (Barry and Perry, 1973). It has undergone a resurgence of interest in recent years due to the avail-

ability of high quality reanalysis data sets, increased computational power and the need to gain a better understanding of regional climate change (Huth et al., 2008). Classifications have generally been undertaken independently in different regions, hence there is little standardization between studies. For example the Hess-Brezowsky classification was developed for Germany (Huth et al., 2008), the Lamb catalogue for the British Isles, and a Self Organised Map (SOM) scheme has been used in Australia (Hope et al., 2006; Hope, 2006). In New Zealand (NZ), the work of Kidson (2000) has defined the most widely used synoptic classification scheme, but alternative schemes such as Jiang et al. (2004) and Jiang (2010) also exist.

One of the few comparisons of classification systems is that of Huth et al. (2008) which provides a comprehensive review, focused on Europe. Philipp et al. (2010) discusses 17 different classification systems devised for Europe as part of the"Harmonisation and Applications of Weather Type Classification for European regions" project. One finding was that for objective classification systems the data pre-processing and distance metric used is as important as the algorithm used in determining each type. Studies have suggested that the output from GCMs can be used for synoptic classification McKendry et al. (2006); Anagnostopoulou et al. (2009), however additional caution has been strongly recommended (Huth, 2000; Sheridan and Lee, 2010). Care is required due to the varied response and biases of different GCMs in different regions, which means that appropriate GCMs for the study region must be selected. Schuenemann and Cassano (2010) used GCM output and SOMs to investigate weather patterns and precipitation over Greenland and their methodology incorporated the GCM output into the initial training of the SOM, which produced positive results.

For NZ, the ability of GCMs to recreate current regional circulation patterns is sometimes questionable, as highlighted in Drost et al. (2007) when using a nested Regional Climate Model (RCM). Work detailed in Mullan and Dean (2009) also indicates weaknesses in model output, for example the modelled westerly wind maximum is biased equatorward; a bias that affects

modelled regional precipitation over NZ (Sturman and Tapper, 2006). Mullan and Dean (2009) investigated a selection of 18 GCMs using a variety of parameters, and identified a preferred ensemble of twelve GCMs. Later in this study we will utilize a subset of GCMs, which correspond to the better performing models identified in Mullan and Dean (2009).

As previously indicated, the work of Kidson (2000) forms the basis of most of the synoptic classification work in NZ in recent years, although related methodologies have been explored (Jiang et al., 2004; Jiang, 2010). The Kidson Types (KTs) stem from a series of studies (Kidson, 1994a,b, 1997) culminating in Kidson (2000), which identified twelve prevalent patterns in the 1000 hPa geopotential height field. These studies explored a variety of classification procedures and weather patterns in the NZ region. In particular, Kidson (1997) investigated the use of combining upper level (500 hPa) and surface level data in a classification scheme. Incorporation of these two levels would be desirable as both levels provide complementary information. The upper level flow can provide information on development and steering of the lower level systems. The lower level is strongly linked to surface weather and is the most commonly used field for depiction of weather forecasts. The interaction of the near-surface flow with topography can provide information on orographic precipitation. However, implementation is difficult due to the large amount of possible combinations of classes (Kidson, 1997). The KTs have become widespread in research focussed on NZ, (McKerchar et al., 2010; Griffiths, 2011; Renwick, 2011), including paleoclimate research (Lorrey et al., 2007; Ackerley et al., 2011). In addition, the use of the classification scheme detailed in Kidson (2000), also has similarities to a number of other schemes, such as McKendry et al. (2006), Jiang (2010) and Coggins et al. (2013).

Here, Kidson's synoptic classification scheme is applied to GCM output to examine changes in the occurrence frequency of the different types to identify future circulation changes over NZ. The GCM output used is from the Coupled Model Inter-comparison Project 3 (CMIP3) experiments reported in the IPCC AR4 (IPCC,

2007). We consider the 20th Century control run (20C3M), plus SRES (Nakicenovic et al., 2000) A1B (medium emission) and A2 (high emission) forcing scenarios in our analysis.

4.3 METHODOLOGY

Synoptic classification systems attempt to reduce the complexity of data by partitioning into representative groups or discrete types. Ideally, the process used minimizes the difference within each type while maximizing the difference between types. The resulting types should be clearly defined and connected to distinct anomaly patterns in surface climate variables, such as temperature and precipitation. Huth et al. (2008) and Sheridan and Lee (2010) indicate that the initial decisions in forming the groups can strongly influence any outcomes and the process needs to be robust and well documented. Care must be taken when performing this form of analysis as too much simplification can reduce its value Cuell and Bonsal (2009); Sheridan and Lee (2010).

This study applies the Kidson (2000) typing methodology to daily Mean Sea Level Pressure (MSLP) reanalysis and GCM model output. It is based on a k-means clustering using the normalised principal components of the first five empirical orthogonal functions (EOFs) of the 1000 hPa field over NZ.

4.3.1 *Data Sources*

Reanalysis data in the period 1981-2000 are used, to match the period of the GCM 20C3M output. Reanalyses are sourced from the NCEP/NCAR2 (Kanamitsu et al., 2002) and ERA40 (Uppala et al., 2005) reanalyses projects. In future work, this analysis will be extended to incorporate ERA-Interim and CMIP5 output. The Kidson types were originally determined using NCEP/NCAR1 (Kalnay et al., 1996) data during 1958-1997 (Kidson, 2000) and this period is also analysed to show consistency

between the reanalysis at later dates and the period used in the earlier work.

We also use climate model output from the World Climate Research Programs (WCRPs) CMIP3 data collection, the availability of daily MSLP data and studies of model quality define the model ensemble used in this study (see details in Table 4.2). Where multiple realisations of a particular scenario are available from a specific model we use the first run.

4.3.2 *Kidson Types*

The methodology employed in Kidson (2000) to define synoptic types uses Principal Component Analysis (PCA) and an iterative k-means clustering process. Further information on PCA in climatology can be found in Preisendorfer (1988); Yarnal (1993) and Yarnal et al. (2001) and MacQueen (1967) for k-means clustering. Kidson's methodology is well presented and developed over a series of papers, (Kidson, 1994a,b, 1997), culminating in Kidson (2000), on which this study is based. The region examined is a domain of latitude 25°- 55°South and longitude 160°East - 175°West. Kidson (2000) used twelve-hourly 1000 hPa geopotential height anomalies from the NCEP/NCAR1 reanalysis data set (Kalnay et al., 1996), taking anomalies defined by removing the overall mean of the data set but retaining the seasonal cycle. PCA (S-mode) was performed on the anomalies and the first 5 PCs were retained and normalised for input into an iterative k-means clustering process. This clustering was run many times, initialised each time with a different set of 100 random seeds and each map assigned to a cluster. At each step the two closest clusters are merged and the assignment process repeated, this process continues until a single cluster remains. A set of 12 stable clusters was selected in Kidson (2000) and Figure 4.1 shows the mean MSLP field for each of the twelve Kidson types. The 12 types are also grouped into 3 regimes, Trough, Zonal and Blocking, these regimes are shown in Table 4.1. The type associated with a particular set of observations is derived

by calculating the Euclidean distance between the normalized PCs associated with that day and the twelve cluster centres and assigned to a particular type based on the minimum Euclidean distance.

In this study, we use the cluster centres and EOFs determined by Kidson (2000). We project MSLP anomalies, determined by removing the 20-year linear trend of each data set, onto the five EOF patterns from Kidson (2000) to determine the weightings for comparison with the cluster centres. The substitution of MSLP instead of geopotential height does not materially affect the result. We then use the minimum Euclidian distance to determine each daily type, the root-mean squared difference is calculated between the five cluster mean centres and the matching weightings derived from projecting the MSLP anomalies onto the Kidson EOF patterns. We use the 1981-2000 period as our historical average (20C3M). When applying this methodology to GCM output bi-linear interpolation to the common 2.5°grid over NZ was required.

4.3.3 *Lund Map Classification*

A second synoptic classification system is used to compare the results derived from the Kidson scheme. Here, the methodology of Lund (1963) is used, because this scheme was elegant in concept and implementation. The Lund Map Classification (LMC) technique uses the correlation between maps as the classifier and thus provides a quite different methodology to that detailed in Kidson (2000). The scheme is comprised of the following steps.

1. Each anomaly map in the time series (of length i) is cross correlated with all the other maps, resulting in an i x i matrix of correlations, with a self correlation of 1 on the diagonal. The map with the highest number of correlations above a predefined threshold (we use 0.8), becomes type 1. Each map associated with this type is then assigned and removed from the data set. This process is repeated until twelve types are assigned,

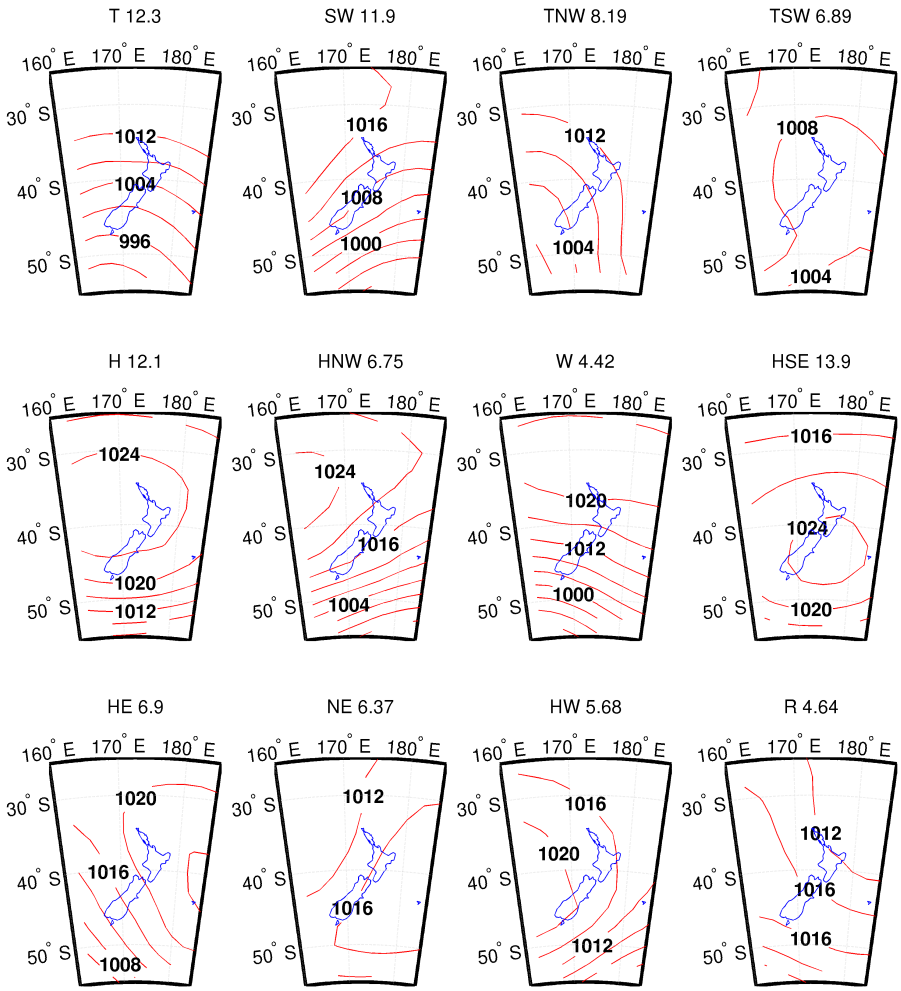

Figure 4.1: The twelve Kidson types and frequency of occurrence generated using the mean MSLP of each type population from the 1981-2000 NCEP/NCAR2. Types are given descriptive names, as determined by Kidson (2000), Trough (T), South Westerly (SW), Trough North West (TNW), Trough South West (TSW), High (H), High North West (HNW), Westerly (W), High South East (HSE), High East (HE), North Easterly (NE), High West (HW) and Ridge (R). The occurrence frequency (%) of each type when applied to the 1981-2000 NCEP/NCAR2 MSLP is also identified in the figure.

this number was selected to allow direct comparability with the Kidson types. Due to the high correlation threshold used, some of the MSLP patterns will remain unclassified. The mean MSLP for each type is then determined.

2. The entire data set is then correlated with the twelve patterns generated in the previous step and each daily MSLP pattern is assigned to one of the twelve representative patterns based on this correlation. The mean MSLP pattern and frequency of occurrence is then generated from this population. Figure 4.2 displays the twelve types identified by the LMC method.

These twelve MSLP patterns are then correlated with the GCM data, as in step 2, to confirm and test the sensitivity of the second synoptic classification scheme. In determining the LMC types a range of correlations were trialed, 0.4 to 0.95, in 0.05 increments, with 0.8 being the final selection. Increasing the correlation threshold results in an increased number of unclassified patterns. However, with a low correlation threshold, the first type is correlated with the majority of the data, resulting in an unbalanced system, with one type having the majority of members and fewer unclassified patterns. The correlation threshold used and number of types is a subjective decision, which we make based on data exploration and uniformity with the twelve KTs.

4.3.4 *Intercomparsion*

To compare results between the GCMs and reanalysis we use the root mean squared difference (RMSD) calculated between the annual frequency of occurrence of each synoptic type as a metric of their similarity. The five 20C3M GCMs with the lowest RMSD values and with data availability across all scenarios and time frames are then selected for later use. The SRES 20C3M (top five) type frequencies are used as a baseline for testing the future A1B and A2 scenarios. We are concerned with the difference in type frequency between each model's 20C3M run and its future scenarios.

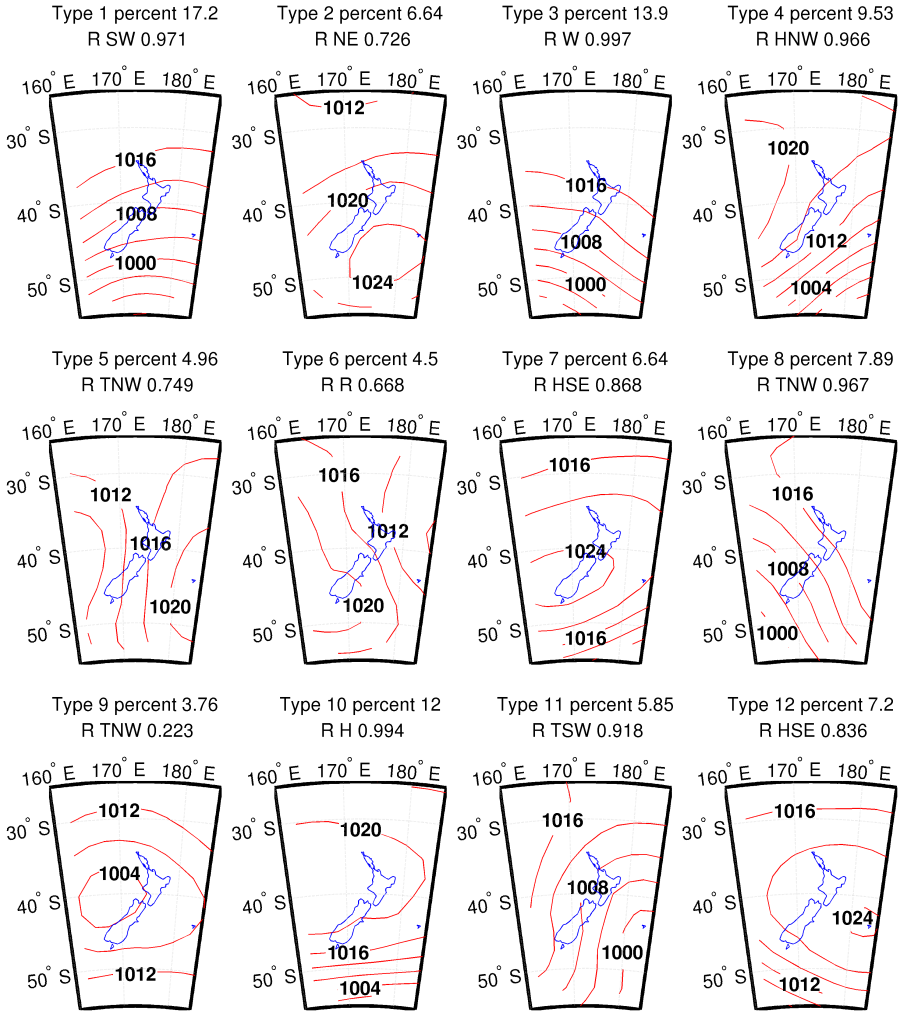

Figure 4.2: The generated mean MSLP map patterns using the LMC synoptic classification methodology and the frequency of occurrence, with a threshold correlation of 0.8. Many of the patterns also resemble the Kidson types. The highest Kidson type and correlation are also shown.

Table 4.1: Reanalysis data type frequencies using MSLP from 1981-2000, NCEP/NCAR2 and ERA40. H1000 is the 1000 hPa geopotential height NCEP/NCAR from 1958-1997 data. The RMSD uses Kidson (2000) as a base.

Frequencies, annual percentage of occurrence (%)					
Regime	Type	Kidson(2000)	H1000	ERA40	NCEP/NCAR2
Trough	T	12.3	12.3	12.0	12.4
	SW	11.3	11.2	12.4	11.9
	TNW	7.6	7.6	8.4	8.20
	TSW	7.3	7.3	6.5	6.9
Zonal	H	12.9	12.8	11.7	12.1
	HNW	6.9	6.9	6.9	6.8
	W	4.8	4.9	4.4	4.4
Blocking	HSE	13.7	13.7	13.5	13.9
	HE	7.1	7.1	7.3	6.9
	NE	6.3	6.2	6.4	6.4
	HW	5.4	5.3	5.7	5.7
	R	4.7	4.7	4.7	4.6
	RMSD	0	0.07	0.60	0.40

4.4 RESULTS

The occurrence frequencies of the synoptic types for the different reanalyses are displayed in Table 4.1. Comparison of these frequencies with those in Kidson (2000) show very similar type frequencies independent of the reanalysis used, and demonstrates that substituting MSLP for 1000hPa height does not bias our results.

As expected the 1000 hPa geopotential height has the lowest RMSD value relative to Kidson (2000), since it closely resembles the data set used in Kidson (2000). However, as we are con-

cerned with future scenarios our results use the MSLP daily data sets for comparison with the GCMs from this point on, since this field was more readily available at daily resolution. To examine the reproduction of the frequencies of the synoptic scale patterns over NZ in the GCMs, the daily MSLP output from each model over a 20-year period representative of the late 20th century are classified and then ranked using the RMSD metric (see Table 4.2. The calculation of the GCM RMSD uses frequencies derived from the NCEP/NCAR2 reanalysis 1981-2000 daily MSLP as the reference value.

The models are also compared against the ERA40 frequencies using the RMSD metric. Comparison between the GCM ordering using the RMSD derived from NCEP/NCAR2 and the ERA40 data shows only two shifts in ordering demonstrating the robustness of this measure (Table 4.2). Table 4.2 shows an analysis for the 20C3M GCM runs against reanalysis datasets, which shows general agreement with the Kidson values. The NCEP/NCAR2 and ERA40 reanalysis and top five GCM 20C3m Kidson type frequencies are shown in Figure 4.3. The largest occurrence types in the reanalysis data are also the most frequently occurring types in the 20C3M runs. Therefore, the models seem to be able to represent similar patterns to the reanalysis in the reference period. The results in Figure 4.3 and Table 4.2 broadly agree with the assessment of model performance detailed in Mullan and Dean (2009).

As we are concerned with the GCMs portrayal of the change between the present (20C3M) and future climates (A1B, A2), the reanalysis is used as a guide for selecting the most representative GCMs. Overall, the analysis detailed in this section highlights that the AR4 models selected for examination in this study are capable of simulating the MSLP field over NZ and reproducing Kidson type frequencies similar to those derived from reanalysis.

To examine the relative change in circulation we compare the frequencies derived from the A1B and A2 scenarios with those from the model's control run (20C3M). Figures 4.4 and 4.5 show the frequency anomaly between the A1B and A2 scenarios de-

Table 4.2: GCM type frequencies for the 20C3M control simulations, ranked against NCEP/NCAR2 by using the RMSD values. ERA40 RMSD values are also shown. The selected (Y) models have data availability across all of the time ranges, scenarios and are used as the top five.

Model	NCEP (RSMD)	ERA (RSMD)	Selected
giss er	0.66	0.82	Y
miroc32 hi res	0.87	1.09	
iap fgoals 10g	0.96	1.09	
mri cgcm	1.05	1.23	Y
csiro mk35	1.21	1.29	Y
ncar ccsm3.0	1.22	1.39	Y
mpi echam5	1.29	1.51	
ingv echam4	1.40	1.42	Y
gfdl cm21	1.42	1.57	
cccma cgcm31	1.43	1.61	
miroc32 medres	1.54	1.77	
ipsl cm4	1.55	1.63	
giss aom	1.75	1.84	
cnrm cm3	2.22	2.32	
bccr bcm20	2.30	2.41	
Top Five GCM	0.74	0.96	

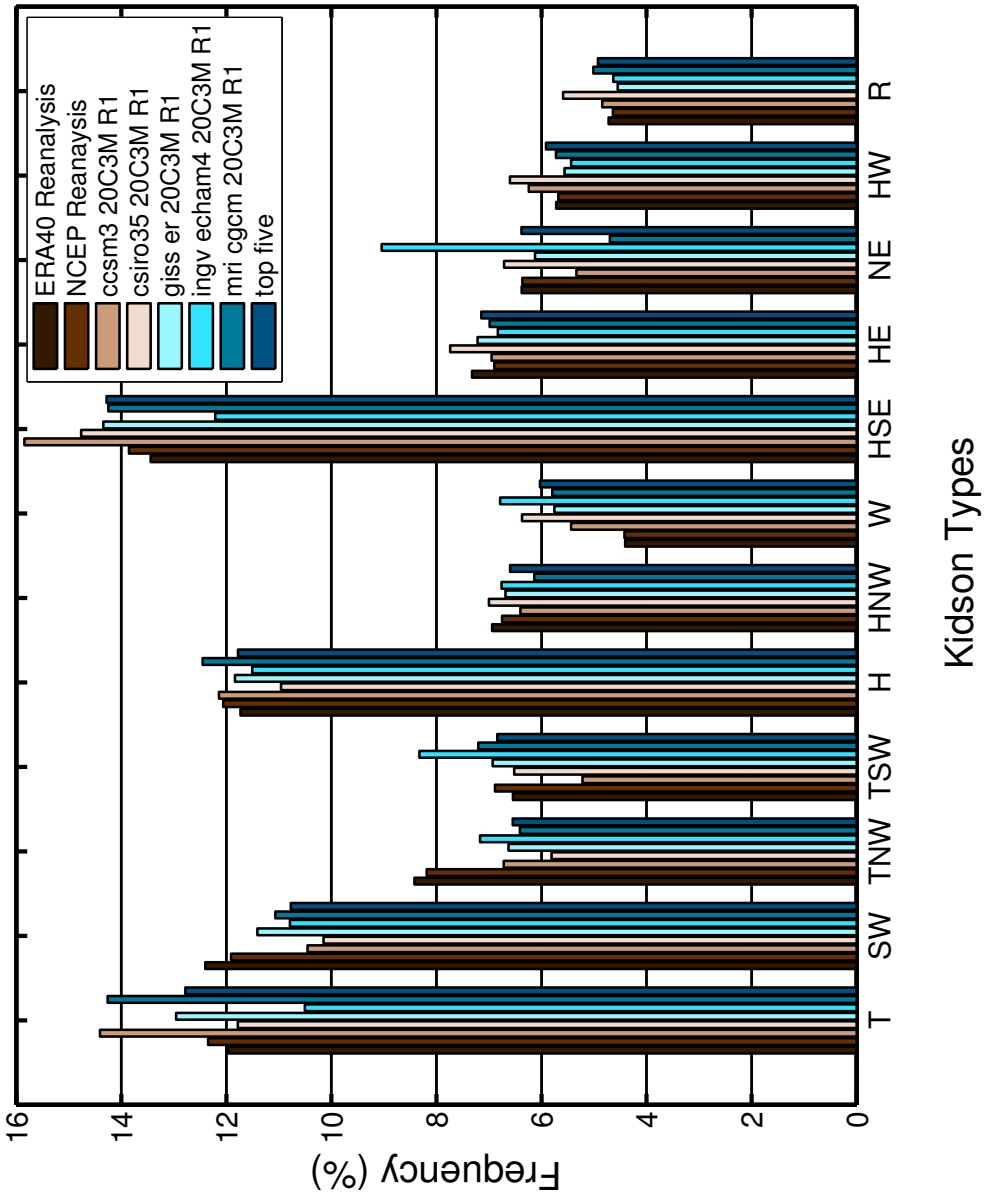

Figure 4.3: The Kidson type frequencies for the reanalysis data and top five 20C3M GCMs, 1981-2000. The GCM ensemble mean (top five) is also shown.

rived from the period 2081-2100, respectively, and each models 20C3M run. The median difference, interquartile ranges derived from the five models and whiskers denoting the spread of values are displayed. Examination of the range of differences between the 20C3M type frequencies and the top five model outputs for the A1B emission scenario displayed in Figure 4.4 show that only the HW type is statistically different from the values derived in the 20C3M run. Seven of the types (SW, TSW, HNW, W, HSE, HE and R) do not differ from zero more than the interquartile range. With 11 of the types displaying very wide model spreads with both positive and negative differences. Type NE shows the largest median increase, however the spread of values means that both positive and negative changes in the model outputs are observed based on the selection of the top 5 best-performing models. This analysis indicates that the majority of type frequencies derived in the 20C3M control runs and the values from the A1B 2081-2100 are not significantly different.

Figure 4.5 shows the model output using the A2 emissions scenario for 2081-2100, again the majority of the types are also not significantly different to the 20C3M control runs, and have similar patterns to the A1B scenario for the same period (Figure 4.4). The main difference is that the different model outputs for the A2 scenario have larger interquartile ranges than those for the A1B scenarios. As in the A1B scenario (Figure 4.4) there is a reduction in type HW and an increase in type NE. This result concurs with Mullan (2011), which also detected an increase in the NE type in annual type frequencies for A1B and A2 scenarios.

The annual variation observed is generally smaller than the variation between model runs, for some cluster types, e.g. R and T. Figure 4.5 illustrates the spread of different models is typically 2-3 %. For the HW type which has an annual frequency of occurrence of 5.68 %, $\approx$ 20 days per year of this weather pattern, the annual change of $\approx$ 0.5% corresponds to an annual reduction of $\approx$ 1.8 days a year.

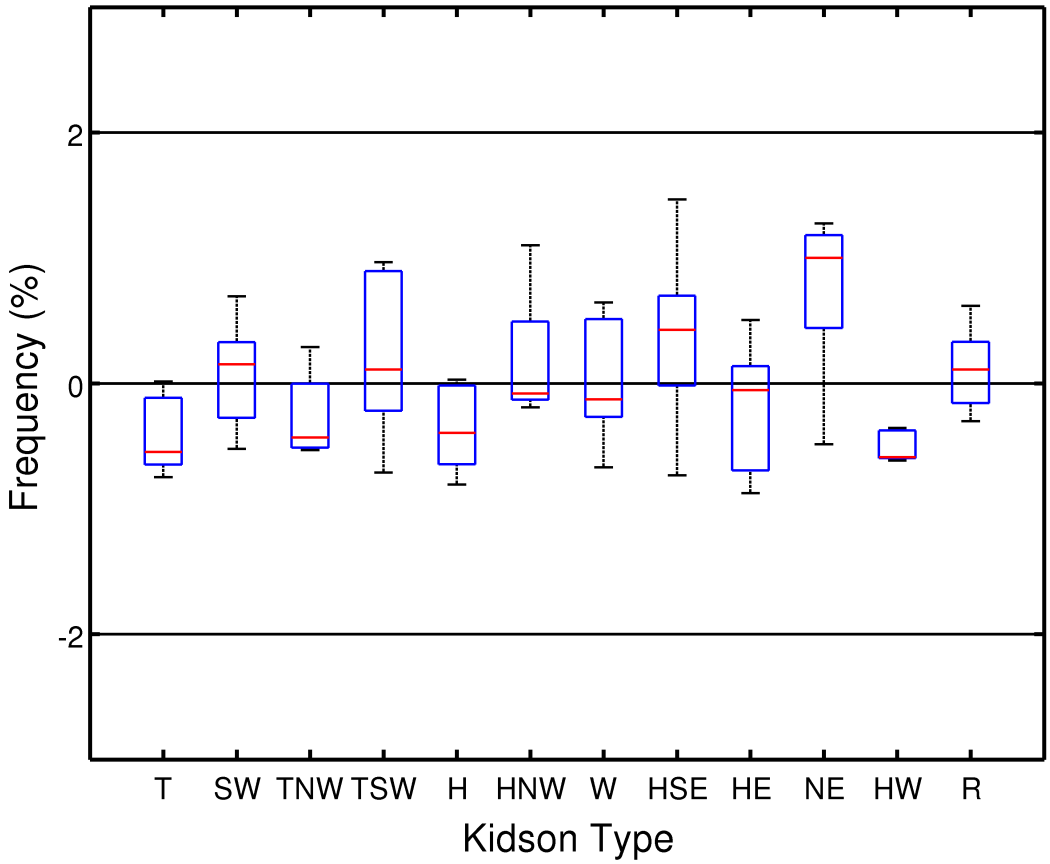

Figure 4.4: A1B 2081-2100 Type Frequency Anomalies from 20C3M 1981-2000 top five models. The box and whisker figures are used to represent the model spread. The boxes show the upper and lower quartiles, the centre is the median and whiskers the range of results.

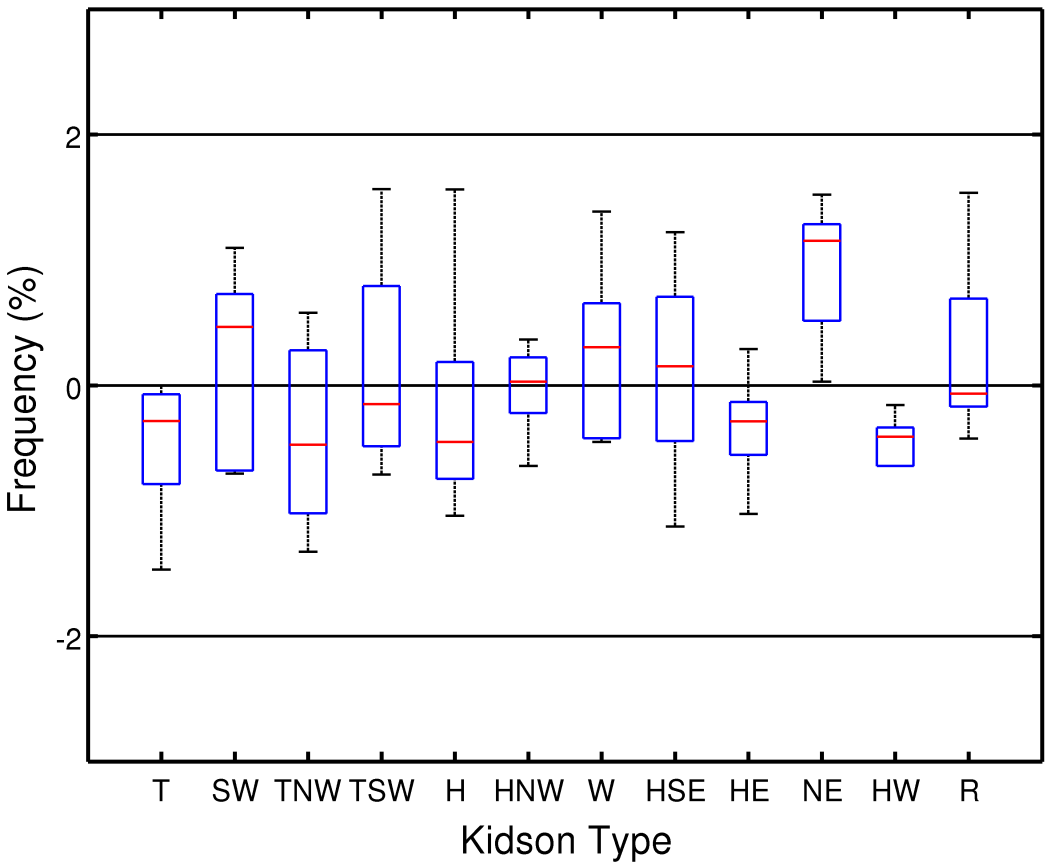

Figure 4.5: A2 2081-2100 Type Frequency Anomalies from 20C3M 1981-2000. 5 top five models

The apparent lack of change in type frequencies is surprising given the work of Kidston et al. (2010) and Swart and Fyfe (2012), which has shown that models often display a poleward movement of the jet stream in the southern hemisphere under certain emission scenarios, which would imply significant shifts in features such as the storm tracks. This lack of change suggests that circulation changes will not impact NZ's future climate and requires careful examination. Possible reasons for the apparent lack of change may be due to:

1, change in seasonal timing of the Kidson types, resulting in no net annual change.

2, model deficiencies linked to poor simulation of the jet and changes in the jet position under different forcing scenarios may mean that the MSLP over NZ is not representative.

3, the synoptic classification scheme is insensitive to small changes in circulation.

4, the circulation patterns over NZ do not change as the global climate changes.

Possibilities 1, 2 and 3 would mean that a climate shift has occurred, but this form of analysis will not resolve this change.

To examine the type frequencies in more detail, we examine the occurrence frequencies for individual months to determine whether a timing change of the different synoptic types has occurred between the 20C3M and A1B or A2 scenarios, Figure 4.6 and 4.7 respectively. A shift in the timing of the types would produce little annual variation in the types, but could have significant climate impacts. Figure 4.6 illustrates the wide range of 20C3M output in the monthly type frequencies derived from the top 5 models. However, the correspondence between the mean from the top five GCM runs (black line) and the NCEP/NCAR2 reanalysis (red line) is generally good. The boxes in Figure 4.6 show upper and lower quartiles and the whiskers the range. The range of values is particularly large in the higher frequency types, T, H and HSE.

Analysing the types in monthly increments provides a view of the seasonality of the different type frequencies (see Figure 4.6). As we increase our temporal resolution the range of GCM type frequencies also tends to increase. The monthly type frequencies shown in Figures 4.6 and 4.7 for the 20C3M and A2 scenarios show strong monthly variations. An annual variation is observed in the T, HSE, H and HW types. However, a semi-annual frequency pattern was observed in the majority of the KTs.

Figure 4.7 displays the monthly frequencies of the top five models for the A2 emission scenario for the period 2081-2100, the black line representing the top 5 model mean for the 20C3M scenario. Examination of the model output and reanalysis model mean shows some seasonal changes larger than the model spread. However, in the majority of months no change larger than the variation between the models is observed. For the Trough types T and SW there is a reduction in summer and the start of autumn (DJFM). TSW increases during summer and reduces during winter. The Zonal types, H, HNW, and W, all display an increase in the winter months and a reduction in the summer. Finally for the Blocking types, NE shows an increase in summer and a reduction in winter. Similar seasonal changes have also been documented in Mullan (2011).

To further test the previous results a second synoptic classification scheme was applied to the reanalysis and the same five GCMs used previously. The twelve LMC MSLP patterns from the NCEP2 1981-2000 (r=0.8) are presented in Figure 4.2, along with their correlations with the KT. The LMC exhibited comparable behaviour to the Kidson method, with some of the dominant KT patterns represented, cf. Figures 4.1 and 4.2.

The A2 2081-2100 annual LMC anomalies from the individual 20C3M model mean are shown in Figure 4.8. Similar to Figures 4.4 and 4.5, there is a widespread of model values and a lack of model consensus, with types 1, 2, 3, 4 and 7 showing both positive and negative frequencies anomalies. Types 5, 6, 8, 9, and 11 display a small reduction in frequency. While types 10 and 12 display increased frequencies. More variation in the an-

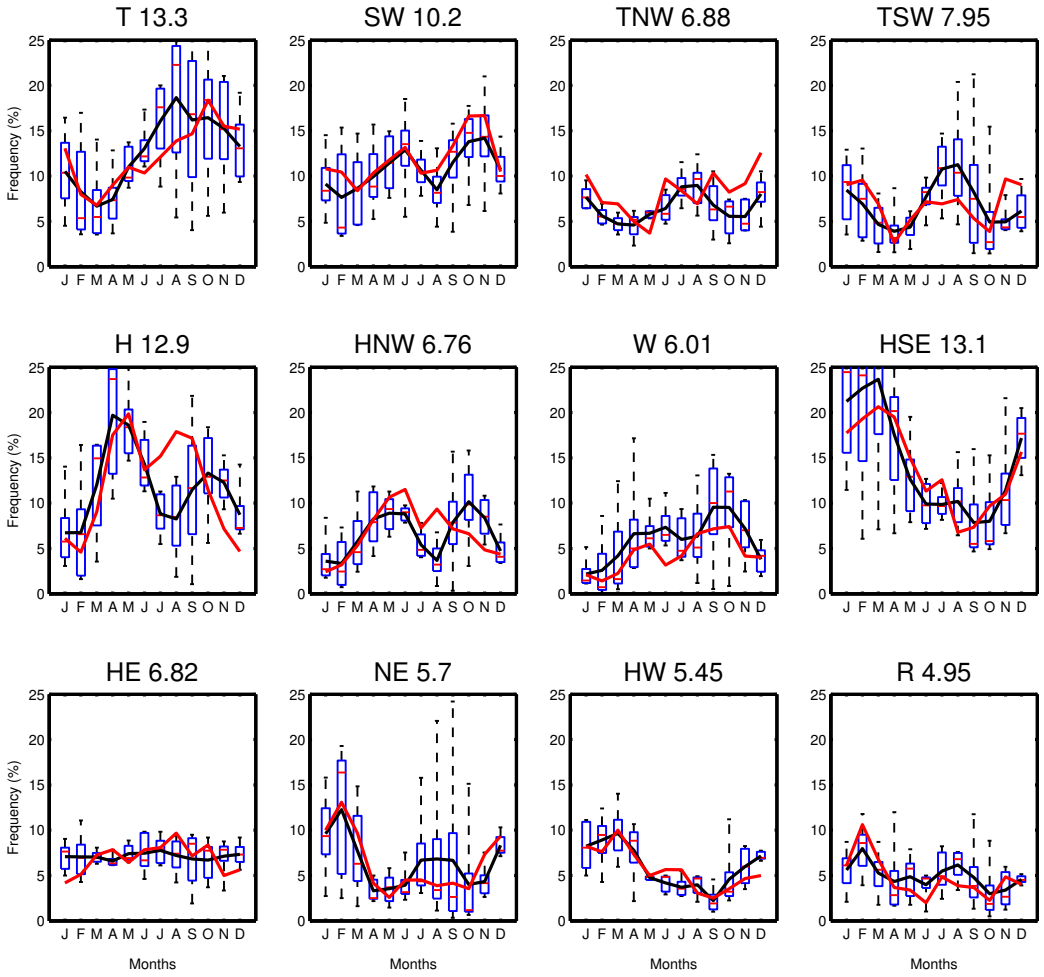

Figure 4.6: The top five 20C3M GCMs 1981-2000 Monthly Type Frequency. The annual frequency is shown next to the type. The red line is the NCEP/NCAR2 reanalysis result and the black line is the ensemble top five mean.

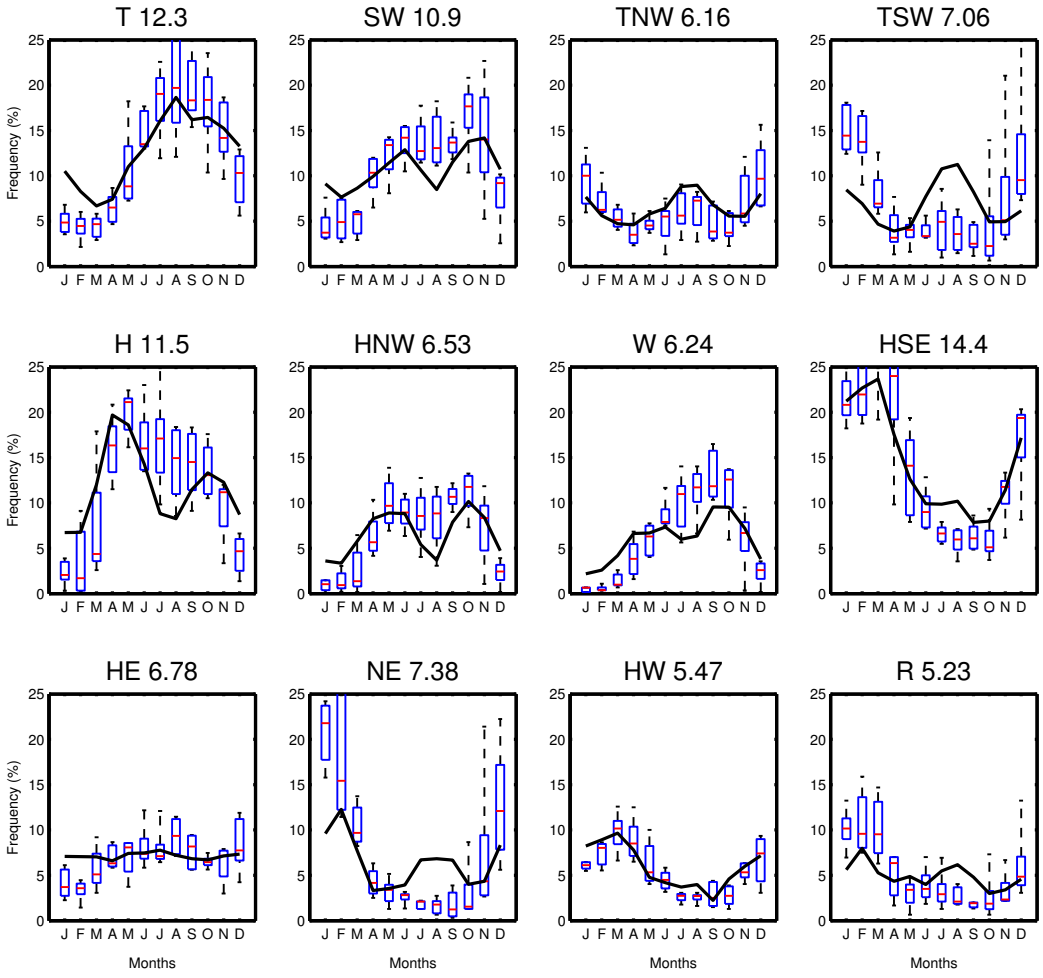

Figure 4.7: A2 2081-2100 Monthly Type Frequencies. The black line is the 20C3M ensemble top five GCM mean, from Figure 4.6

nual LMC types than identified in the KTs is therefore observed (cf. Figure 4.5 and 4.8). Consideration of the LMC types (Figure 4.2) and their correlation to the KTs (Figure 4.1) indicates that corresponding types do not agree in terms of their variation. For example LMC type 10 and 12 correlate highly with the KT H and HSE, respectively. However, there is no increase in the annual frequency for KT H or HSE identified in Figure 4.5, but more significant variation observed in LMC types, which suggests that the Kidson typing may have a sensitivity issue.

Figure 4.9 shows the monthly LMC type frequencies of the models for the A2 scenario for the period 2081-2100. As before the majority of months show no change in the type frequency greater than the spread associated with the 5 models selected. In this case, Type 3, which correlates with KT W, shows an increase in frequency during the winter months and a reduction in the late summer (FM) which is also observed in the Kidson scheme, Figure 4.7.

4.4.1 *Sensitivity Study*

As indicated previously, the lack of annual type frequency change is rather unexpected (see Figures 4.4 and 4.5). To examine this result, a sensitivity test was performed simulating a southerly displacement in the jet position, as projected to occur during the 21st Century (Arblaster and Meehl, 2006; Karpechko et al., 2010; Simpkins and Karpechko, 2012). The grid used in the synoptic classification scheme was shifted in the meridional direction by up to $\pm$ 10°latitude, in 2.5°increments using the NCEP/NCAR2 reanalysis data set. The resulting changes in KT frequencies from each grid displacement are displayed in Figure 4.10 and Figure 4.11 for the LMC types. The grey bars identify the percentage of the original members of each type. Thus these are at a maximum when the grid is in the normal position and reduce as the grid is displaced. For both schemes each type shows a clear reduction in the number of original members re-

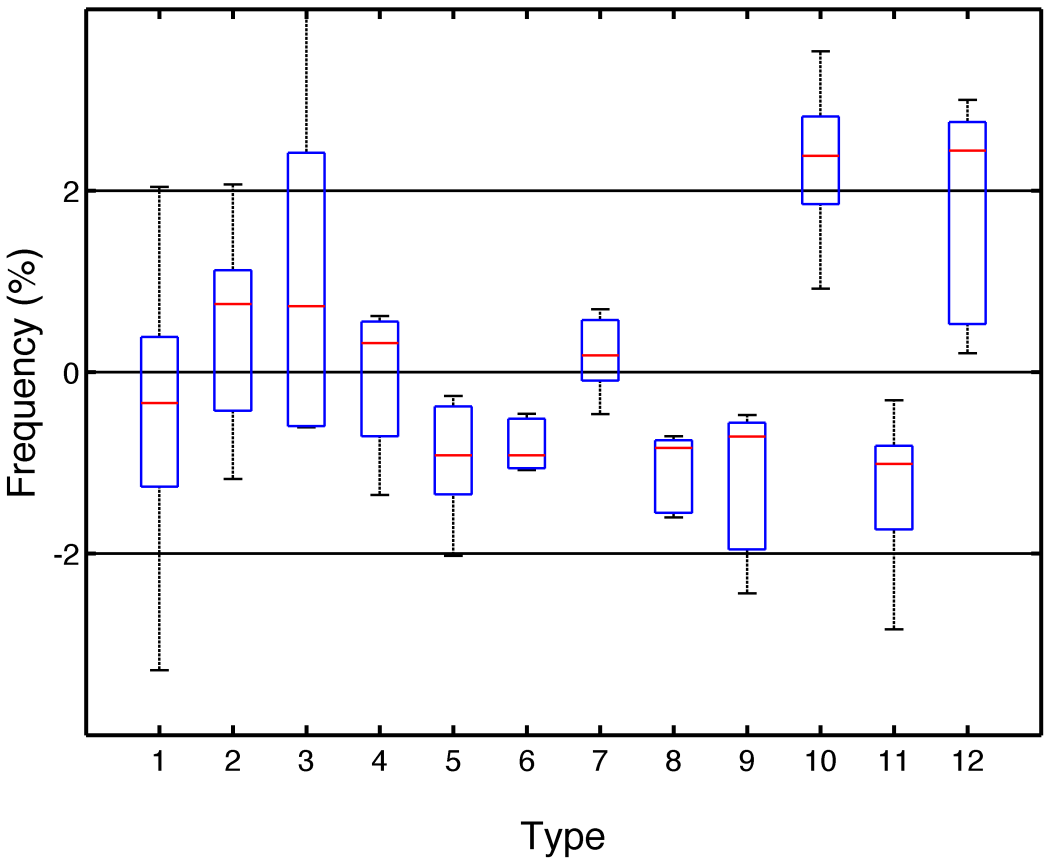

Figure 4.8: LMC, A2 2081-2100 Type Frequency Anomalies from the 20C3M top five mean 1981-2000.

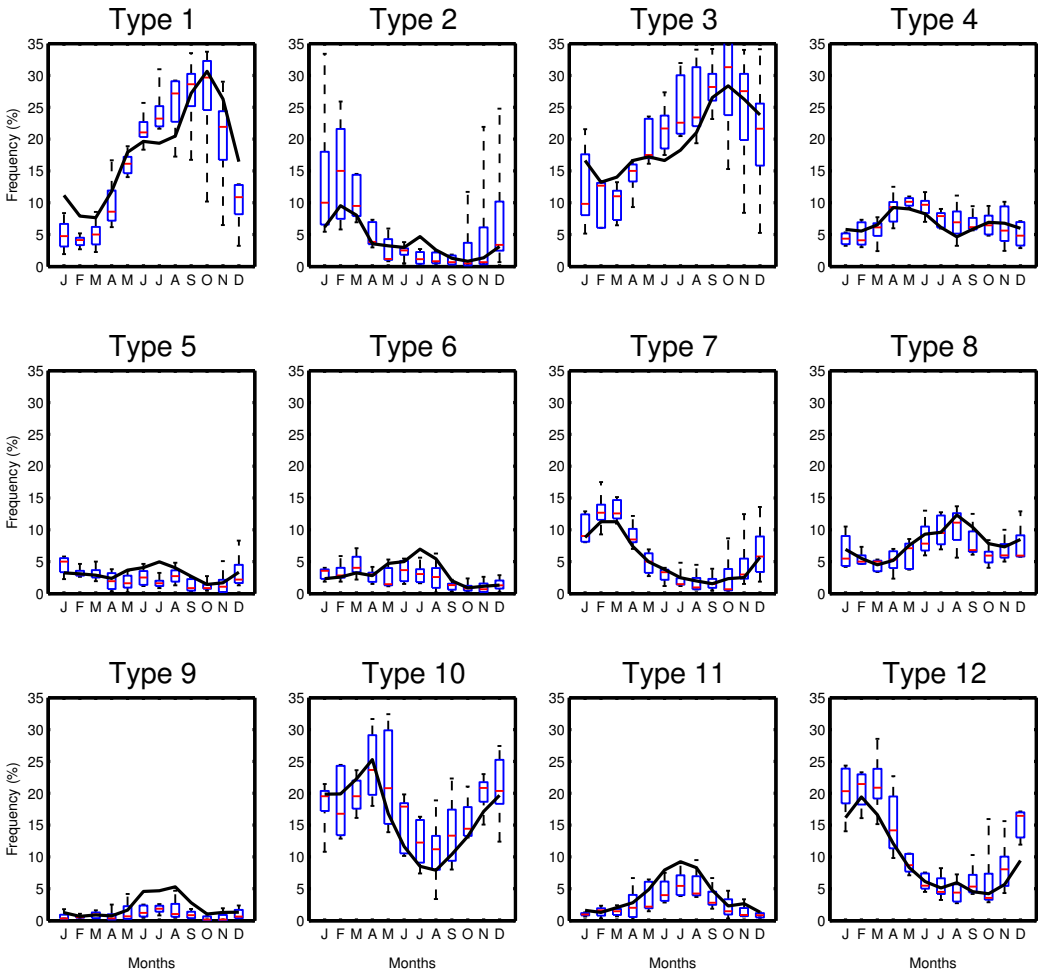

Figure 4.9: LMC A2 2081-2100 Monthly Type Frequencies. The black line is the 20C3M ensemble top five GCM mean.

maining within that type as the latitude is displaced from the normal position.

The changes in the frequency of the KTs for the different grid displacements, coloured bars, are often rather modest (NE and R types), Figure 4.10. This results in some types maintaining nearly constant frequency, which can be explained by inter-type transfer. It is apparent that the two methodologies have a different response to the grid shifting with the LMC scheme displaying a higher sensitivity to the grid displacement. In particular, the higher frequency LMC types, 1, 2 and 3, show considerable variation as the grid is incrementally shifted.

This simple analysis demonstrates that a large spatial shift in the position of the jet is required to obtain a significant change in type frequency using the Kidson methodology, typically ten degrees of latitude for a two percent change in annual type frequency. The disparity in the changes displayed in Figure 4.10 and 4.11 also suggests that the methodology used in Kidson (2000) can be insensitive to significant variation in the average circulation. In general the Kidson scheme seems to favour the existing distributions, as a very large shift is required to perturb the type frequencies. This combined with the range of model responses makes it hard to draw any conclusions about frequency changes on the annual time scale.

4.5 DISCUSSION

We also analysed multiple GCM realisations over longer time series. The CCSM3.0 model provides four runs forced by A1B and A2 scenarios between 2000 and 2099. The four CCSM3.0 runs exhibit a range of type frequencies as expected. For the A2 scenario the yearly type frequencies are plotted and overlaid with the trend lines from each run in Figure 4.12. Large inter-run variability is apparent, with some types displaying both positive and negative trends, SW, HSE and HE.

Another limitation of the methodology is that it does not measure the magnitude/intensity of the types and thus does not ac-

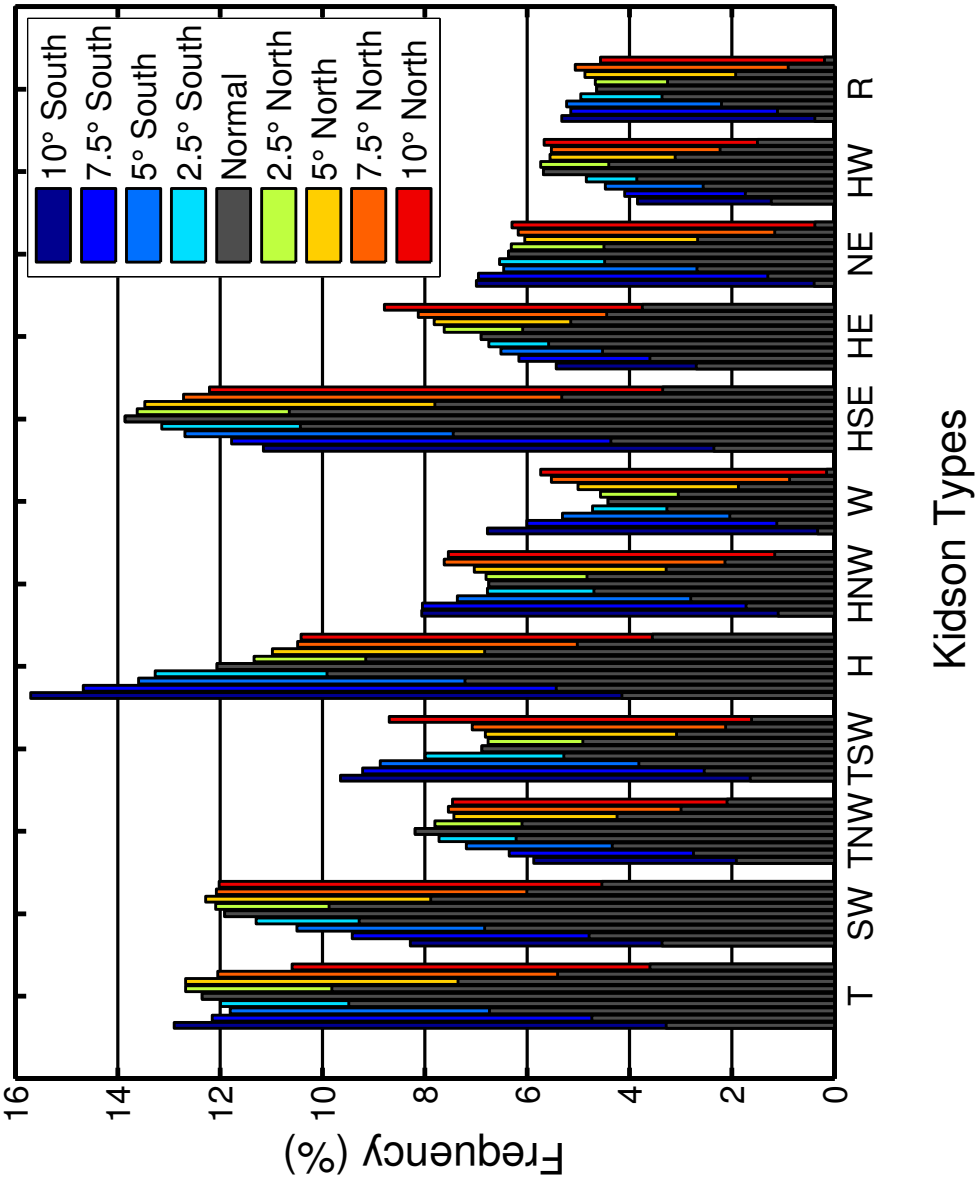

Figure 4.10: Annual Type frequency obtained by shifting the grid in 2.5°increments. The overlaid gray bars are the original type members, which reduce as the type is displaced.

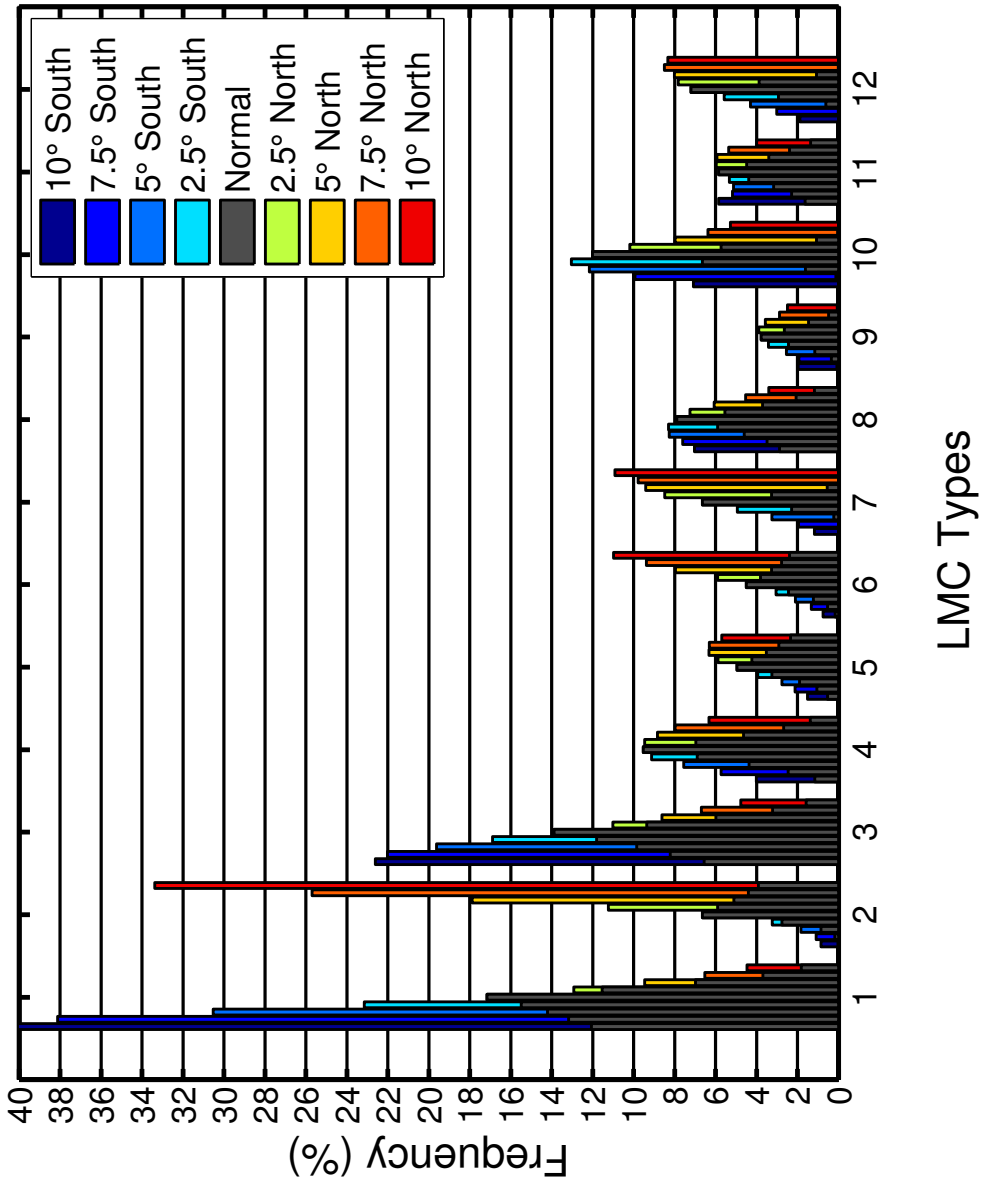

Figure 4.11: LMC Type frequency obtained by shifting the grid in 2.5°increments. The overlaid gray bars are the original type members, which reduce as the type is displaced.

count for increasing/decreasing trends in the intensity of pressure anomalies. The MSLP anomalies from the 20c3m model mean and A2 2081-2100 for each type are shown in Figure 4.13, with type TSW showing a 2-3 hPa anomaly. A1B and A2 2045-2065 projections have reduced anomalies when compared with the A2 2081-2100 period (not shown). Figure 4.14 shows the MSLP for the NCEP/NCAR2 reanalysis, top five models 20C3M, A2 2081-2100 and anomalies from A2 2081-2100 20C3M. Figure 4.14 shows the mean flow inferred from geostrophic winds varies little (≈1 hPa) between the 20C3M and A2 scenarios.

The initial selection of 12 types used in the Kidson scheme was based on stability and repeatability during the iterative clustering process (Kidson, 2000). This stability and low number of classes may contribute to the lack of sensitivity observed. Schuenemann and Cassano (2010) incorporated GCM data into the training data set of their SOM. We believe the inclusion of this data into the training phase enhances the response of the classification scheme to future scenarios. Also the increased number of types/nodes, 35 compared to Kidson's 12, may aid sensitivity.

4.6 CONCLUSION

Our results suggest that the principal synoptic climatology methodology used in this study, namely Kidson typing, is relatively insensitive to changes in large-scale circulation, on an annual scale. This insensitivity combined with the range of GCM output, inter-run variability and inter-model variability, impedes statistically significant results being identified. Therefore the Kidson typing classification scheme may not be sensitive enough to identify subtle projected regional climate change given model uncertainty, as a small pressure gradient difference is not enough to change the inter-type assignment. The methodology favours the existing distributions and patterns formed from the initial clustering process and highlights that initial clustering should

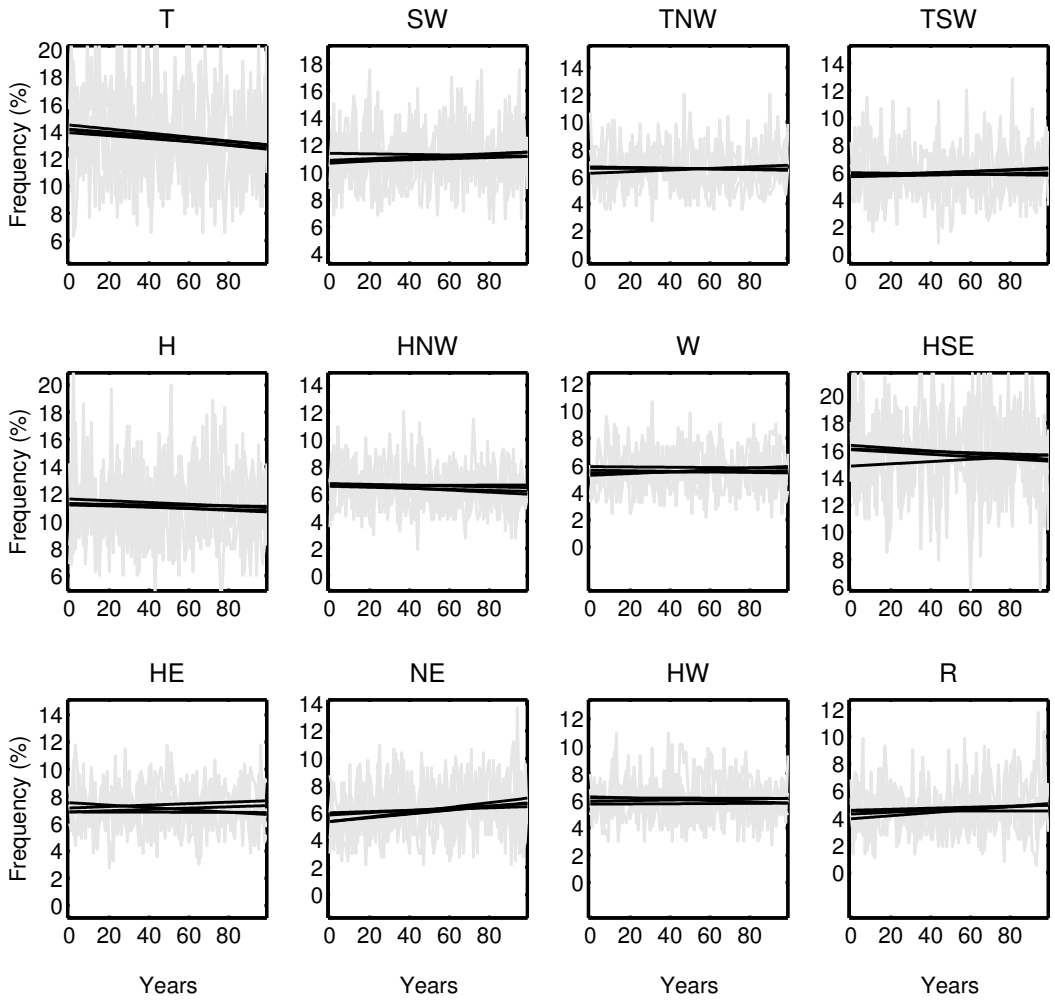

Figure 4.12: CCSM3.0 A2 2000-2099, (4 runs). The yearly frequency of the 4 runs is shown in the grey and the black trend lines from each run.

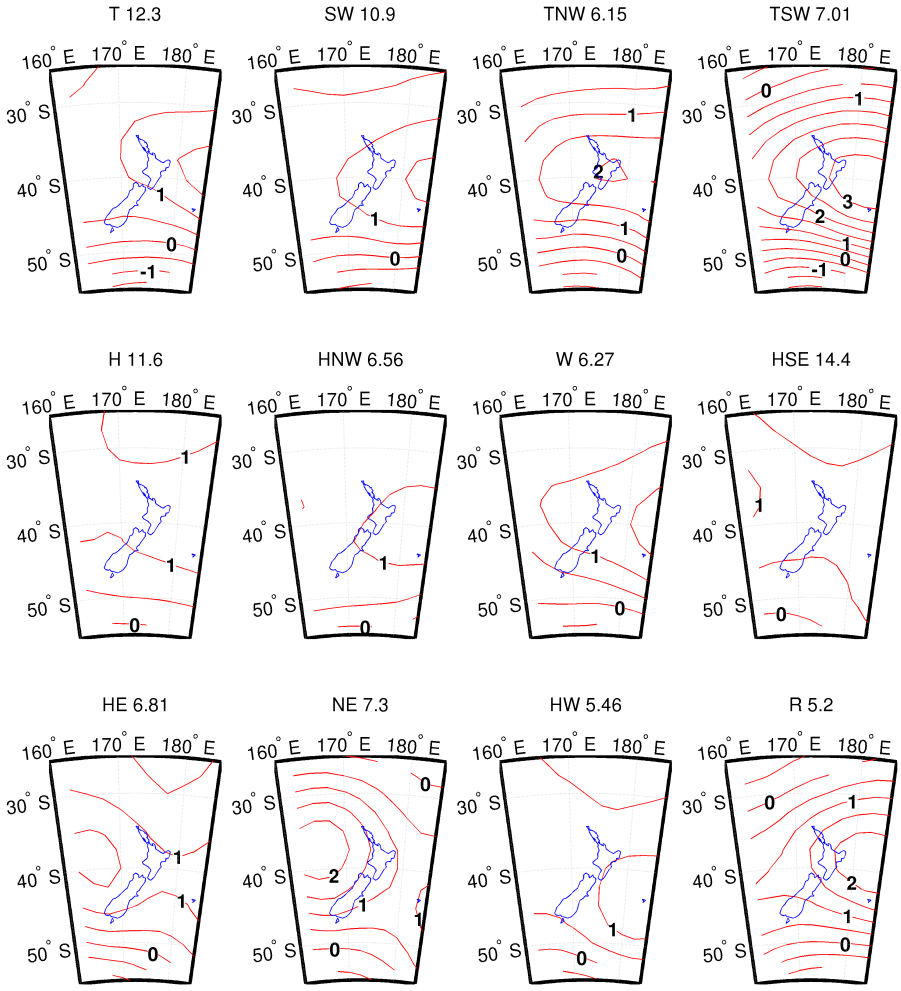

Figure 4.13: A2 2081-2100 Kidson type anomalies from the 20C3M top five mean 1981-2000 (hPa).

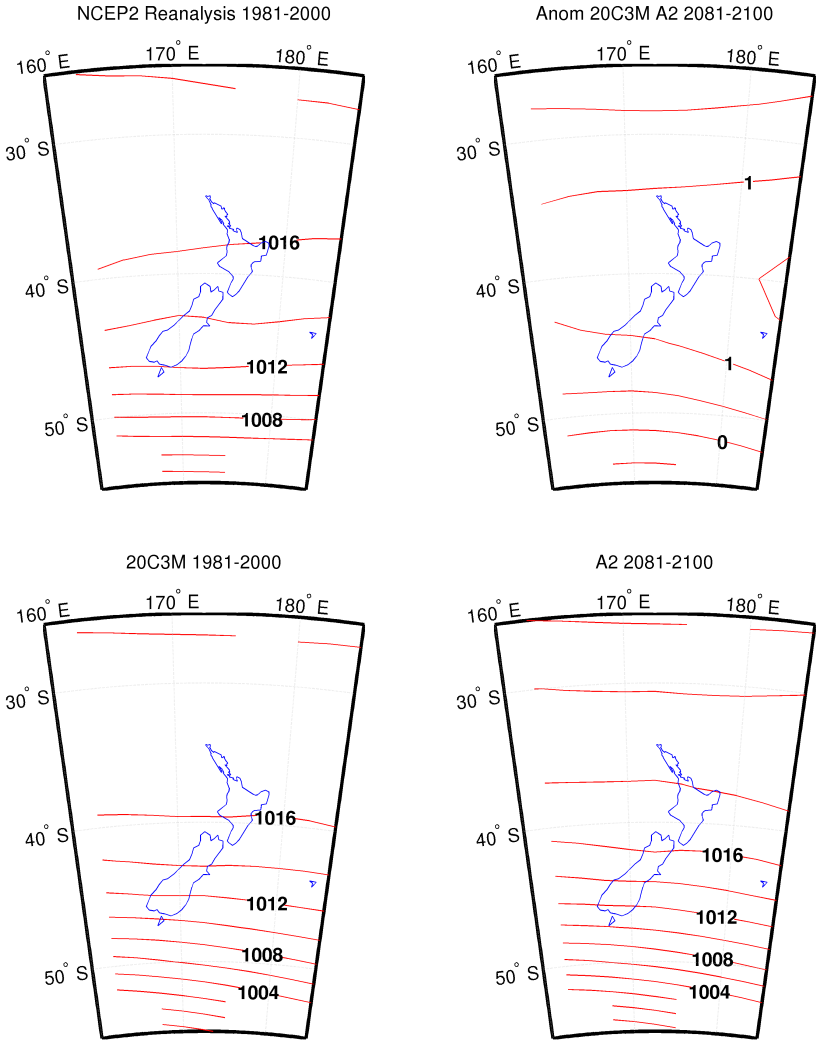

Figure 4.14: MSLP for the NCEP2 reanalysis and 5 top models (20C3M, A2 2081-2100, A2- 20C3M anomalies).

likely include GCM output. The twelve predetermined cluster types, while valid and representative of real world features, inhibit the inter-type variability and transfer. Having a larger number of clusters may increase the level of sensitivity. Results in this study also suggest that when creating a classification system it is important to consider the data to which the scheme may be applied and the variable of interest or research area. For example, the application of the Kidson scheme to GCM output for climate sensitivity studies was not initially envisaged.

We reiterate that these results are limited to our test region; the surface level data used, MSLP; Kidson and LMC methodology and the GCMs used, and may not be indicative of other regions. As seen in Figure 4.14 there was little variation between the 20C3M and A2 model MSLP projections, thus MSLP may not be the best variable for investigation of future circulation patterns in the NZ region. However, the results concerning sensitivity, with the use of the shifting grid, may have ramifications for other synoptic classification schemes using a similar methodology. In addition, this study does not diminish the usefulness of Kidson types in other applications or synoptic climatology, but it does suggest that the Kidson classification methodology may not be suitable for examining climate change scenarios over NZ.

While the usefulness of synoptic climatology methodologies is not questioned here, this study suggests that care must be undertaken when using type or regime frequency variation as a proxy for change. These warnings have been previously identified in Cuell and Bonsal (2009) and Sheridan and Lee (2010), and should be investigated when using principal component analysis methodologies for synoptic climatology or other synoptic classification techniques.

5

KIDSON TYPES IN THE SOUTHERN HEMISPHERE

5.1 INTRODUCTION

Smaller scale weather events can be overridden and dominated by the larger circulation (Oke, 1987; Sturman and Tapper, 2006). Thus, the synoptic scale patterns that the Kidson Types (KTs) represent can be modulated by the large scale circulation and modes of inter-annual variability. Refer to Chapter 4 or Section 2.2.3 for further explanation of the KTs and their function. Previously in Chapter 4 the future changes in the KT frequency of occurrence were investigated using General Circulation Model (GCM) projections in the 2045-2065 and 2081-2100 periods, there was no consideration given to the role of the larger circulation or inter-annual variability in that work. The motivation of this chapter is to amend this and expand the exploration of the KTs to the hemispheric scale. Additionally this chapter provides further scrutiny into the KTs, to determine if trends within the type frequency are present.

This analysis is conducted with reanalysis data only, thus avoiding the internal variability associated with GCMs, while retaining the variability observed in the reanalyses. The range of responses from a large GCM ensemble may mask model consensus and smaller trends (Parsons et al., 2014).

It is apparent that the Kidson methodology may be insensitive to small shifts in the jet position. This conclusion was de-

termined in Chapter 4 by incrementally shifting the domain in the meridional direction, to simulate a projected change in the jet location. However, the KTs still have utility, as they are the de facto Synoptic Climatology (SC) method used in New Zealand (NZ) and have been widely used, see Renwick (2011); Parsons et al. (2014) and references within.

In this chapter, three supplementary forms of analyses are undertaken on the KTs, and they are described as follows:

OBSERVED DOMAIN SIZE. The Kidson Types are used to determine composites of the Mean Sea Level Pressure (MSLP) and these composites are then examined over an enlarged domain, which encompasses the South Pacific Ocean (SPO) and Southern Hemisphere (SH).

INTER-ANNUAL VARIABILITY. The Kidson Types are investigated with consideration to the larger modes of variability, the Southern Annular Mode (SAM) and El Niño - Southern Oscillation (ENSO).

TREND ANALYSIS. The trends within the annual frequencies of occurrence, of the Kidson Types and Regimes, are investigated using a wider range of reanalysis output than that examined previously in Chapter 4.

The latest generation of reanalyses data, detailed in Table 5.1, is utilised to ascertain the daily occurrence of the KTs. The daily KT information is then used to create hemispheric composites of the MSLP for each of the KTs. Earlier reanalysis data have suffered from some erroneous data assimilation and a lack of observation data in the SH prior to the satellite era (Kidson, 1999; Marshall, 2003; Renwick, 2004; Jones and Lister, 2007), see Section 3.1 for further discussion on reanalysis data.

The KT frequencies are also determined during the positive, neutral and negative phases of the SAM and ENSO indices. SAM is a large mode of variability that can affect the NZ region (Ummenhofer and England, 2007; Kidston et al., 2009). The Southern Annular Mode Positive Phase (SAM+) manifests as an increase in positive pressure anomalies over NZ, this induces a

reduction in the Westerly wind in the mid latitudes, and the opposite response occurs in the polar regions, with an increase in the intensity of the polar vortex. SAM is currently projected to be trending towards a positive phase, SAM+, (Arblaster et al., 2011; Son et al., 2010). The increase in SAM+ is linked to the Antarctic Ozone Hole (AOH) and this occurs during the austral summer (Simpkins and Karpechko, 2012). See Section 2.3.3 for a further discussion on SAM.

The Southern Oscillation Index (SOI) is a measure of the atmospheric component of the coupled ocean-atmosphere mode of variability, known as ENSO. It is defined as the pressure difference between two main centres, Tahiti and Darwin. The SOI index is negatively correlated with Sea Surface Temperature (SST) indices used in determining El Niño and La Niña events, such that a Southern Oscillation Index Positive Phase (SOI+) goes with negative SST anomalies in the eastern Pacific (La Niña) and a Southern Oscillation Index Negative Phase (SOI-) goes with positive SST anomalies in the eastern Pacific (El Niño). For NZ, during the SOI-, El Niño , there are stronger south westerly winds and during SOI+, La Niña , generally calmer conditions prevail (Kidson, 2000). The SOI is described further in Section 2.3.2.

The KTs are defined by a domain, of 25°S - 55°S and 160°E - 175°W, over NZ and the reanalysis data is also constrained with observational data from NZ. However, the assimilation of the erroneous higher latitude data in the SH still affected the quality of the NCEP/NCAR1 (NCEP1) reanalysis data that the KTs use. Additionally, a break point in the data is apparent at 1979, which is the beginning of satellite data assimilation (Renwick, 2004).

As the Kidson (2000) methodology utilises NCEP1 reanalysis from 1958-1996, trend analysis using data pre 1979 might bias and overstate an apparent trend. In the original work of Kidson (2000) no trend analysis was presented. Trends in KT frequency have been reported previously, (Renwick, 2011; Sturman and Quénol, 2013), caution is advisable with results that are based on the NCEP1 reanalysis. This is due to the well known quality

issues with the NCEP1 reanalysis data (Kidson, 1999; Kanamitsu et al., 2002; Marshall, 2003; Bromwich et al., 2007), also see Section 3.1.

In Chapter 4 trends were determined for the CCSM3.0 model projections between 2000-2099 using four realisations of the A2 forcing scenario. In the four runs the SW, HE and HSE Types displayed both negative and positive trends, thus highlighting the year to year variability of the KTs and the uncertainty in determining significant trends.

The Twentieth Century Reanalysis (20CR) is used to investigate the frequencies of occurrence and trends in the KTs from 1871-2010, this data set provides an opportunity to investigate past trends in the annual frequencies of the KTs. Refer to Section 3.1 for further information regarding the 20CR. Trend analysis is also undertaken with the ERA Interim (ERA-I) and NCEP1 reanalyses output to provide a comparison with the 20CR. An overlapping period of the three data sets is used, between 1979-1997.

In summary, three extensions of the KT analyses are undertaken; using composite analysis the domain is expanded to encompass the SH; the KTs are investigated with respect to phases of the SAM and SOI modes of variability; and trends within the types and regime frequency of occurrence are also investigated.

5.2 METHODOLOGY

The methodology used in determination of the KTs is based on Parsons et al. (2014) and is described in further detail in Chapter 4, thus it is only summarised here.

5.2.1 *Data*

Three reanalyses products are used in this Chapter, see Table 5.1. Two of them are later generations of reanalyses when com-

pared to the reanalyses output used in Chapter 4. The ERA-I is a high resolution reanalysis data set from the European Centre for Medium-Range Weather Forecasts (ECMWF), that supersedes the European Reanalysis 40 (ERA40) (Dee et al., 2011). The 20CR is a longer duration reanalysis data set, that is intended to enable the study of events which occur across larger time scales, such as ENSO and SAM. The 20CR assimilated surface observations only and spans the available instrumentation record, this also avoids any change due to the inclusion of satellite data post 1979 (Compo et al., 2011). The 20CR is currently the longest reanalysis product, back to 1871. However, the lack of observations in the SH during the early period of this data set needs to be noted. Section 3.1 provides further discussion on the 20CR and Figure 3.2 displayed the number of observations used in the reanalysis.

The NCEP1 reanalysis is used to compare the trends observed in 20CR and ERA-I, as NCEP1 is the data set that Kidson (2000) used and NCEP1 has also been used in subsequent KT work. The reanalyses data sets are archived at 6 hourly time intervals. However, we use only one measurement from 12:00 GMT for each day for the ERA-I and 20CR reanalyses. This reduces the data overheads, particular with the longer 20CR time series and the size of the expanded SH domain. Kidson (2000) used 12 hourly 1000 hPa geopotential height data, however daily and once daily temporal resolution MSLP data has been successfully used with the KTs before (Parsons et al., 2014).

The NCEP1 reanalysis data is 1000 hPa geopotential height data at 12 hourly, as used in Kidson (2000). For each data set the anomalies are determined by subtracting the dataset mean from the entire period. The NCEP1 data is only used for comparison in the trend analysis.

5.2.2 *Kidson Types*

To determine the KTs the reanalysis data are bi-linearly interpolated into a 2.5°x 2.5°latitude longitude grid, at the same resolu-

Table 5.1: Data Sources

Model	Institution	Country	Reference
NCEP/NCAR1	NCAR	USA	Kalnay et al. (1996)
ERA Interim	ECMWF	Europe	Dee et al. (2011)
20Cth Reanalysis V2	NCAR	USA	Compo et al. (2011)

tion and location as the original KTs. The data are then projected onto the 5 Kidson Empirical Orthogonal Function (EOF) pattens, from Kidson (2000), to ascertain the daily weightings. These are then normalized and assigned to the closest of the 12 Kidson clusters, based on minimum euclidean distance, to determine a "type" for each observation. Thus, the reanalysis data are used to determine a time series of KTs. The resultant time series is then used to determine composites of surface pressure in the larger SPO and SH domains. The larger domains, SPO and SH, are shown at their original resolutions, at 0.5°x 0.5°for the ERA-I reanalysis. The SPO domain is defined as 15°S - 65°S and 120°E - 140°W. For further information on the KT see Section 2.2.3 or Chapter 4.

5.2.3 *Inter-Annual Variability*

For the inter-annual study the KTs are aggregated into their three regimes, Blocking, Trough and Zonal. Dependant on the phases of the SAM and SOI the frequencies of occurrence for each regime is then determined. Upper and lower quartiles are used for the positive and negative phases, with the remainder defining the neutral phase.

The SAM index is determined using the normalised zonal mean MSLP differences between latitudes 40°S and 65°S, as detailed in Gong and Wang (1999) and Section 2.3.3. The SOI is determined using the Troup (1965) method, in which pressure differences

between Darwin and Tahiti define the index, as detailed in Section 2.3.2. Both of these methods use normalised differences in MSLP at set locations. Further discussion and the indices determined from ERA-I are presented in the BACKGROUND, in Sections 2.3.2 and 2.3.3.

5.2.4 *Trend Analysis*

The 20CR reanalysis data set provides an opportunity to investigate trends in the frequency of the KTs over longer period of data, the ERA-I and NCEP1 trends are also displayed for comparison.

The annual type and regime frequencies are determined for each year in the data. A linear trend line is then fitted, using the least squares fit. The NCEP1 reanalysis data is used for a comparison between the 20CR and ERA-I reanalysis data. Due to the different length of data an overlapping subset, 1979-1997, is also investigated.

5.3 RESULTS

The same methodology and analysis has been undertaken with each of the three reanalyses. To avoid repetition, the presented results are limited to the most appropriate section. Thus ERA-I is presented in Section 5.3.1; 20CR in Section 5.3.2 and all three reanalyses in Section 5.3.3.

Using the Kidson typing methodology, the Type and Regime frequency of occurrence has been determined for each of the three reanalyses data sets, NCEP1, 20CR and ERA-I, see Table 5.2. Even though we have used quite different data sets and time ranges the annual type frequencies are similar to each other and our previously presented results in Chapter 4 (Table 4.1), with the NCEP1 regimes frequency being nearly identical to the 20CR.

Figure 5.1 displays the twelve MSLP type patterns, determined from the ERA-I data set. Unsurprisingly the resultant mean pattens of the KTs, Figure 5.1 is similar to previously presented results in Figure 4.1.

Table 5.2: Kidson Types and Regimes, frequency of occurrence (%). As determined from NCEP1, 20CR and ERA-I. The regime frequency is displayed at the end of each regime column as the total of the regime member types

Regime	Type	NCEP1 1958-1997	20CR 1871-2010	ERA-Interim 1979-2008
Trough	T	12.3	12.5	12.1
	SW	11.2	10.1	11.9
	TNW	7.6	7.8	8.16
	TSW	7.3	7.8	6.46
		38.4	38.2	38.6
Zonal	H	12.8	12.5	11.7
	HNW	6.9	6.7	6.76
	W	4.9	5.5	4.85
		24.5	24.6	23.4
Blocking	HSE	13.7	12.8	14.0
	HE	7.1	7.1	7.52
	NE	6.2	6.6	5.92
	HW	5.3	6.8	5.63
	R	4.7	4.0	4.95
		37.1	37.3	38.0

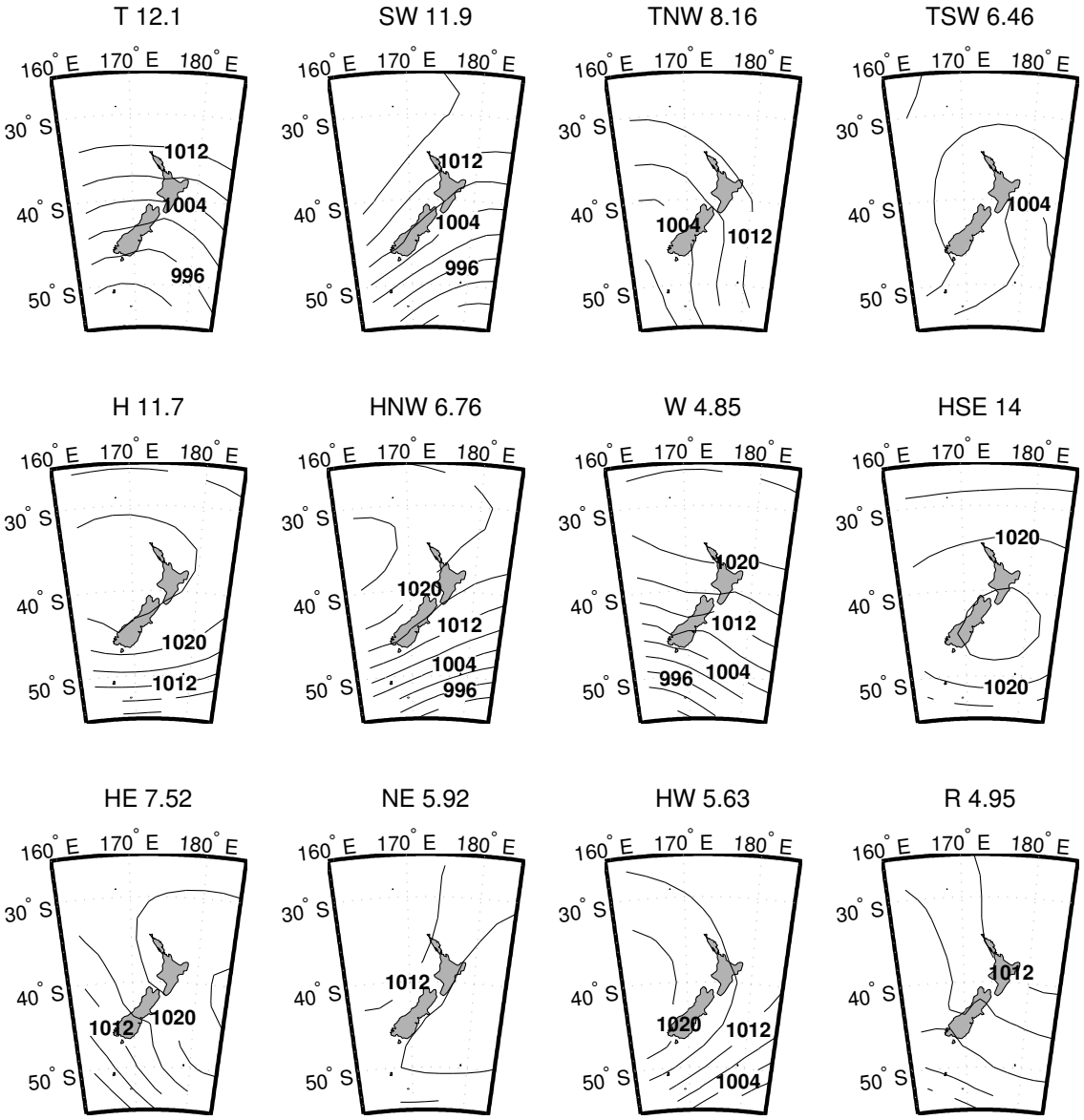

Figure 5.1: Kidson Types MSLP, from ERA-Interim 1979-2008. The annual frequency of occurrence (%) of each Kidson Type is displayed above the MSLP field and the contour interval is 4 hPa. The Kidson domain is located at 25°S - 55°S and 160°E - 175°W.

5.3.1 *Kidson Types in the Southern Hemisphere*

Using the daily time series of KTs extracted from the ERA-I data the size of the domain is now extended and examined via compositing. Figure 5.2 displays the MSLP of the KTs in the SPO, effectively it is an enlarged version of Figure 5.1 at 0.5°x 0.5°resolution. It is apparent that the dominant feature is the westerly flow that circumnavigates Antarctica and the location of blocking Anticyclones (ACs).

As the westerly flow vacillates between a more northerly and southerly direction it modulates the NZ weather and thus the KTs. This meridional vacillation is known to be highly correlated with the temperature in NZ (Trenberth, 1976; Dean and Stott, 2009), with cooler temperatures when the flow is from a more southerly and warmer from a more northerly direction.

The location of blocking anticyclones can also inhibit this flow. For example the High South East (HSE) type, from the Blocking regime grouping, can be seen to be diverting the flow south of NZ in Figure 5.2.

The displayed domain is now further enlarged to incorporate Antarctica. As the Kidson typing methodology is defined by a domain centred over NZ, the further from NZ the closer to the climatological mean the KT patterns are. This is more apparent when the anomalies are displayed, see Figure 5.3. The largest anomalies are still within the Kidson domain centred over NZ. Further from the Kidson domain the anomalies are reduced and the SH becomes the background state. Thus the KTs can be considered as high (anticyclones) and low (cyclones) systems superimposed on the climatological mean.

Figure 5.4 displays the MSLP Kidson anomalies, as seen in Figure 5.3, however the projection is altered to be centred on the Kidson domain while also displaying Antarctica.

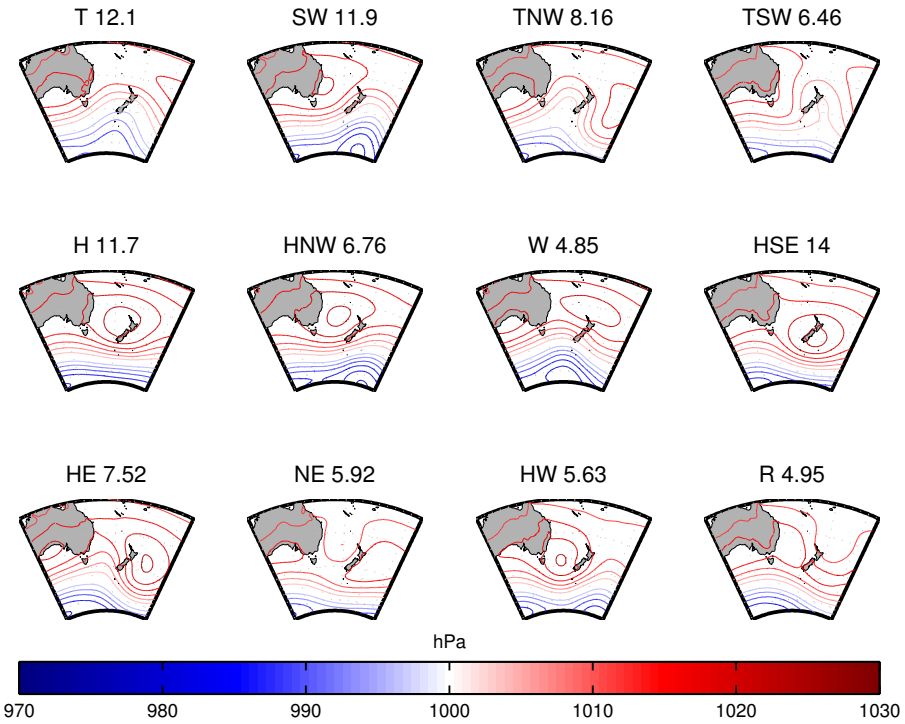

Figure 5.2: Kidson Types MSLP, from ERA-Interim 1979-2008. The annual frequency of occurrence (%) of each Kidson Type is displayed above the enlarged domain of the MSLP field and the contour interval is 4 hPa.

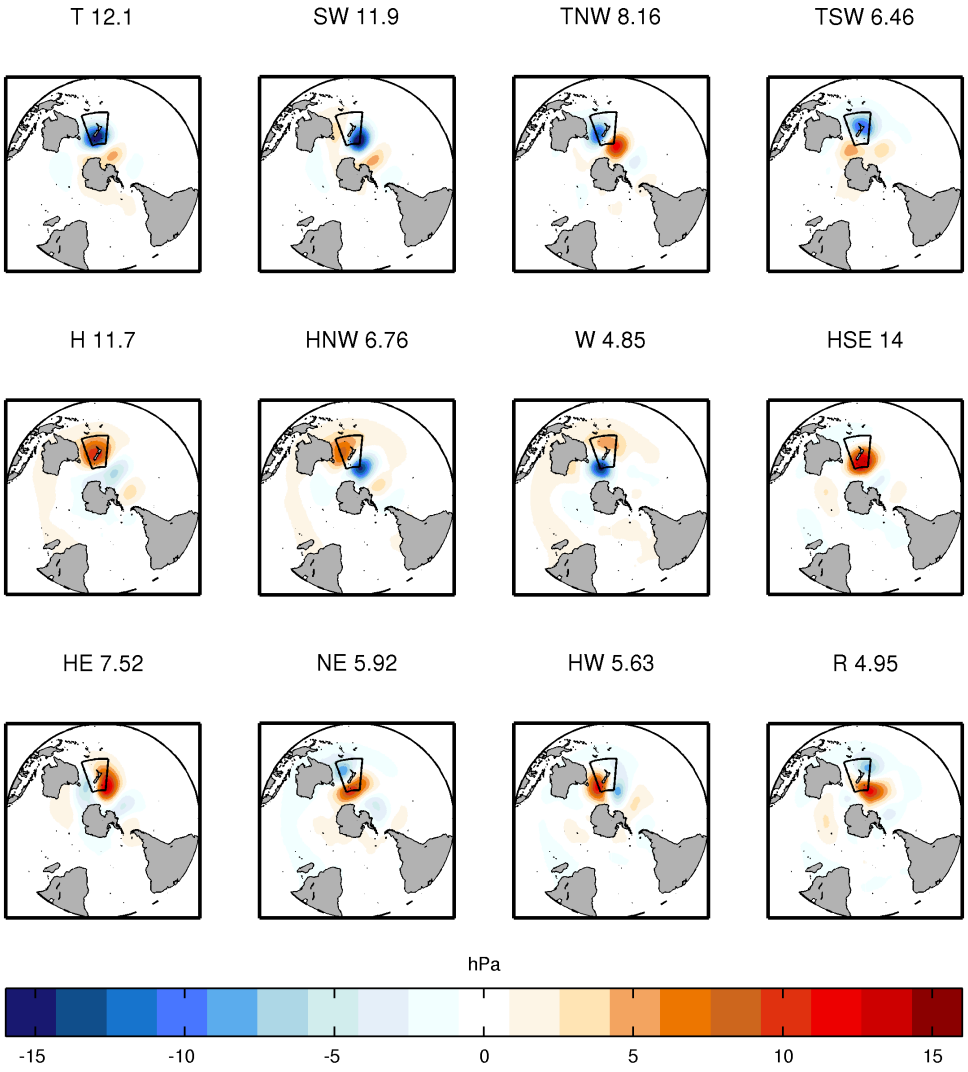

Figure 5.3: Kidson Types Annual MSLP Anomalies in the Southern Hemisphere, using ERA-I 1979-2008. The Kidson domain is outlined over NZ. The field is MSLP anomalies in hPa.

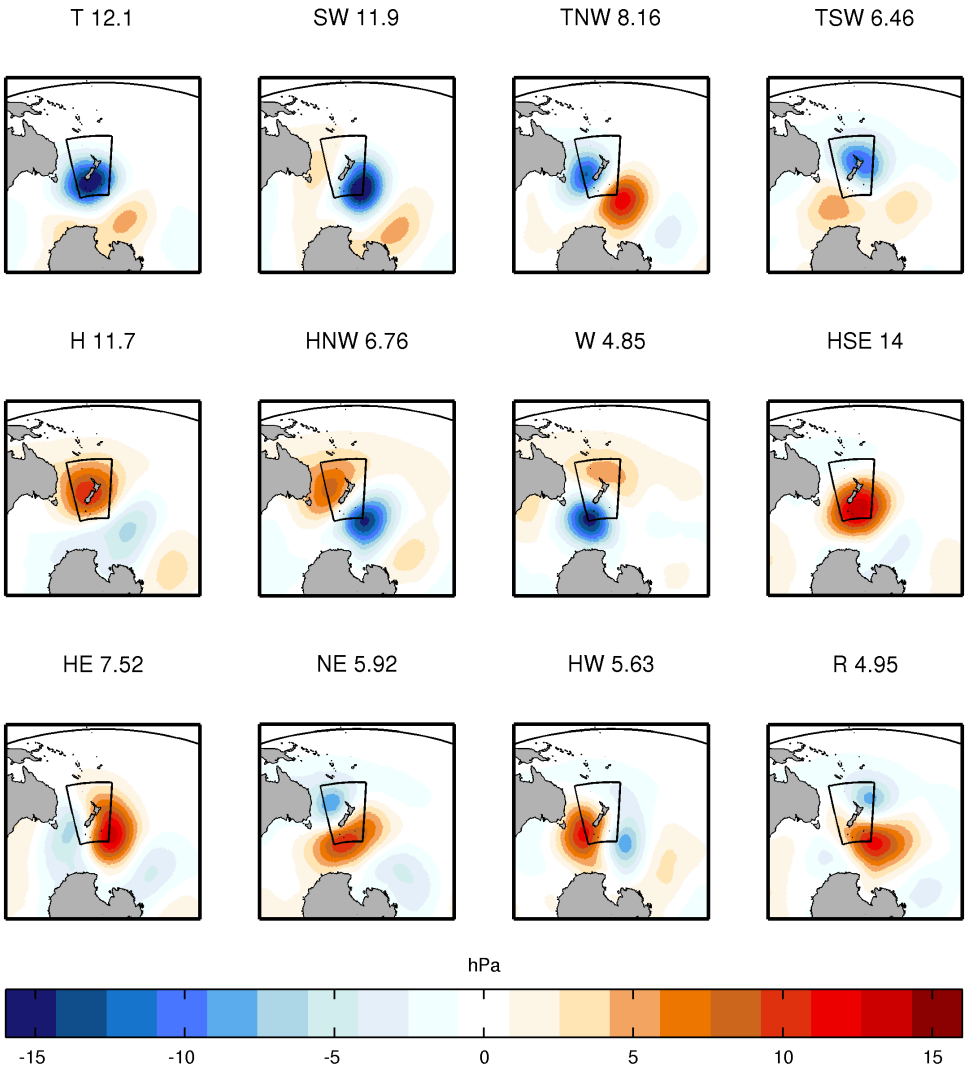

Figure 5.4: Kidson Types Annual MSLP Anomalies in the Southern Hemisphere (altered projection), using ERA-I 1979-2008. The Kidson domain is outlined over NZ. The field is MSLP anomalies in hPa.

5.3.2 *Inter-Annual Variability*

The long term 20CR is used for the analysis of the inter-annual variability. The KTs are aggregated into their three regimes, Trough, Zonal and Blocking. The regime seasonal frequency is determined during the SAM and SOI phases, as these modes of variability have strong seasonal features. The seasons are defined as Summer (DJF), Autumn (MAM), Winter (JJA) and Spring (SON).

The Southern Annular Mode (SAM) indices are presented in Figure 5.5 and in a monthly form in Figure 5.7. The SOI is presented in Figure 5.6. The SAM and SOI indices are both smoothed with a three month (91 day) running mean. The inter-annual variability for the ERA-I reanalysis is displayed in the BACKGROUND Chapter, in Sections 2.3.3 and 2.3.2 for SAM and SOI, respectively.

In Figures 5.5 and 5.6 the upper and lower quartiles are indicated. These quartile partitions are used in determination of the positive, neutral and negative phases of the SAM and SOI. The trend towards a SAM+ phase is clearly evident in Figure 5.5, this is also seen in Figure 5.7 where the SAM+ phase is observed to be more influential in the Summer months, particularly post 1990.

The seasonal regime frequencies derived for SAM+, neutral and Southern Annular Mode Negative Phase (SAM-) and SOI+, neutral and SOI- are presented in Figures 5.8 and 5.9 respectively, each regime is displayed as a separate graph. The frequency of occurrence is displayed and grouped into annual and seasonal frequencies during the phases of each index. The sum of each column in each graph totals to 100%.

Figure 5.8 displays the seasonal regime frequencies of occurrence, during their respective SAMs phases. It is apparent that SAM+ increases the blocking regimes and suppresses the Troughs, as per Renwick (2011). This is particularly evident in Summer and Spring. For SAM- the opposite occurs, Troughs are more common and blocking is reduced, this variation has its largest

variation during Winter and Spring. The Zonal types appear to be less affected by the phases of SAM, as per Renwick (2011). The SOI regimes are displayed in Figure 5.9. During SOI+ Blocking is increased and Trough reduced. Increased variation is seen when the seasons are considered. This is also observed during Summer and Spring.

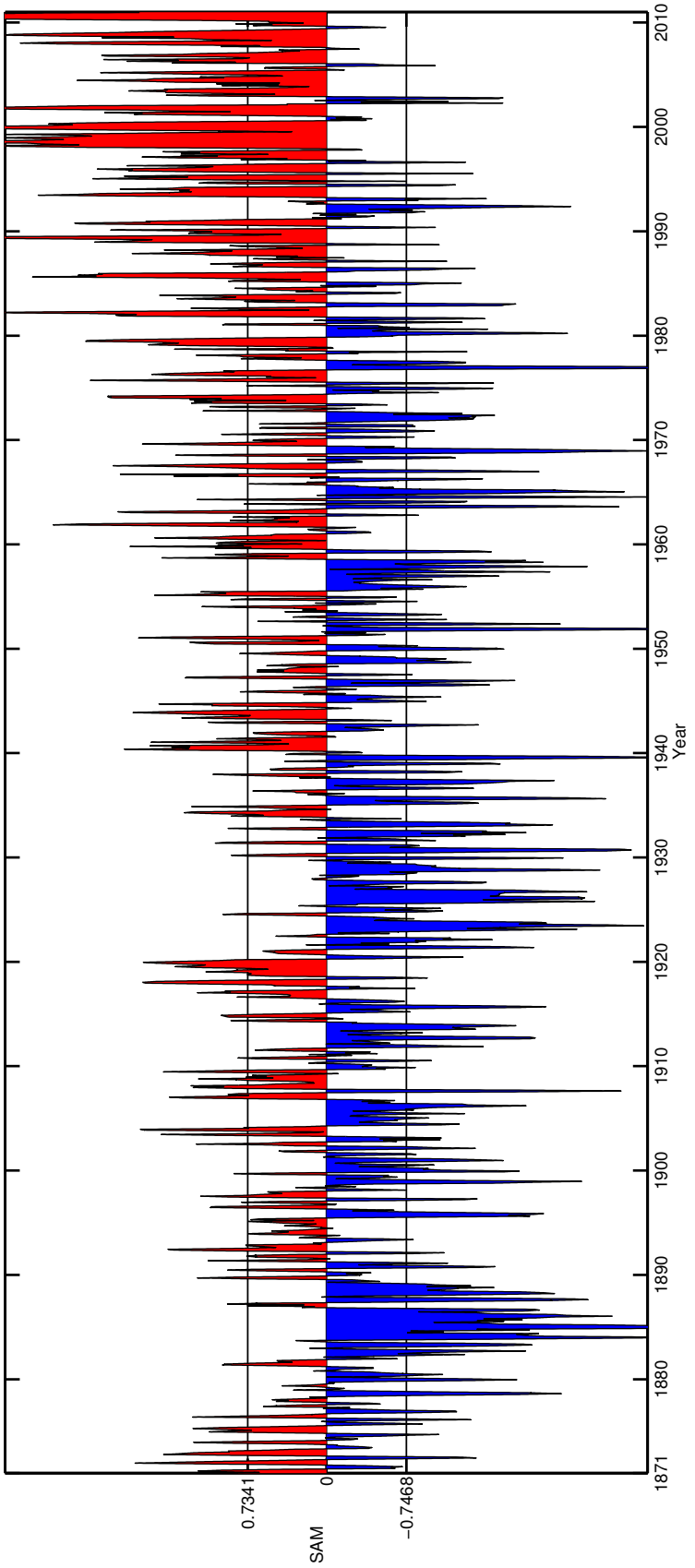

Figure 5.5: SAM Index, 20CR 1871-2010. The black lines indicate the location of the cut off points used in determining the composites and these are defined as the upper and lower quartiles.

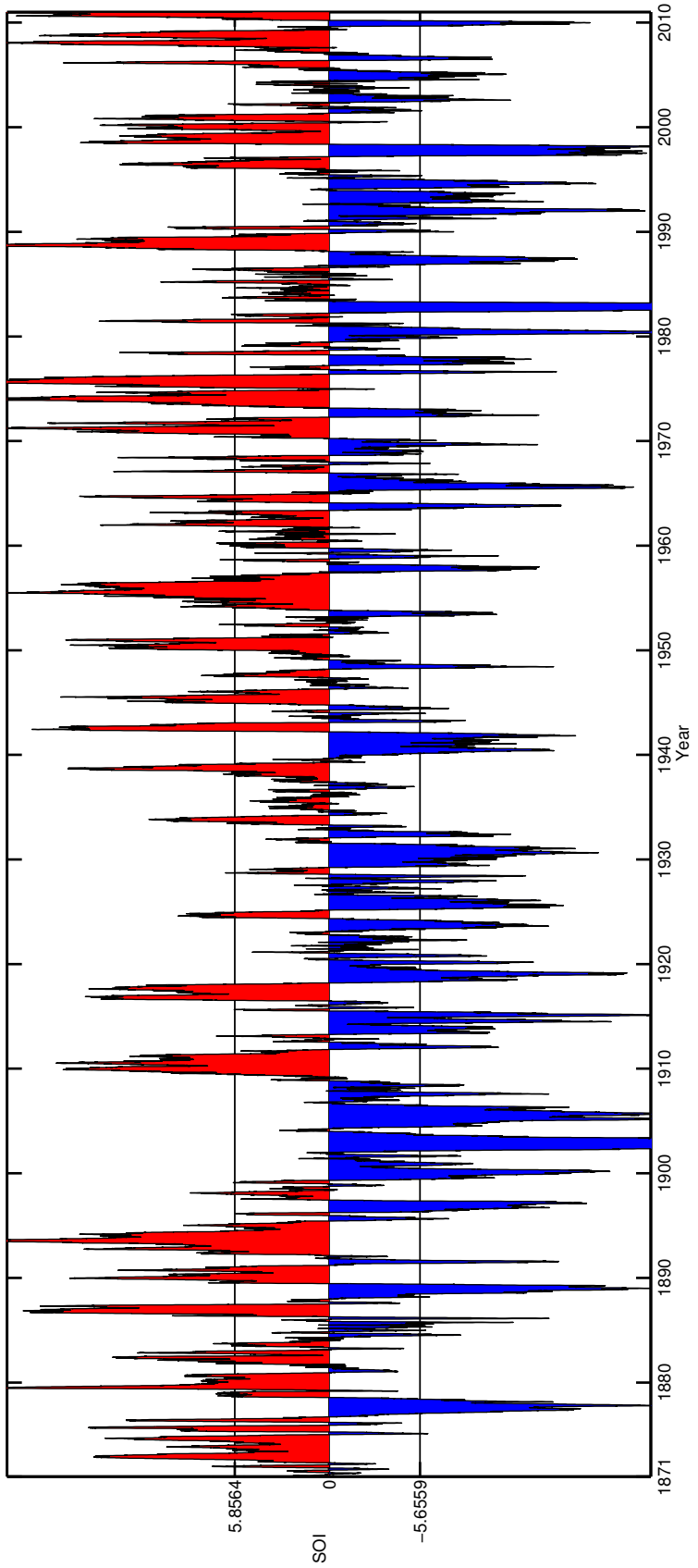

Figure 5.6: SOI, 20CR 1871-2010. The black lines indicate the location of the cut off points used in determining the composites and these are defined as the upper and lower quartiles.

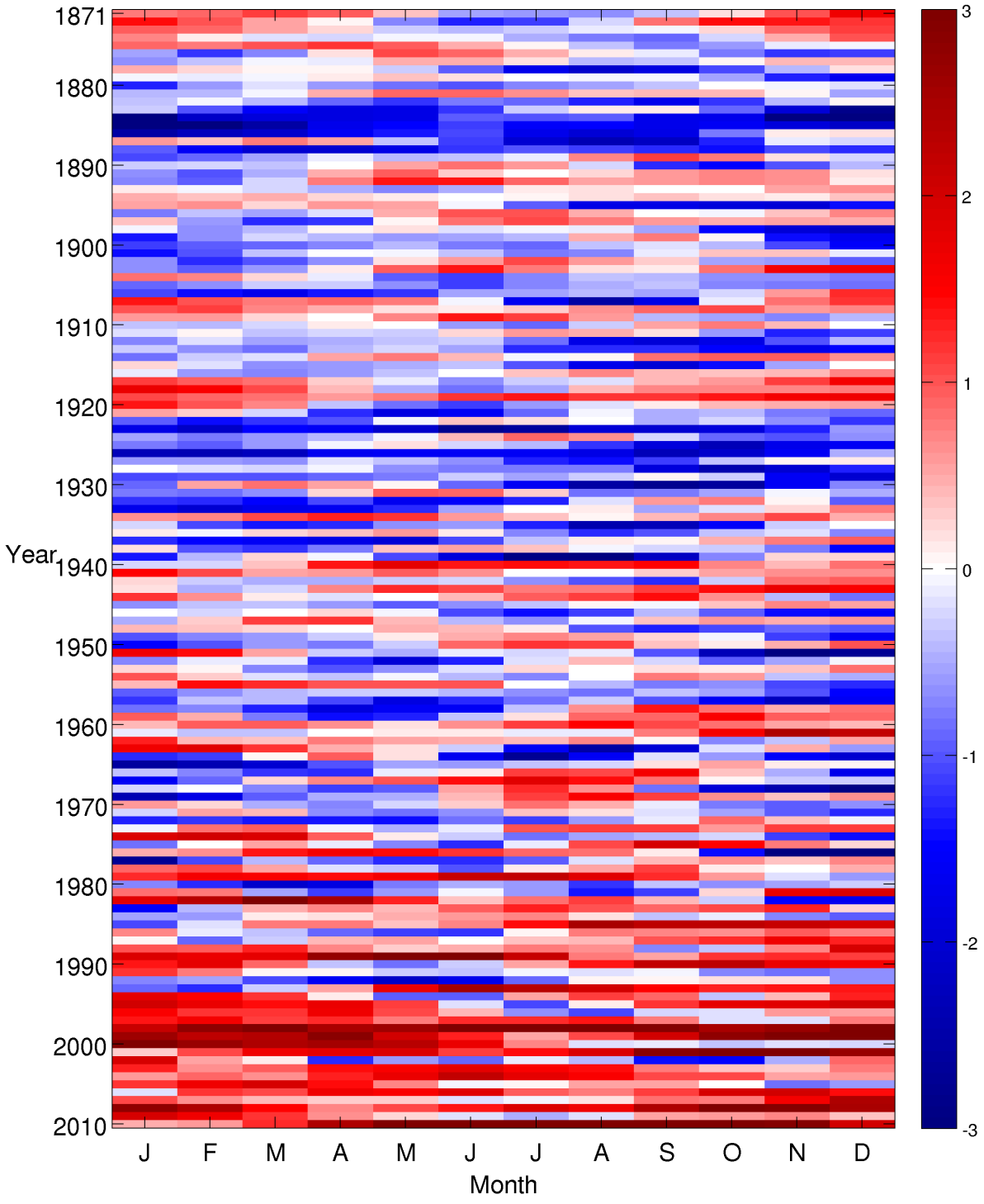

Figure 5.7: Monthly SAM Indices. 20CR 1871-2010

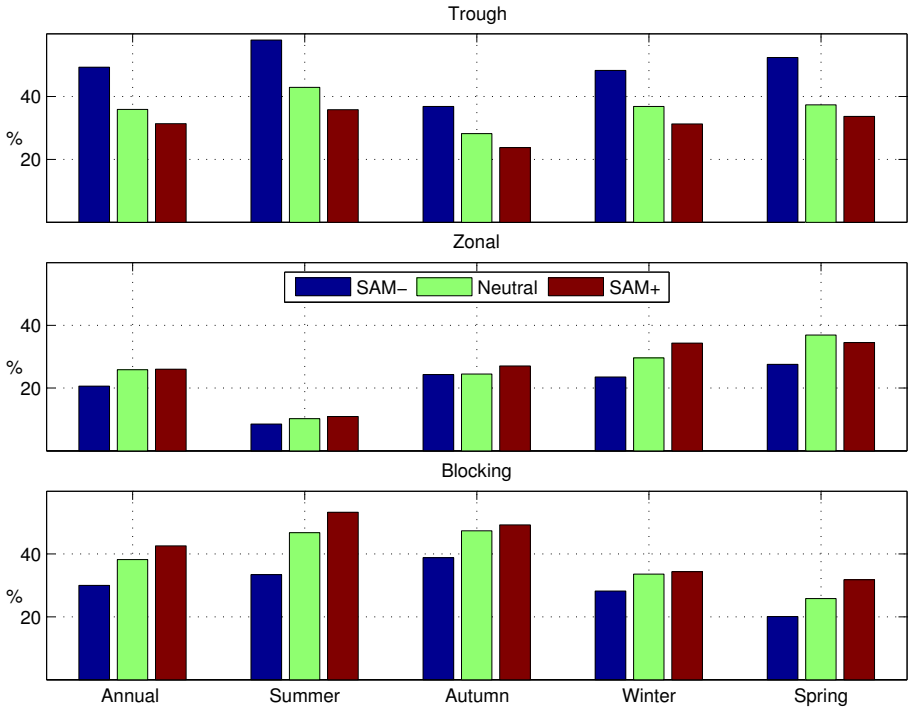

Figure 5.8: Seasonal Regimes during SAM phases. 20CR 1871-2010

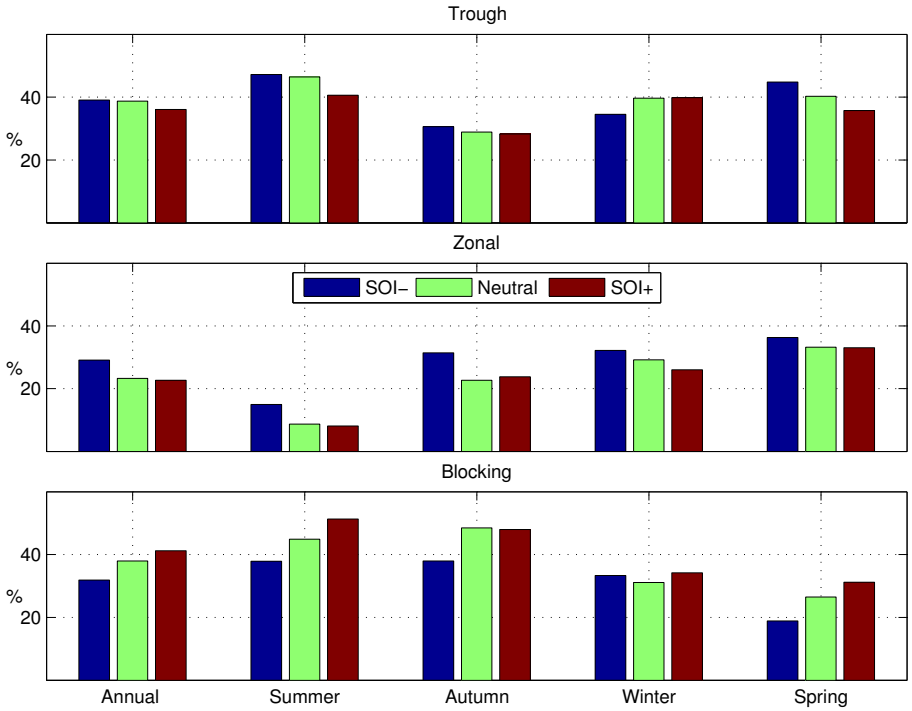

Figure 5.9: Seasonal Regimes during SOI phases. 20CR 1871-2010

5.3.3 *Trend Analysis*

Trends within the frequency of occurrence are of much interest, as the KTs provide a measure of synoptic scale variability, or effectively an objective integrated measure of the weather over NZ. Thus any trends could provide an insightful metric of changing weather patterns, which is the motivation of this thesis. For each calendar year the frequencies of occurrence for each type and regime are determined and the annual frequency is plotted. There is considerable year to year variability observed in the annual frequencies of the types and regimes, and this is observed across all three reanalyses. The individual types can show large trends. However, when the types are aggregated into their regimes these trends are less pronounced.

As different reanalysis data becomes available it is also advantageous to understand if the KTs are portrayed differently in these data. The trends are determined across the entire range of the reanalyses, thus a different length of data for each reanalysis. Therefore, it is expected that different trends will be observed for the different reanalysis in the different periods. Trends are also determined for a subset of overlapping data, 1979-1997, for reanalyses intercomparison.

The Type and Regime trends for the 20CR, are displayed in Figures 5.10 and 5.11 respectively. A t-test is used to determine the significance of the linear regression, the P-value and the R^2 are also displayed. Trends are displayed as a percentage frequency change per decade.

The Type and Regime trends for NCEP1, ERA-I and 20CR are compiled in Table 5.3. Levels of significance are denoted by asterisks, with significance only observed in the 20CR, which is also the longest time series. Discussion on the trends between the different reanalysis output is further elaborated in Section 5.4.

We focus on the regimes and the types with significant trends and the more frequent types, those with an annual frequency of greater than 10%. The four largest occurring types T, SW, H

and HSE, which account for approximately 50% of observed patterns are therefore detailed.

In the NCEP1 reanalysis the types SW and HSE increase and the H and T reduce, these same trends are also observed in the 20CR. In the ERA-I reanalysis the types H and T also reduce. However, there is also a reduction in the SW type.

The NCEP1 reanalysis has an 0.44% per decade increase in Blocking, and a 0.23% per decade increase in Trough regimes. This is compensated by a 0.67% decadal reduction in Zonal frequency. The ERA-I regimes have a reduction in Zonal regimes, -0.27% per decade, and Trough 0.54% per decade. The largest trend is observed in the ERA-I Blocking regime, with an increase of 0.82% per decade.

The regime trends observed in the 20CR reanalysis are reduced when compared to the other reanalyses. The Zonal regime reduces at -0.32% per decade and the Blocking and Trough regimes increases at approximately 0.15% per decade.

Only the 20CR displays statistically significant trends. Within the Trough regime, there is a reduction in TSW and an increase in SW types, both of these trends are highly significant. However, there is no significant change in the Trough regime itself. Likewise within the Blocking regime there are significant type trends, positive (HE and R) and negative (HW), however there is no significant regime trend. However, the 0.32% per decade reduction in the Zonal regime is significant, with types H and W both having significant downward trends.

Table 5.3: Kidson Types and Regimes, Trends (%) per decade. As determined from NCEP1, 20CR and ERA-I. The regime trend is displayed at the end of each regime column. * denotes significance at α 0.05 and ** at α 0.01 levels.

Regime	Type	NCEP1 1958-1997	20CR 1871-2010	ERA-Interim 1979-2008
Trough	T	-0.162	-0.009	-0.541
	SW	0.342	0.364**	-0.010
	TNW	0.288	0.035	-0.172
	TSW	-0.236	-0.223**	0.179
		0.231	0.167	-0.544
Zonal	H	-0.447	-0.163*	-0.256
	HNW	-0.207	0.033	0.518
	W	-0.0146	-0.188**	-0.534
		-0.669	-0.317*	-0.272
Blocking	HSE	0.338	0.144	0.190
	HE	-0.099	0.127*	0.406
	NE	-0.291	-0.089	0.358
	HW	0.236	-0.218**	0.049
	R	0.256	0.186**	-0.181
		0.441	0.150	0.821

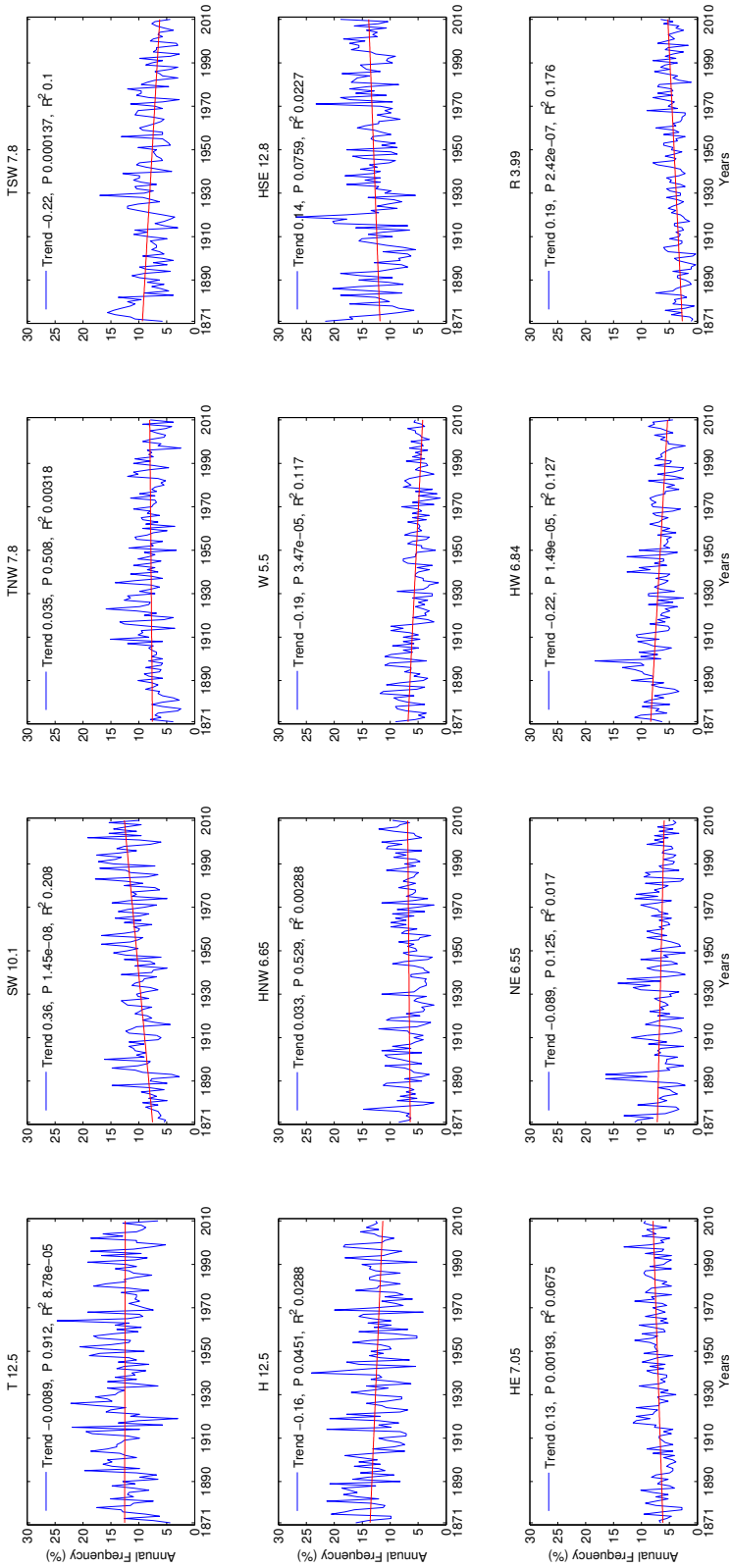

Figure 5.10: 20CR Kidson Type Trends 1871-2010. Frequency of occurrence. Trends are % change per 10 years.

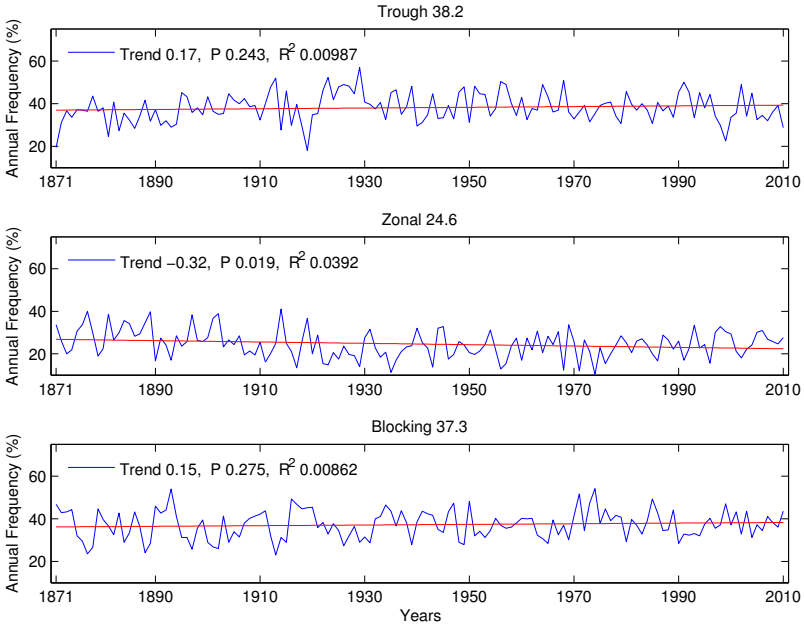

Figure 5.11: 20CR Kidson Regime Trends 1871-2010. Frequency of occurrence. Trends are % change per 10 years.

5.4 DISCUSSION

The KT anomalies when seen within the SH are of interest, as they display a snapshot of the transient synoptic systems within the hemisphere. Figure 5.3 displays the KT MSLP anomalies, as determined from the annual MSLP. Since the KT domain is defined over NZ this region shows the greatest departure from the mean. The SH generally averages out towards the mean further from NZ. The four most common types (T, SW, H and HSE) make up 50 % of the assigned weather patterns. In Figure 5.4 these types display a distinct anomaly over NZ, for T and SW it is negative and for H and HSE positive. Whilst on a hemispheric scale these slight location differences may appear insignificant, on a local level when combined with the orography there can be considerable variation in precipitation and temperature fields linked to these changes (Kidson, 2000; Renwick, 2011).

As seen in Figure 5.4 the annual KT anomalies appear as highs and lows superimposed on the climatological mean. While this in itself is unsurprising, there are other anomalies that are present and further removed from the KT domain which are of interest. Figure 5.12 displays the SW Kidson Type with the Kidson domain placed over NZ. The SW type describes a weather type in which a South Westerly flow is present across NZ. While this flow in itself is not remarkable and is a common occurrence, with an annual occurrence of 11.9 % (ERA-I 1979-2008). The SW has a highly significant increasing trend of 0.364 % per decade, when determined from the 20CR.

The location of an anomalous positive region close to Antarctica, positioned far from the domain, is of interest as Persistent Positive Anomalies (PPAs) or Blocking Events (BEs) are known to occur in this region (Renwick, 2005). They are also known as BEs because of their ability to block, split and or deviate the mean flow. BEs can also be thought of as long lived or slow moving ACs. Figure 5.12 may display evidence of this, whereby positive anomalies deflect/disrupt the mean flow and the resul-

tant affect for NZ is a SW flow across the country, this may also be symptomatic of the South Pacific wave train.

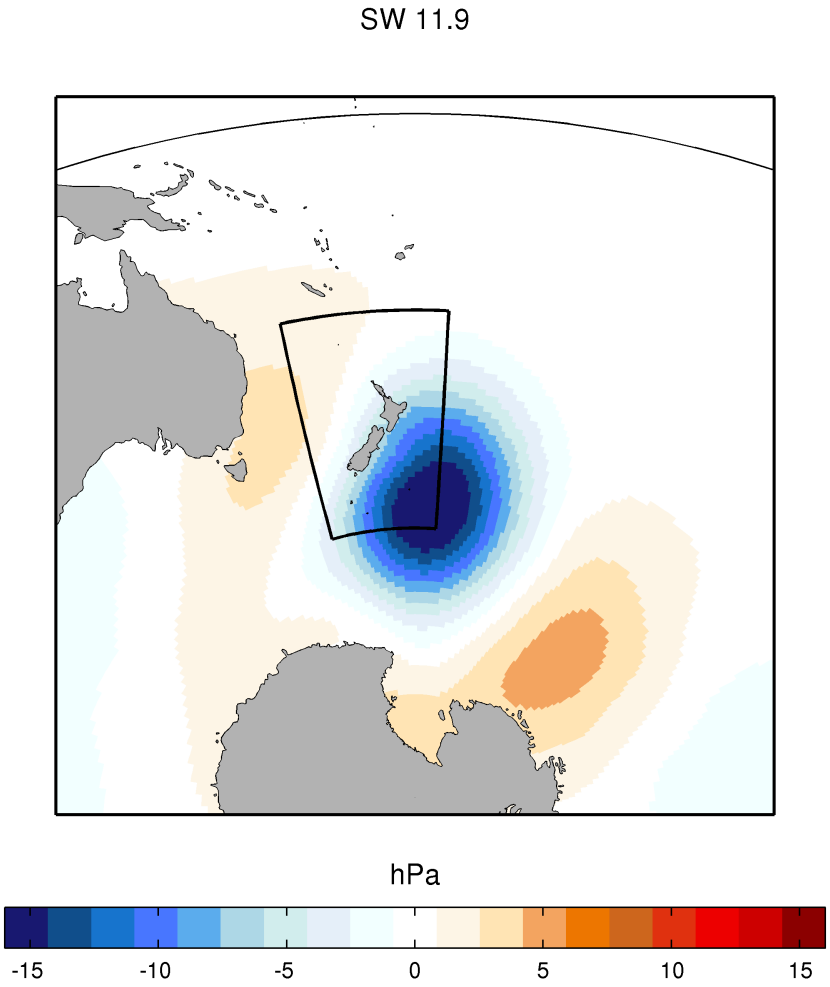

Figure 5.12: Kidson Type South Westerly (SW) Annual Anomaly. Determined from ERA-I 1979-2008.

SAM is an important consideration as the SAM+ trend is projected to continue until the mid 21st century, however as the AOH recovers the Green House Gas (GHG) forcing becomes more important (Arblaster et al., 2011; Christensen et al., 2013). The SAM+ trend is apparent in the 20CR reanalysis, in Figure 5.5. The seasonality of SAM+ is clearly evident in Figure 5.7, where the majority of SAM+ occurs during the Summer. During SAM+

Blocking Regimes increase and Troughs are reduced, the opposite occurs during SAM-.

A reduction in Troughs occur during SAM+ phase, Figure 5.8. As the SAM+ occurs during the later of the 20th century and the ERA-I data range is 1979-2008 this coincides with the majority of the SAM+ events.

To compare the trends observed in the three sets of reanalysis data, they are overlaid on the same plot. Figure 5.13 displays the three regimes with each of the reanalysis overlaid and trend lines fitted. The trend lines are fitted from the full data range, thus the 20CR trend line is fitted from the 1871-2010 data.

There is considerable yearly variability in the Regime frequencies and this is observed in all of the reanalyses. However, when the three reanalyses data sets are overlaid, there is agreement in the pattern of the signal.

The ERA-I Trough Regime trends, shown in Table 5.3 and Figure 5.13, indicate a negative trend of -0.544 % per decade. This negative trend is not observed in the NCEP1 or 20CR reanalyses. The only regime to display a significant trend is the 20CR Zonal regime.

The trends are fitted to different lengths of data, thus it is reasonable to expect different trends in each of the reanalyes. The trends were also examined with a overlapping period of data for this reason.

In Figure 5.14 a subset of overlapping data is used, between 1979-1997. For each of the KTs the gradient, frequency of occurrence and P value from the t-test are displayed. It is visually observable that there is agreement in the annual frequencies between each reanalysis. However, all of the trends have high P values and thus are not significant over this shorter period. The short time series also impedes the statistics, as the 20CR has significant trends as seen in Table 5.3 and Figures 5.10 and 5.11. This may also explain the lack the lack of significant results for the NCEP1 and ERA-I trends.

Figure 5.15 displays the three reanalyses yearly output of the HE type and their trend lines and an overlapping subset, 1979-1997. The 20CR and ERA-I show positive rends, 0.127% and 0.406% per decade, while the NCEP1 has a slight negative -0.098 % trend. There is still good agreement with the three reanalyses after 1979, however less with 20CR and NCEP1 prior to 1979. If the data is constrained to the period 1979-1996, the longest overlap period, then the reanalysis all show agreement with respect to their trends.

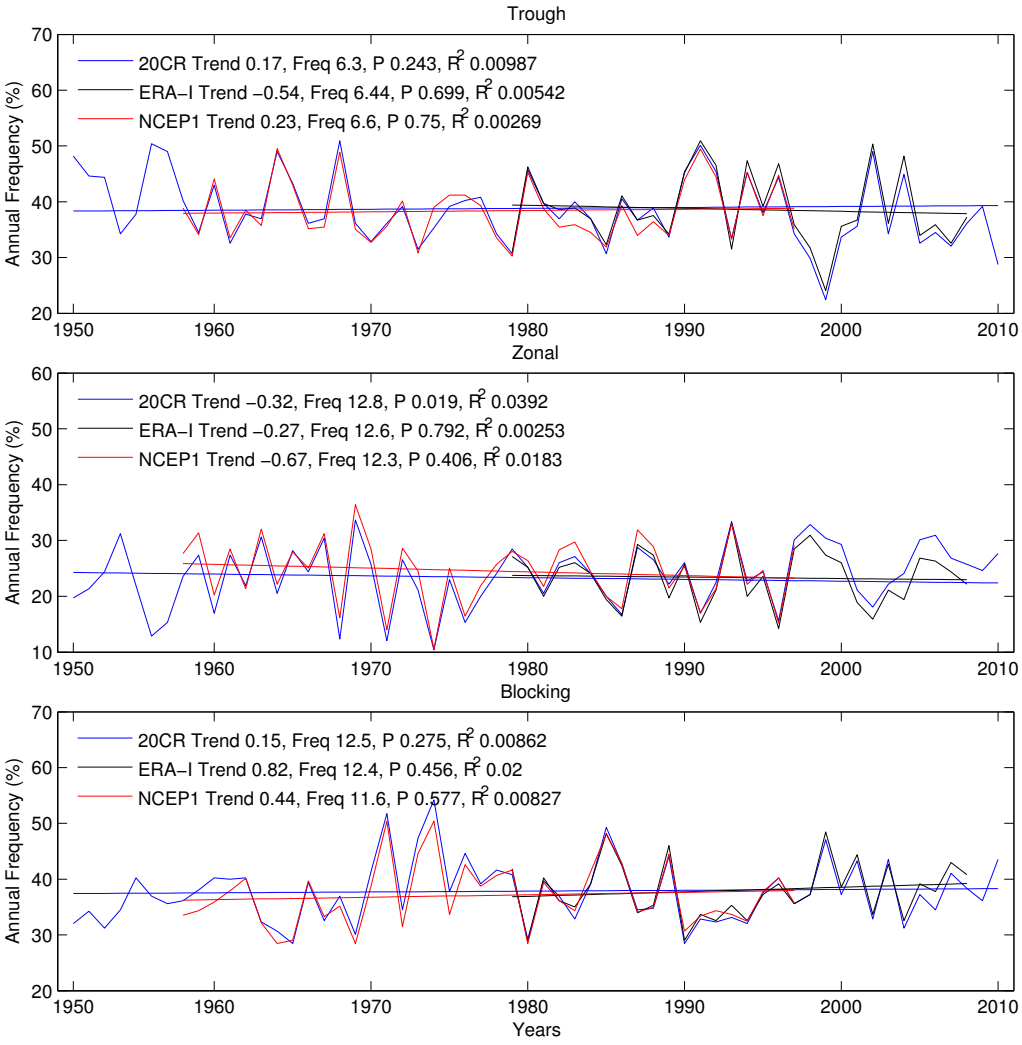

Figure 5.13: Reanalyses Regimes. Trends are % change per decade and fitted over the entire data range.

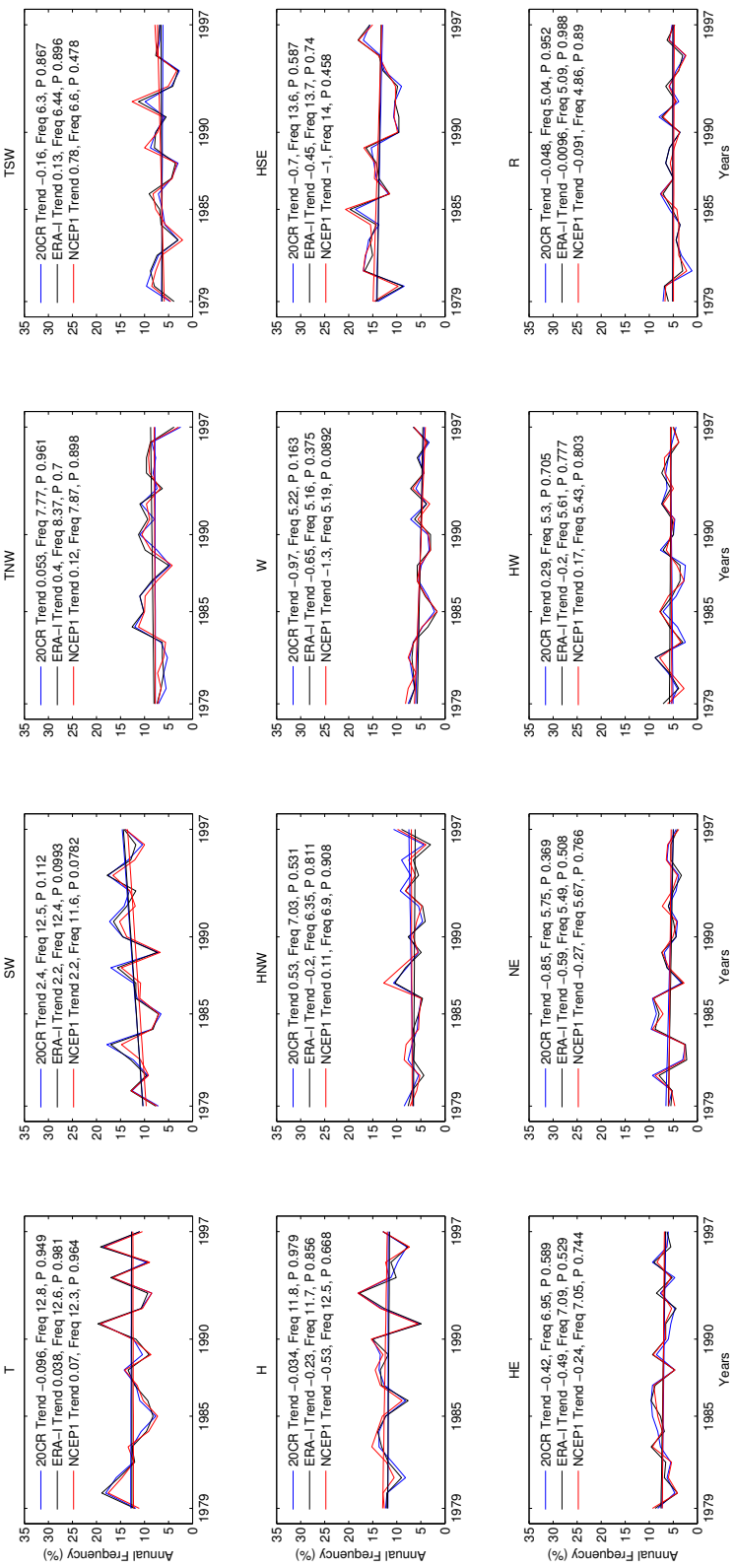

Figure 5.14: Subset 1979-1997 Kidson Type Trends. Frequency of occurrence. Trends are % change per decade.

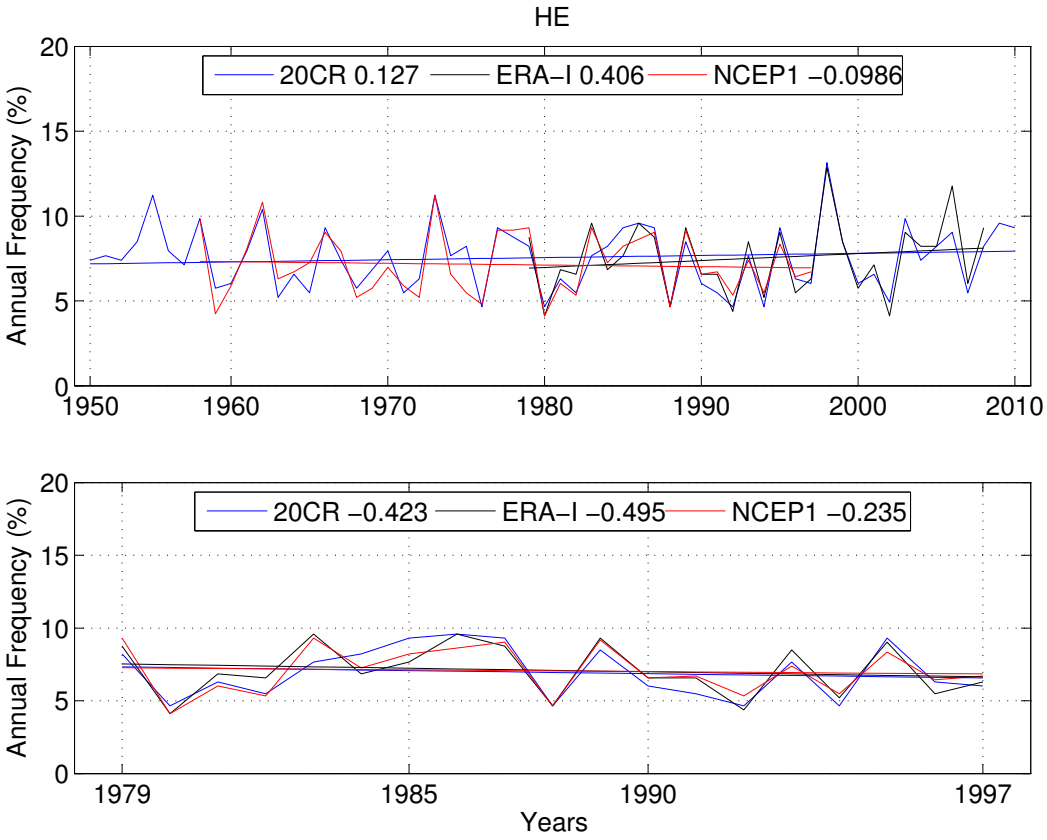

Figure 5.15: HE Trend and subset 1979-1997. Trends are % change per 10 years.

5.5 CONCLUSION

This chapter has detailed a further investigation of the KTs. Three additional analyses have been undertaken using two later generation reanalyses and the original KT NCEP1 reanalysis.

Firstly, the Kidson typing methodology has been expanded to examine composites over the SH, with the use of ERA-I reanalysis data. Allowing the KT patterns to be observed within the context of the larger circulation. As seen in Figures 5.4 and 5.12 anomalies further afield from the NZ and the KT domain are still present. These positive anomalies positioned in the SPO are of interest, as they may be indicative of BEs which are known to perturb the mean flow and primarily occur in this region (Renwick, 2005).

Secondly, the seasonal frequencies of the Kidson Regimes were determined during each phase of the SAM and SOI. The SAM and SOI were analysed using upper and lower quartiles to determine positive and negative phases of the indices. During SAM+ there is an increase in the Blocking Regime and a reduction in Troughs and the Zonal Regime is less affected by SAM+. SAM- increases the Trough Regime, particularly during Summer and Spring. The Blocking and Zonal Regimes are also less frequent during SAM-.

The Trough Regime is less affected by the SOI, with a slight reduction during SOI+. During SOI- there is an increase in the Zonal Regime and a reduction in the Blocking Regimes across all of the seasons and the opposite applies for the SOI+. These results, both SAM and SOI, are in agreement with previous work by Renwick (2011).

Finally, the 20CR reanalysis has been used to investigate trends within the KTs, over an extended period from 1871-2010. Whilst, some of the 20CR KT trends are statistically significant it must be reiterated that there is scarcity of observations in the SH prior to the satellite era, see Section 3.1. The 20CR data set does not suffer from the erroneous data assimilation that occurred in the NCEP1 reanalysis. The observed trends in the 20CR are still

treated with some caution, due to a lack of observational data in the SH during the early period of the reanalysis.

The SW and TSW Types both display significant trends, positive and negative respectively, as seen in Figure 5.10. Both are members of the Trough Regime. However there is no significant trend observed in the Trough Regime. The Zonal Regime is the only regime that exhibits a significant trend, a reduction at −0.32 % per decade. The Zonal regime members H and W both have significant negative trends. The Blocking Regime has no significant trend, however there are trends with its Type members, both positive (HE, R) and negative (HW). The negative Zonal Regime trend is also observed in the NCEP1 and ERA-I output, however it is not significant.

The shorter periods of data from NCEP1 and ERA-I and combined with the highly variable annual frequencies has meant that no trends with statistical significance were determined for these data sets. At times conflicting Type trends are apparent from each of theses reanalyses. Due to the low R^2 care should be taken when assessing the validity of the presented trends. Caution is advisable when using early generation reanalysis data sets, such as NCEP1, when determining trends. As trends may have been overstated, due to the quality of the early reanalysis data and the length of the data. When the Types are aggregated into their Regimes there is agreement with the sign of the trends, apart from the ERA-I Trough Regime.

When trends are fitted to a period of overlapping data (1979-1997), there is more agreement with the observed trends, Figures 5.14 and 5.15, though significance is not observed.

The robustness of the KTs is such that the frequencies and patterns can be easily replicated by different reanalysis data sets and over different time periods. However, as mentioned in Parsons et al. (2014) this robustness and stability may limit the usefulness when investigating climate sensitivity.

The Kidson Types (KTs) are a regional weather typing scheme that has been widely utilised in NZ, see Kidson (2000); Renwick (2011); Parsons et al. (2014) and Chapter 4 and references

within. The KTs can be considered highs and lows, imposed on the mean background flow, as seen if Figure 5.4. While the Kidson Types (KTs) are defined over NZ, some MSLP anomalies are located substantially further from the defining domain. Larger scale phenomena such as BEs located further from NZ can influence local weather patterns, this is the focus of the Chapter 6.

6

BLOCKING IN THE SOUTHERN HEMISPHERE

6.1 ABSTRACT

This study is concerned with Blocking Events (BEs), or Persistent Positive Anomalies (PPAs), in the Southern Hemisphere (SH) and the future projections of these BEs. The ERA Interim (ERA-I) reanalysis is used to compare the historical Coupled Model Inter-comparison Project 5 (CMIP5) output from four General Circulation Models (GCMs) which also simulate the response to the Representative Concentration Pathway (RCP) 4.5 and 8.5 future projections. The historical simulation, CMIP5 output, agrees well with the ERA-I reanalysis for annual and seasonal BE locations and frequencies, with the higher latitudes of the South Pacific Ocean (SPO) being the primary blocking region in the SH and with BEs occurring predominately during winter.

A reduction in BEs is observed in the SPO during the RCP 4.5 projections and this is more pronounced during the 8.5 projections, and occurs predominantly during the summer and spring seasons. The ensemble annual maximum BE frequency from the RCP 8.5 (2071-2100) decreases by 2.4 % (relative 15.7 %), from the historical (1976-2005) maximum of 15.3 %. High BE variability and a lack of model consensus is apparent when the BE data is further scrutinized.

The Southern Annular Mode (SAM) is negativity correlated with the BEs observed in the SPO region, -0.765 during summer and -0.633 in winter. This negative correlation is also observed in

the GCM historical output. However, during the RCP projections this correlation is reduced in three of the models during summer. This suggests that SAM may be less influential in summer time blocking in the future. However, these results need to be tempered by the small GCM ensemble and the high year to year variability in BEs.

6.2 INTRODUCTION

In the midlatitudes of the Southern Hemisphere (SH) the passage of cyclones and anticyclones form the basis of synoptic weather (Trenberth and Mo, 1985). These features have a predisposition to form at certain locations and travel along favored paths, due to a combination of atmospheric and geographical conditions. Blocking is a large scale feature which can exist on longer time scales when compared to other synoptic scale features, thus it can also influence the paths of these transient synoptic scale features (Trenberth and Mo, 1985; Liu, 1994; Sinclair, 1996).

Blocking has been previously defined as occurring when the mean flow is split around the blocking anomaly (Rex, 1950a,b), the deflection of the flow can be detected by gradients in the geopotential height field (Tibaldi et al., 1994; Matsueda et al., 2009). This occurs in the higher latitudes, however in the lower latitudes it tends to be related to subtropical anticyclones (Renwick, 2005). Thus, in the midlatitudes Blocking Events (BEs) can also be thought of as Persistent Positive Anomalies (PPAs) or as long lived stationary/slow moving anticyclonic systems. Whilst these PPAs events may not fit the classic definition of BEs by Rex (1950a) they still embody features of blocking, such as their persistent nature and ability to influence the passage of synoptic scale events. These BEs can be identified by finding PPAs in the data field, a prolonged positive departure from the mean based on a subjective threshold can therefore be used to identify BEs. This methodology has been used in a variety of studies (Dole and Gordon, 1983; Sinclair, 1996; Renwick, 2005) and is utilised in this study.

The underlying mechanisms of blocking are not yet fully understood (Barnes et al., 2012; Cowan et al., 2013; Christensen et al., 2013). However, some mechanisms have been suggested, the blocking system appears to maintains itself by absorbing smaller positive transient eddies through meridional transport from low latitudes, thus maintaining the anticyclonic (positive) anomaly (Trenberth and Mo, 1985; Yamazaki and Itoh, 2009).

In the SH, Zonal Wave 3 (ZW_3) is also thought to reinforce BEs (Trenberth and Mo, 1985; Renwick, 2005; Berrisford et al., 2007). However, the higher zonal wind speed in the SH is also thought to reduce the duration of BEs compared to the Northern Hemisphere (NH) (Trenberth and Mo, 1985; Kiladis and Mo, 1998).

This study is concerned with BEs, or PPAs as defined by Renwick (2005), and the future projections of these BEs in the SH, using General Circulation Model (GCM) output from the Coupled Model Inter-comparison Project (CMIP)5 archive. We are interested in investigating if there is a change in the future BE frequencies and the in geographical distribution.

Initial studies of blocking were motivated by a desire to enhance weather forecasting ability, as these stable long-lived positive features were considered an ideal candidate to assist in providing an extended weather forecast. Blocking can also interrupt the regional weather sequences, thereby causing anomalous weather patterns upstream (Sinclair, 1996). Another reason for their study is that the prediction of blocking has long been difficult and prone to error (Liu, 1994; Tibaldi et al., 1994; Renwick and Wallace, 1996).

The majority of blocking studies have focussed on the NH, which has had the benefit of a higher density observational network for a longer period of time, than the SH. This is primarily linked to the scarcity of observations, particularly in the Southern Ocean (SO) before the advent of satellite data being assimilated into reanalysis products.

In the SH, the mean westerly flow is relatively zonally symmetric compared to the more perturbed NH jet stream, this is due to the lack of topography in comparison to the NH. Weaker and shorter blocking events in the SH are observed, compared to the the NH and strong BEs are generally limited to the South Pacific Ocean (SPO) region (Wiedenmann et al., 2002). New Zealand (NZ) has also been noted as a primary region in which blocking events occur, this region may also be enhanced by quasi stationary planetary waves, ZW_3, (Trenberth and Mo, 1985; Renwick, 2005).

Trenberth and Mo (1985) provided a detailed statistical analysis of the BE frequency and distributions in the SH, BEs were determined from a PPA approach. During winter it is noted that a ZW3 pattern appears to reinforce the BE and also the BEs have a tendency to reform at the same location. Although, as noted in Renwick (2005), they used an early data set that was deficient in detail over much of the SO. Hence, more recent studies with the benefit of later reanalyses must be considered more reliable than Trenberth and Mo (1985).

Sinclair (1996) also provides an overview of anticyclones and blocking, this study used an objective tracking scheme for the anticyclones and a PPA methodology in determination of the BEs. Five day and 6 hPa and 15 hPa anomaly thresholds were used in determining the BEs. Stronger BEs, greater than 15 hPa, were limited to the SPO region and only found during winter.

Oliveira et al. (2013) investigated the role of El Niño - Southern Oscillation (ENSO) and Southern Annular Mode (SAM) on blocking and established a climatology using the NCEP/NCAR1 (NCEP1) reanalysis. However, no statistically significant trends in the blocking were determined within the reanalysis data. However, a significant ($p < 0.05$) reduction in blocking was observed during La Niña events, occurring between longitudes 175°W and 130°W. Additionally the use of the older NCEP1 data set is questionable, as the veracity of the NCEP1 in the SH is considered problematic (Kistler et al., 2001; Marshall, 2003; Simmonds et al., 2003).

Precipitation patterns in Australia have been related to blocking, these have been caused by the BE modifying the position of a subtropical ridge which in turn displaces the mid latitude westerlies resulting in modified precipitation patterns (Cowan et al., 2013). Extreme weather events can also be influenced by these features (Barnes et al., 2012; Dunn-Sigouin and Son, 2013). The location of the BEs can also impede the movement of fronts, which can cause extreme weather events such as flooding by prolonged precipitation as the front stalls overland. Australia is also susceptible to heat waves, drought and wildfires and these have also been linked to BE (Pezza et al., 2011).

The ability of GCMs output to portray BEs has been questionable, as they have previously underestimated blocking frequency (Palmer et al., 2008). This has been linked to the low spatial resolution of GCM, which means that they are not able to accurately represent smaller eddies which are thought to aid the maintenance of blocking anomalies (Masato et al., 2013).

Matsueda et al. (2009), using three different horizontal resolutions (20, 60 and 180km), found only the highest GCM resolution was able to simulate the observed blocking. This could possibly be due to lower resolution not resolving transient eddies, which would in turn give some support to the concept that small eddies have an important role in maintaining BEs.

Barnes et al. (2012) investigated 14 CMIP3 GCMs and determined that the blocking persistence remained constant, however, a significant reduction in blocking frequency was observed in the NH with increased Green House Gas (GHG) forcing.

Barriopedro et al. (2010b) combined previous studies to determine an index which can be applied to a multitude of different studies and this methodology was then applied to reanalysis and GCM output in the NH (Barriopedro et al., 2010a). The GCM underestimated blocking activity and this was linked to the models inability to correctly resolve the strength and position the zonal winds (Barriopedro et al., 2010a). Dunn-Sigouin and Son (2013) investigated blocking in the NH with reanalysis and CMIP5 models, using historical and Representative Concentration Pathway (RCP) 8.5 projections. The CMIP5 models tested were generally able to reproduce the reanalysis blocking climatology. A reduction in blocking was observed in the North Atlantic and North Pacific regions during the RCP 8.5 scenario.

The Antarctic Ozone Hole (AOH) can also influence SAM, as the reduction of ozone in the austral autumn and winter causes a reduction in stratospheric temperature. This temperature reduction then causes a change in the geopotential height, which in turn causes a strengthening of the circumpolar flow (Arblaster and Meehl, 2006; Thompson et al., 2011). Therefore, we might expect some variability in SH blocking and this should be ob-

served due to projected increase in the positive phase, SAM+. However, there are competing forcings, ozone and GHGs. As the ozone depletion recovers GHGs are expected to continue to rise. Ozone is more important in the 20th century, however GHGs will be more important than ozone by the middle of the 21st century (Son et al., 2010; Arblaster et al., 2011; Christensen et al., 2013).

Ho et al. (2012) investigated a variety of SAM indices in relation to Australian precipitation and concluded that they all provide comparable information. However, indices based on station data have the added benefit of a longer time series for historical investigations. There are also well known "issues" with reanalysis products in the southern hemisphere prior to the inclusion of satellite products in 1979, for example SAM is over estimated in the NCEP1 reanalysis (Marshall, 2003). The SAM index used in this is determined with surface pressure zonal mean differences at latitudes 40° and 65°, as described in Gong and Wang (1999).

There is a consensus of observed blocking event climatology in the SH from these different methodologies using reanalysis data, namely the majority of BEs occur in the SPO during winter. The IPCC Fifth Assessment Report (AR5) has noted, with only "medium confidence" that future SH BEs will not increase in frequency, however persistence and intensity of BEs is uncertain (Christensen et al., 2013). The literature is currently deficient in SH GCM blocking studies. Thus, further knowledge of blocking using the latest reanalysis and GCM projections is beneficial to increase confidence and understanding of this important phenomena. Additionally, this study also provides further insight into a process which can potentially impact the weather of NZ.

6.3 METHODOLOGY

6.3.1 *Data*

We use the following data sources in our analysis; ERA Interim (ERA-I) reanalysis (Dee et al., 2011) and CMIP5 GCM output (Taylor et al., 2012), using the historical run and RCPs 8.5 and 4.5 for our future scenarios. RCP 8.5 represents "business as usual", with continuing high forcings and RCP 4.5 is a lower emission future, that rises then stabilizes in the mid 21st century thus assuming some mitigation strategies have been implemented (Moss et al., 2010). We organize the GCM data into 30 year periods; 1976-2005, 2011-2040, 2041-2070 and 2071-2100. The ERA-I reanalysis data is not available before 1979 and the GCM historical data run after 2006, thus there is a 4 year period with no overlap between the historical (1976-2005) and reanalysis (1979-2008).

It was deemed beneficial to have a longer period, at the expense of the 4 year reanalysis/historical non-overlap. This is because we are concerned with any changes in BEs, determined by the difference between each models historical run and its projection. The majority of the analysis is based on the GCM output, thus the 4 year lack of overlap period between the reanalysis and the GCM historical run is of less importance.

The first GCM run/realization is selected when multiple realizations are available. The reanalysis and selected GCMs data has been bi-linearly interpolated to a common grid resolution. This spatial resolution was selected as the coarser of the GCMs used, 1.25 latitude x 1.875 longitude, resulting in a 65 by 192 point grid (12480 data points).

Our SH region is limited to 5°S-85°S. Pressure at Sea Level (PSL) data was utilised due to the availability of this data in the CMIP5 archive at 6hr frequency. This high temporal frequency data was used as it was also required for a forthcoming complimentary study. Previous studies of PPAs and blocking have often utilized higher level data, i.e. 500 mb, however, the patterns

Table 6.1: Data Sources

Model	Institution	Country	Reference
ERA-I	ECMWF	Europe	(Dee et al., 2011)
ACCESS10	CSIRO	Australia	(Bi et al., 2013)
CCSM4	NOAA	USA	(Gent et al., 2011)
HAGDGEM2 ES	MOHC	UK	(Collins et al., 2011)
MIROC5	AORI	Japan	(Watanabe et al., 2010)

seen at this level are also well represented at the surface level (Renwick, 2005).

The model selection, is shown in Table 6.1, and was influenced from work detailed in Mullan (pers. comms.) in which CMIP5 GCMs were ranked by their ability to simulate 62 metrics that are of concern in the SH and to NZ. In chapter 4 the use of a smaller ensemble was beneficial in the synoptic analysis. Thus the decision to use a small ensemble of "good" GCMs that have been tested with consideration given to the SH circulation.

6.3.2 *Blocking*

Our blocking methodology is similar to that of Renwick (2005), hereafter R2005, this form of methodology has also been used in Dole and Gordon (1983) and Sinclair (1996). We define Blocking Events (BEs) to be positive anomalies that exist for an extended period of time, hence Persistent Positive Anomalies (PPAs). The anomaly for each grid point is determined by removing that grid point's overall mean, determined from the full 30 year dataset. Each grid point is then tested to determine if it's anomaly is greater than a subjective threshold (8 hPa). If 5 days worth of consecutive data at that grid point is above the threshold, it is then considered a BE and those 5 days are added to the blocking frequency. Blocking anomalies are defined in relation to the current 30 year time period in question to remove the

Table 6.2: Blocking Thresholds

MSLP Anomaly	2.5 Days	5 Days	10 Days
6 hPa	✔	✔	✔
8 hPa	✔	✔	✔
12 hPa		✔	✔
16 hPa		✔	

potential impacts of changing Mean Sea Level Pressure (MSLP) over the entire record.

A range of thresholds were evaluated, detailed in Table 6.2. The subjective choice of 8 hPa is based on this data exploration, and comparison with the earlier work of R2005 (Renwick pers, comms), and is used for the majority of the analysis. However, 5 days and 16 hPa is also used for some comparison with the work of Sinclair (1996). The largest point of difference in methodology between this work and R2005 is that we use PSL anomalies, our thresholds are 5 days and 8 hPa instead of 500 hPa geopotential height anomalies of a 100m, 5 day threshold. However, R2005 noted that patterns between the 500 hPa and 1000 hPa levels were similar.

A BE is determined, by a continuous positive anomaly lasting at least 5 days, each day of the BE adds to the blocking frequency not just the single event. Thus one 10 day BE is equivalent to two 5 day BEs, in terms of blocking frequency in our analysis. We use an annual frequency of occurrence for GCM intercomparison, this is due to the different amount of days in the data sets, as the reanalysis and GCMs use different calenders, e.g. no leap years or 360 days. The quantity of blocking events are then summed and divided by the total number of days to determine the annual frequency of occurrence for each model and 30 year period. This metric is also used for the seasonal results, with each season displaying the annual percentage of BEs that occur within the three month season. Thus the sum of the seasons equals the annual frequency.

A smaller region in the SPO is used for determination of statistical trends. It is defined as latitudes 45°S - 70°S and longitudes 180°- 270°and is displayed in Figure 6.1 as the red outlined domain. The mean frequency of occurrence is determined in this region.

6.4 RESULTS

Our primary concern is the investigation of future BEs. We focus our analysis and discussion on the differences between the GCM historical runs and RCP projections. The reanalysis data is predominantly used to compare our results with previous work and the GCM historical runs, to identify the integrity of the results from the various GCMs.

The differences are determined between the historical and future projections for each of the individual models. The mean of the four model differences are then presented and reported as an absolute percentage. Thus a frequency of 10 % represents $\approx$ 36.5 days of blocking activity and an anomaly of -5% a reduction of $\approx$ 18.25 days. The seasonal results are reported in a similar manner, however the as a seasonal percentage.

The results and discussion focus on the 8 hPa threshold unless otherwise stated. In Figure 6.1 the red outline displays the SPO region, latitudes 45°S - 70°S and longitudes 180°- 270°, which is used in further analysis in Section 6.4.5.

6.4.1 *Reanalysis*

The ERA-I 1979-2008 annual frequency of occurrence of BEs is displayed in Figure 6.1, as a percentage of annual occurrence. The BE maximum is observed in the SPO, located at 60°S and between 135° - 90°W. These patterns have been observed in a number of previous studies, (Kiladis and Mo, 1998; Sinclair, 1996; Renwick, 2005).

The seasonality of BEs is displayed in Figure 6.2. The majority of BEs occur during Winter (JJA), in the SPO at 60°S and between 135° - 90°West, in the same region as observed in the annual pattern. Autumn displays the next highest frequency of occurrence. The location of the maximum is still in the SPO, though reduced in intensity. The blocking activity also extends south of Australia, centered at 45°S to 90°E into the Indian Ocean (IO). During summer (DJF) the highest frequency of BEs occurs poleward of 60° S, peaking in the SPO, close to the Ross Sea. Another band of BE is centered on 45°S between 90°W - 90°E. Spring (SON) has the least BEs when compared to the other seasons. Though, the spring BE maximum is still located in the same SPO region, although this maxima is more diffuse than in other seasons. Secondary regions are also present to the east of NZ and in the South Atlantic Ocean.

A higher threshold of 16 hPa was also tested. With this threshold, blocking is limited to the SPO and occurs primarily during the winter, Figures 6.3 and 6.4 respectively. This agrees with the findings of Sinclair (1996), who also found BEs to be limited to the SPO and winter when using a high threshold of 15 hPa.

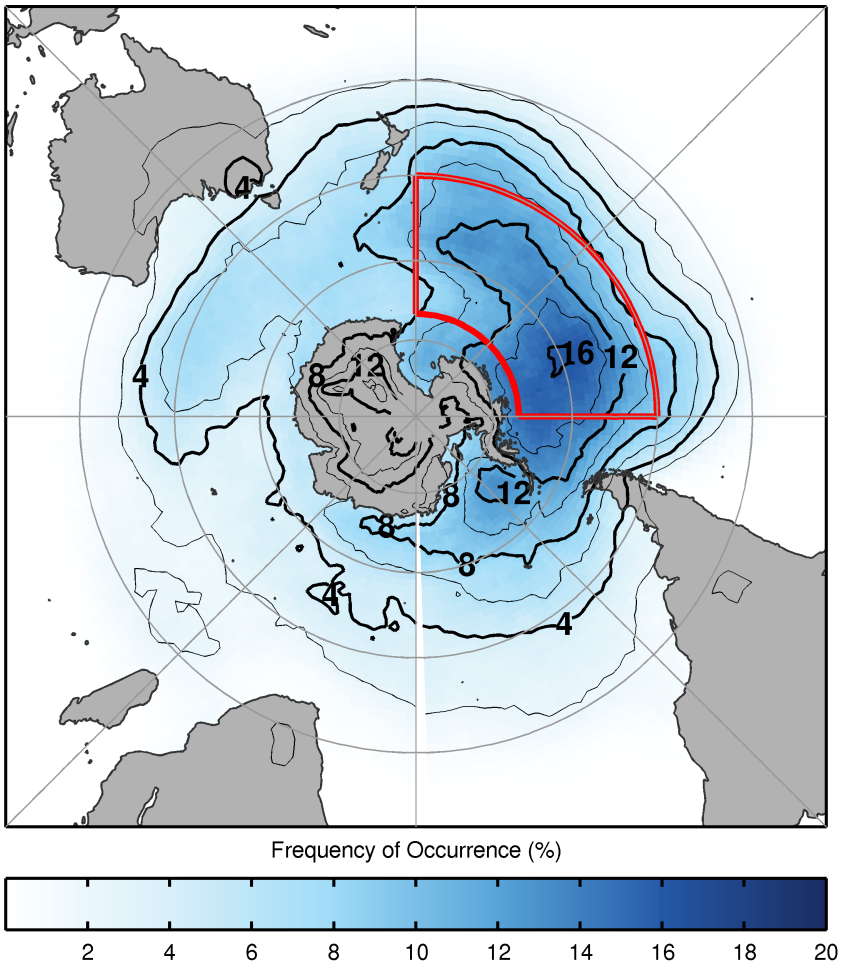

Figure 6.1: ERA-Interim BE 1979-2008. Annual mean frequency of occurrence (%). The contour interval is 2, starting at 2, and every second contour line is thickened and labelled. The red outline displays the SPO region, latitudes 45°S - 70°S and longitudes 180°- 270°, used in further analysis in the discussion.

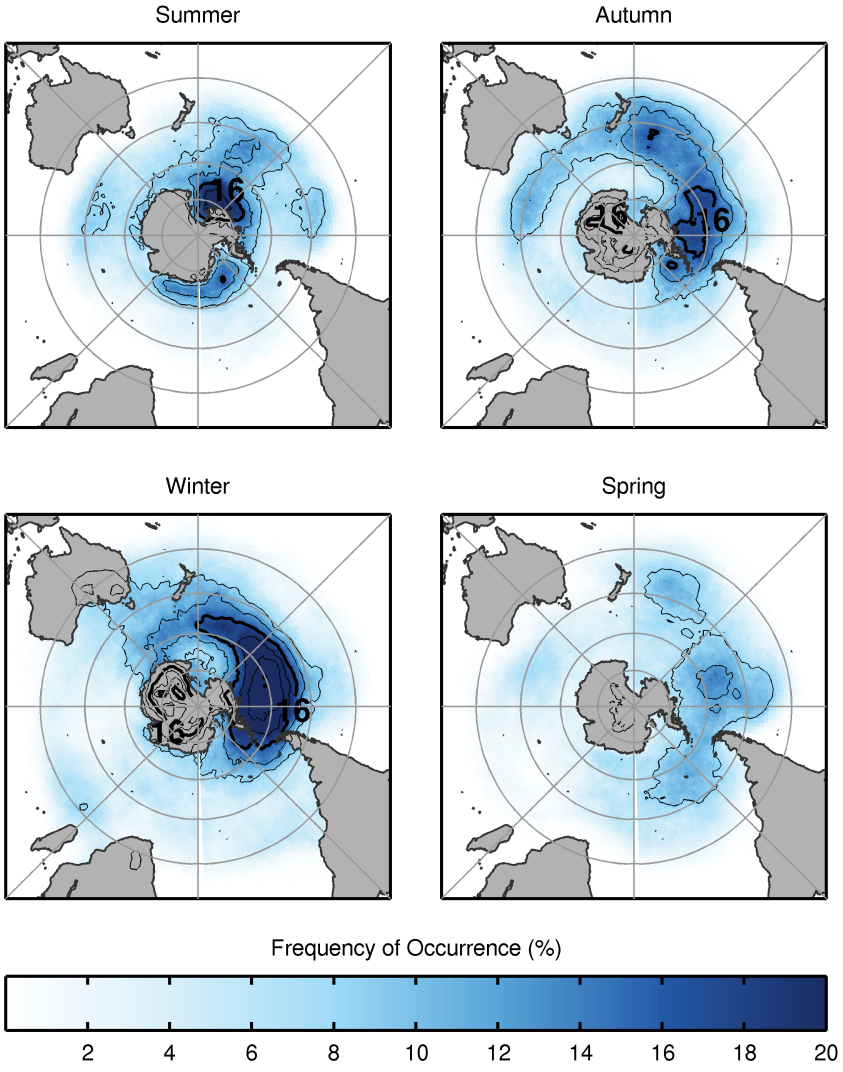

Figure 6.2: ERA-Interim BE 1979-2008. Seasonal mean frequency of occurrence (%). The contour interval is 4, starting at 8, and the 16 contour line is thickened and labelled.

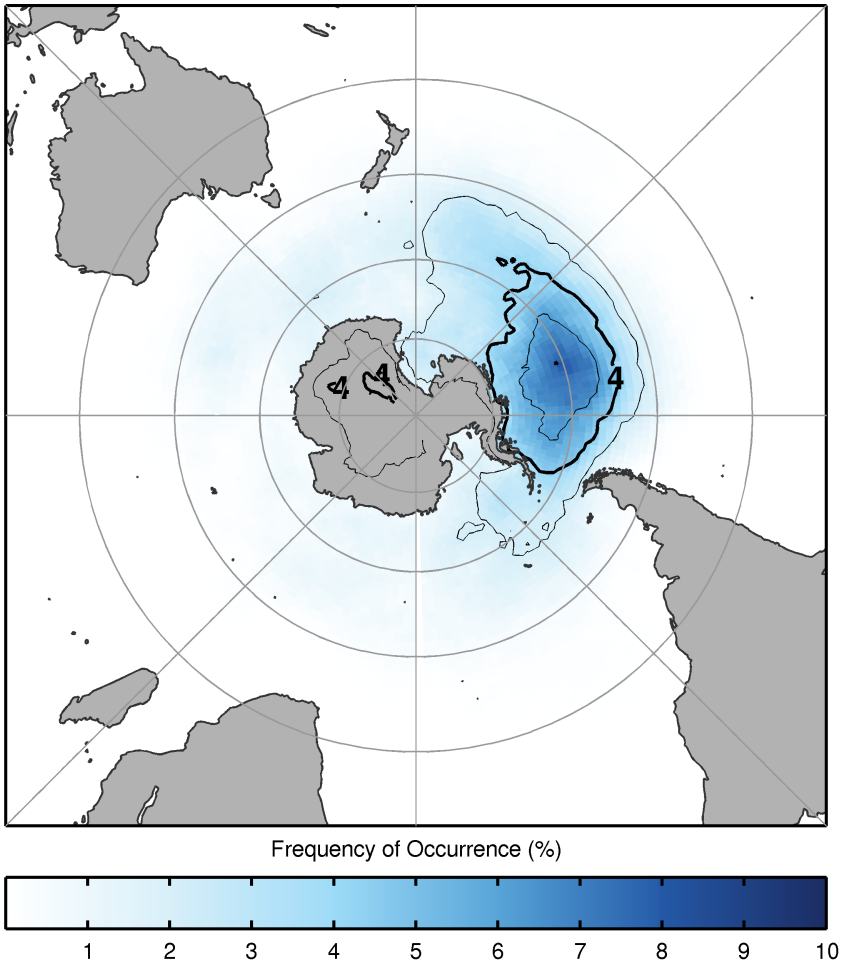

Figure 6.3: ERA-Interim BE 1979-2008. High threshold (16 hPa) annual mean frequency of occurrence (%). The contour interval is 2, starting at 2, and every second contour line is thickened and labelled.

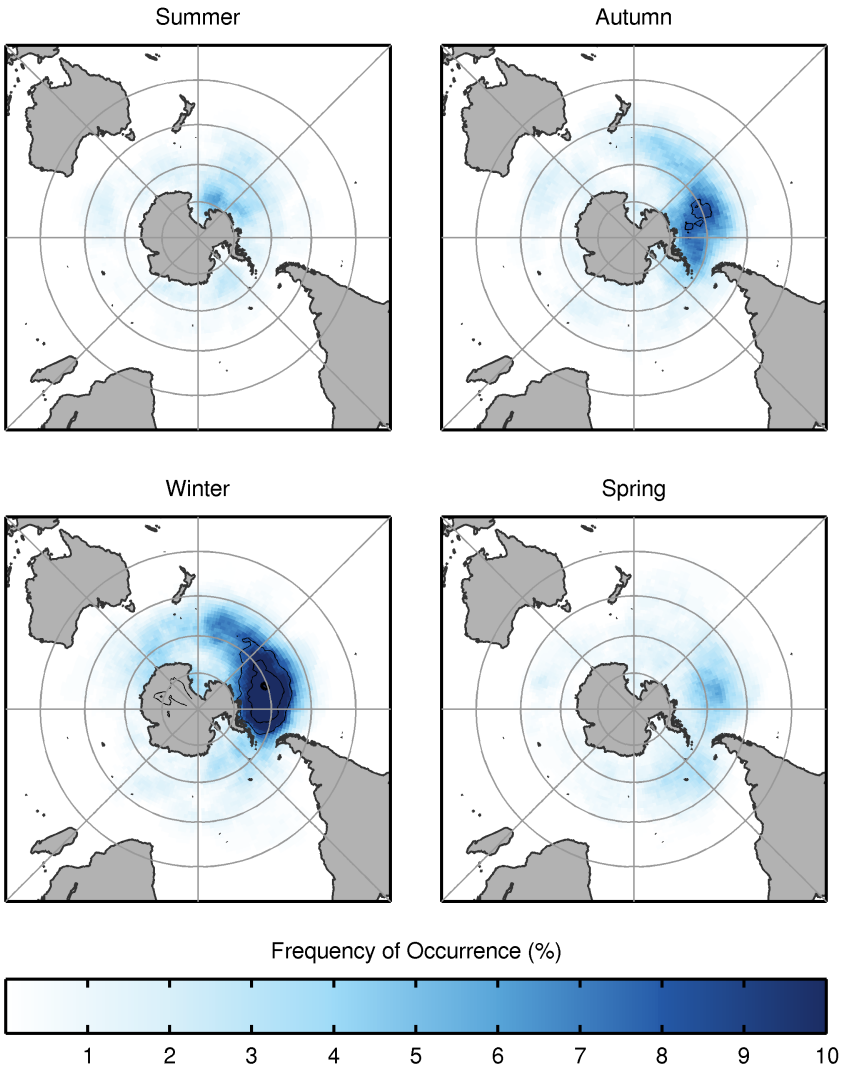

Figure 6.4: ERA-Interim BE 1979-2008. High threshold (16 hPa) seasonal mean frequency of occurrence (%). The contour interval is 4, starting at 8, and the 16 contour line is thickened and labelled.

6.4.2 *GCM Historical Output*

We now examine the BEs from the GCM historical output and compare them with the reanalysis to determine the quality of the representation of BEs, as an ensemble and individually. The ensemble annual and seasonal means are presented first, then the higher 16 hPa threshold and finally the individual GCMs. The correlation coefficient between the historical GCM and ERA-I output is displayed above the Figures and used as a comparative measure of the spatial pattern, this information is also presented in Table 6.3.

The mean of the GCM historical runs are displayed in Figure 6.5. A similar distribution as seen in the reanalysis is apparent, with the maximum located in the SPO at 60°S, however, the BE frequency is reduced in the ensemble of the four model runs compared to that derived from the ERA-I reanalysis. The GCM historical BEs also extend further into the IO and South Atlantic Ocean than the reanalysis, effectively circumnavigating Antarctica at 45°S. Despite these small variations the GCM ensemble, Figure 6.5, spatial pattern and frequency compares well with the ERA-I reanalysis, Figure 6.1, as shown by the correlation of 0.976.

The seasonal GCM historical BE frequencies are displayed in Figure 6.6. As in the seasonal reanalysis, Figure 6.2, the highest frequency of BEs occur during winter and these BEs are also predominantly located in the SPO between 45° - 60°S and 135°W - 90°E. However, in the historical output the band of BEs between 45° - 60°S extends further east. Spring also has a more diffuse distribution than the reanalysis, with higher occurrence BEs in the SPO. Summer also has a maximum occurrence of BEs poleward of 60°S, surrounding the coast of Antarctica. Secondary regions of elevated BEs are approximately centred on 45°S in the South Pacific (SP) and 90°E in the IO. During autumn a more annular structure of BEs occurs and is centred on 45°S, with a maximum at 90°W. With the seasonal correlations ranging between 0.922 - 0.930, which is slightly less than the annual results at 0.976.

Figure 6.7 displays the ensemble annual mean for the higher 16 hPa threshold. As previously there is a high correlation of 0.957 with the reanalysis, Figure 6.3, and the BEs occur in the SPO. The seasonal GCM historical high threshold ensemble is displayed in Figure 6.8 with correlations ranging between 0.864 and 0.921. As seen previously, BEs are more frequent in the SPO and during winter.

We now consider the response of the individual GCM in the ensemble, these results are also displayed in Table 6.3. The annual correlation coefficients between the each historical GCM run and the reanalysis are above 0.953, Figure 6.9, which compares well with the ensemble mean of 0.976. Thus, the GCMs are capable of emulating the broad scale BE patterns observed in the SH. However, as we increase our temporal resolution from annual to seasonal, greater disparity between the reanalysis and GCM output is evident, as seen in the reduced correlation coefficients.

Figures 6.11 and 6.12 display the GCM output for summer and winter during the 8hPa threshold, respectively. MIROC5 displays the lowest BE frequency of the ensemble during summer and the largest during winter. Figure 6.13 displays the higher 16 hPa threshold during winter from the four GCMs, as seen in the 8hPa results MIROC5 displays a highest frequency of BEs.

Based on the correlation coefficients in Table 6.3 the four model ensemble out performs any of the individual model during the annual or seasonal periods. This clearly shows that the GCM ensemble is capable of generating the observed blocking as geographical patterns do not change appreciably. However, MIROC5 appears positively biased during winter and negativity biased in summer when compared to the other GCMs. We will only discuss results using 8 hPa threshold from this point on.

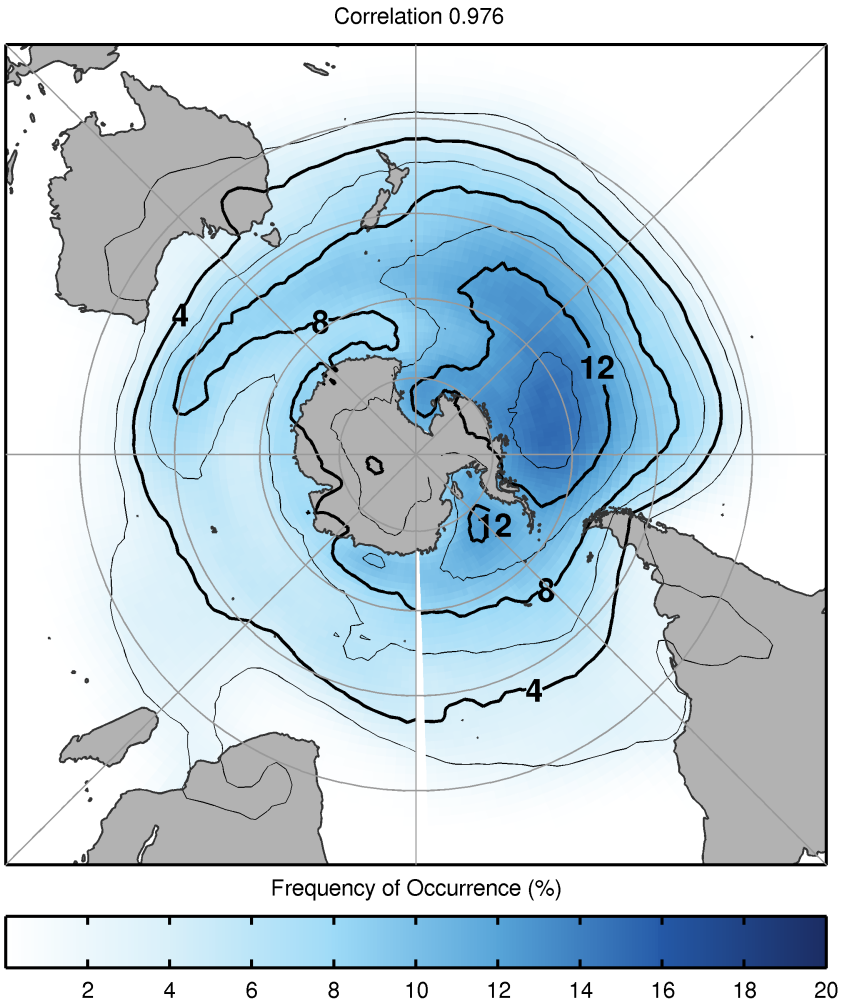

Figure 6.5: Historical GCMs BE Ensemble Annual Mean 1976-2005. 8 hPa threshold, Annual mean frequency of occurrence (%). The contour interval is 2, starting at 2, and every second contour line is thickened and labelled. The correlation with the reanalysis is also displayed at the top of the figure.

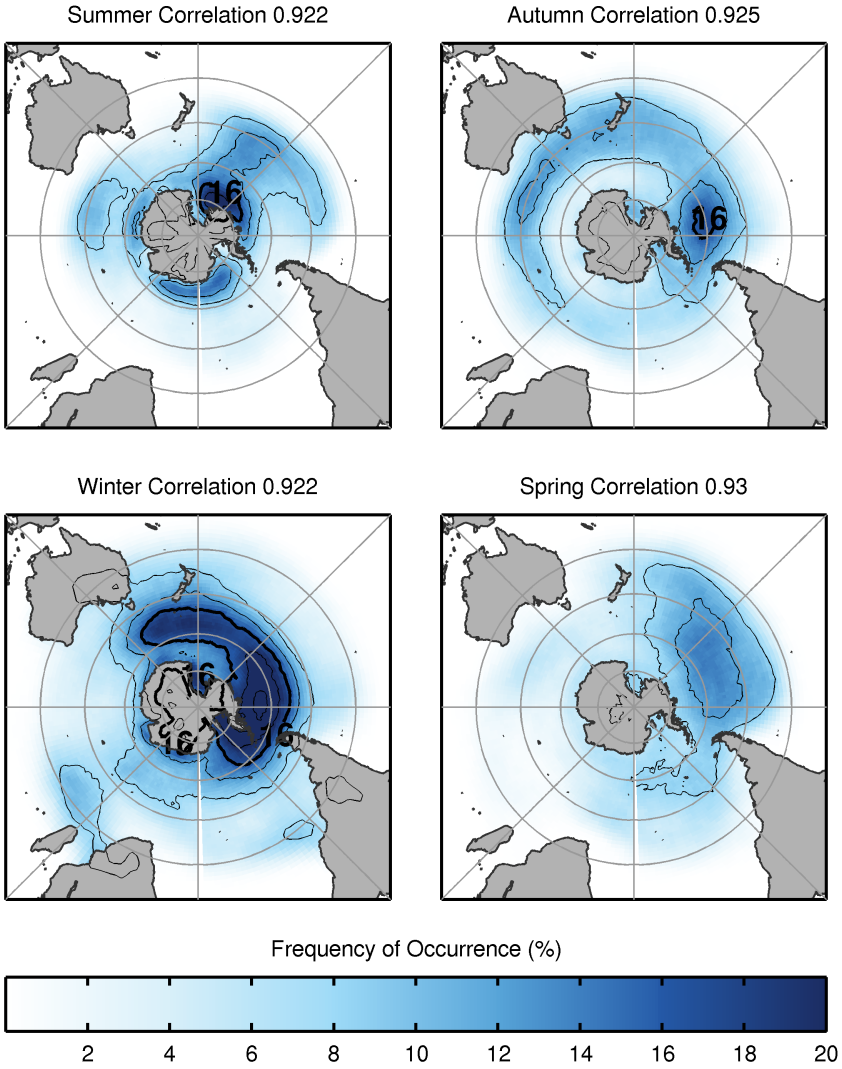

Figure 6.6: Historical GCMs BE Ensemble Seasonal Mean 1976-2005. 8 hPa threshold, Seasonal mean frequency of occurrence (%). The contour interval is 4, starting at 8, and the 16 contour line is thickened and labelled. The correlation with the reanalysis is also displayed at the top of the figure.

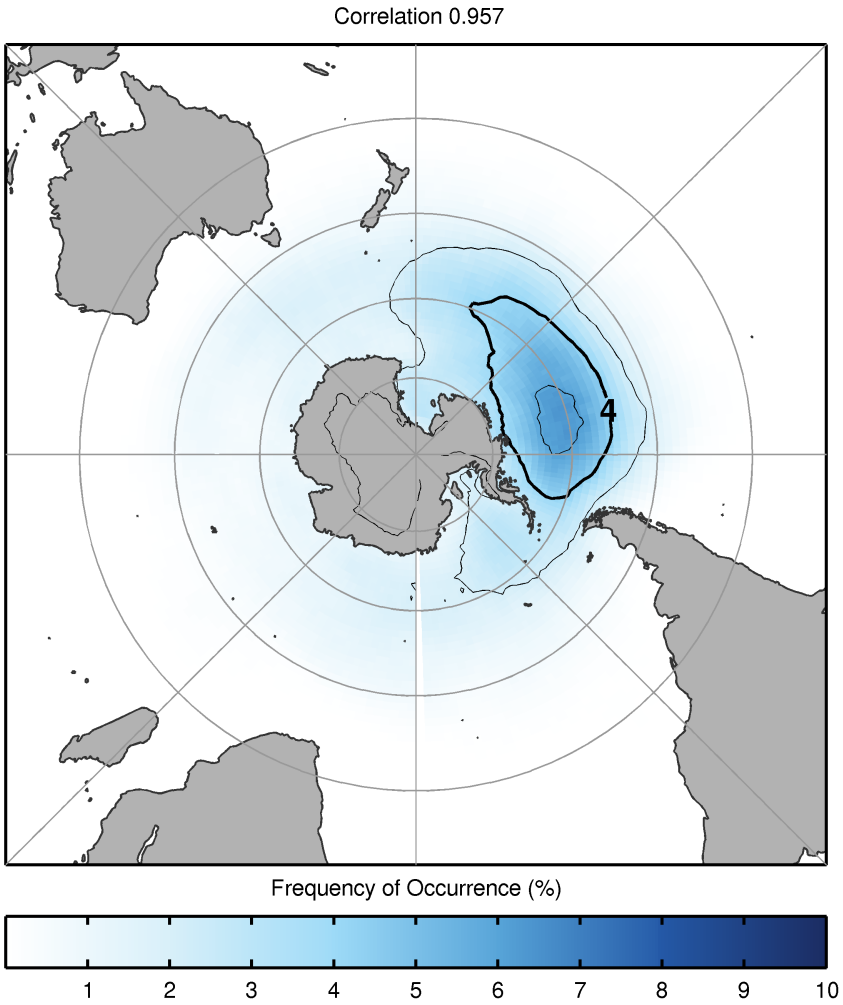

Figure 6.7: Historical GCMs BE Ensemble Annual Mean 1976-2005. High threshold (16 hPa) Annual mean frequency of occurrence (%). The contour interval is 2, starting at 2, and every second contour line is thickened and labelled. The correlation with the reanalysis is also displayed at the top of the figure.

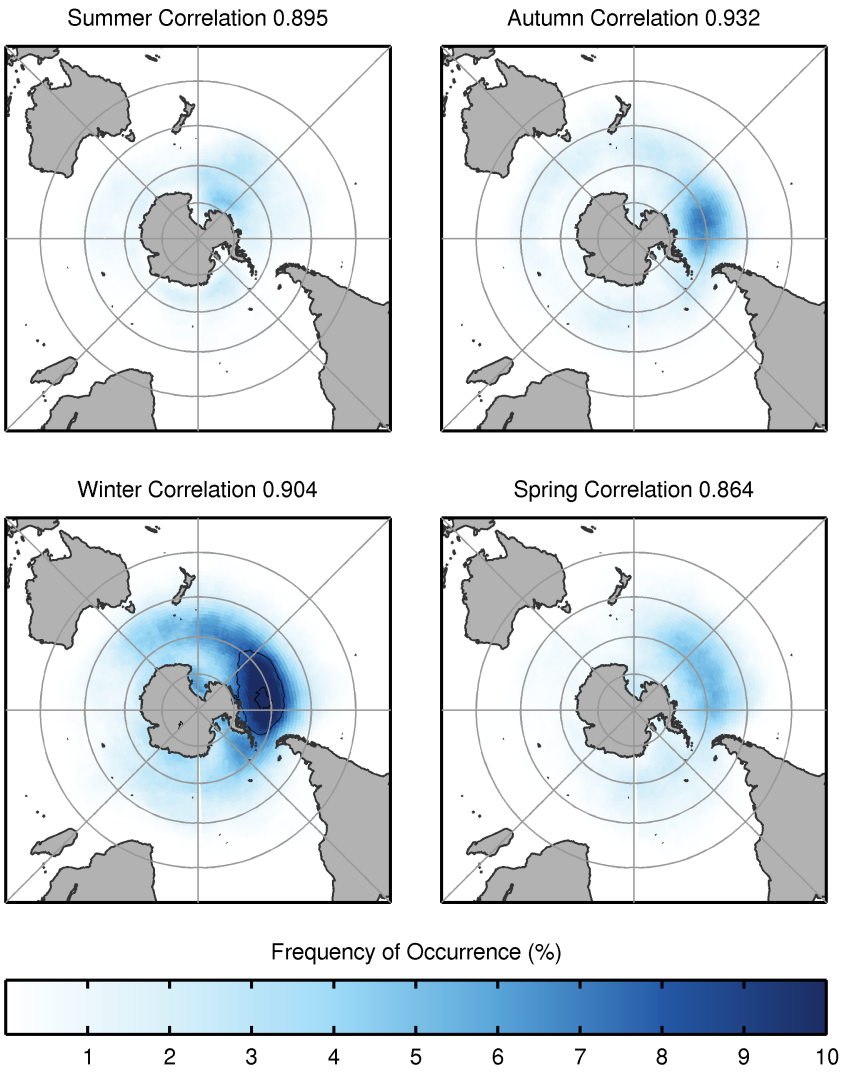

Figure 6.8: Historical GCMs BE Ensemble Seasonal Mean 1976-2005. High threshold (16 hPa) Seasonal mean frequency of occurrence (%). The contour interval is 4, starting at 8, and the 16 contour line is thickened and labelled. The correlation with the reanalysis is also displayed at the top of the figure.

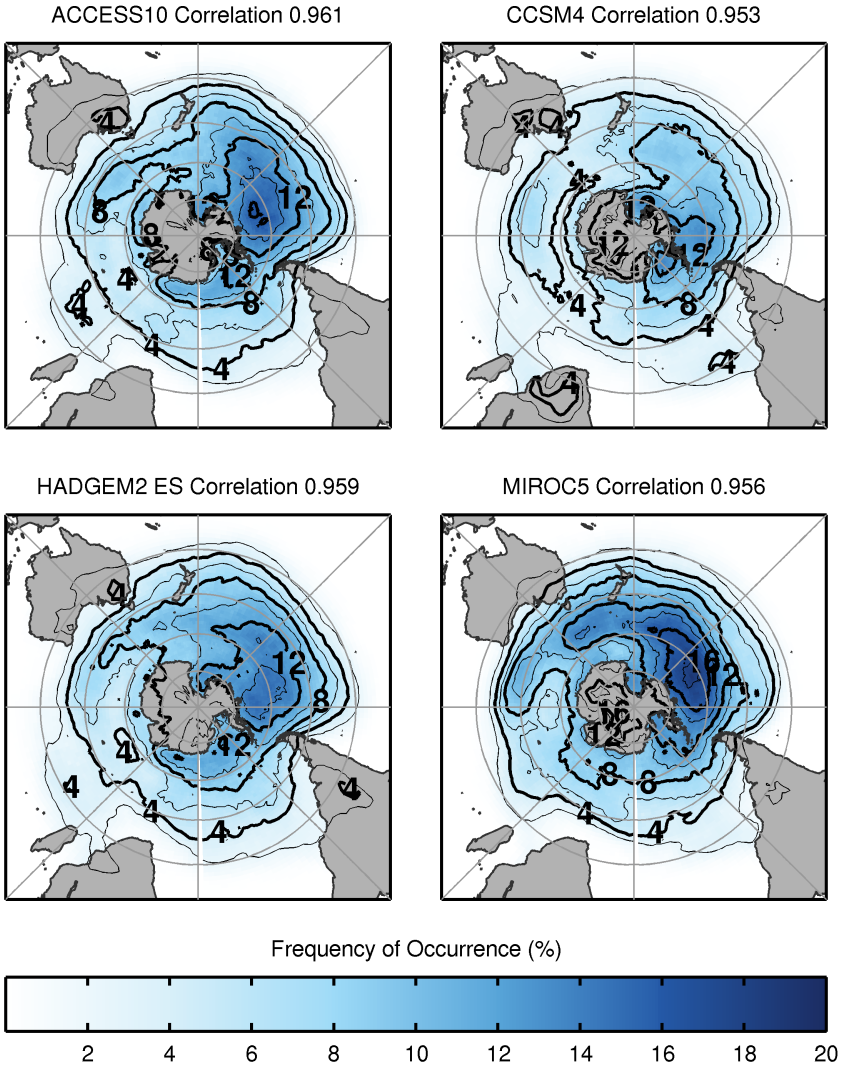

Figure 6.9: Historical GCMs BE Annual mean frequency of occurrence (%). The contour interval is 2, starting at 2, and every second contour line is thickened and labelled. The correlation with the reanalysis is also displayed at the top of the figure.

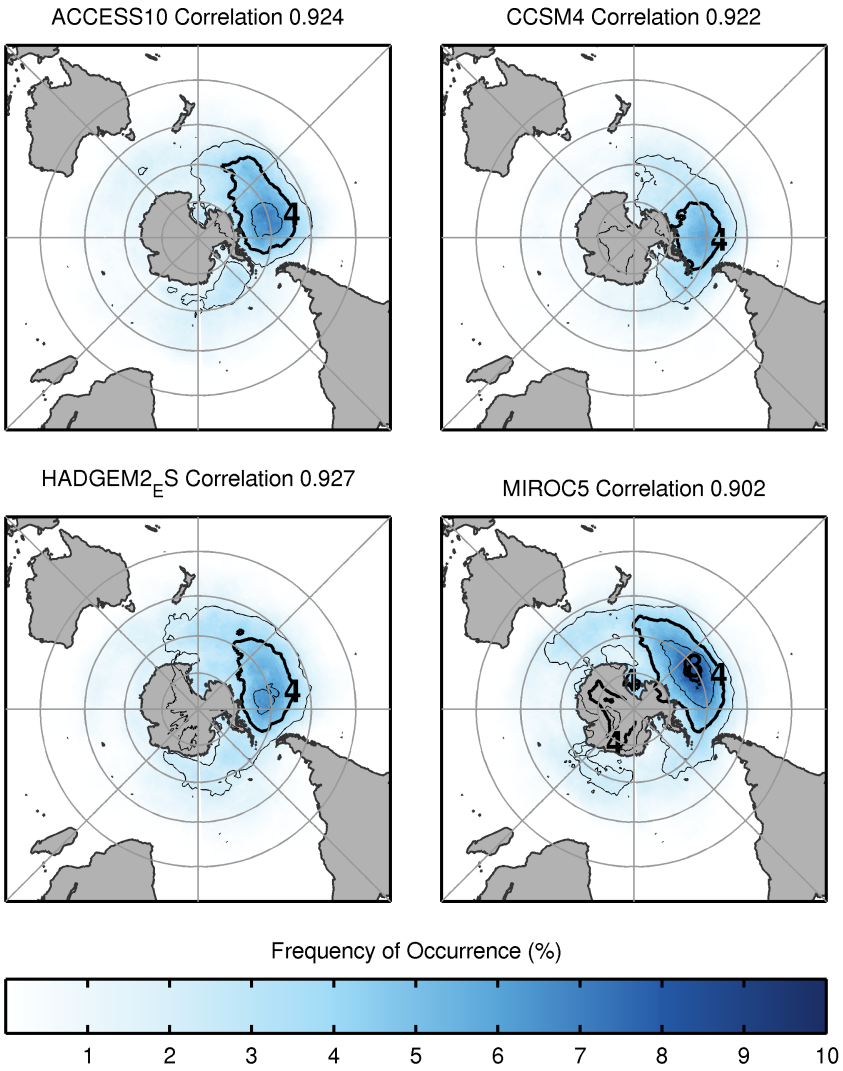

Figure 6.10: Historical GCMs BE Annual mean frequency of occurrence (%). High threshold (16 hPa). The contour interval is 2, starting at 2, and every second contour line is thickened and labelled.

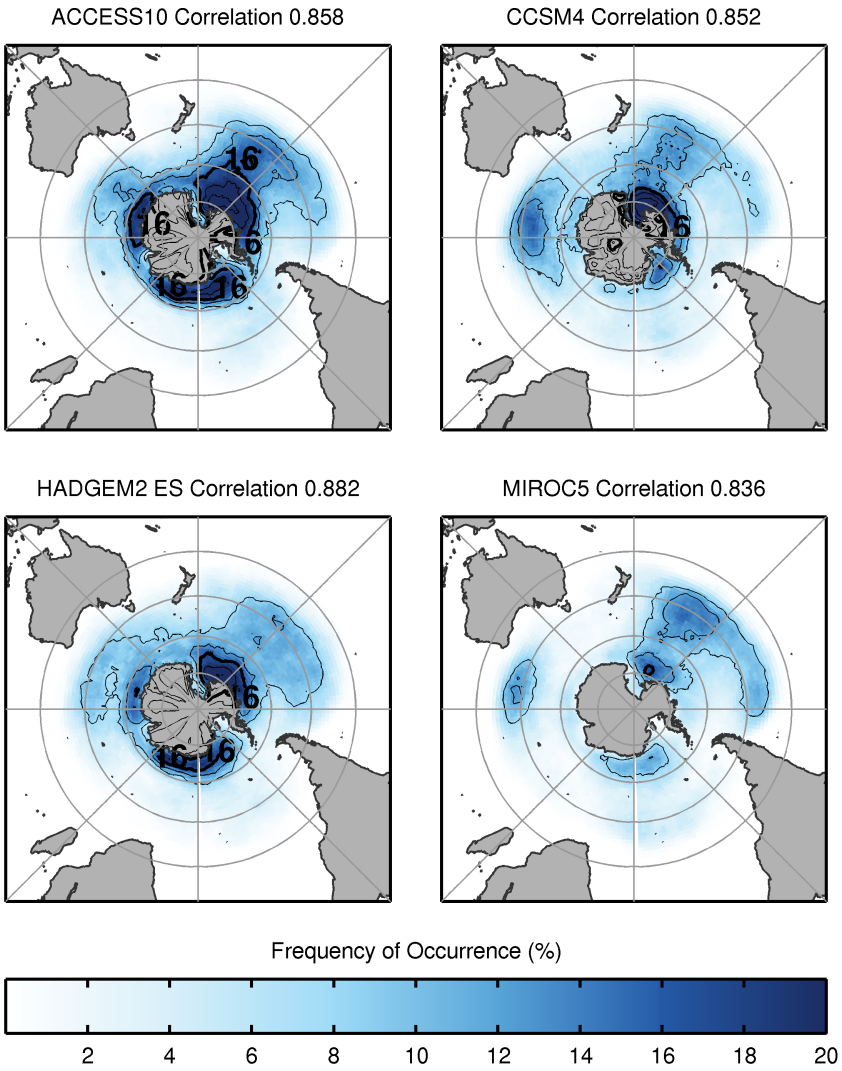

Figure 6.11: GCM Historical BE Summer 1976-2005. Seasonal mean frequency of occurrence (%). The contour interval is 4, starting at 8, and the 16 contour line is thickened and labelled.

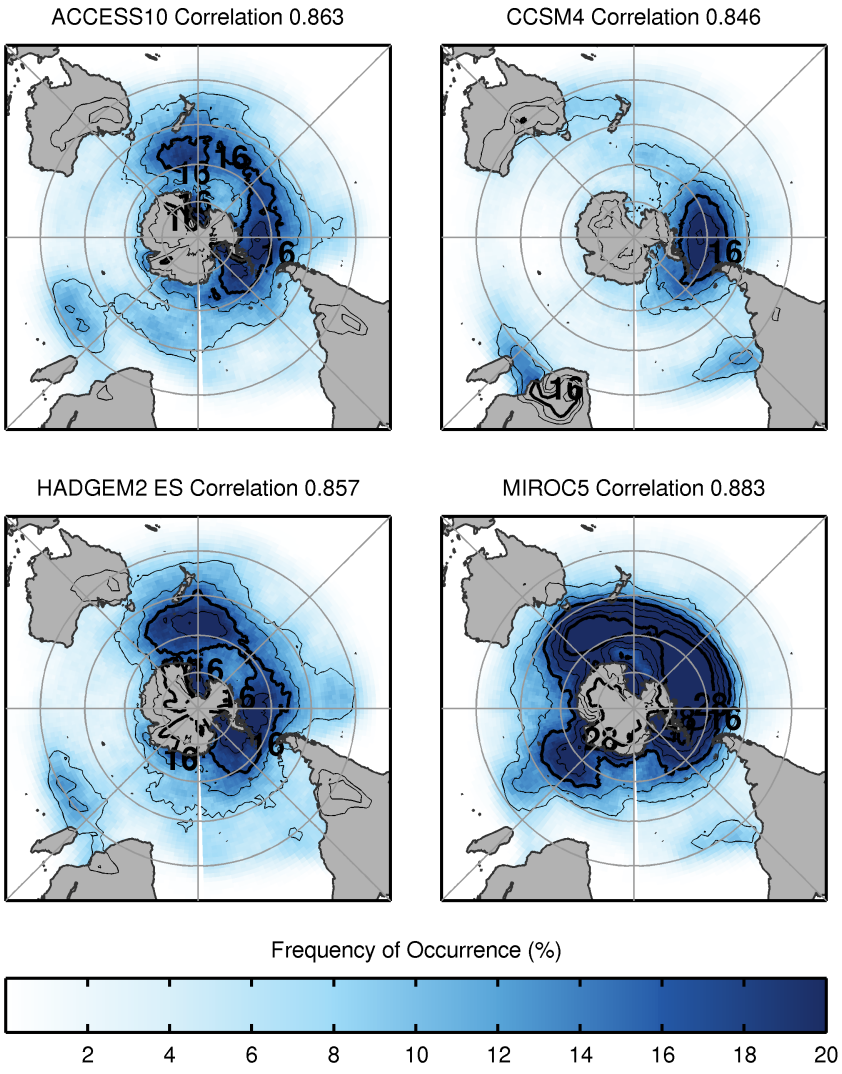

Figure 6.12: GCM Historical BE Winter 1976-2005. Seasonal mean frequency of occurrence (%). The contour interval is 4, starting at 8, and the 16 contour line is thickened and labelled.

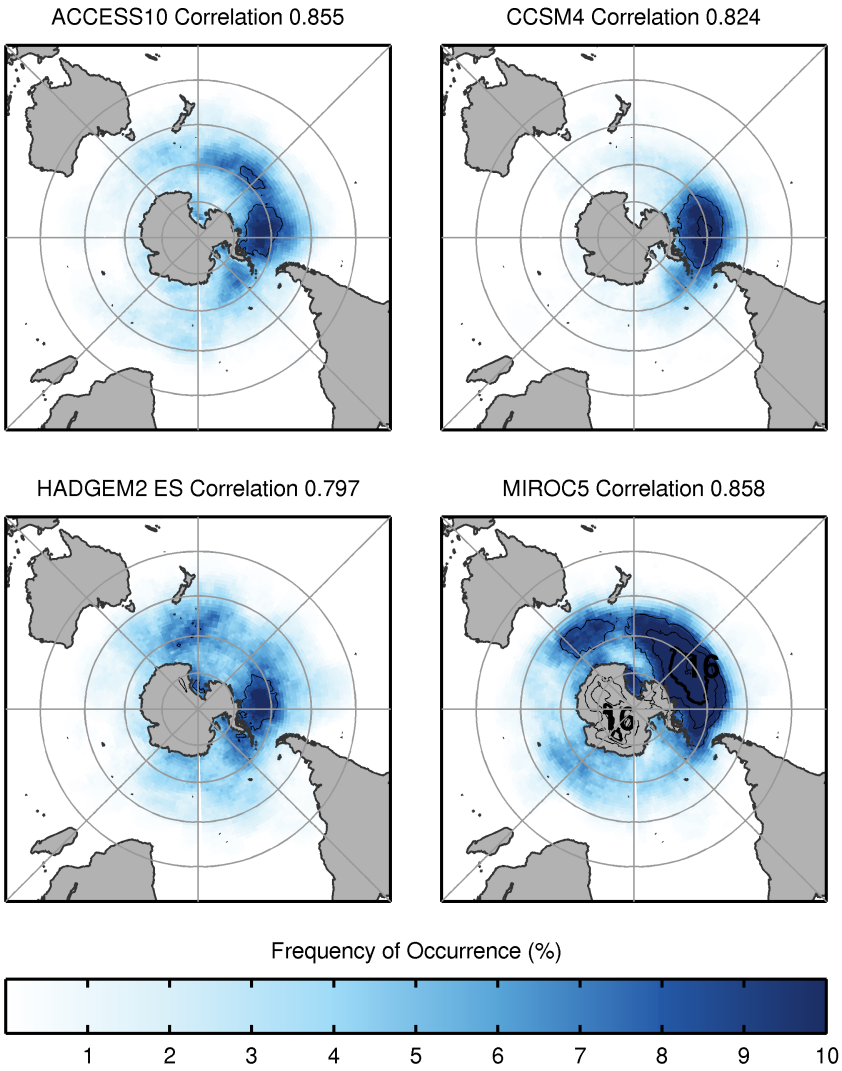

Figure 6.13: GCM Historical BE Winter 1976-2005 High threshold (16 hPa). Seasonal mean frequency of occurrence (%). The contour interval is 4, starting at 8, and the 16 contour line is thickened and labelled.

Table 6.3: GCM Historical and Reanalysis Correlation Coefficients

	Annual	Summer	Autumn	Winter	Spring
8 hPa					
ACCESS10	0.961	0.858	0.863	0.863	0.795
CCSM4	0.953	0.852	0.846	0.846	0.809
HADGEM2 ES	0.959	0.882	0.857	0.857	0.895
MIROC5	0.956	0.836	0.883	0.883	0.857
Ensemble	0.976	0.922	0.925	0.922	0.930
16 hPa					
ACCESS10	0.924	0.836	0.863	0.855	0.748
CCSM4	0.922	0.765	0.846	0.824	0.742
HADGEM2 ES	0.927	0.854	0.857	0.797	0.812
MIROC5	0.902	0.687	0.883	0.858	0.758
Ensemble	0.957	0.895	0.932	0.904	0.864

6.4.3 *GCM RCP4.5*

Figures 6.14 and 6.15 display the annual mean BE frequency for the 2011-2040 and 2071-2100 period for the RCP 4.5 projections, respectively. The geographical distribution of the BEs is similar between each of the three time periods (2041-2070 not shown). However, there are less BEs in the the primary SPO region in the later period. A reducing trend in annual BE frequency is apparent over the three periods in the RCPs 4.5 projection, however it is relatively minor.

6.4.4 *GCM RCP8.5*

Figures 6.16 and 6.17 display the annual mean BE frequency for the 2011-2040 and 2071-2100 period for the RCP 8.5 projections, respectively. The geographical distribution of the BEs is similar between both and as seen in the RCP 4.5 results in Figures 6.14 and 6.15. However, there are again less BEs in the the primary SPO region in the later period. The reduction in annual BE frequency is particularly apparent in the SPO.

6.4.5 *South Pacific Ocean (SPO)*

The previous results have given a qualitative description of the projected BEs in the SH. In order to provide a more quantitative analysis, we now focus our analysis on the SPO region defined as latitudes 45°S - 70°S and longitudes 180°- 270°and displayed in Figure 6.1. Since the majority of the observed blocking occurs in this region it is deemed worthy of further investigation.

The mean of the 21 x 49 grid points, in the SPO region, is determined for each season and year of the 30 year period. These are then presented as an annual BE frequency of occurrence (%), thus the four seasons blocking frequency sums to the annual frequency. The ensemble means and standard deviations for the SPO region BE frequency of occurrence are presented in

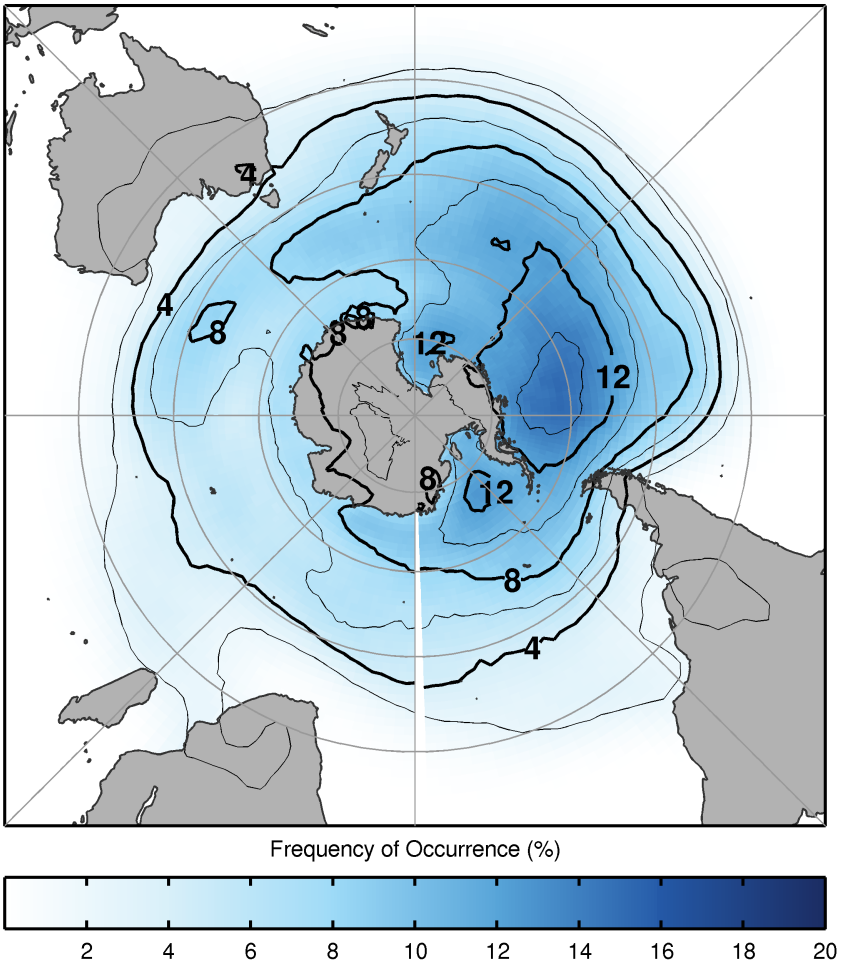

Figure 6.14: RCP 4.5 GCMs BE Annual Mean Frequency of Occurrence, 2011-2040. The contour interval is 2, starting at 2, and every second contour line is thickened and labelled.

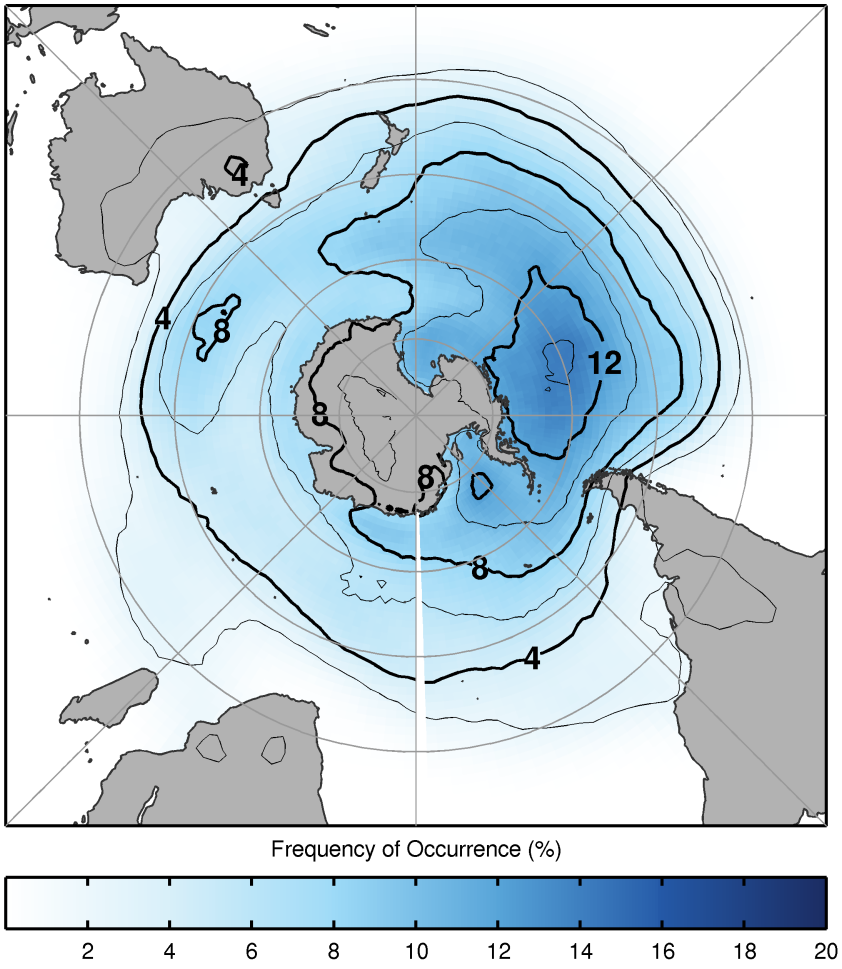

Figure 6.15: RCP 4.5 GCMs BE Annual Mean Frequency of Occurrence, 2071-2100. The contour interval is 2, starting at 2, and every second contour line is thickened and labelled.

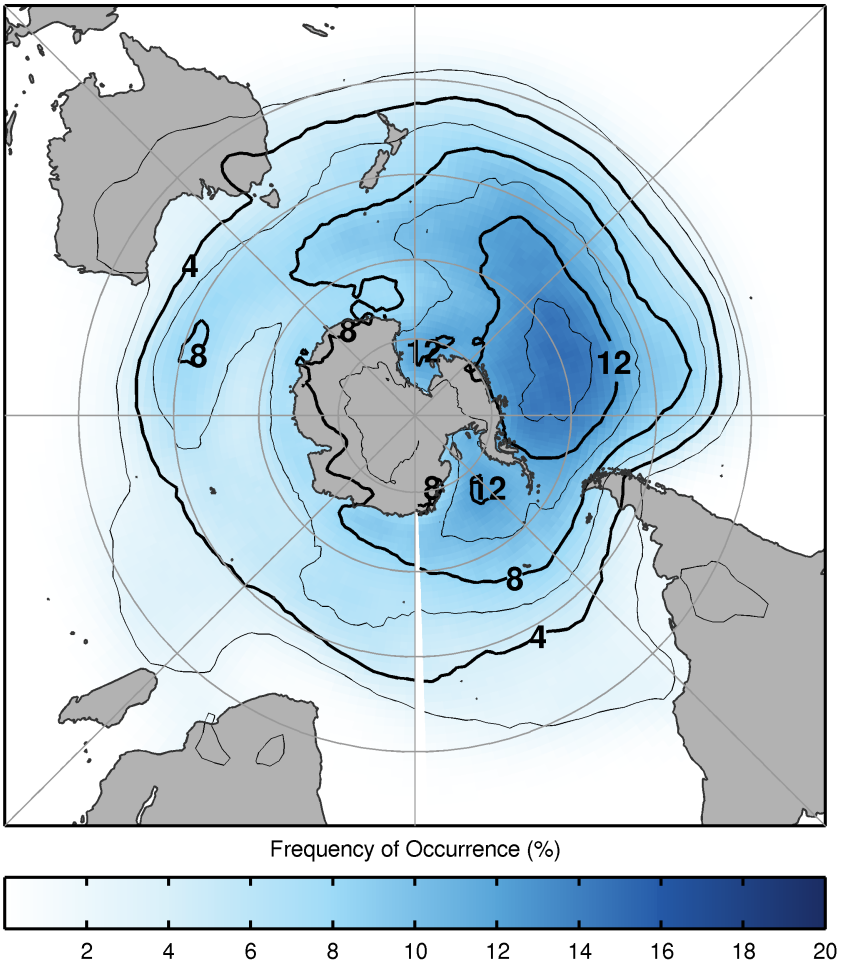

Figure 6.16: RCP 8.5 GCMs BE Annual Mean Frequency of Occurrence, 2011-2040. The contour interval is 2, starting at 2, and every second contour line is thickened and labelled.

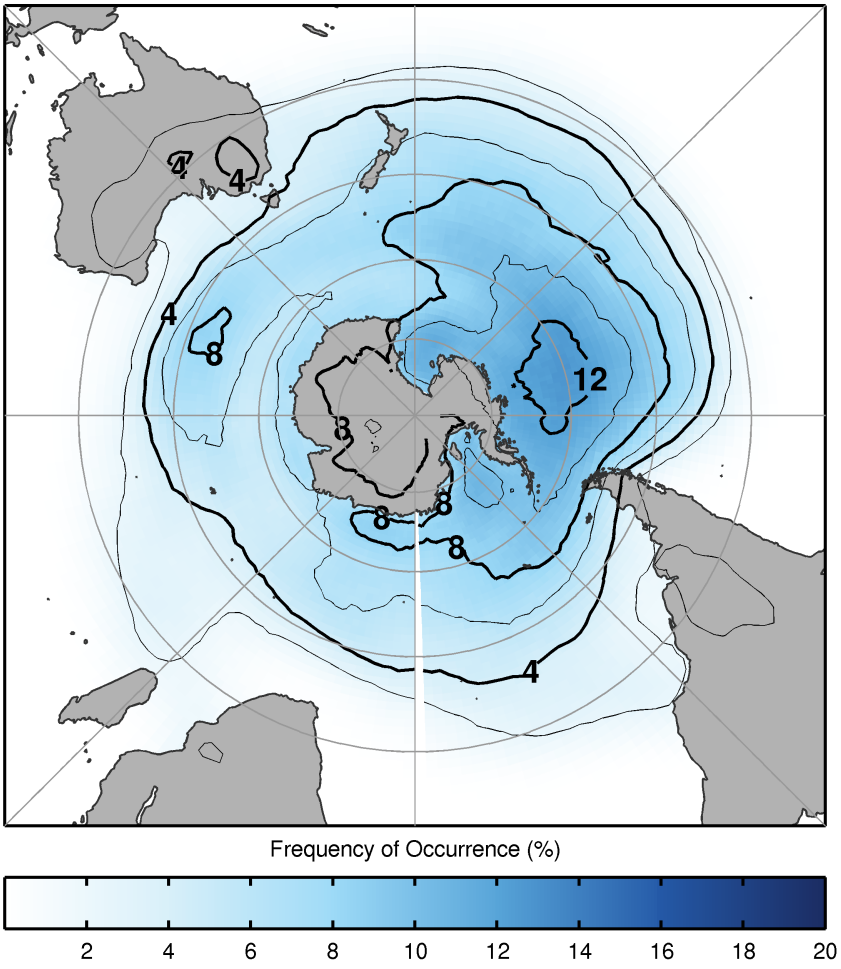

Figure 6.17: RCP 8.5 GCMs BE Annual Mean Frequency of Occurrence, 2071-2100. The contour interval is 2, starting at 2, and every second contour line is thickened and labelled.

Table 6.4. The differences are generated between the reanalysis and historical and using the latter period (2071-2100) for the historical and RCP projections. These values represent the ensemble SPO area mean, thus are reduced in value when compared to the previously seen spatial patterns, such as the reanalysis in Figure 6.5 and the historical and RCP8.5 differences, Figure 6.27, and the previously discussed maximum values.

Figures 6.18 and 6.19, display the ERA-I and the individual GCM historical output, respectively. The reanalysis has a mean BE frequency of 12.19% with standard deviation 3.16. Similar results are also observed in the historical GCM output with the BE frequency of occurrence ranging between 9.19 to 14.12% and standard deviation of 2.86 to 3.83 for the four GCMs, with an ensemble mean of 12.05% and standard deviation 3.42. The reducing trend, -0.09 % per/year, observed in the reanalysis is also replicated in all of the GCMs, ranging between -0.12 to -0.03 % per/year. As seen in Figures 6.18 and 6.19 the BEs exhibit high year to year variability, for this reason this study has used 30 year aggregates in displaying the spatial patterns.

The RCP4.5 mean ensemble displays a reduction across all three time periods, Table 6.4. However, this reduction is subtle when the standard deviation is taken into consideration and the RCP4.5 reductions reflect the previously seen differences in the spatial distributions, Figures 6.26 and 6.28. The RCP4.5 2071-2100 ensemble has a reduction of 1.0% in the annual frequency of occurrence of BEs and this occurs predominantly during summer and spring seasons.

As before, the RCP8.5 projection displays a greater reduction in BEs when compared to the RCP4.5 projection. The reductions observed are of borderline significance, less than 1 standard deviation. However, despite the high uncertainties the reduction in the SPO BEs is consistent across the three time periods and in the annual and seasonal periods. There is an annual BE reduction of 2.01%, with a standard deviation 2.95%. This reduction occurs mostly in the summer and spring, with a reduction of -0.86% and -0.85%, respectively.

These results are the absolute frequency of occurrence. When a relative frequency of occurrence is used the reduction is more striking. A BE reduction of 32.6% during summer and 31.3% during spring, between the historical and RCP8.5 2071-2100 period is identified. However, these results need to be tempered by the high standard deviation and the size of the SPO region.

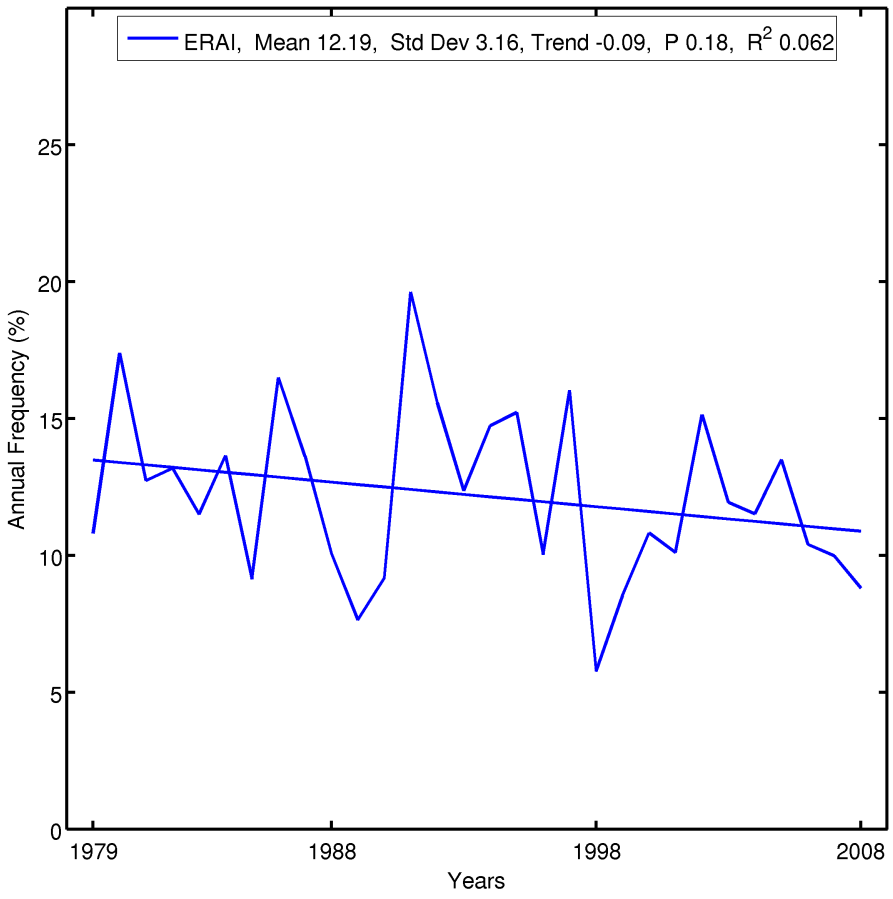

Figure 6.18: ERA-Interim BE yearly mean frequency of occurrence (%) in the SPO region, 1979-2008.

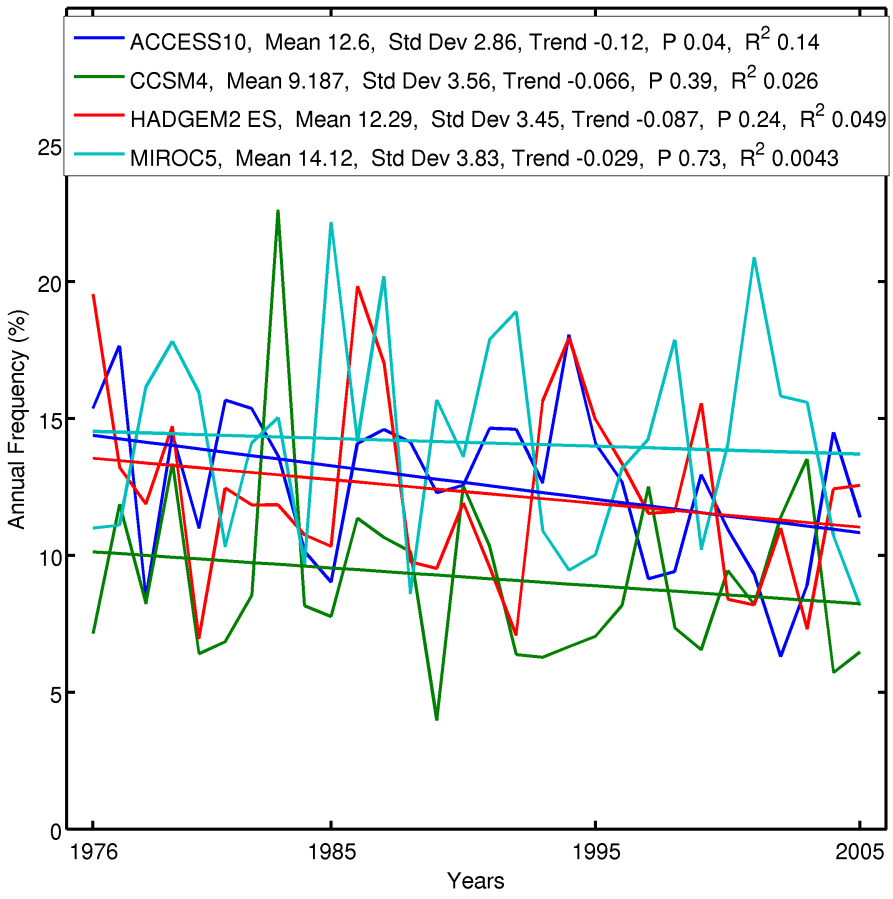

Figure 6.19: GCM Historical BE yearly mean frequency of occurrence (%) in the SPO region, 1976-2005.

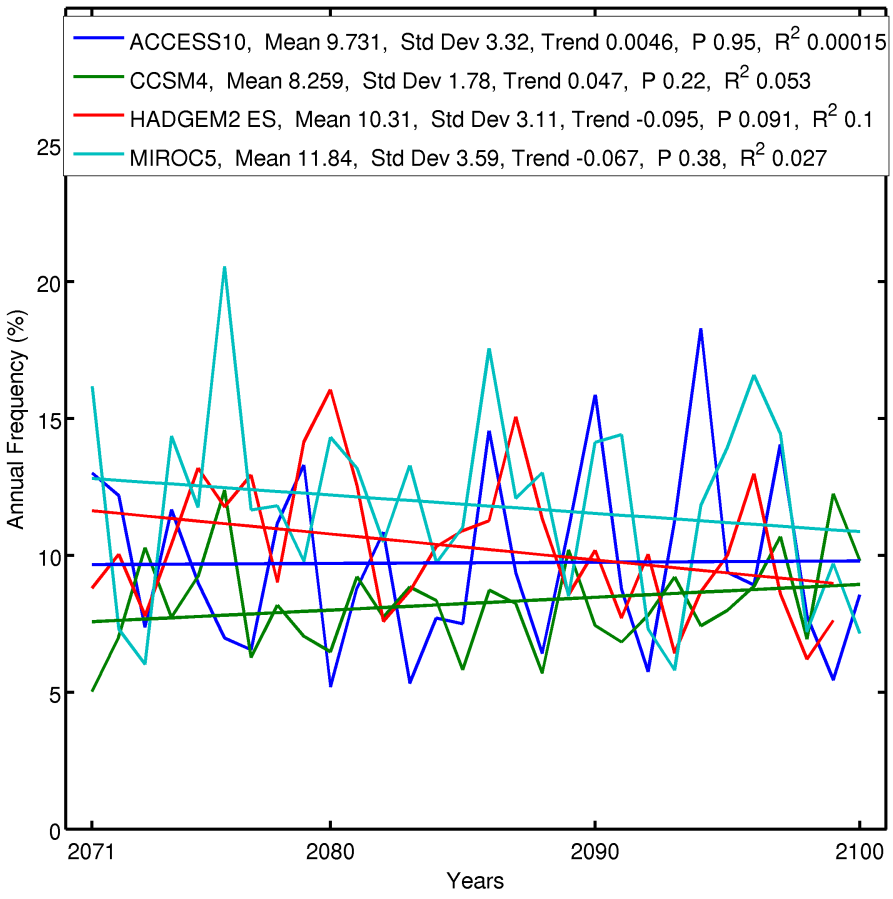

Figure 6.20: RCP8.5 BE yearly mean frequency of occurrence (%) in the SPO region, 2071-2100.

Table 6.4: SPO Region Ensemble means & standard deviation, in brackets, of the annual BE frequency of occurrence (%). The absolute differences are generated between the reanalysis and historical and the historical and RCP projections, using the later period (2071-2100). The differences as a relative percentage are also shown.

	Annual	Summer	Autumn	Winter	Spring
Reanalyis					
1979-2008	12.19 (3.16)	2.56 (1.58)	3.13 (1.4)	4.36 (1.63)	2.13 (1.05)
Historical					
1976-2005	12.05 (3.42)	2.65 (1.25)	2.61 (1.09)	4.09 (1.69)	2.72 (1.52)
Differences	-0.136	0.0859	-0.513	-0.271	0.584
Relative	-1.12	3.35	-16.4	-6.22	27.4
RCP 4.5					
2011-2040	11.76 (2.83)	2.46 (1.41)	2.64 (1.27)	4.14 (1.47)	2.54 (1.16)
2041-2070	11.16 (2.94)	2.34 (1.31)	2.47 (1.23)	4.16 (1.47)	2.18 (1.2)
2071-2100	11.04 (3.12)	2.05 (0.965)	2.51 (1.25)	4.26 (1.76)	2.23 (1.19)
Differences	-1.0	-0.605	-0.106	0.174	-0.487
Relative	-8.34	-22.8	-4.04	4.26	-17.9
RCP 8.5					
2011-2040	12.02 (2.79)	2.33 (1.25)	2.6 (1.25)	4.56 (1.66)	2.55 (1.27)
2041-2070	11.02 (3.02)	2.2 (1.04)	2.45 (1.28)	4.02 (1.49)	2.36 (1.32)
2071-2100	10.03 (2.95)	1.79 (0.989)	2.38 (1.13)	3.92 (1.69)	1.87 (1.02)
Differences	-2.01	-0.864	-0.232	-0.164	-0.851
Relative	-16.7	-32.6	-8.87	-4.02	-31.3

6.4.5.1 *SPO Persistence*

The persistence is the duration of the BE. Our methodology requires that a minimum of five days is required before an event satisfies our threshold. Since the BE frequency of occurrence metric is insensitive to the duration of individual events, such that a 10 day event is equivalent to two 5 day events, examination of persistence allows us to distinguish if there is a change in duration of BEs. This is a interesting metric as it is effectively a change in the duration of BEs, that the blocking frequency of occurrence may not reveal. Longer duration BEs have been linked to extreme weather events and this is therefore an important consideration (Pezza et al., 2011).

The duration, in 6 hourly time increments, of all of the BEs for each grid point in the SPO region is determined. The frequency of the BE duration is then counted for each grid point. The mean count of each of the time increments in the SPO region is then calculated. The persistence analysis is conducted on the 30 year time period. No seasonal analysis is undertaken, thus avoiding the complication of BEs that occur across the seasons.

Figure 6.21 displays the persistence for the ERA-I reanalysis and the four historical GCM runs. Unsurprisingly, there are more counts at the shorter durations than longer, with the maximum amount of counts occurring at the 5 day threshold. The duration of BEs is asymptotic and by 25 days is zero. Figure 6.22 is the same data as seen in Figure 6.21, however it is displayed as differences from the reanalysis, with the ensemble mean and standard deviation of the differences also displayed. The dotted line, is $\pm$ 1 standard deviation from the ensemble mean. As before the differences are generated between each of the model's historical output and its future projection.

In figure 6.22, the four GCMs under represent the shorter duration BEs, less the 7 days. Two of the models, ACCESS10 and MIROC5, are positively biased towards longer duration BEs, with BEs longer than 10 days. HADGEM2 ES shows agreement with the reanalysis at 10 day durations, while CCSM4 displays a reduced count compared to the reanalysis. The ensemble mean

displays a reduction in shorter duration events. However, the 10 day duration is comparable with the reanalysis. Thus, the models are under representing the shorter duration BEs, which are also more frequent.

Figures 6.23, 6.24 and 6.25 display the differences between the GCM historical and RCP8.5 projections in the three 30 year time periods, 2011-2040, 2041-2070 and 2071-2100, respectively. The three time periods are shown in order to give an appreciation of the evolution of the persistence.

In the first RCP8.5 period, 2011-2040 Figure 6.23, the ensemble mean is negative at the starting 5 day threshold and displays an increase at $\approx$ 6-8 days. ACCESS10 and MIROC5 have a positive anomaly and CCSM4 and HADGEM2 ES display a negative anomaly. Thus the standard deviation is spread across both positive and negative differences from $\approx$ 5-7 days.

In Figure 6.24 the disparity between the GCMs is apparent, as seen by the large standard deviation. The ensemble mean displays an increase in $\approx$ 5-6 day duration events and then a reduction in the mid to longer duration events from approximately 7 days onwards, slowly trending back the the historical values by 20 days. The ensemble mean positive anomaly at 5-6 days may be due to the influence of MIROC5 and the small ensemble size.

At the end of the century, 2071-2100 Figure 6.25, ACCESS10 has the largest reduction between $\approx$ 7-12 days, however at 5 days the initial count is similar to the historical simulation. MIROC5 has an initial increase in 5 day events before reducing close to the mean. There is less agreement between the GCMs in Figure 6.25 as seen by the large standard deviation, particularly at the 5-6 day duration. Whilst there is a reduction overall, the large inter model variability and related standard deviation makes this analysis less certain.

Of interest is the evolution of the ensemble mean across the three RCP8.5 time periods. From the initial 2011-2040 period, Figure 6.23, to 2041-2070 there is a increase in the negative anomaly from -0.2 to -0.4 at $\approx$ 7-10 days. From 10 days the

mean is negative, trending towards zero. However, the positive anomaly observed from 5-7 days is possibly skewed by the MIROC5. In the later periods, between 2041-2070 and 2071-2100 Figures 6.24 and 6.25 respectively, the negative anomaly further deepens to -0.6 and expands to $\approx$ 6-12 days. The previous positive anomaly is reduced, however MIROC5 is still positive between 5-6 days, possibly skewing mean and standard deviation.

The use of a small selection of GCMs has been advantageous in the previous work, Chapter 4. A larger ensemble or additional realizations from the selected GCMs may have been beneficial in this analysis due to model disagreement. For example MIROC5's response in the persistence analysis, Figure 6.25 and RCP8.5 Winter 2071-2100 differences, Figure 6.30.

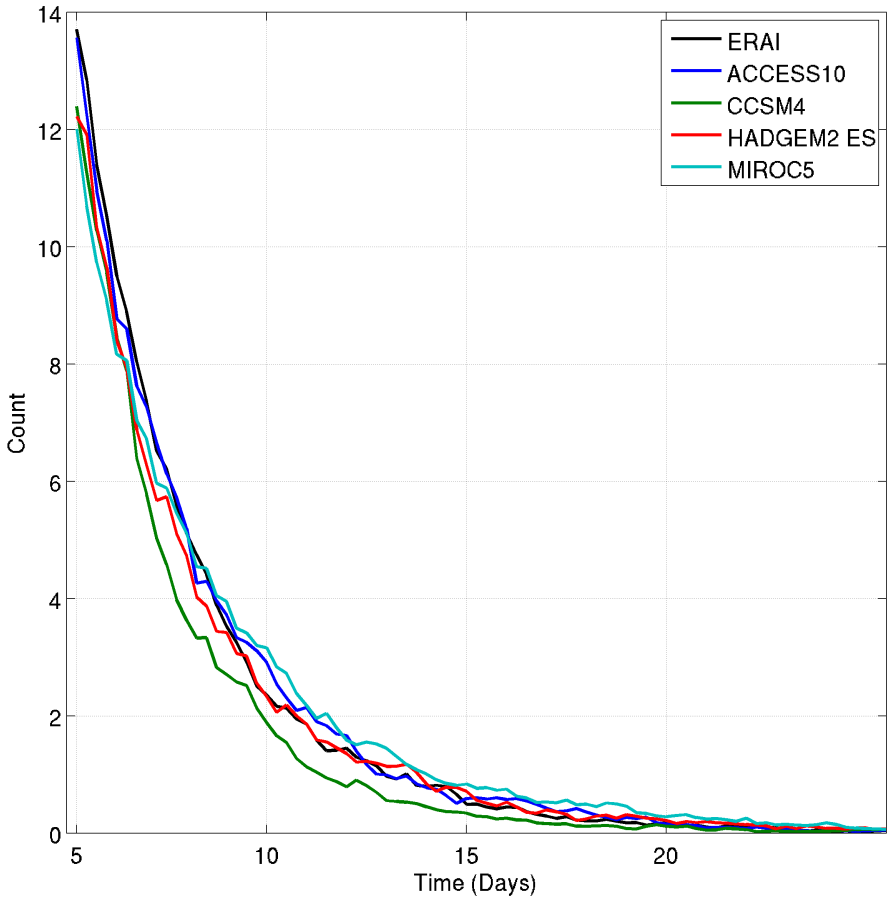

Figure 6.21: Reanalysis and Historical SPO Mean Persistence.

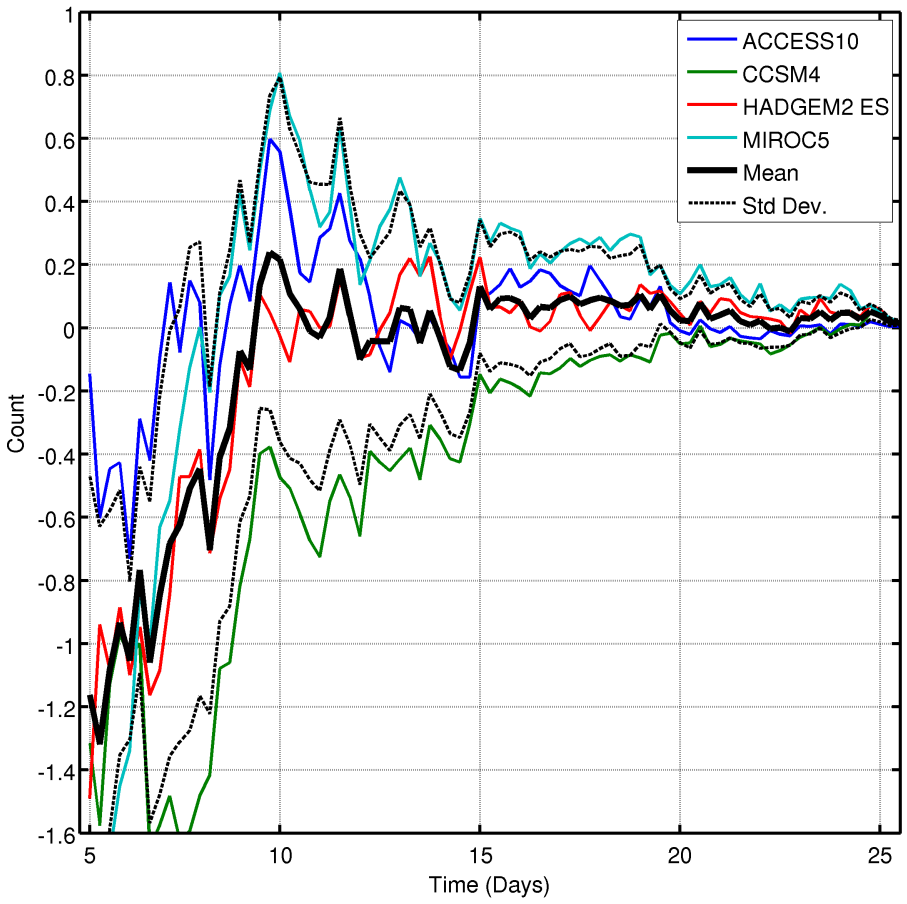

Figure 6.22: Reanalysis and Historical SPO Mean Persistence differences. The mean and standard deviation of the differences is also displayed.

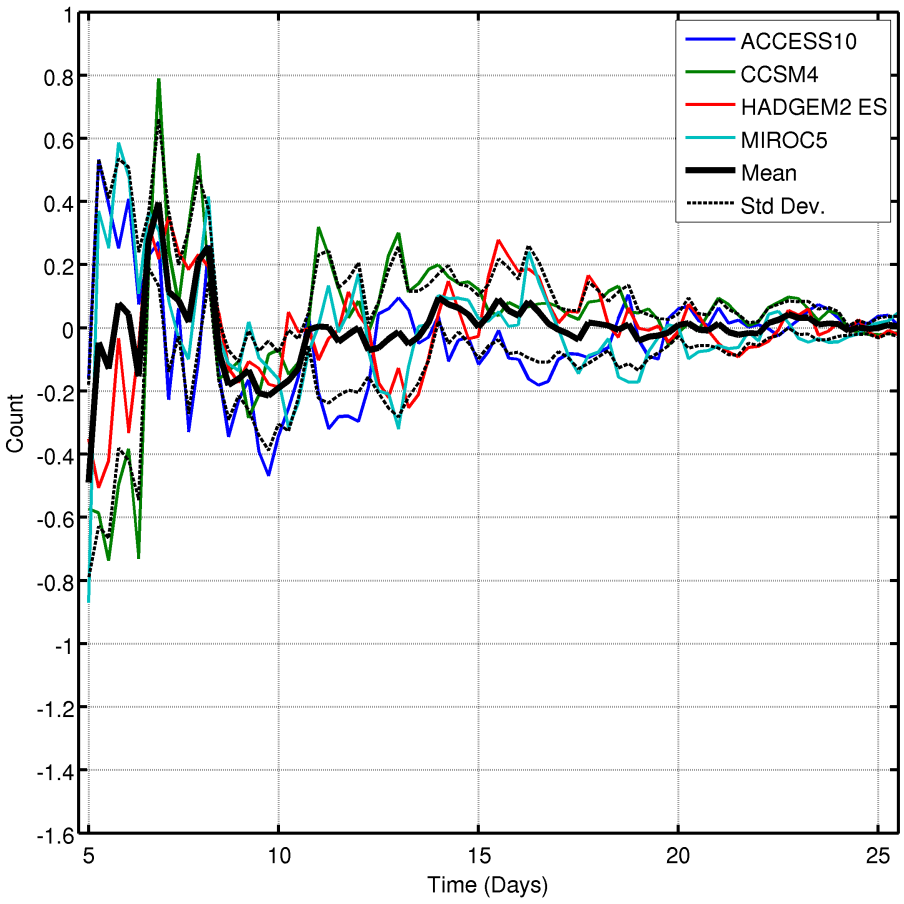

Figure 6.23: RCP8.5 SPO Persistence differences, 2011-2040. The mean and standard deviation of the differences is also displayed.

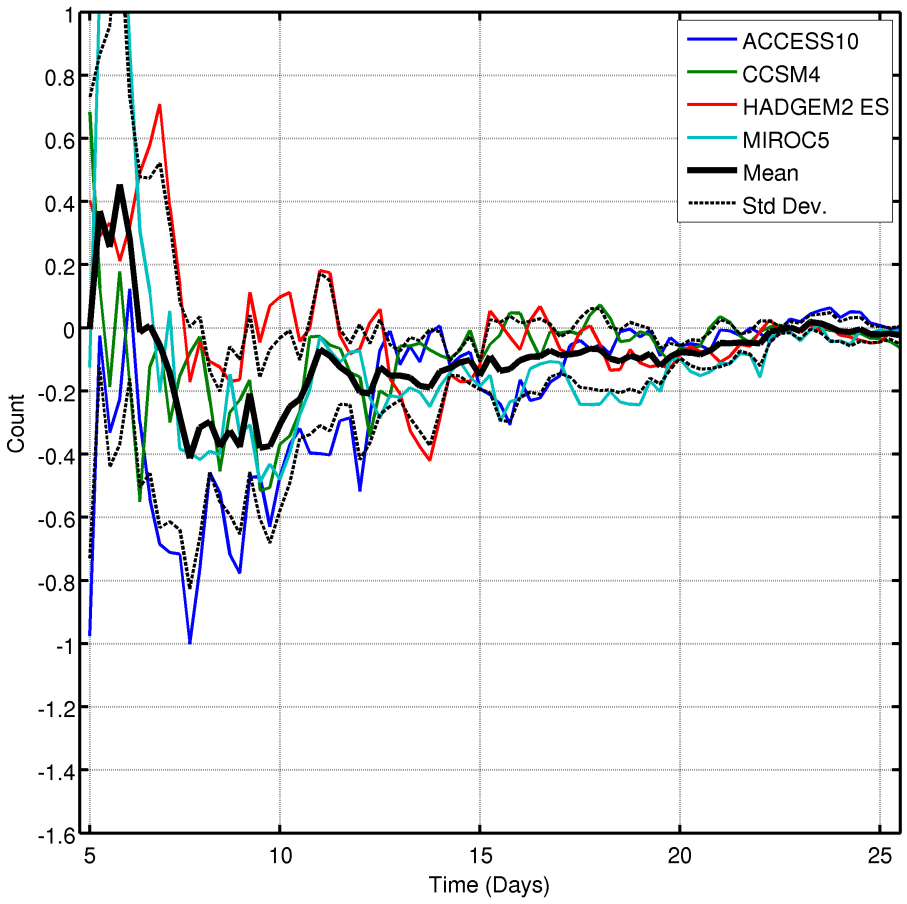

Figure 6.24: RCP8.5 SPO Persistence differences, 2041-2070. The mean and standard deviation of the differences is also displayed.

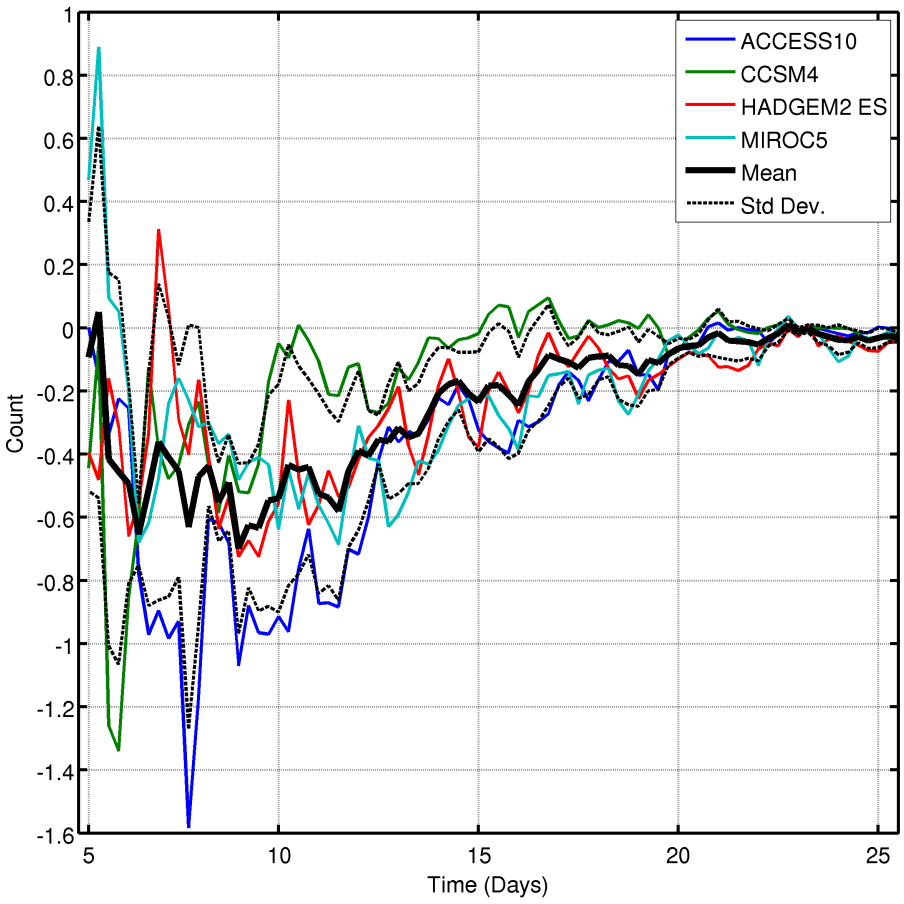

Figure 6.25: RCP8.5 SPO Persistence differences, 2071-2100. The mean and standard deviation of the differences is also displayed.

6.5 DISCUSSION

The ensemble annual mean changes between the RCP 4.5 and 8.5 projections at 2071-2100 and the historical output are displayed in Figures 6.26 and 6.27, respectively. A reduction in the BEs is evident during both of the RCP projections and is more pronounced in the RCP 8.5 projection, Figure 6.27. The largest change is observed in the SPO where the BE maximum is reduced in extent and frequency. This reduction in BEs from 60°S to Antarctica is seen across each of the three 30 year time steps in both RCP projections.

There is also a small increase in BEs in the midlatitudes, centred on 30°S in the SPO. The IO has a decrease between 30° - 45°S and a small increase at 45° - 65°S, effectively identifying a sight poleward shift in BE activity. Finally the South Atlantic Ocean has a slight increase in BE.

The mean GCM historical BE frequency maximum was 15.3 % and the RCP 8.5 2071-2100 is reduced to 12.9 %. This 2.4 % reduction relates to a relative decrease of -15.7% or ≈9 days less of BE per annum in the region of the maxima.

The seasonal BE structure follow a similar pattern, in that the RCP 8.5 displays the same variability pattern as the RCP 4.5, but with a larger reduction in the frequency of occurrence. Figures 6.28 and 6.29 display the seasonal mean BE differences between the RCP 4.5 and 8.5 projections, for the 2071-2100 period and the historical output, respectively.

During the summer there is a change in location and frequency of the BEs. A reduction in the previous maxima located at 45°S, 135°W and an increase in BE between 45° - 60°S in the IO. Autumn has a reduction in the SPO and an increase in the South Atlantic Ocean relative to the historical patterns. During winter there is a large reduction in BE south of Tasmania, a $ZW3$ like pattern is also evident. Spring also displays a general reduction in BE across the SH, however an equatorward shift in latitude is observed in the SPO. These seasonal changes are seen in both

RCPs, however they are more pronounced in the RCP 8.5 (Figure 6.29).

The GCM ensemble contains four models, while there is agreement in the annual BE distributions the seasonal variation between models is more varied. The small ensemble size also means that a single model output could also dominate the ensemble mean. Figures 6.30 and 6.31 display the winter and summer BE frequency differences for the four GCMs during the RCP 8.5 2071-2100 period, respectively. During the winter season, Figure 6.30, MIROC5 displays strong reduction in BEs that resembles a ZW_3 pattern, this is not observed in the other models. However during the Summer seasons, Figure 6.31, all of the GCMs display a consensus with a BE reduction in the SPO region, though of varying magnitude.

Figure 6.30 also displays some smaller BE increases. An increase in BEs centred at 30°S in the SPO is also observed in all of the GCMs. This results in an increase in BE to the North and North East of NZ and a reduction to the South of NZ, effectively NZ is positioned between a positive and negative BE change.

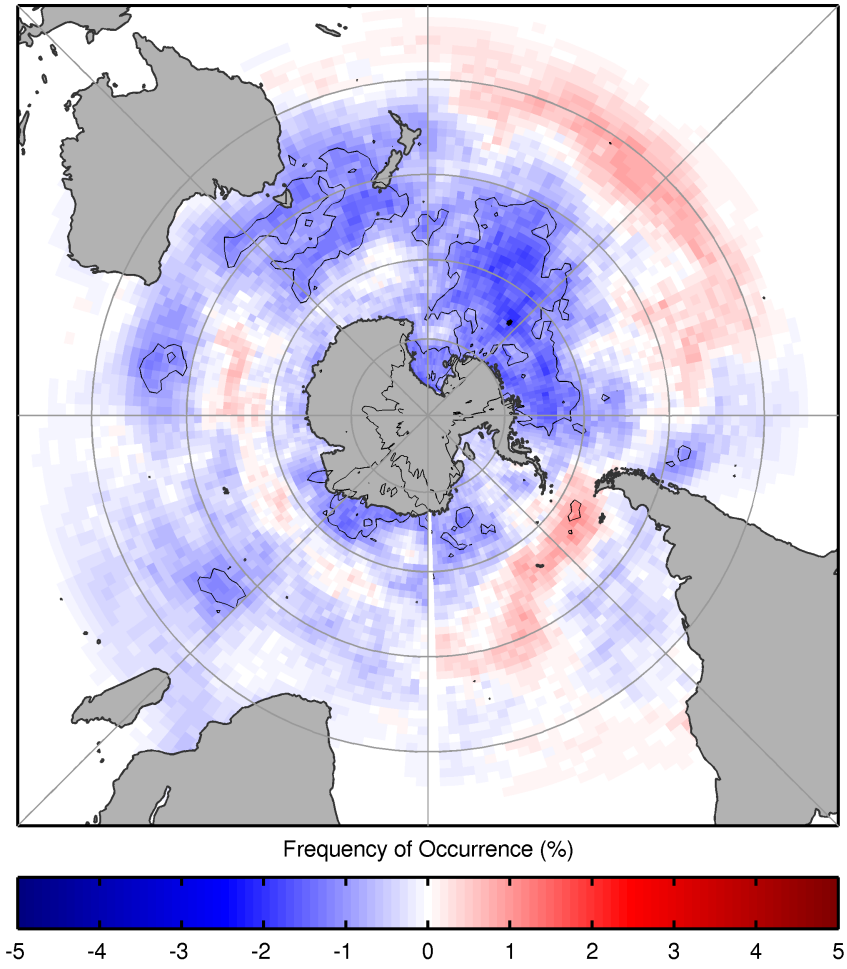

Figure 6.26: RCP4.5 BE annual differences, 2071-2100. The contour intervals start at ± 1 with an interval of 1 and every second contour is thickened.

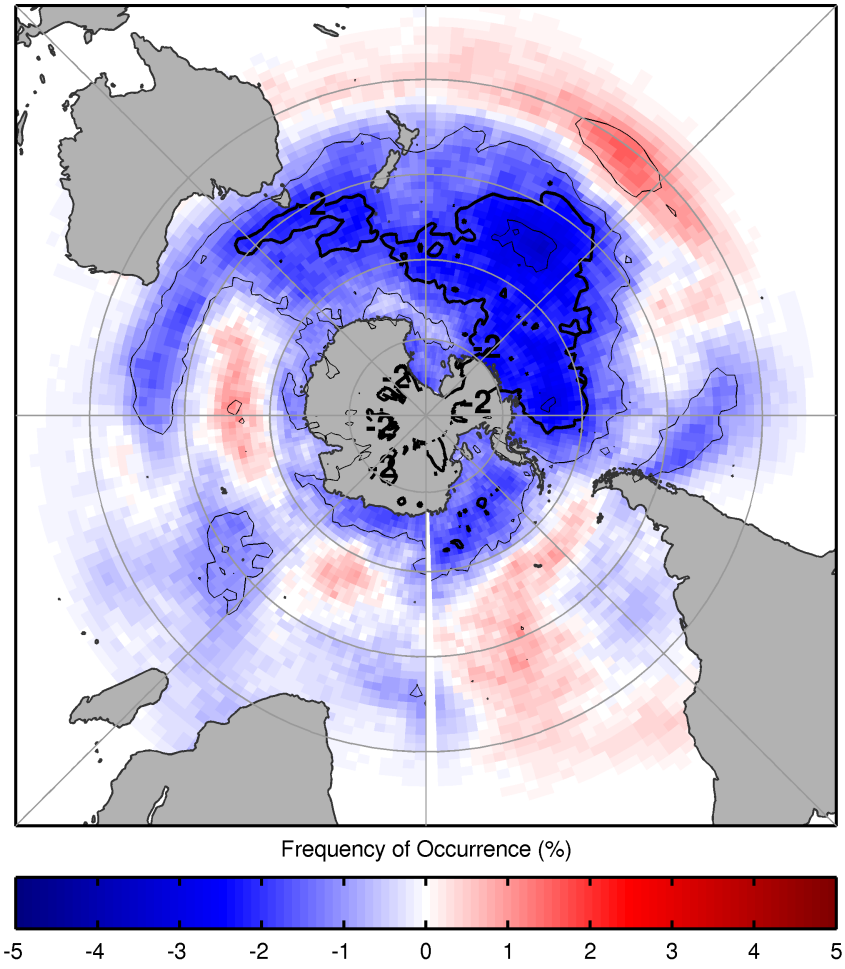

Figure 6.27: RCP8.5 BE annual differences, 2071-2100. The contour intervals start at $\pm$ 1 with an interval of 1 and every second contour is thickened.

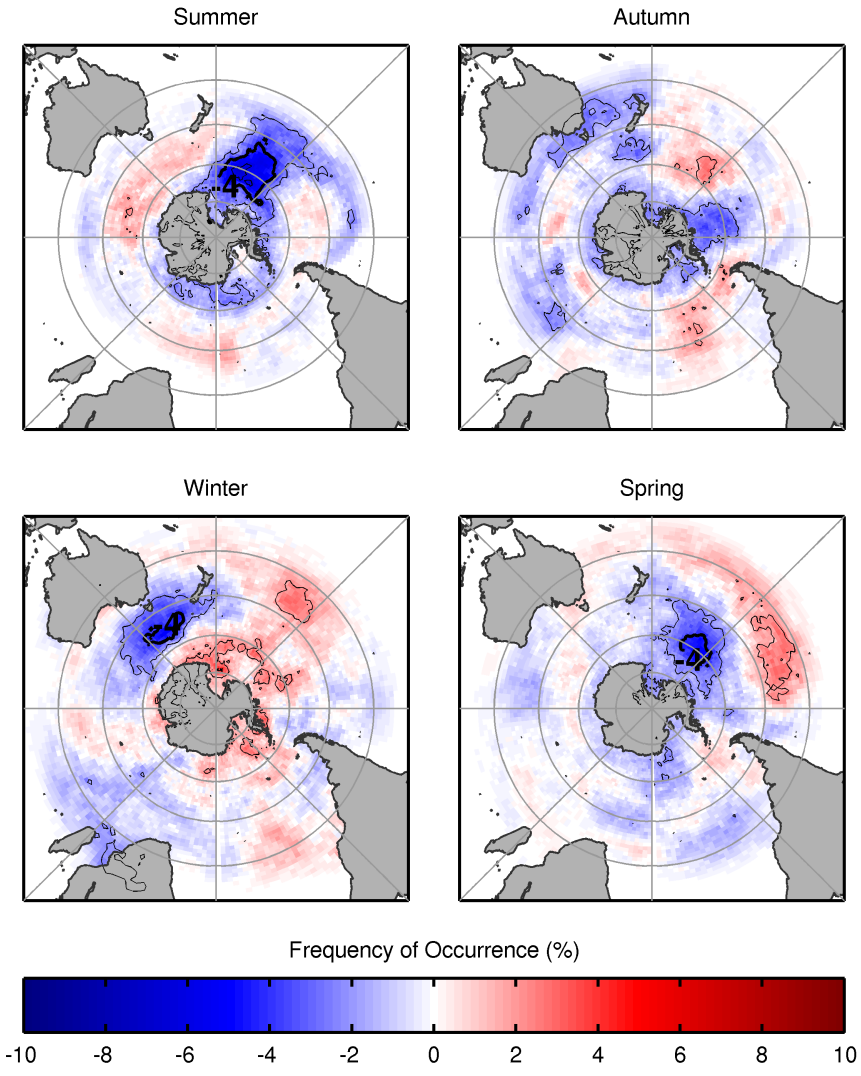

Figure 6.28: Historical RCP4.5 Seasonal BE differences, 2071-2100. The contour intervals start at ± 2 with an interval of 2 and every second contour is thickened and labelled.

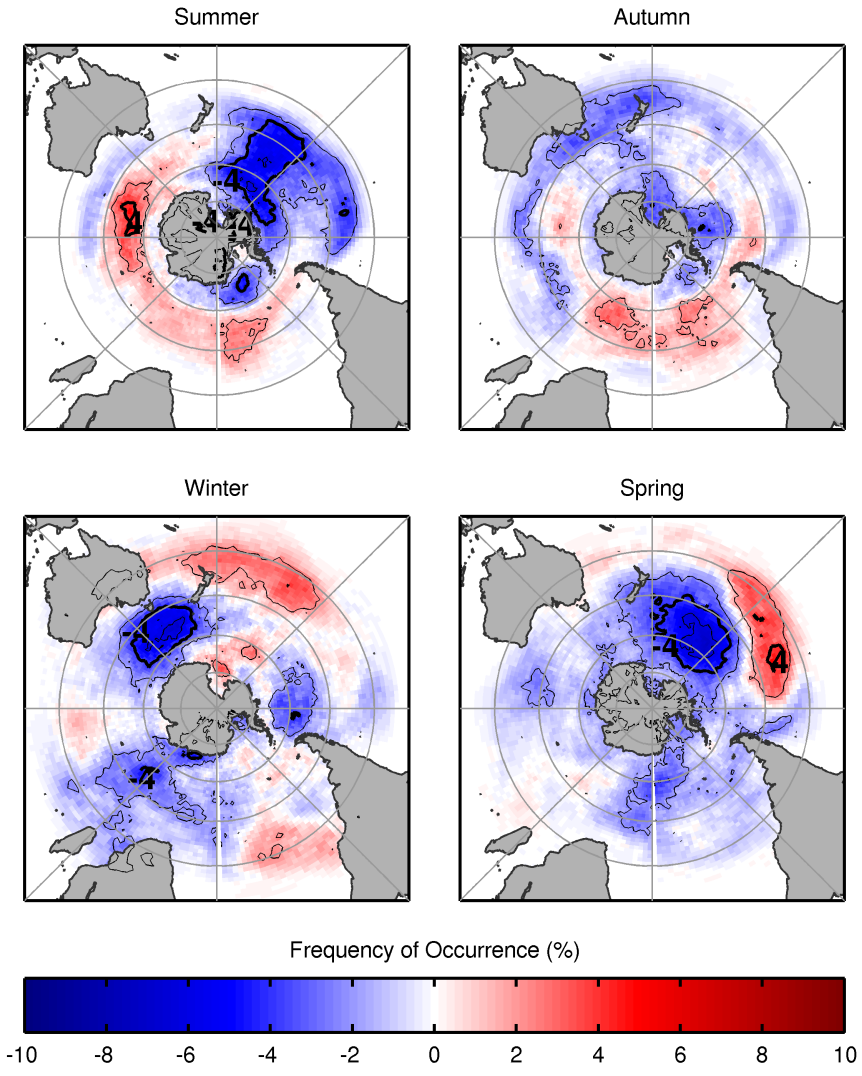

Figure 6.29: Historical RCP8.5 Seasonal BE differences, 2071-2100. The contour intervals start at ± 2 with an interval of 2 and every second contour is thickened and labelled.

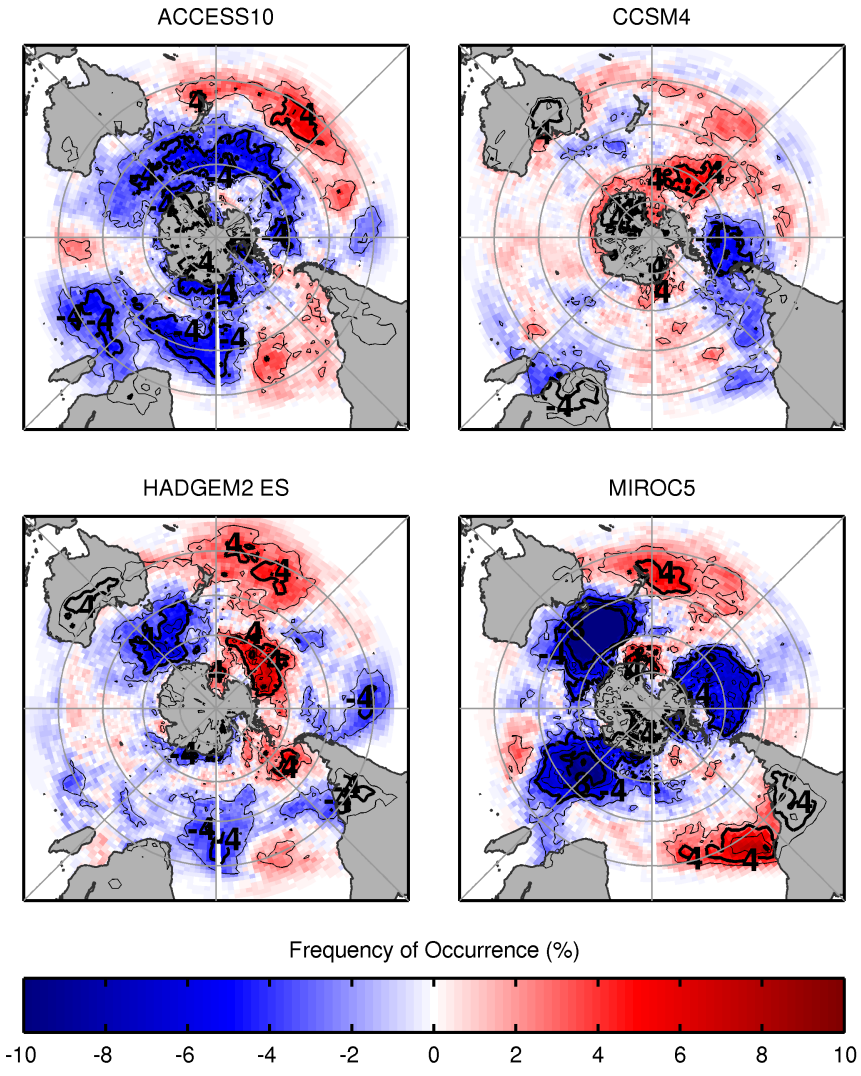

Figure 6.30: Historical RCP8.5 GCM Winter BE differences, 2071-2100. The contour intervals start at ± 2 with an interval of 2 and every second contour is thickened and labelled.

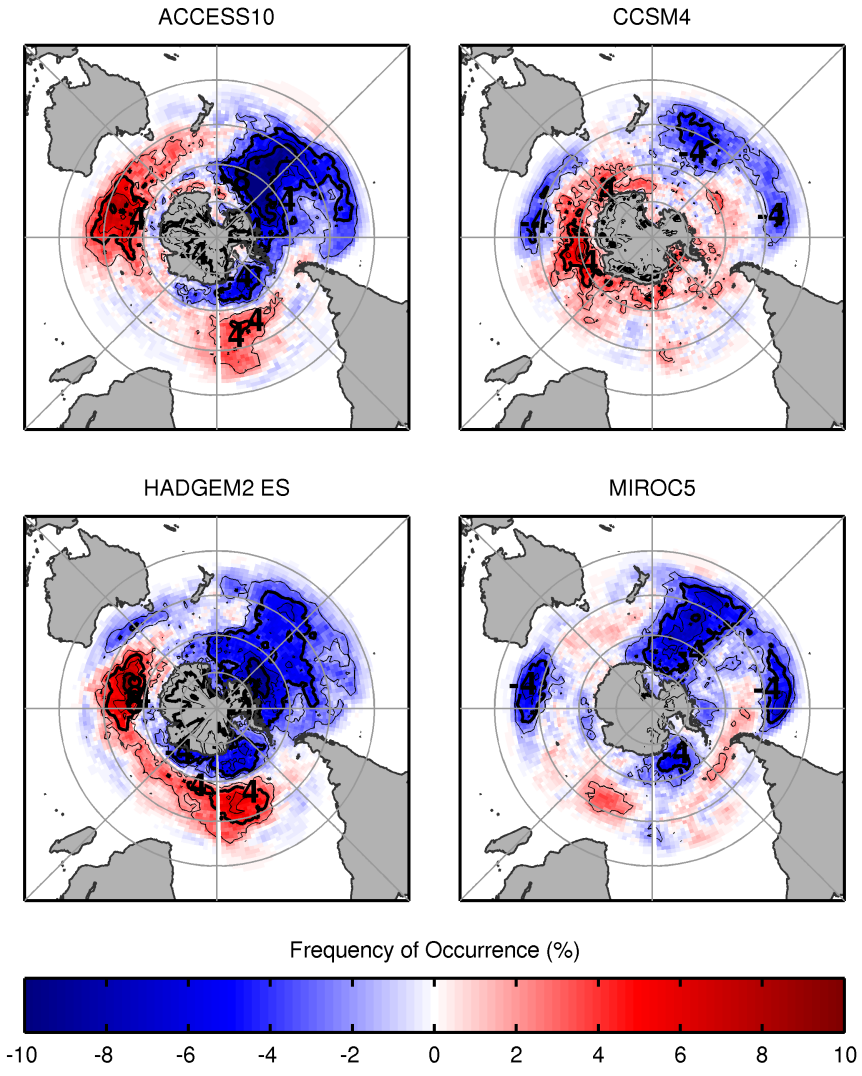

Figure 6.31: Historical RCP8.5 GCM Summer BE differences, 2071-2100. The contour intervals start at ± 2 with an interval of 2 and every second contour is thickened and labelled.

6.5.1 *Zonal Wave 3*

ZW3 has also been thought to have a role in the formation and reinforcement of BEs (Trenberth and Mo, 1985; Renwick, 2005; Berrisford et al., 2007). A ZW3 index was determined and investigated using the methodology of Raphael (2004), see Section 2.3.7.

Histograms of the ZW3 index were determined using 0.1 bins between -3 and 3 for each simulation. Figure 6.32 displays the histogram of the ZW3 index for the reanalysis data and the mean of the 4 histograms for the GCM historical period and Figure 6.33 displays the historical and RCP8.5 2071-2100 output.

No significant variation in the distribution of the ZW3 index was observed between the GCM historical and RCP8.5 projections. Additionally the methodology of Raphael (2004) may be insensitive to a phase change, as it relies on three static areas in determination of the index. However, ZW3 is still considered an important phenomena and this is identified in Section 7.1.1 as an area of further research.

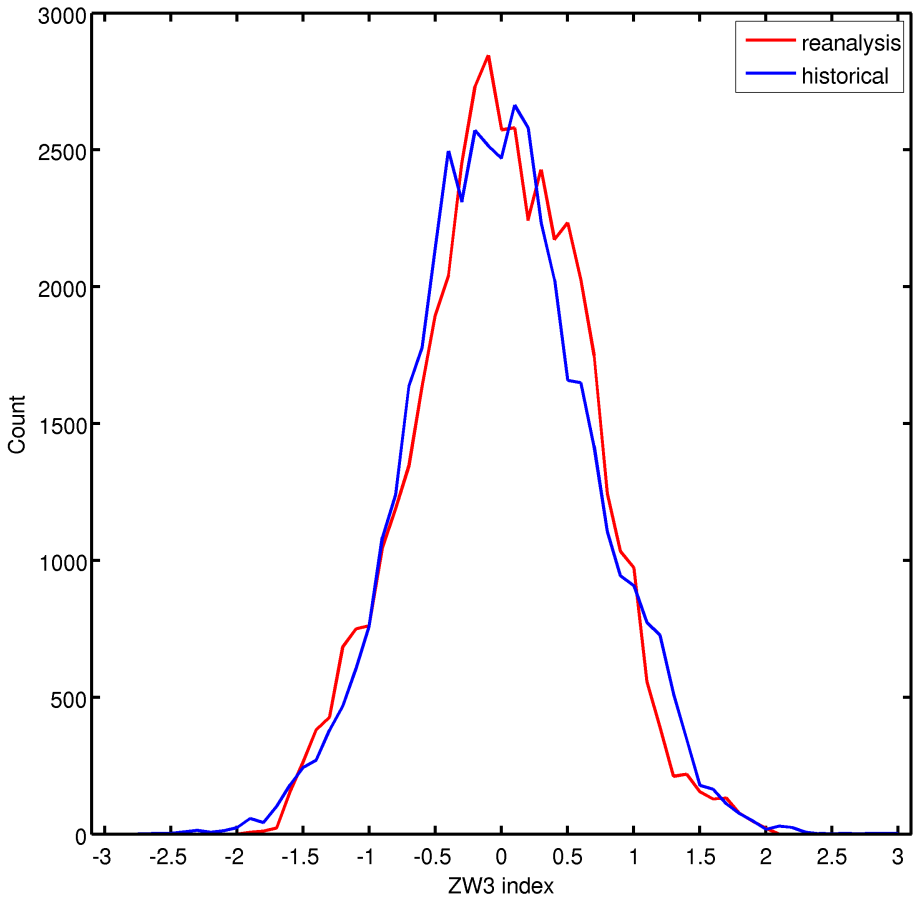

Figure 6.32: Mean ZW3 histograms. Reanalysis and Historical GCM output.

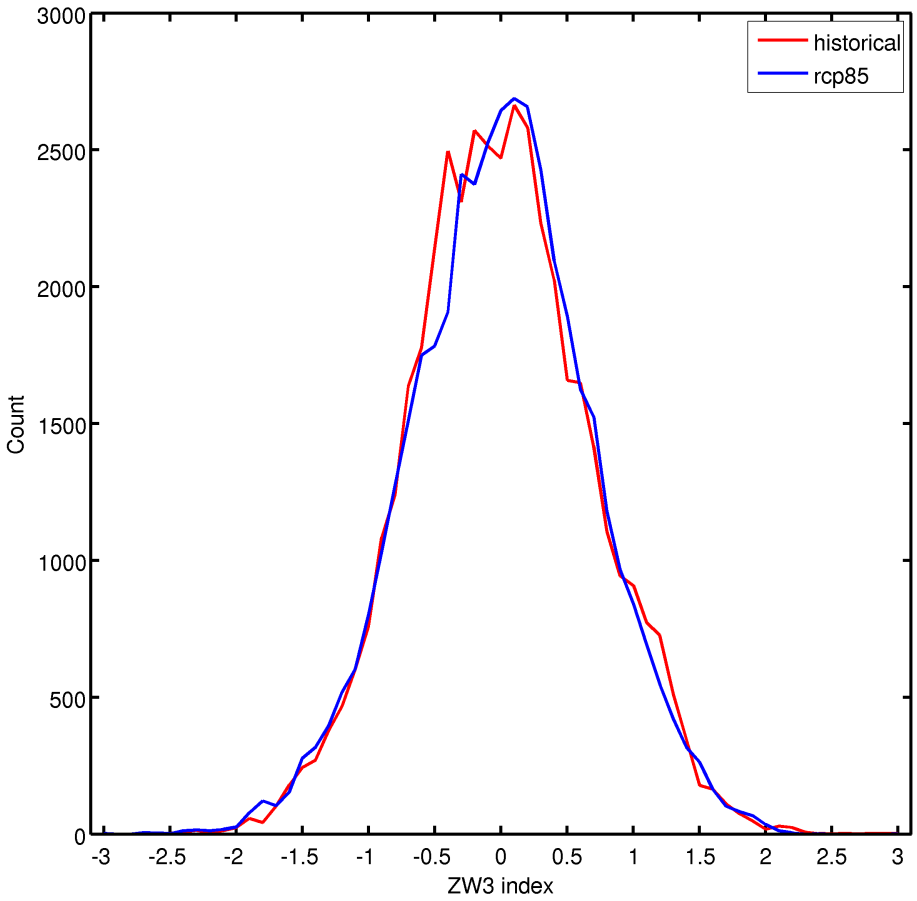

Figure 6.33: Mean ZW3 histograms. Historical and RCP 8.5 2071-2100 output.

6.5.2 *Southern Annular Mode (SAM)*

SAM has a large influence on the climate in the SH, during SAM+ the wind speed in the SH higher latitudes is enhanced and in the mid latitudes it is reduced (Arblaster and Meehl, 2006; Thompson et al., 2011). The seasonality of SAM is also an important factor, with SAM being more pronounced during summer. Thus we would expect BEs to be less frequent during SAM+ and summer as the increased wind speed disrupts the blocking events, see Section 2.3.3 for further discussion on SAM.

Figure 6.34 displays the frequency of occurrence of yearly BEs in the SPO region and the SAM index from the ERA-I reanalysis during summer. There is a high negative correlation of -0.765 between the BEs and the SAM index. A positive trend of 0.0515 BE % per/year is observed in the SAM index, while the BEs experience a reducing trend of -0.0425 % per/year. The observed trend towards SAM+ is a well accepted occurrence in the literature (Son et al., 2010; Arblaster et al., 2011) and has been linked to increased GHG and the reduction of stratospheric ozone.

In winter, Figure 6.35, there is still a high negative correlation of -0.633 between the BEs and SAM. However, the trends previously observed in summer, negative BE and SAM+, are not evident. A substantial reduction in BEs occurs in the winter of 1998. This was also observed by Oliveira et al. (2013), despite using a different methodology and data, they noted that a reduction in the blocking occurred during SAM+ and Southern Oscillation Index Positive Phase (SOI+) or La Niña .

Figure 6.36 displays the mean yearly summer BEs in the SPO region and the SAM index for each of GCMs during the historical period, 1976-2005. Each GCM is a different realisation, thus the models should not be directly compared to to each other on a year to year basis. The overall trend and correlation from the period is important. All of the GCMs display a strong negative correlation, ranging from -0.55 to -0.78 and are trending towards SAM+, while also displaying a reduction in BEs, thus in good agreement with the ERA-I reanalysis.

Table 6.5 displays the correlation coefficients between the SAM index and BE frequency in the SPO during summer, winter and monthly for each GCM and time period. A three monthly running mean is applied to the monthly BEs and SAM index. Of interest is the latter period 2071-2100 in both RCPs 4.5 and 8.5 projections where the correlation coefficient is reduced in three of the models during summer, Figure 6.37. During winter the historical and RCP projection correlations appear to be more stable and do not display the reduction observed in CCSM4, HADGEM2 ES and MIROC5 during the summer.

This would suggest that SAM is potentially less important, or correlated, in suppressing BE towards the end of the 21st century. However, the correlation response across the models is quite varied during the RCPs projections. Additionally the SAM in the GCM projections may be less certain due to competing forcings, ozone recovery and increased GHG, and how the individual GCMs parametrize these processes.

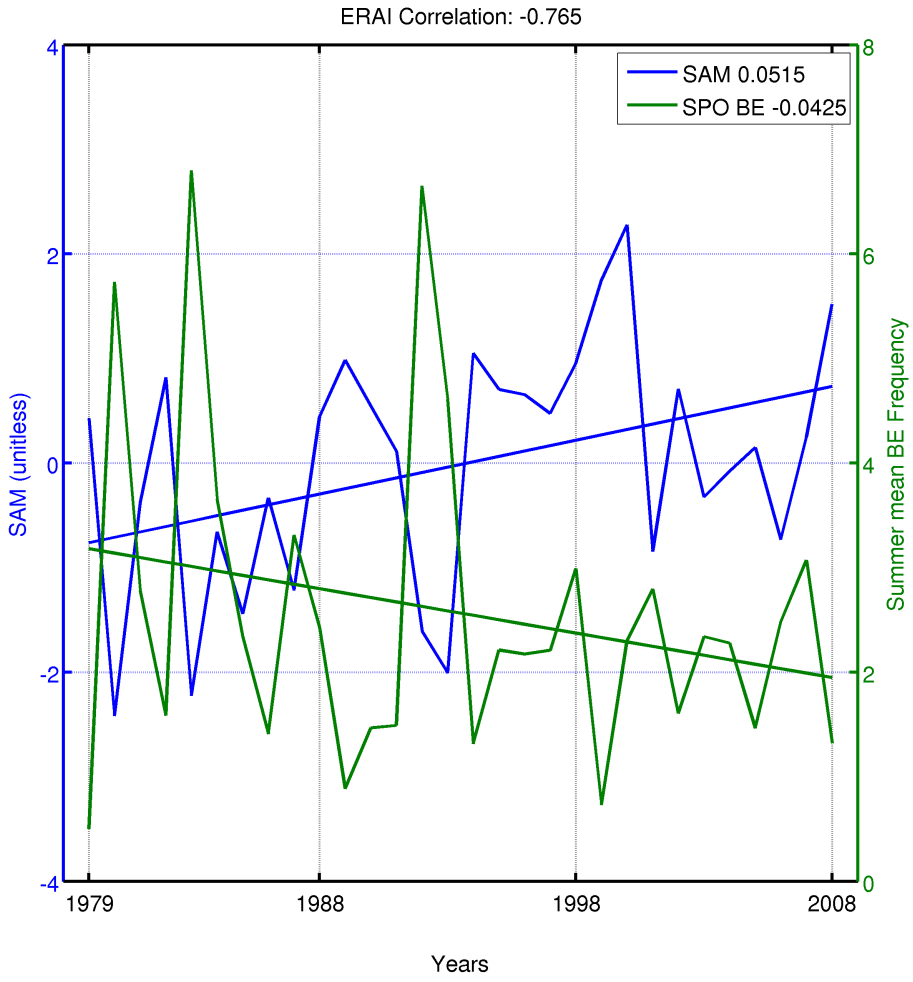

Figure 6.34: ERA-I Summer SAM & BE Correlation, 1979-2008. The trend per/year is displayed in the legend.

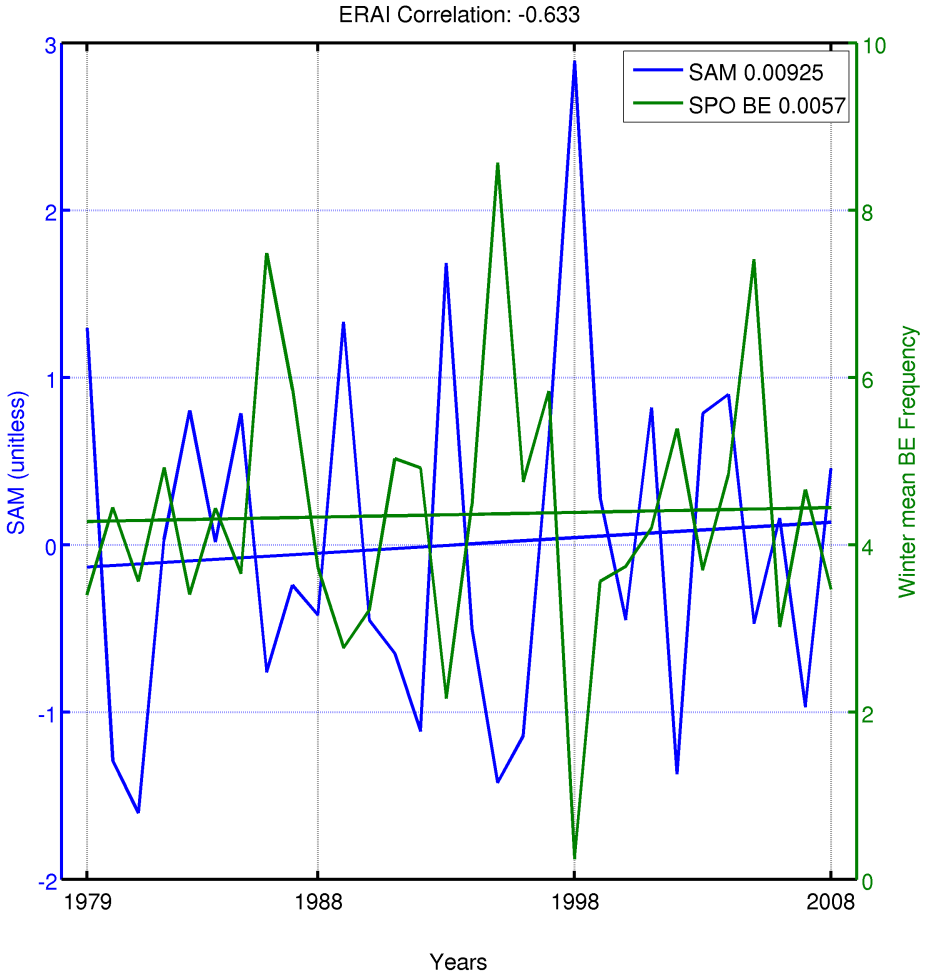

Figure 6.35: ERA-I Winter SAM & BE Correlation, 1979-2008. The trend per/year is displayed in the legend.

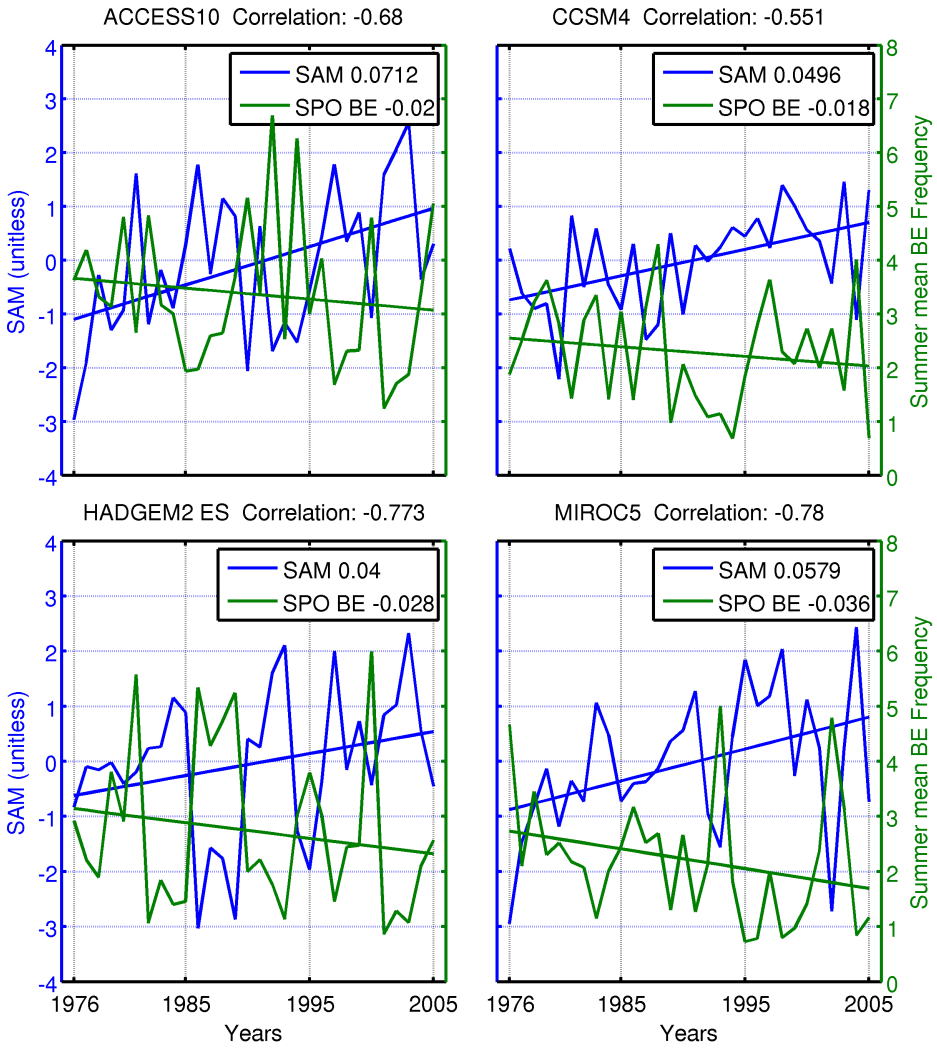

Figure 6.36: Historical GCMs Summer SAM & BE Correlation, 1976-2005. The trend per/year is displayed in the legend.

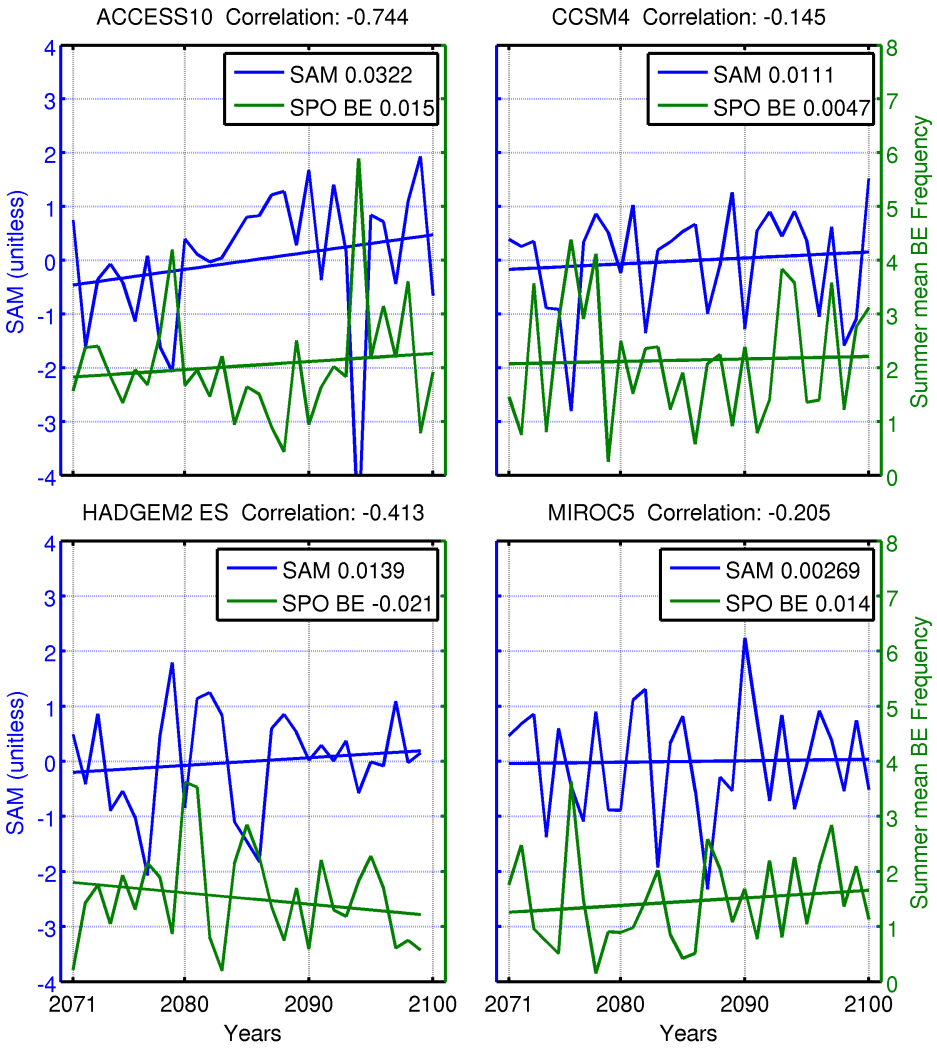

Figure 6.37: RCP 8.5 GCMs Summer SAM & BE Correlation, 2071-2100. The trend per/year is displayed in the legend.

Table 6.5: SPO region BE and SAM Correlations during Summer (DJF), Winter (JJA) and Monthly (mon) for the individual GCMs, a 3 month running mean has been applied to the monthly data.

		ACCESS10	CCSM4	HADGEM2 ES	MIROC5
Historical					
1976-2005	DJF	-0.680	-0.551	-0.773	-0.780
	JJA	-0.613	-0.587	-0.733	-0.802
	mon	-0.616	-0.518	-0.579	-0.494
RCP 4.5					
2011-2040	DJF	-0.769	-0.325	-0.729	-0.752
	JJA	-0.580	-0.596	-0.671	-0.672
	mon	-0.593	-0.428	-0.541	-0.507
2041-2070	DJF	-0.850	-0.371	-0.791	-0.595
	JJA	-0.474	-0.467	-0.562	-0.805
	mon	-0.627	-0.364	-0.498	-0.457
2071-2100	DJF	-0.610	-0.344	-0.397	-0.424
	JJA	-0.547	-0.756	-0.737	-0.580
	mon	-0.494	-0.450	-0.503	-0.387
RCP 8.5					
2011-2040	DJF	-0.591	-0.335	-0.643	-0.361
	JJA	-0.464	-0.771	-0.701	-0.676
	mon	-0.525	-0.497	-0.507	-0.358
2041-2070	DJF	-0.719	-0.173	-0.703	-0.537
	JJA	-0.460	-0.685	-0.504	-0.725
	mon	-0.572	-0.420	-0.410	-0.485
2071-2100	DJF	-0.744	-0.145	-0.413	-0.215
	JJA	-0.637	-0.535	-0.713	-0.701
	mon	-0.544	-0.282	-0.422	-0.405

6.6 CONCLUSION

A persistent positive anomaly methodology has been applied to the ERA-I reanalysis and four CMIP5 GCMs over the SH and regions of blocking activity have been determined. The annual BEs spatial distributions from the the reanalysis data and the CMIP5 historical GCM output broadly agree with each other with correlations >0.9. These results also agree with previous studies, which show the majority of BEs occur during the winter and are located in the SPO (Kiladis and Mo, 1998; Sinclair, 1996; Renwick, 2005). However, as we increase the temporal resolution, from annual to seasonal, increased variation in the BEs response from individual GCMs is evident.

We have illustrated a reduction in extent and frequency of future blocking events, between the CMIP5 historical and both RCP projections. In particular, in the SPO the annual frequency of BEs at the higher latitudes is reduced, as the extent of the historical maxima contracts in size and frequency. The SPO region has been previously noted as the main center of blocking activity in the SH (Kiladis and Mo, 1998; Sinclair, 1996; Renwick, 2005), and this is therefore an important finding. While both RCP projections display a reduction this is considerably more pronounced in the RCP 8.5, the higher forcing scenario. This agrees in sign with work detailed in Barnes et al. (2012), who observed a reduction in blocking frequency with increased GHG forcing in the NH. To the best of our understanding this is the first SH blocking study to utilises CMIP5 output and the first SH blocking GCM study to use a PPA methodology.

The BE reduction which occurs during the austral summer and spring and is observed in all four of the GCMs. The mean GCM historical annual BE frequency maximum was 15.3 % and the RCP 8.5 2071-2100 is reduced to 12.9 %. This 2.4 % reduction relates to a relative decrease of -15.7 %. Smaller BE increases are also observed, but are not robust between models.

In the SPO region the ensemble, as seen in Figure 6.19 and Table 6.4, shows large year to year variability in BE frequency,

thus resulting in a high standard deviation. A reduction in annual BEs is observed, -8.34% and -16.7% relative to the historical output for the 2071-2100 period in RCP 4.5 and 8.5, respectively. This occurs predominantly during the summer and spring, with the RCP8.5 showing a -32.6% relative reduction. However, the changes observed are less than 1 standard deviation, thus their significance is questionable.

The persistence study illustrates that the GCMs are negatively biased in their representation of shorter, 5 day, BEs. Longer duration events, 10 day BEs, display a better agreement with the reanalysis, however these events are also less frequent. During the RCP projections there is a reduction in the mid to long duration BEs, $\approx$ 6-12 days. The evolution of the persistence in the RCP projection ensemble mean shows a reduction in mid to long term duration BEs. Short, 5 day, BEs increase relative to the historical output, then reduce by 2071-2100. This positive anomaly observed at may be associated with the MIROC5 model, which displays an high positive anomaly. Thus the veracity of these persistence results may be impeded by the small ensemble size, this is observed as a large standard deviation between the models.

As expected SAM is negatively correlated with BE in the SPO region. In the SPO region the ERA-I reanalysis BEs are negatively correlated, -0.765, with the SAM index during summer, Figure 6.34. The GCMs also exhibit this negative correlation, ranging between -0.55 to -0.78, Figure 6.36. However, during the RCP projections the GCM response is less consistent, as seen in Table 6.3. ACCESS10 maintains a high negative correlation in across both scenarios and time periods. The negative correlation is reduced in the other models, CCSM4, HADGEM2 ES and MIROC5. Whilst during winter the models retain the negative correlations previously observed in the historical period. Thus, it appears that the negative relationship observed in summer between BE frequency and SAM is less related in the RCP projections than in the historical period.

ZW3 has also been thought to play a supporting role in the formation and reinforcement of BEs. ZW3 was investigated using

the methodology of Raphael (2004). No significant variation in the distribution of the ZW_3 index was observed, additionally the methodology of Raphael (2004) may be insensitive to phase changes, as it relies on static "centres of action".

In summary, the GCM ensemble has a consensus displaying a reduction in BE during summer and spring. However, due to the high year to year variability of BEs these values, while large relative to the historical period, are less than 1 standard deviation thus the significance is questionable. We have shown a high negative correlation between SAM and BE in the SPO, during periods of SAM+ BE are reduced in summer. The summer BE reduction may be associated with SAM. However the GCM projections do not show a clear consensus on this point.

Investigating the persistence of BE we have determined that the GCMs under report 5 day BE in the historical output. However, varied response from the GCMs impede the usefulness of this measure. Whilst this study has been informative and the results are beneficial, further work to increase the size of the GCM ensemble and testing the veracity of SAM in the GCM output is needed.

7

CONCLUSIONS AND FUTURE WORK

The goal of this thesis was "to understand what New Zealand's future weather may entail", with the use of Intergovernmental Panel on Climate Change (IPCC) assessment data in conjunction with Synoptic Climatology (SC) techniques.

The intention was to downscale the results back to New Zealand (NZ). However, this was superseded by the results in Chapter 4 and the research process has led further afield. This has highlighted the teleconnections that are present and the importance of the wider circulation to NZ. Thus, it is apparent that the larger scale circulation needs to be considered in conjunction with, if not before, the synoptic scale. However, some key findings for the Kidson Types (KTs) and Southern Hemisphere (SH) blocking were determined.

1. The Kidson methodology is insensitive to change in the circulation on an annual scale in the General Circulation Model (GCM) analysis.
2. Trends in the annual frequency of occurrence of the Kidson Types may be overstated depending on the length of data used, due to the high year to year variability.
3. Composite analysis with the KTs revealed Mean Sea Level Pressure (MSLP) anomalies located far from the KT domain, highlighting the importance of teleconnections to particular weather types and regimes. Modes of variability, such as Southern Annular Mode (SAM) and Southern

Oscillation Index (SOI), modulated the frequency of the Kidson Regimes.

4. A reduction of Blocking Events (BEs) in the South Pacific Ocean (SPO) during summer and spring is observed between 2071-2100 and this is larger in the higher emission scenario.

5. There is a strong negative correlation between Southern Annular Mode Positive Phase (SAM+) and BEs in the SPO in the present. However, the correlation is reduced in the future, based on the Representative Concentration Pathway (RCP)8.5 scenario.

The starting point of our analysis, in Chapter 4, expanded on the SC method of Kidson (2000). The KT are an important SC research tool for NZ and can provide an interpretation of complex weather patterns by a reduction and simplification into classes or types of weather. Our methodology incorporated the Kidson technique while allowing the use of GCM MSLP fields. This approach was successful as it allowed the KTs methodology to be applied to a variety of output, whilst retaining the original KTs. This was an important consideration as the intention was to build on the Kidson work, rather than replace it. The KTs were then determined using GCM output from the Coupled Model Inter-comparison Project (CMIP)3 archive, in order to gain understanding of future weather patterns over NZ.

The historical (20C3M) CMIP3 output from 15 GCMs were able to generate similar annual frequencies of occurrence to the KT frequencies observed in the reanalysis. The top five GCMs, as determined by root mean squared difference between the annual frequencies of the types and the NCEP/NCAR2 (NCEP2) reanalysis, were used in further analysis with the A1B and A2 scenarios.

The difference between the annual type frequencies for the historical and the A1B and A2 projections were determined for each of the top five models. For the 2081-2100 period with the A1B scenario only the HW type was statistically different from the values derived in the 20C3M run and 11 of the types dis-

played wide model spread, both positive and negative. Similar patterns were also observed in the A2 2081-2100 period, where the majority of the types are also not significantly different from their 20C3M control runs. The main difference is that the A2 scenario has larger interquartile ranges than those observed in the A1B scenarios. Increased variation is observed in the monthly KTs, however the model consensus is also reduced. During the A2 2081-2100 period there is an increase in TSW and NE during summer, but other changes are not statistically significant given the large variability.

The lack of annual type frequency change was unexpected, as a southerly displacement in the eddie-driven jet is projected to occur during the 21st Century (Arblaster and Meehl, 2006; Karpechko et al., 2010; Simpkins and Karpechko, 2012) and this might be expected to result in changes to the weather pattern frequencies. To examine this result, a sensitivity test simulating a southerly displacement in the jet position was performed by shifting the KT domain in the meridional direction. The changes in the frequency of the KTs for the different grid displacements were small, with some types maintaining nearly constant frequency. This analysis demonstrated that a large spatial shift in the position of the jet is required to obtain a significant change in annual type frequency using the Kidson methodology. The Kidson scheme therefore seems to favour the existing distributions and be relatively insensitive to change in this framework.

Trends were also determined for 4 realisations of the CCSM3.0 model using the A2 forcing scenario between 2000-2099. The SW, HE and HSE Types displayed both negative and positive trends, thus highlighting the high year to year variability of the KTs and the uncertainty in determining significant trends from model output. Thus, when combined with the range of model responses it was concluded that it is hard to draw any conclusions about frequency changes on the annual time scale. The KTs therefore do not appear to be an appropriate tool for analysis in this context.

It must also be remembered that the KT were not originally devised for this form of analysis and the KTs still have utility as an

objective classification system. The KTs have been widely used and therefore it would be beneficial to build on the existing body of work, rather than proposing a new synoptic climatology methodology for NZ.

In Chapter 5 versions of the KTs were generated with the ERA Interim (ERA-I) and Twentieth Century Reanalysis (20CR) reanalyses. The intention of this chapter was to further examine the KTs with respect to their wider context in the SH circulation, inter-annual variability and annual trends of the KTs. The inter-annual variability results, in terms of relationships between KT frequency and variations in the SAM and SOI are in agreement with previous work by Renwick (2011).

Composite analysis was also undertaken using the ERA-I reanalysis. The KTs were determined with the same methodology used in Chapter 4 and the resultant KT time series is then used to determine MSLP composites in the SH for each type. Viewing the KTs within the larger domain is insightful. For example, the westerly flow can be inferred from the MSLP, via the geostrophic approximation, and it is apparent that this flow is a dominant feature for NZ. Additionally synoptic scale systems, cyclones and anticyclones, can be thought of as superimposed on the mean flow. This inspired the development of a cyclone tracking algorithm.

Since the KTs are defined over NZ, at distances away from NZ the MSLP becomes closer to the climatological mean when compositing data based on KTs. During this analysis a particularly interesting feature was revealed in the KT MSLP anomalies, especially considering the number of members that make up one of the KT composites. As expected the largest MSLP anomalies are located within and close to the KT domain. However, a positive anomaly was revealed far from NZ with the South Westerly (SW) type. This is of interest as BEs are known to occur in this region (Renwick, 2005) and this also highlights that specific KTs may be linked to larger teleconnection patterns. This result was the motivation for Chapter 6, as a change in BE in this region could be directly linked to NZ weather.

As discussed in Chapter 3, the veracity of reanalyses in the SH prior to the satellite record is questionable. The 20CR provides a long term data set based on surface observations only, thus avoiding discontinuities associated with assimilation of data from different observation platforms. However, there is still a deficit of observations in the SH, particularly before 1950.

For each year the KT frequency of occurrence is determined for the 20CR, ERA-I and NCEP/NCAR1 (NCEP1) reanalyses. As expected there is high year to year variability. The only significant trends are observed with the 20CR, as this data series has the longest record, from 1871-2010. There are conflicting positive and negative trends across the three reanalysis for the different types and regimes. However, when the trends are compared over a period of overlapping data, between 1979-1997, consensus is observed with the sign of the trends. The lack of significant trends is related to the high year to year variability and the length of data record, thus the only significant regimes trends are observed in the 20CR. Which displays a reduction in the Zonal regime of 0.317 % per decade.

The motivation for the blocking study in Chapter 6 is that a MSLP positive anomaly was located far from the Kidson domain, in a region in which blocking occurs, during the composite analysis of the KTs. Additionally, there is a lack of literature regarding this important phenomenon, particularly with regard to GCM studies, thus this is a topic worthy of study. To our knowledge, this is the first study using GCM output using the Persistent Positive Anomaly (PPA) methodology in the SH and this is advantageous as the spatial pattern, latitude and longitude, of the BEs is determined. Additionally this is also the first blocking study using CMIP5 output in the SH to our knowledge.

The methodology used in Chapter 6 is similar to that of Renwick (2005) and uses CMIP5 output from four GCMs. The ensemble size of four GCMs was influenced by results from Chapter 4. A ten member ensemble was initially used in Chapter 4, however the range of GCM response diluted the significance of the results. The ensemble was then reduced to the five best per-

forming members. The approach of using a small ensemble of the best performing GCMs was therefore used in Chapter 6, the GCMs selection was influenced by work detailed in Mullan et al. (2013) and data availability.

The BE annual spatial patterns from the four GCMs historical output are highly correlated with the reanalysis. This was tested using a 8 hPa and a higher 16 hPa threshold to identify anomalies. The GCM historical seasonal output is also well correlated, though more variation is present. These results are in agreement to previous results in the literature (Kiladis and Mo, 1998; Sinclair, 1996; Renwick, 2005), with the majority of BEs occurring during winter and located in the SPO.

Since the majority of BE occur in the SPO a smaller domain was used for further analysis. The SPO region was defined as latitudes 45°S - 70°S and longitudes 180°- 270°. In the SPO region the persistence, duration of the BE, was determined. The historical GCMs display less 5 day events than the reanalysis. However, by 10 days the count was similar to the reanalysis. The persistence and spatial pattens agree with the literature, which also notes that blocking frequency is under reported in GCM output (Palmer et al., 2008).

A BE reduction occurs in the SPO and it steadily decreases during the 21st century. This is observed in both the RCP4.5 and 8.5 scenarios, however it is largest in the RCP8.5. The ensemble displays an annual BE relative frequency change of -8.34% and -16.7% for the RCP4.5 and 8.5 projections, respectively for the 2071-2100 period. During summer, this becomes -22.8% and -32.6% and the summer BE reduction is observed in all of the models in the SPO. However, during winter there is less model agreement. There was less model consensus with the persistence during the RCP projections.

Since the SPO BE reduction was strongest in summer and Matsueda et al. (2009) suggested that SAM could be related to a reduction of blocking observed in the SH. SAM was correlated against the BE frequency in the SPO. SAM+ was found to be highly negatively correlated with BEs in the SPO in the reanaly-

sis and the historical output from the four GCMs. However, the correlation is reduced in three of the GCMs towards the end of the 21st century in both RCP projections. This could be associated with a change in the dominant forcing of SAM from ozone to green house gases (Arblaster et al., 2011). Additionally, the GCMs use different processes to parametrise or prescribe stratospheric ozone.

The small ensemble size may also have impeded these results. This is due to the varied response and lack of consensus from the model projections in the persistence analysis, during winter and SAM correlations during the future projections. A larger ensemble or more realisations from the GCMs selection may be beneficial in clarifying the results, or highlighting errant model behaviour.

7.0.1 *Thesis Synthesis*

This work followed a narrative that began with the KTs and progressed to the larger circulation. In Chapter 5 the modes of variability, SAM and El Niño - Southern Oscillation (ENSO), modulated the Kidson types and MSLP anomalies were observed located far from NZ. In Chapter 6 SAM also modulated the frequency of SPO blocking events. Thus the SAM provides an important linkage between the large scale and regional climate. A benefit of synoptic climatology methodologies is the simplification of complex weather systems. However, the larger circulation needs to be considered and incorporated into the these classification systems.

Climate studies often employ GCM output, thus the suitability of these GCMs needs to be examined and justified. A smaller ensemble of suitable GCMs may be beneficial instead of a large ensemble, this was observed in the range of KTs frequencies in Chapter 4. However, in Chapter 6 the small GCM selection may have been a hindrance.

The goal of this thesis was "to understand what New Zealand's future weather may entail". However, in order to understand fu-

ture weather patterns the future teleconnections and circulation changes must first be understood.

7.1 FUTURE WORK

The KTs have been widely used and thus it would be beneficial to build on this existing body of work and methodology, rather than proposing a new synoptic climatology method for NZ. Therefore, further SC work in NZ needs to incorporate the KTs or provide robust linkages to the KTs, while addressing the sensitivity shortcomings.

A version of the KTs was generated using the ERA-I reanalysis and these are currently being used in a study which investigates ocean wave heights around New Zealand by another researcher.

Chapter 5 is to be reworked for submission. Since this work focuses on the KT, thus of interest mainly to the NZ, the NZ journal Weather and Climate is appropriate for publication.

7.1.1 *Blocking*

Chapter 6 is currently being reformatted and worked on for submission. Whilst a paper is to be submitted, there is still room for further investigation in this area.

1. A larger GCM ensemble might be beneficial in obtaining greater model consensus and could also highlight any errant model behaviour. This could also assist by increasing the statistical robustness of the results.
2. While a reduction in blocking frequency was observed with the GCM projections in chapter 6, the implications and mechanism of this reduction have not yet been adequately answered. Further work is required and could include investigation of linkages to SOI and Sea Surface Temperature (SST).

3. SAMs relationship with BEs needs further study, in particular the reduction in the correlation observed in the RCP projections.
4. Repercussions from the projected reduction of BEs in the SPO for NZ needs to be considered. How this changes the circulation and the meteorological impacts for NZ. This work could link to the KTs
5. Further investigation of Zonal Wave 3 (ZW_3) and its effect on SH blocking would be conducted using a Fourier analysis methodology.

7.1.2 *Cyclone & Anticyclone Climatologies*

In Chapter 5 it was apparent that synoptic scale weather in the mid-latitudes can be considered as cyclones and anticyclones superimposed on the mean flow. As alluded to in the Introduction and Literature Review, in Sections 1.2 and 2.3.5, a tracking scheme was developed. While this tracking work is not presented, it is still worthy of mention. Whilst promising at first, refining the algorithm and tuning of the subjective threshold slowed progress. Additionally, when considering the amount of GCM data to process, the speed of the program made this analysis untenable in the remaining thesis timeframe.

However, the rationale for this work is still valid and worthy of further investigation. The CMIP5 archives data at a high temporal (6 hour) and spatial resolution. Thus, the GCM output would be suitable for Lagrangian methodology. This climatology could provide beneficial information regarding projected mid latitude weather systems that impact NZ.

1. In order to process the volume of GCM data required a simpler scheme which is optimised for speed would be necessary.
2. Reducing the domain size from the SH to the larger NZ region would also reduce the computational requirements.

This is an ideal candidate for further investigation and my intention is to continue with aspects of this work.

BIBLIOGRAPHY

Ackerley, D., S. Dean, A. Sood, and A. Mullan, 2012: Regional climate modelling in New Zealand: Comparison to gridded and satellite observations. *Weather and Climate*, **32**, 3–22.

Ackerley, D., et al., 2011: Using synoptic type analysis to understand New Zealand climate during the mid-holocene. *Climate of the Past*, **7 (4)**, 1189–1207, doi:10.5194/cp-7-1189-2011, URL http://www.clim-past.net/7/1189/2011/.

Ainley, D., J. Russell, S. Jenouvrier, E. Woehler, P. O. Lyver, W. R. Fraser, and G. L. Kooyman, 2010: Antarctic penguin response to habitat change as earth's troposphere reaches 2 °c above preindustrial levels. *Ecological Monographs*, **80 (1)**, 49–66, doi:10.1890/08-2289.1, URL http://dx.doi.org/10.1890/08-2289.1.

Anagnostopoulou, C., K. Tolika, and P. Maheras, 2009: Classification of circulation types: a new flexible automated approach applicable to NCEP and GCM datasets. *Theoretical and Applied Climatology*, **96**, 3–15, doi:10.1007/s00704-008-0032-6.

Arblaster, J. M. and G. A. Meehl, 2006: Contributions of external forcings to Southern Annular Mode trends. *Journal of Climate*, **19**, 2896, doi:10.1175/JCLI3774.1.

Arblaster, J. M., G. A. Meehl, and D. J. Karoly, 2011: Future climate change in the Southern Hemisphere: Competing effects of ozone and greenhouse gases. *Geophysical Research Letters*, **38**, doi:10.1029/2010GL045384.

Barnes, E., J. Slingo, and T. Woollings, 2012: A methodology for the comparison of blocking climatologies across indices, models and climate scenarios. *Climate Dynamics*, **38 (11-12)**, 2467–2481, doi:10.1007/s00382-011-1243-6.

Barriopedro, D., R. García-Herrera, J. F. González-Rouco, and R. M. Trigo, 2010a: Application of blocking diagnosis methods to general circulation models. part ii: model simulations. **35 (7-8)**, 1393–1409, doi:10.1007/s00382-010-0766-6, URL http://dx.doi.org/10.1007/s00382-010-0766-6.

Barriopedro, D., R. García-Herrera, and R. M. Trigo, 2010b: Application of blocking diagnosis methods to general circulation models. part I: A novel detection scheme. *Climate Dynamics*, **35 (7-8)**, 1373–1391, doi:10.1007/s00382-010-0767-5.

Barry, R. G. and A. H. Perry, 1973: *Synoptic climatology; methods and applications [by] R. G. Barry and A. H. Perry*. Methuen London,, xvi, 555 p. pp.

Bengtsson, L., S. Hagemann, and K. I. Hodges, 2004: Can climate trends be calculated from reanalysis data? *Journal of Geophysical Research: Atmospheres*, **109 (D11)**, doi:10.1029/2004JD004536, URL http://dx.doi.org/10.1029/2004JD004536.

Berrisford, P., B. J. Hoskins, and E. Tyrlis, 2007: Blocking and rossby wave breaking on the dynamical tropopause in the southern hemisphere. *Journal of the Atmospheric Sciences*, **64 (8)**, 2881–2898, doi:10.1175/JAS3984.1, URL http://dx.doi.org/10.1175/JAS3984.1.

Bi, D., et al., 2013: The access coupled model: Description, control climate and evaluation. *Aust Met Oceanog J*, **63**, 9–32.

Bindoff, N., et al., 2013: *Climate Change 2013: The Physical Science Basis. Contribution of Working Group I to the Fifth Assessment Report of the Intergovernmental Panel on Climate Change*, chap. 10. Cambridge University Press, Cambridge, United Kingdom.

Bjerknes, J., 1966: A possible response of the atmospheric hadley circulation to equatorial anomalies of ocean temperature. *Tellus*, **18 (4)**, 820–829, doi:10.1111/j.2153-3490.1966.tb00303.x, URL http://dx.doi.org/10.1111/j.2153-3490.1966.tb00303.x.

Bjornsson, S. A., H. Venegas, 1997: *A manual for EOF and SVD analyses of Climatic Data*. McGill University.

Blackmon, M. L., 1976: A climatological spectral study of the 500 mb geopotential height of the Northern Hemisphere. *Journal of the Atmospheric Sciences*, **33 (8)**, 1607–1623, doi:10.1175/1520-0469(1976)033<1607:ACSSOT>2.0.CO;2, URL http://dx.doi.org/10.1175/1520-0469(1976)033<1607:ACSSOT>2.0.CO;2.

Bromwich, D. H., R. L. Fogt, K. I. Hodges, and J. E. Walsh, 2007: A tropospheric assessment of the ERA-40, NCEP, and JRA-25 global reanalyses in the polar regions. *Journal of Geophysical Research: Atmospheres*, **112**, 10 111, doi:10.1029/2006JD007859.

Bromwich, D. H., J. P. Nicolas, and A. J. Monaghan, 2011: An assessment of precipitation changes over Antarctica and the Southern Ocean since 1989 in contemporary global reanalyses. *Journal of Climate*, **24 (16)**, 4189–4209, doi:10.1175/2011JCLI4074.1, URL http://dx.doi.org/10.1175/2011JCLI4074.1.

Christensen, J., et al., 2013: *Climate Phenomena and their Relevance for Future Regional Climate Change 2013: The Physical Science Basis. Contribution of Working Group I to the Fifth Assessment Report of the Intergovernmental Panel on Climate Change*, chap. 14. Cambridge University Press, Cambridge, United Kingdom.

Christensen, W. I. and R. A. Bryson, 1966: An investigation of the potential of component analysis for weather classification. *Monthly Weather Review*, **94**, 697–709, doi:10.1175/1520-0493(1966)094<0697:AIOTPO>2.3.CO;2.

Coggins, J. H. J., A. J. Mcdonald, G. Plank, M. Pannell, B. Jolly, S. Parsons, and T. Delany, 2013: SNOW-WEB: a new technology for Antarctic meteorological monitoring. *Antarctic Science*, **25 (04)**, 583–599.

Collins, M., et al., 2010: The impact of global warming on the tropical pacific ocean and el nino. *Nature Geosci*, **3 (6)**, 391–397, URL http://dx.doi.org/10.1038/ngeo868.

Collins, W. J., et al., 2011: Development and evaluation of an Earth-System model – HadGEM2. *Geoscientific Model Development Discussions*, **4 (2)**, 997–1062, doi:10.5194/gmdd-4-997-2011.

Compo, G. P., J. S. Whitaker, and P. D. Sardeshmukh, 2006: Feasibility of a 100-year reanalysis using only surface pressure data. *Bulletin of the American Meteorological Society*, **87 (2)**, 175–190, doi:10.1175/BAMS-87-2-175, URL http://dx.doi.org/10.1175/BAMS-87-2-175.

Compo, G. P., et al., 2011: The twentieth century reanalysis project. *Quarterly Journal of the Royal Meteorological Society*, **137 (654)**, 1–28, doi:10.1002/qj.776, URL http://dx.doi.org/10.1002/qj.776.

Cowan, T., P. van Rensch, A. Purich, and W. Cai, 2013: The association of tropical and extratropical climate modes to atmospheric blocking across Southeastern Australia. *Journal of Climate*, **26 (19)**, 7555 – 7569, doi:10.1175/JCLI-D-12-00781.1.

Cuell, C. and B. Bonsal, 2009: An assessment of climatological synoptic typing by principal component analysis and kmeans clustering. *Theoretical and Applied Climatology*, **98**, 361–373, URL http://dx.doi.org/10.1007/s00704-009-0119-8, 10.1007/s00704-009-0119-8.

Dean, S. and P. Stott, 2009: The effect of local circulation variability on the detection and attribution of New Zealand temperature trends. *Journal of Climate*, **22 (23)**, 6217–6229.

Dee, D. P., et al., 2011: The ERA-Interim reanalysis: configuration and performance of the data assimilation system. *Quarterly Journal of the Royal Meteorological Society*, **137 (656)**, 553–597, doi:10.1002/qj.828.

Doherty, S., et al., 2009: Lessons learned from IPCC AR4: Scientific developments needed to understand, predict, and respond to climate change. *Bulletin of the American Meteorological Society*, **90 (4)**, 497–513.

Dole, R. M. and N. D. Gordon, 1983: Persistent anomalies of the extratropical Northern Hemisphere wintertime circulation: Geographical distribution and regional persistence characteristics. *Monthly Weather Review*, **111 (8)**, 1567–1586, doi:10.1175/1520-0493(1983)111<1567:PAOTEN>2.0.CO;2, URL http://dx.doi.org/10.1175/1520-0493(1983)111<1567:PAOTEN>2.0.CO;2.

Drost, F., J. Renwick, B. Bhaskaran, H. Oliver, and J. McGregor, 2007: Simulation of New Zealand's climate using a high-resolution nested regional climate model. *International Journal of Climatology*, **27 (9)**, 1153–1169, doi:{10.1002/joc.1461}.

Dunn-Sigouin, E. and S.-W. Son, 2013: Northern Hemisphere blocking frequency and duration in the CMIP5 models. *Journal of Geophysical Research: Atmospheres*, **118 (3)**, 1179–1188, doi:10.1002/jgrd.50143.

Flato, G., et al., 2013: *Climate Change 2013: The Physical Science Basis. Contribution of Working Group I to the Fifth Assessment Report of the Intergovernmental Panel on Climate Change*, chap. 9. Cambridge University Press, Cambridge, United Kingdom.

Fogt, R. L., J. M. Jones, and J. Renwick, 2012: Seasonal zonal asymmetries in the Southern Annular Mode and their impact on regional temperature anomalies. *Journal of Climate*, **25 (18)**, 6253 – 6270, doi:10.1175/JCLI-D-11-00474.1.

Gent, P. R., et al., 2011: The community climate system model version 4. *Journal of Climate*, **24 (19)**, 4973–4991, doi:10.1175/2011JCLI4083.1.

Gillett, N. P., T. D. Kell, and P. D. Jones, 2006: Regional climate impacts of the Southern Annular Mode. *Geophysical Research Letters*, **33**, L23 704, doi:10.1029/2006GL027721.

Gong, D. and S. Wang, 1999: Definition of Antarctic Oscillation index. *Geophysical Research Letters*, **26**, 459–462, doi:10.1029/1999GL900003.

Gordon, N. D., 1986: The Southern Oscillation and New Zealand Weather. *Monthly Weather Review*, **114**, 371–+, doi:

10.1175/1520-0493(1986)114<0371:TSOANZ>2.0.CO;2.

Griffiths, G., 2011: Drivers of extreme daily rainfalls in New Zealand. *Weather and Climate*, **31**, 24–49.

Harvey, B. J., L. C. Shaffrey, T. J. Woollings, G. Zappa, and K. I. Hodges, 2012: How large are projected 21st century storm track changes? *Geophysical Research Letters*, **39**, doi:10.1029/2012GL052873.

Hawkins, E. and R. Sutton, 2009: The potential to narrow uncertainty in regional climate predictions. *Bulletin of the American Meteorological Society*, **90 (8)**, 1095–1107.

Hewitson, B. C. and R. G. Crane, 2002: Self-organizing maps: applications to synoptic climatology. *Climate Research*, **22 (1)**, 13–26, URL http://www.int-res.com/abstracts/cr/v22/n1/p13-26/.

Ho, M., A. S. Kiem, and D. C. Verdon-Kidd, 2012: The Southern Annular Mode: a comparison of indices. *Hydrology and Earth System Sciences*, **16 (3)**, 967–982, doi:{10.5194/hess-16-967-2012}.

Hobbs, W. R. and M. N. Raphael, 2007: A representative time-series for the southern hemisphere zonal wave 1. *Geophysical Research Letters*, **34 (5)**, doi:10.1029/2006GL028740, URL http://dx.doi.org/10.1029/2006GL028740.

Hobbs, W. R. and M. N. Raphael, 2010: Characterizing the zonally asymmetric component of the SH circulation. *Climate Dynamics*, **35 (5)**, 859–873, doi:10.1007/s00382-009-0663-z.

Hope, P. K., 2006: Projected future changes in synoptic systems influencing southwest Western Australia. *Climate Dynamics*, **26**, 765–780, doi:10.1007/s00382-006-0116-x.

Hope, P. K., W. Drosdowsky, and N. Nicholls, 2006: Shifts in the synoptic systems influencing southwest Western Australia. *Climate Dynamics*, **26 (7-8)**, 751–764, doi:10.1007/s00382-006-0115-y.

Hoskins, B. J. and K. I. Hodges, 2005: A new perspective on southern hemisphere storm tracks. *Journal of Climate*, **18 (20)**, 4108–4129, doi:10.1175/JCLI3570.1.

Huth, R., 2000: A circulation classification scheme applicable in GCM studies. *Theoretical and Applied Climatology*, **67**, 1–18, doi:10.1007/s007040070012.

Huth, R., C. Beck, A. Philipp, M. Demuzere, Z. Ustrnul, M. Cahynová, J. Kyselỳ, and O. Tveito, 2008: Classifications of atmospheric circulation patterns. *Annals of the New York Academy of Sciences*, **1146 Trends and Directions in Climate Research**, 105–152.

IPCC, 2007: Climate change 2007: The physical science basis: Contribution of working group i to the fourth assessment report of the intergovernmental panel on climate change. Cambridge University Press, Cambridge [etc.].

Jiang, N., 2010: A new objective procedure for classifying New Zealand synoptic weather types during 1958-2008. *International Journal of Climatology*, **31 (6)**, 863–879, doi:10.1002/joc.2126.

Jiang, N., K. N. Dirks, and K. Luo, 2013a: Classification of synoptic weather types using self-organising map and its application to climate and air quality data visualisation. *Weather and Climate*, **33**, 52–75.

Jiang, N., G. Griffiths, and A. Lorrey, 2013b: Influence of large-scale climate modes on daily synoptic weather types over New Zealand. *International Journal of Climatology*, **33 (2)**, 499–519, doi:10.1002/joc.3443, URL http://dx.doi.org/10.1002/joc.3443.

Jiang, N., J. E. Hay, and G. W. Fisher, 2004: Classification of New Zealand synoptic weather types and relation to the Southern Oscillation Index. *Weather and Climate*, **23 (24)**, 3–23.

Jin, E., et al., 2008: Current status of enso prediction skill in coupled ocean–atmosphere models. *Climate Dynamics*, **31**, 647–664, 10.1007/s00382-008-0397-3.

Jones, D. and I. Simmonds, 1994: A climatology of Southern Hemisphere anticyclones. *Climate Dynamics*, **10 (6-7)**, 333–348, doi:10.1007/BF00228031, URL http://dx.doi.org/10.1007/BF00228031.

Jones, P. D. and D. H. Lister, 2007: Intercomparison of four different Southern Hemisphere sea level pressure datasets. *Geophysical Research Letters*, **34**, L10 704, doi:10.1029/2007GL029251.

Kalnay, E., et al., 1996: The NCEP/NCAR 40-year reanalysis project. *Bulletin of the American Meteorological Society*, **77**, 437–472, doi:10.1175/1520-0477(1996).

Kanamitsu, M., W. Ebisuzaki, J. Woollen, S.-K. Yang, J. J. Hnilo, M. Fiorino, and G. L. Potter, 2002: NCEP-DOE AMIP-II Reanalysis (R-2). *Bulletin of the American Meteorological Society*, **83**, 1631–1643, doi:10.1175/BAMS-83-11-1631(2002)083<1631:NAR>2.3.CO;2.

Karpechko, A. Y., N. P. Gillett, L. J. Gray, and M. Dall'Amico, 2010: Influence of ozone recovery and greenhouse gas increases on Southern Hemisphere circulation. *Journal of Geophysical Research: Atmospheres*, **115 (D22)**, doi:10.1029/2010JD014423, URL http://dx.doi.org/10.1029/2010JD014423.

Kidson, J. W., 1994a: An automated procedure for the identification of synoptic types applied to the New Zealand region. *International Journal of Climatology*, **14**, 711–721, doi:10.1002/joc.3370140702.

Kidson, J. W., 1994b: Relationship of New Zealand daily and monthly weather patterns to synoptic weather types. *International Journal of Climatology*, **14**, 723–737, doi:10.1002/joc.3370140703.

Kidson, J. W., 1997: The utility of surface and upper air data in synoptic climatological specification of surface climatic variables. *International Journal of Climatology*, **17**, 399–413.

Kidson, J. W., 1999: Principal modes of southern hemisphere low-frequency variability obtained from ncep–ncar reanalyses. *Journal of Climate*, **12 (9)**, 2808–2830, doi:10.1175/1520-0442(1999)012<2808:PMOSHL>2.0.CO;2, URL http://dx.doi.org/10.1175/1520-0442(1999)012<2808:PMOSHL>2.0.CO;2.

Kidson, J. W., 2000: An analysis of New Zealand synoptic types and their use in defining weather regimes. *International Journal of Climatology*, **20 (3)**, 299–316.

Kidson, J. W. and J. A. Renwick, 2002a: Patterns of convection in the tropical pacific and their influence on New Zealand weather. *International Journal of Climatology*, **22**, 151–174, doi:10.1002/joc.737.

Kidson, J. W. and J. A. Renwick, 2002b: The Southern Hemisphere evolution of ENSO during 1981-99. *Journal of Climate*, **15**, 847–863, doi:10.1175/1520-0442(2002)015<0847:TSHEOE>2.0.CO;2.

Kidson, J. W. and M. R. Sinclair, 1995: The influence of persistent anomalies on Southern Hemisphere storm tracks. *Journal of climate*, **8 (8)**, 1938–1950.

Kidson, J. W. and C. S. Thompson, 1998: A comparison of statistical and model-based downscaling techniques for estimating local climate variations. *Journal of Climate*, **11 (4)**, 735–753, doi:10.1175/1520-0442(1998)011<0735:ACOSAM>2.0.CO;2, URL http://dx.doi.org/10.1175/1520-0442(1998)011<0735:ACOSAM>2.0.CO;2.

Kidston, J., D. Frierson, J. Renwick, and G. Vallis, 2010: Observations, simulations, and dynamics of jet stream variability and annular modes. *Journal of Climate*, **23 (23)**, 6186–6199, cited By (since 1996) 1.

Kidston, J. and E. P. Gerber, 2010: Intermodel variability of the poleward shift of the austral jet stream in the cmip3 integrations linked to biases in 20th century climatology. *Geophysical Research Letters*, **37 (9)**, doi:10.1029/2010GL042873, URL http://dx.doi.org/10.1029/2010GL042873.

Kidston, J., J. A. Renwick, and J. McGregor, 2009: Hemispheric-Scale Seasonality of the Southern Annular Mode and Impacts on the Climate of New Zealand. *Journal of Climate*, **22**, 4759–4770, doi:10.1175/2009JCLI2640.1.

Kiladis, G. N. and K. C. Mo, 1998: *Interannual and intraseasonal variability in the Southern Hemisphere*, Vol. 27, chap. 8, 307–336. The American Meteorological Society: Meteorological Monographs.

Kistler, R., et al., 2001: The NCEP-NCAR 50-Year Reanalysis: Monthly Means CD-ROM and Documentation. *Bulletin of the American Meteorological Society*, **82**, 247–268, doi:10.1175/1520-0477(2001)082<0247:TNNYRM>2.3.CO;2.

Knutti, R., R. Furrer, C. Tebaldi, J. Cermak, and G. A. Meehl, 2010: Challenges in combining projections from multiple climate models. *Journal of Climate*, **23**, 2739–2758, doi:10.1175/2009JCLI3361.1.

Lee, C. C. and S. C. Sheridan, 2012: A six-step approach to developing future synoptic classifications based on GCM output. *International Journal of Climatology*, **32 (12)**, 1792–1802, doi:10.1002/joc.2394, URL http://dx.doi.org/10.1002/joc.2394.

Liang, X.-Z., K. E. Kunkel, G. A. Meehl, R. G. Jones, and J. X. L. Wang, 2008: Regional climate models downscaling analysis of general circulation models present climate biases propagation into future change projections. *Geophysical Research Letters*, **35 (8)**, doi:10.1029/2007GL032849, URL http://dx.doi.org/10.1029/2007GL032849.

Liu, Q., 1994: On the definition and persistence of blocking. *Tellus A*, **46 (3)**, URL http://www.tellusa.net/index.php/tellusa/article/view/15479.

Lorrey, A., A. M. Fowler, and J. Salinger, 2007: Regional climate regime classification as a qualitative tool for interpreting multi-proxy palaeoclimate data spatial patterns: A new zealand case study. *Palaeogeography, Palaeoclimatology, Palaeoecology*, **253 (3-4)**, 407 – 433, doi:10.1016/j.palaeo.

2007.06.011, URL http://www.sciencedirect.com/science/article/pii/S0031018207003306.

Lund, I. A., 1963: Map pattern classification by statistical methods. *Journal of Applied Meteorology*, **2**, 56–65.

MacQueen, J. B., 1967: Some methods for classification and analysis of multivariate observations. *Proc. of the fifth Berkeley Symposium on Mathematical Statistics and Probability*, L. M. L. Cam and J. Neyman, Eds., University of California Press, Berkeley, CA, University of California, Vol. 1, 281–297.

Mahlstein, I., P. R. Gent, and S. Solomon, 2013: Historical Antarctic mean sea ice area, sea ice trends, and winds in CMIP5 simulations. *Journal of Geophysical Research: Atmospheres*, **118 (11)**, 5105–5110, doi:10.1002/jgrd.50443, URL http://dx.doi.org/10.1002/jgrd.50443.

Mahlstein, I. and R. Knutti, 2010: Regional climate change patterns identified by cluster analysis. *Climate Dynamics*, **35 (4)**, 587–600, doi:10.1007/s00382-009-0654-0, URL http://dx.doi.org/10.1007/s00382-009-0654-0.

Marshall, G. J., 2003: Trends in the Southern Annular Mode from observations and reanalyses. *Journal of Climate*, **16**, 4134–4143, doi:10.1175/1520-0442(2003)016<4134:TITSAM>2.0.CO;2.

Masato, G., B. J. Hoskins, and T. Woollings, 2013: Winter and summer northern hemisphere blocking in CMIP5 models. *Journal of Climate*, **26 (18)**, 7044–7059, doi:10.1175/JCLI-D-12-00466.1, URL http://dx.doi.org/10.1175/JCLI-D-12-00466.1.

Matsueda, M., H. Endo, and R. Mizuta, 2009: Future change in Southern Hemisphere summertime and wintertime atmospheric blockings simulated using a 20-km-mesh AGCM. *Geophysical Research Letters*, **37 (2)**, doi:10.1029/2009GL041758, URL http://dx.doi.org/10.1029/2009GL041758.

Mayewski, P. A., et al., 2009: State of the Antarctic and Southern Ocean climate system. *Reviews of Geophysics*, **47 (1)**, doi:

10.1029/2007RG000231, URL http://dx.doi.org/10.1029/2007RG000231.

McGuffie, K. and A. Henderson-Sellers, 2005: *A Climate Modelling Primer*. John Wiley & Sons, Ltd, 165–212 pp., doi:10.1002/0470857617.ch5.

McKendry, I. G., K. Stahl, and R. D. Moore, 2006: Synoptic sea-level pressure patterns generated by a general circulation model: comparison with types derived from NCEP/NCAR re-analysis and implications for downscaling. *International Journal of Climatology*, **26 (12)**, 1727–1736, doi:10.1002/joc.1337.

McKerchar, A., J. Renwick, and J. Schmidt, 2010: Diminishing streamflows on the east coast of the South Island New Zealand and linkage to climate variabilty and change. *Journal of Hydology (NZ)*, **49**, 1–14.

McPhaden, M. J., S. E. Zebiak, and M. H. Glantz, 2006: ENSO as an integrating concept in earth science. *Science*, **314 (5806)**, 1740–1745, doi:10.1126/science.1132588, URL http://www.sciencemag.org/content/314/5806/1740.abstract.

Meehl, G. A., G. J. Boer, C. Covey, M. Latif, and R. J. Stouffer, 2000: The coupled model intercomparison project (cmip). *Bulletin of the American Meteorological Society*, **81 (2)**, 313–318, doi:10.1175/1520-0477(2000)081<0313:TCMIPC>2.3.CO;2, URL http://dx.doi.org/10.1175/1520-0477(2000)081<0313:TCMIPC>2.3.CO;2.

Meehl, G. A., C. Covey, T. Delworth, M. Latif, B. McAvaney, J. F. B. Mitchell, R. J. Stouffer, and K. E. Taylor, 2007: The WCRP CMIP3 multimodel dataset - a new era in climate change research. *Bulletin of the American Meteorological Society*, **88 (9)**, 1383–1394, doi:DOI10.1175/BAMS-88-9-1383.

Meehl, G. A., et al., 2009: Decadal prediction. *Bulletin of the American Meteorological Society*, **90 (10)**, 1467–1485, doi:10.1175/2009BAMS2778.1, URL http://dx.doi.org/10.1175/2009BAMS2778.1.

Mo, K. C. and G. H. White, 1985: Teleconnections in the Southern Hemisphere. *Monthly Weather Review*, **113 (1)**, 22–37, doi:10.1175/1520-0493(1985)113<0022:TITSH>2.0.CO;2, URL http://dx.doi.org/10.1175/1520-0493(1985)113<0022:TITSH>2.0.CO;2.

Moss, R. H., et al., 2010: The next generation of scenarios for climate change research and assessment. *Nature*, **463**, 747–756, doi:10.1038/nature08823.

Mullan, A., 1998: Southern hemisphere sea-surface temperatures and their contemporary and lag association with New Zealand temperature and precipitation. *International Journal of Climatology*, **18 (8)**, 817–840.

Mullan, A., S. Dean, and S. Stuart, 2013: How good are the CMIP5 models? *New Zealand Climate Change Conference*.

Mullan, B., 2011: Scenarios of storminess and regional wind extremes under climate change. Tech. rep., NIWA.

Mullan, B. and S. Dean, 2009: AR4 Climate Model Validation and Scenarios for New Zealand. Tech. rep., NIWA.

Murray, R. J. and I. Simmonds, 1991: A numerical scheme for tracking cyclone centres from digital data. part i: Development and operation of the scheme. *Australian Meteorological Magazine*, **39 (3)**, 155–166.

Nakicenovic, N., et al., 2000: *Special report on emissions scenarios. Special report of Working Group III of the Intergovernmental Panel on Climate Change*. Cambridge University Press, Cambridge.

Neu, U., et al., 2012: Imilast: A community effort to intercompare extratropical cyclone detection and tracking algorithms. *Bulletin of the American Meteorological Society*, **94 (4)**, 529–547, doi:10.1175/BAMS-D-11-00154.1, URL http://dx.doi.org/10.1175/BAMS-D-11-00154.1.

Oke, T. R., 1987: *Boundary Layer Climates*, Vol. 5. 2d ed., Methuen, London.

Oliveira, F. N. M., L. M. V. Carvalho, and T. Ambrizzi, 2013: A new climatology for Southern Hemisphere blockings in the winter and the combined effect of ENSO and SAM phases. *International Journal of Climatology*, doi:10.1002/joc.3795, URL http://dx.doi.org/10.1002/joc.3795.

Palmer, T. N., F. J. Doblas-Reyes, A. Weisheimer, and M. J. Rodwell, 2008: Toward seamless prediction: Calibration of climate change projections using seasonal forecasts. *Bulletin of the American Meteorological Society*, **89 (4)**, 459–470, doi:10.1175/BAMS-89-4-459, URL http://dx.doi.org/10.1175/BAMS-89-4-459.

Parsons, S., A. J. McDonald, and J. A. Renwick, 2014: The use of synoptic climatology with general circulation model output over New Zealand. *International Journal of Climatology*, doi:10.1002/joc.3919, URL http://dx.doi.org/10.1002/joc.3919.

Peters, G. P., et al., 2013: The challenge to keep global warming below 2c. *Nature Climate Change*, **3 (1)**, 4–6, URL http://dx.doi.org/10.1038/nclimate1783.

Pezza, A., P. van Rensch, and W. Cai, 2011: Severe heat waves in Southern Australia: synoptic climatology and large scale connections. *Climate Dynamics*, 1–16, doi:10.1007/s00382-011-1016-2.

Pezza, A. B., I. Simmonds, and J. A. Renwick, 2007: Southern Hemisphere cyclones and anticyclones: recent trends and links with decadal variability in the Pacific Ocean. *International Journal of Climatology*, **27**, 1403–1419, doi:10.1002/joc.1477.

Philipp, A., et al., 2010: Cost733cat - A database of weather and circulation type classifications. *Physics and Chemistry of the Earth*, **35**, 360–373, doi:10.1016/j.pce.2009.12.010.

Preisendorfer, R., 1988: *Principal Component Analysis in Meteorology and Oceanography*. Elsevier.

Raphael, M. N., 2004: A zonal wave 3 index for the Southern Hemisphere. *Geophysical Research Letters*, **31 (23)**, doi:

10.1029/2004GL020365, URL http://dx.doi.org/10.1029/2004GL020365.

Renwick, J., 2004: Trends in the Southern Hemisphere polar vortex in NCEP and ECMWF reanalyses. *Geophysical Research Letters*, **31 (7)**, L07 209 1–4.

Renwick, J., 2011: Kidson's Synoptic Weather Types and Surface Climate Variability over New Zealand. *Weather and Climate*, **31**, 3–23.

Renwick, J., A. Mullan, and A. Porteous, 2009: Statistical downscaling of New Zealand climate. *Weather and Climate*, **29**, 24–44.

Renwick, J. A., 2005: Persistent positive anomalies in the Southern Hemisphere Circulation. *Monthly Weather Review*, **133**, doi:10.1175/MWR2900.1.

Renwick, J. A., J. J. Katzfey, K. C. Nguyen, and J. L. McGregor, 1998: Regional model simulations of New Zealand climate. *Journal of Geophysical Research*, **103**, 5973–5982, doi:10.1029/97JD02939.

Renwick, J. A. and M. J. Revell, 1999: Blocking over the south pacific and rossby wave propagation. *Monthly Weather Review*, **127 (10)**, 2233–2247, doi:10.1175/1520-0493(1999)127<2233:BOTSPA>2.0.CO;2, URL http://dx.doi.org/10.1175/1520-0493(1999)127<2233:BOTSPA>2.0.CO;2.

Renwick, J. A. and D. Thompson, 2006: The southern annular mode the southern annular mode and new zealand climate. *Water & Atmosphere*, **14**, 24–25.

Renwick, J. A. and J. M. Wallace, 1996: Relationships between north pacific wintertime blocking, El Niño, and the PNA pattern. *Monthly Weather Review*, **124 (9)**, 2071–2076, doi:10.1175/1520-0493(1996)124<2071:RBNPWB>2.0.CO;2.

Rex, D. F., 1950a: Blocking action in the middle troposphere and its effect upon regional climate. *Tellus*, **2 (3)**, 196–211, doi:10.1111/j.2153-3490.1950.tb00331.x, URL http://dx.doi.org/10.1111/j.2153-3490.1950.tb00331.x.

Rex, D. F., 1950b: Blocking action in the middle troposphere and its effect upon regional climate. *Tellus*, **2 (4)**, 275–301, doi:10.1111/j.2153-3490.1950.tb00339.x, URL http://dx.doi.org/10.1111/j.2153-3490.1950.tb00339.x.

Saha, S., et al., 2010: The NCEP Climate Forecast System Reanalysis. *Bulletin of the American Meteorological Society*, **91**, 1015–1057, doi:10.1175/2010BAMS3001.1.

Salinger, M. J. and A. B. Mullan, 1999: New Zealand climate: temperature and precipitation variations and their links with atmospheric circulation 1930-1994. *International Journal of Climatology*, **19**, 1049–1071, doi:10.1002/(SICI)1097-0088(199908)19:10<1049::AID-JOC417>3.0.CO;2-Z.

Schuenemann, K. C. and J. J. Cassano, 2009: Changes in synoptic weather patterns and greenland precipitation in the 20th and 21st centuries: 1. evaluation of late 20th century simulations from ipcc models. *Journal of Geophysical Research: Atmospheres*, **114 (D20)**, n/a–n/a, doi:10.1029/2009JD011705, URL http://dx.doi.org/10.1029/2009JD011705.

Schuenemann, K. C. and J. J. Cassano, 2010: Changes in synoptic weather patterns and Greenland precipitation in the 20th and 21st centuries: 2. analysis of 21st century atmospheric changes using self-organizing maps. *Journal of Geophysical Research*, **115 (D5)**, D05 108, doi:10.1029/2009JD011706, URL http://dx.doi.org/10.1029/2009JD011706.

Shapiro, M., et al., 2010: An earth-system prediction initiative for the 21st century. *Bulletin of the American Meteorological Society*.

Sheridan, S. and C. Lee, 2010: Synoptic climatology and the general circulation model. *Progress in Physical Geography*, **34 (1)**, 101–109.

Sheridan, S. C. and C. C. Lee, 2011: The self-organizing map in synoptic climatological research. *Progress in Physical Geography*, **35 (1)**, 109–119, doi:10.1177/0309133310397582, URL http://ppg.sagepub.com/content/35/1/109.abstract,

http://ppg.sagepub.com/content/35/1/109.full.pdf+html.

Simmonds, I., K. Keay, and E.-P. Lim, 2003: Synoptic activity in the seas around Antarctica. *Monthly Weather Review*, **131 (2)**, 272–288, doi:10.1175/1520-0493(2003)131<0272:SAITSA>2.0.CO;2, URL http://dx.doi.org/10.1175/1520-0493(2003)131<0272:SAITSA>2.0.CO;2.

Simmons, A. J., et al., 2004: Comparison of trends and low-frequency variability in CRU, ERA-40, and NCEP/NCAR analyses of surface air temperature. *Journal of Geophysical Research: Atmospheres*, **109 (D24)**, doi:10.1029/2004JD005306, URL http://dx.doi.org/10.1029/2004JD005306.

Simpkins, G. and A. Karpechko, 2012: Sensitivity of the Southern Annular Mode to greenhouse gas emission scenarios. *Climate Dynamics*, **38 (3-4)**, 563–572, doi:10.1007/s00382-011-1121-2, URL http://dx.doi.org/10.1007/s00382-011-1121-2.

Sinclair, M. R., 1994: An objective cyclone climatology for the Southern Hemisphere. *Monthly Weather Review*, **122 (10)**, 2239–2256, doi:10.1175/1520-0493(1994)122<2239:AOCCFT>2.0.CO;2, URL http://dx.doi.org/10.1175/1520-0493(1994)122<2239:AOCCFT>2.0.CO;2.

Sinclair, M. R., 1995: A climatology of cyclogenesis for the Southern Hemisphere. *Monthly Weather Review*, **123 (6)**, 1601–1619, doi:10.1175/1520-0493(1995)123<1601:ACOCFT>2.0.CO;2, URL http://dx.doi.org/10.1175/1520-0493(1995)123<1601:ACOCFT>2.0.CO;2.

Sinclair, M. R., 1996: A climatology of anticyclones and blocking for the Southern Hemisphere. *Monthly Weather Review*, **124 (2)**, 245–264, doi:10.1175/1520-0493(1996)124<0245:ACOAAB>2.0.CO;2, URL http://dx.doi.org/10.1175/1520-0493(1996)124<0245:ACOAAB>2.0.CO;2.

Sinclair, M. R., 1997: Objective identification of cyclones and their circulation intensity, and climatology. *Weather and forecasting*, **12 (3)**, 595–612.

Solomon, S., D. Qin, M. Manning, Z. Chen, M. Marquis, K. B. Avery, M. Tignor, and H. L. Miller, (Eds.) , 2007: *Climate change 2007: The physical science basis : contribution of Working Group I to the Fourth Assessment Report of the Intergovernmental Panel on Climate Change*. Cambridge University Press, Cambridge.

Son, S. W., et al., 2010: Impact of stratospheric ozone on Southern Hemisphere circulation change: A multimodel assessment. *Journal of Geophysical Research*, **115**, doi:{10.1029/2010JD014271}.

Stevenson, S. L., 2012: Significant changes to ENSO strength and impacts in the twenty-first century: Results from CMIP5. *Geophysical Research Letters*, **39 (17)**, L17703, doi:10.1029/2012GL052759, URL http://dx.doi.org/10.1029/2012GL052759.

Sturman, A. and H. Quénol, 2013: Changes in atmospheric circulation and temperature trends in major vineyard regions of New Zealand. *International Journal of Climatology*, **33 (12)**, 2609–2621, doi:10.1002/joc.3608, URL http://dx.doi.org/10.1002/joc.3608.

Sturman, A. and N. Tapper, 2006: *The Weather and Climate of Australia and New Zealand*. Oxford University Press, Melbourne.

Swart, N. C. and J. C. Fyfe, 2012: Observed and simulated changes in the Southern Hemisphere surface westerly wind-stress. *Geophysical Research Letters*, **39**, doi:{10.1029/2012GL052810}.

Tait, A., R. Henderson, R. Turner, and X. Zheng, 2006: Thin plate smoothing spline interpolation of daily rainfall for New Zealand using a climatological rainfall surface. *International Journal of Climatology*, **26 (14)**, 2097–2115, doi:{10.1002/joc.1350}.

Taljaard, J. J., 1967: Development, distribution and movement of cyclones and anticyclones in the Southern Hemisphere during the IGY. *Journal of Applied Meteorology*, **6 (6)**, 973–987, doi:10.1175/1520-0450(1967)006<0973:DDAMOC>2.

o.CO;2, URL http://dx.doi.org/10.1175/1520-0450(1967)006<0973:DDAMOC>2.0.CO;2.

Taylor, K. E., R. J. Stouffer, and G. A. Meehl, 2012: An overview of CMIP5 and the experiment design. *Bulletin of the American Meteorological Society*, **93 (4)**, 485–498, doi:10.1175/BAMS-D-11-00094.1, URL http://dx.doi.org/10.1175/BAMS-D-11-00094.1.

Tebaldi, C. and R. Knutti, 2007: The use of the multi-model ensemble in probabilistic climate projections. *Philosophical Transactions of the Royal Society A: Mathematical, Physical and Engineering Sciences*, **365 (1857)**, 2053–2075, doi:10.1098/rsta.2007.2076, URL http://rsta.royalsocietypublishing.org/content/365/1857/2053.abstract, http://rsta.royalsocietypublishing.org/content/365/1857/2053.full.pdf+html.

Thompson, D. W. J., S. Solomon, P. J. Kushner, M. H. England, K. M. Grise, and D. J. Karoly, 2011: Signatures of the Antarctic ozone hole in Southern Hemisphere surface climate change. *Nature Geoscience*, **4 (11)**, 741–749, URL http://dx.doi.org/10.1038/ngeo1296.

Thompson, D. W. J. and J. M. Wallace, 2000: Annular Modes in the Extratropical Circulation. Part I: Month-to-Month Variability*. *Journal of Climate*, **13**, 1000–1016, doi:10.1175/1520-0442(2000)013<1000:AMITEC>2.0.CO;2.

Tibaldi, S. and F. Molteni, 1990: On the operational predictability of blocking. *Tellus A*, **42 (3)**, 343–365, doi:10.1034/j.1600-0870.1990.t01-2-00003.x, URL http://dx.doi.org/10.1034/j.1600-0870.1990.t01-2-00003.x.

Tibaldi, S., E. Tosi, A. Navarra, and L. Pedulli, 1994: Northern and Southern Hemisphere seasonal variability of blocking frequency and predictability. *Monthly Weather Review*, **122 (9)**, 1971–2003, doi:10.1175/1520-0493(1994)122<1971:NASHSV>2.0.CO;2, URL http://dx.doi.org/10.1175/1520-0493(1994)122<1971:NASHSV>2.0.CO;2.

Trenberth, K. E., 1976: Fluctuations and trends in indices of the Southern Hemispheric circulation. *Quarterly Journal of the Royal Meteorological Society*, **102 (431)**, 65–75, doi:10.1002/qj.49710243106, URL http://dx.doi.org/10.1002/qj.49710243106.

Trenberth, K. F. and K. C. Mo, 1985: Blocking in the Southern Hemisphere. *Monthly Weather Review*, **113 (1)**, 3–21, doi:10.1175/1520-0493(1985)113<0003:BITSH>2.0.CO;2, URL http://dx.doi.org/10.1175/1520-0493(1985)113<0003:BITSH>2.0.CO;2.

Troup, A. J., 1965: The 'Southern Oscillation'. *Quarterly Journal of the Royal Meteorological Society*, **91 (390)**, 490–506, doi:10.1002/qj.49709139009, URL http://dx.doi.org/10.1002/qj.49709139009.

Turner, J., 2004: The El Niño–Southern Oscillation and Antarctica. *International Journal of Climatology*, **24 (1)**, 1–31, doi:10.1002/joc.965, URL http://dx.doi.org/10.1002/joc.965.

Turner, J., T. J. Bracegirdle, T. Phillips, G. J. Marshall, and J. S. Hosking, 2013: An initial assessment of Antarctic sea ice extent in the CMIP5 models. *Journal of Climate*, **26 (5)**, 1473–1484.

Ulbrich, U., G. Leckebusch, and J. Pinto, 2009: Extra-tropical cyclones in the present and future climate: a review. *Theoretical and Applied Climatology*, **96 (1-2)**, 117–131, doi:10.1007/s00704-008-0083-8, URL http://dx.doi.org/10.1007/s00704-008-0083-8.

Ummenhofer, C. C. and M. H. England, 2007: Interannual extremes in New Zealand precipitation linked to modes of Southern Hemisphere climate variability. *Journal of Climate*, **20 (21)**, 5418–5440, doi:10.1175/2007JCLI1430.1.

Uppala, S. M., et al., 2005: The ERA-40 re-analysis. *Quarterly Journal of the Royal Meteorological Society*, **131**, 2961–3012, doi:10.1256/qj.04.176.

van Loon, H. and R. L. Jenne, 1972: The zonal harmonic standing waves in the Southern Hemisphere. *Journal of Geophysical Research*, **77 (6)**, 992–1003, doi:10.1029/JC077i006p00992, URL http://dx.doi.org/10.1029/JC077i006p00992.

Wallace, J. M., G.-H. Lim, and M. L. Blackmon, 1988: Relationship between cyclone tracks, anticyclone tracks and baroclinic waveguides. *Journal of the Atmospheric Sciences*, **45 (3)**, 439–462, doi:10.1175/1520-0469(1988)045<0439:RBCTAT>2.0.CO;2, URL http://dx.doi.org/10.1175/1520-0469(1988)045<0439:RBCTAT>2.0.CO;2.

Watanabe, M., et al., 2010: Improved climate simulation by miroc5: Mean states, variability, and climate sensitivity. *Journal of Climate*, **23 (23)**, 6312–6335, doi:10.1175/2010JCLI3679.1, URL http://dx.doi.org/10.1175/2010JCLI3679.1.

Wiedenmann, J. M., A. R. Lupo, I. I. Mokhov, and E. A. Tikhonova, 2002: The climatology of blocking anticyclones for the Northern and Southern Hemispheres: Block intensity as a diagnostic. *Journal of Climate*, **15 (23)**, 3459–3473, doi:10.1175/1520-0442(2002)015<3459:TCOBAF>2.0.CO;2, URL http://dx.doi.org/10.1175/1520-0442(2002)015<3459:TCOBAF>2.0.CO;2.

Wilks, D. S., 2011: *Statistical methods in the atmospheric sciences*. 3d ed., Academic Press.

Yamazaki, A. and H. Itoh, 2009: Selective absorption mechanism for the maintenance of blocking. *Geophysical Research Letters*, **36 (5)**, L05 803, doi:10.1029/2008GL036770, URL http://dx.doi.org/10.1029/2008GL036770.

Yarnal, B., 1993: *Synoptic Climatology in Environmental Analysis*. Belhaven Press. London, UK. 195pp.

Yarnal, B., A. C. Comrie, B. Frakes, and D. P. Brown, 2001: Developments and prospects in synoptic climatology. *International Journal of Climatology*, **21**, 1923–1950.

Yin, J., 2005: A consistent poleward shift of the storm tracks in simulations of 21st century climate. *Geophysical Research*

Letters, **32 (18)**, doi:{10.1029/2005GL023684}.